UCRL-ID-145269

# Institute for Laser Science and Applications

*H.A. Baldis*

**August 27, 2001**

U.S. Department of Energy

Lawrence Livermore National Laboratory

# Institute for Laser Science and Applications

## ILSA REPORT 2000

Lawrence Livermore National Laboratory

*This work was performed under the auspices of the U.S. Department of Energy by the University of California Lawrence Livermore National Laboratory, through the Institute for Laser Science and Applications, under contract No. W-7405-Eng-48.*

# Institute for Laser Science and Applications

## Report 2000

Edited by
Hector A. Baldis
Institute for Laser Science and Applications
University Relations Program
Lawrence Livermore National Laboratory
and University of California, Davis

**Acknowledgements**

Scientific Editor - Hector A. Baldis
Publication Coordinator - Mary Ann Soby
Publication Editor/Graphics - Marsha McInnis
Copy Edit -Mary Ann Soby

# Table of Contents

**FY00**



## PUBLICATIONS

# ILSA Director's Message

Hector A. Baldis,
Director, Institute for Laser Science and Applications
and University of California, Davis

# PROJECTS

## *Institute for Laser Science and Applications*

PROJECTS

# Theory of Parametric Instabilities

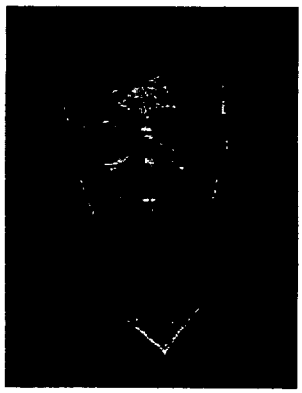

Bruce Cohen, Principal Investigator, LLNL

***Co-PI's:***
*Hector Baldis – LLNL and UC Davis*
*Richard Berger, Ed Williams, Bruce Langdon, Robert Kirkwood – LLNL*
*Christine Labaune – LULI, Ecole Polytechnique, France*

When intense lasers are used to initiate fusion in inertial confinement fusion, plasmas typically form. Because the laser energy flux densities are high, there is a tendency for nonlinear interactions of the laser beam or beams with the plasma to occur. Such interactions can lead to backscatter, focusing, and/or filamentation of the laser beams, all of which may be quite deleterious to the fusion application. This project addresses the theoretical study of laser-plasma interactions and the modeling of laser-plasma interaction experiments. In particular, this project has addressed the modeling of multiple laser-beam experiments with CH target foils at the LULI facility near Paris that demonstrated a number of interesting and important nonlinear features regarding stimulated Brillouin and Raman backscatter (stimulated scattering of an electromagnetic wave by an ion sound wave and an electron plasma wave, respectively, in a plasma). We have applied similar analyses to SRS experiments in NOVA at LLNL and to a proposed cross-beam experiment in OMEGA at Rochester.

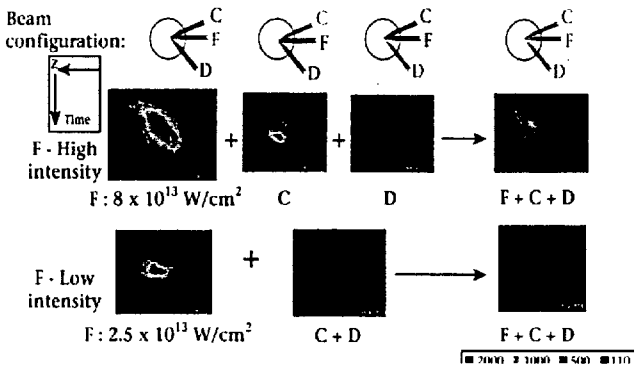


*Influence of multiple-beam irradiation on the amplitude of ion acoustic waves associated with stimulated Brillouin scattering in the LULI experiment.*

## Recent Publications

C. Labaune, H.A. Baldis, B.I. Cohen, W. Rozmus, S. Depierreux, E. Schifano, B.S. Bauer, and A. Michard, *Nonlinear Modification of Laser-Plasma Interaction Processes Under Crossed Laser Beams Irradiation*, (November, 1998), **Phys. Plasmas 6**, 2048 (1999).

K.B. Wharton, R.K. Kirkwood, S.H. Glenzer, K.G. Estabrook, B.B. Afeyan, B.I. Cohen, J.D. Moody, and C. Joshi, *Energy Transfer Between Identical-Frequency Laser Beams* (November, 1998), **Phys. Plasmas 6**, 2144 (1999).

C. Labaune, H.A. Baldis, B.S. Bauer, E. Schifano, and B.I. Cohen, *Spatial and Temporal Coexistence of Stimulated Scattering Processes Under Crossed-Laser-Beam Irradiation*, **Phys. Rev. Lett. 82**, 3613 (1999).

B.I. Cohen, B.F. Lasinski, A.B. Langdon, E.A. Williams, H.A. Baldis, and C. Labaune, *Suppression of Stimulated Brillouin Scattering by Seeded Ion Wave Mode Coupling*, (LLNL Report-JC-129491), **Phys. Plasmas 5**, 3402 (1998).

B.I. Cohen, B.F. Lasinski, A.B. Langdon, E.A. Williams, K.B. Wharton, R.K. Kirkwood, and K.G. Estabrook, *Resonant Stimulated Brillouin Interaction of Opposed Laser Beams in a Drifing Plasma*, **Physics of Plasmas, 5**, 3408 (1998).

K.B. Wharton, C. Joshi, R.K. Kirkwood, S.H. Glenzer, K.G. Estabrook, B.B. Afeyan, B.I. Cohen, and J.D. Moody, *Observation of Energy Transfer Between Identical-Frequency Laser Beams in Flowing Plasmas*, (LLNL Report UCRL-JC-129856) **Physical Rev. Lett. 81**, 2248 (1998).

## Affiliated Institutes

LULI, CNRS, Ecole Polytechnique, 91128 Palaiseau, France; UC Davis

## Modeling Stimulated Scattering in LULI Multiple Beam Experiments

Multiple laser beam experiments with CH target foils at the LULI facility [Baldis, et al., Phys. Rev. Lett. 77, 2957 (1996)] demonstrate anti-correlation of stimulated Brillouin and Raman backscatter (SBS and SRS). Detailed Thomson scattering diagnostics show that SBS always precedes SRS, that secondary electron plasma waves can accompany SRS appropriate to the Langmuir Decay Instability (LDI), and that with multiple interaction laser beams the SBS direct backscatter signal in the primary laser beam is reduced while the SRS backscatter signal is enhanced and onsets earlier in time. Analysis and numerical calculations are presented that evaluate the influences of local pump depletion in laser hot spots due to SBS, of mode coupling of SBS and LDI ion waves, and of optical mixing of secondary and primary laser beams on the competition of SBS and SRS. The calculations quantify the effectiveness of local pump depletion, ion wave mode coupling, and optical mixing in affecting the LULI observations. Both local pump depletion in intense speckles and ion wave mode coupling contribute significantly to influencing the suppression of SBS direct backscatter in multiple-beam experiments and the competition of SBS and SRS.

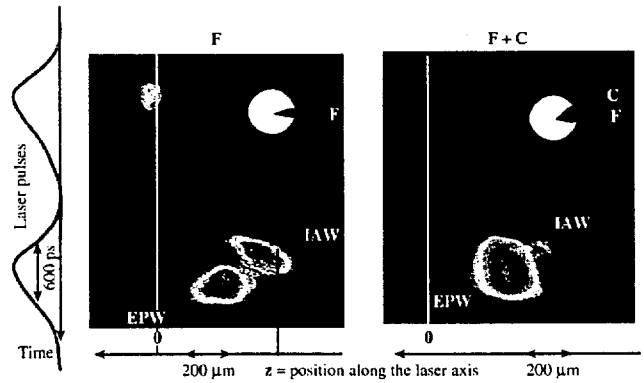


Space and time evolution of Thomson scattered light from IAWs associated with SBS and EPWs associated with SRS

*Modification of the competition between SBS and SRS under crossed beam irradiation: EPWs associated with SRS start earlier in the laser pulse with multiple beams than with single beam, and coexist with IAWs associated with SBS.*

## Contact Information

Bruce Cohen
Ph: (925) 422-9823
Email: bcohen@llnl.gov

PROJECTS

# Plasma Induced Laser Incoherence

Hector Baldis, Principal Investigator, LLNL and UC Davis

*Co- PI's:*
*C. Labaune, S. Depierreux, J. Fuchs – LULI, Ecole Polytechnique*
*D. Pesme – CPT, Ecole Polytechnique*
*W. Rozmus – University of Alberta*
*B. Cohen – LLNL*

The propagation of intense laser pulse through underdense, fully ionized plasmas can be affected by a number of non-linear processes like filamentation, self-focusing or parametric instabilities like stimulated Brillouin and Raman scattering [1]. By reducing the coupling efficiency to the plasma and the illumination symmetry or by allowing coupling between crossed beams, they lead to degraded performances of inertial confinement fusion (ICF) targets. Optical smoothing techniques, which increased spatial and temporal incoherence of laser beams, have been proposed and implemented to reduce the growth of these non-linear processes [2-4].

In addition to such smoothing, recent theoretical studies have suggested [5, 6] that the propagation of the laser beam through the underdense plasma could also induce spatial and temporal incoherence upon an already spatially randomized laser beam by a random phase plate (RPP) [7]. This so-called self-induced plasma smoothing (SIPS) process would develop through the non-linear coupling between stimulated Brillouin forward scattering (SBFS) and the dynamically evoluting hot spots of the beam. SIPS could not only influence laser-plasma interactions but also interfere with the externally applied smoothing techniques and thus modify their expected performances. Its study is therefore of fundamental importance in order to determine the proper beam smoothing strategies for the future megajoule-scale laser facilities.

## Recent Publications

C. Labaune, H.A. Baldis, E. Schifano, B.S. Bauer, A. Maximov, I. Ourdev, W. Rozmus, and D. Pesme, *Enhanced Forward Scattering in the Case of Two Crossed Laser Beams Interacting with a Plasma*, **Phys. Rev. Lett., 85**, 1658 (2000).

J. Fuchs, C. Labaune, S. Depierreux, A. Michard, and H.A. Baldis, *Modification of Spatial and Temporal Gains of Stimulated Brillouin and Raman by Polarization Smoothing*, **Phys. Rev. Lett., 84**, 3089 (2000).

S. Depierreux, J. Fuchs, C. Labaune, A. Michard, H.A. Baldis, D. Pesme, S. Huller, and G. Laval, *First Observation of Ion-Acoustic Waves Produced by the Langmuir Decay Instability*, **Phys. Rev. Lett., 84**, 2869 (2000).

C. Labaune, H.A. Baldis, B.I. Cohen, W. Rozmus, E. Schifano, B.S. Bauer, and A. Michard, *Non-linear Modifiction of Laser-plasma Interaction Processes Under Laser Beams Irradiation*, **Phys. Plasmas, 6**, 2048 (1999).

C. Labaune, H.A. Baldis, B.S. Bauer, E. Schifano, and B.I. Cohen, *Spatial and Temporal Coexistence of Stimulated Scattering Processes under Crossed-Laser Beam Irradiation*, **Phys. Rev. Lett., 82**, 3613 (1999).

C. Labaune, H.A. Baldis, B.S. Bauer, V.T. Tikhonchuk, and G. Laval, *Time-resolved Measurements of Secondary Langmuir Waves Produced by the Langmuir Decay Instability*, **Phys. Plasmas, 5**, 234 (1998).

H.A. Baldis, C. Labaune, J.D. Moody, T. Talinaud, and V.T. Tikhonchuk, *Localization of Stimulated Brillouin Scattering in Random Phase Plate Speckles*, **Phys. Rev. Lett., 80**, 1900 (1998).

## Affiliated Institutes

UC Davis; Laboratoire pour l 'Utilisation des Lasers Intenses (LULI); CNRS, Ecole Polytechnique, France; University of Alberta, Canada

The experiments were performed with five beams of the LULI (Laboratoire pour l'Utilisation des Lasers Intenses) laser facility. The $\lambda_0$=1.053 μm interaction beam was focused with an f/6 lens, through an RPP along the principal axis of a preformed plasma. The resulting randomized speckle distribution had a focal spot diameter of 320 μm full width at half maximum (FWHM), leading to a peak average intensity $10^{14}$ W/cm$^2$. By varying the delay between the plasma creation pulses and the interaction pulse, as well as the thickness of the target and the energy of the plasma-creating beams, it was possible to adjust the density of the target at the time of the interaction. The forward scattered light was collected in two directions : at 0±10° and 22.5±5°.

The time-resolved near-field images of a central slab of the forward scattered light at high intensity is shown in Fig.1. The intensity pattern is much smoother after propagation through the plasma with a smaller contrast ratio of the hot spots which drops from 1 (without plasma) to ~0.3 (with plasma). This is linked with a significant change in the temporal behavior of the pattern which evolves from a stationary to a random dynamical behavior, with intense speckles appearing and vanishing rapidly.

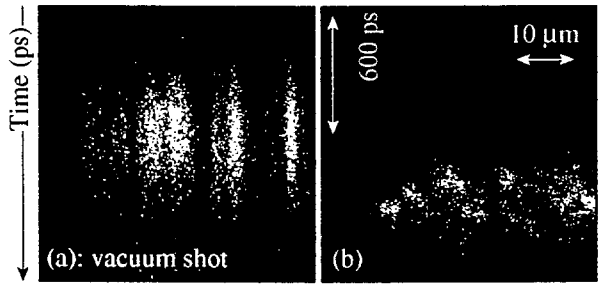


*One-dimensional time-resolved near field images of the forward scattered light at 0±10°. (a) stationary speckle pattern of the f/3 incident light (vacuum shot). (b) through the $n_{max}/n_c$~0.2 plasma and with an intensity of $<I_{14}>=3$.*

The results demonstrate that SIPS is effective in modifying significantly the properties of an intense propagating beam. The main processes that can couple the incident laser light with the plasma and induce such large-angle spreading and large red spectral shifts are filamentation and SBFS. Self-phase modulation could account for part of the shift but, to produce bandwidth >10 Å, an almost complete plasma evacuation inside the speckles is needed.

Numerical simulations [6], with a similar self-focusing/filamentation initial stage, display, at later propagation times, an unsteady behavior of the plasma response with strongly deflected filaments oscillating in and out. This is mainly due to the mixing between the density wells dug by neighbor filaments. Such a rapidly bifurcating motion of the filaments decorrelates the light from the plasma response and smoothes the spatial intensity distribution. In addition, these simulations also display, at high intensity, large redshifts and spectral broadening for the forward scattered light. The fact that deflecting filaments couple to SBFS to produce correlated spatial and temporal incoherence can be understood as follows: first, spreading filaments can stimulate SBFS (which grows more strongly with angle) and second, SBFS frequency broadened spreading can in turn induce filaments to propagate at larger angles.

This additional smoothing, stronger than what external techniques like SSD [4] can achieve, could reduce further growth of other parametric instabilities.

## References:

[1] W. Kruer, *The Physics of Laser Plasma Interactions.* New York: Addison-Wesley, 1988.
[2] C. Labaune, et al, **Phys. Fluids B 4**, 2224 (1992).
[3] W. Seka et al., **Phys. Fluids B 4**, 2232 (1992.
[4] R. Kirkwood, et al., **Phys. Plasmas 4**, 1800 (1997).
[5] V.V. Eliseev, et al., **Phys. Plasmas 4**, 4333 (1997).
[6] A. Schmitt and B. Afeyan, **Phys. Plasmas 5**, 503 (1998).
[7] Y. Kato, et al., **Phys. Rev. Lett. 53**, 1057 (1984).

## Contact Information

Hector A. Baldis
Ph: (925) 422-0101
Email: baldis1@llnl.gov

# Fluctuations and Nonlinear Waves in Laser Produced Plasmas

Wojciech Rozmus, Principal Investigator, University of Alberta

***Co PI:***
*Hector Baldis – LLNL and UC Davis*

***Collaborator:***
*Sigfried Glenzer – LLNL*

***PostDocs and Graduate Students:***
*E. Fourkal, A. Maximov, C. Kirkby, I. Ourdev, Y. Shao – University of Alberta*

Support from ILSA provides my group with different collaborative opportunities in our theoretical and numerical studies of kinetic and wave processes in laser produced plasmas. Nonparaxial electromagnetic wave interaction code has been applied in studies of ion wave response to laser beams. We have identified a forward stimulated Brillouin scattering as one of the processes contributing, in addition to filamentation instability, to a plasma induced loss of coherence of laser beams in experimental results from Janus laser. Resonant instability of laser filaments has been discovered in three dimensional simulations of a single laser hot spot. This rapidly growing perturbation leads to destruction of nonlinearly trapped electromagnetic waves in density channels. It results in spectral and angular broadening of the transmitted light and modifies intensity distribution of a laser light in the plasma.

A nonlocal linear plasma transport theory, which is valid for the arbitrary particle collisionality has been generalized to include an effect of the laser light. Plasma response to randomized laser beams described in terms of the nonlocal hydrodynamics has shown strong enhancement of electrostatic fluctuations.

An ongoing development of the particle code, which includes particle collisions and the interaction with a oscillatory electric field resulted in a new non-Maxwellian distribution functions and preliminary results involving the nonlinear thermal transport.

## Recent Publications

S.H. Glenzer, W.E. Alley, K.G. Estabrook, J.D. DeGroot, M. Haines, J.A. Hammer, J.-P. Jadaud, B.J. MacGowan, J. Moody, W. Rozmus, and L.J. Suter, *Thomson Scattering from Laser Plasmas*, **Phys. Plasmas 6**, 2117 (1999).

V. Eliseev, D. Pesme, W. Rozmus, V. Tikhonchuk and C. Capjack, *Filamentation of a Laser Beam Interacting with an Underdense Plasma and its Coupling to Stimulated Brillouin Scattering*, **Physica Scripta, T75**, 112 (1998).

A. Brantov, V. Yu. Bychenkov, V. Tikhonchuk, and W. Rozmus, *Nonlocal Electron Tansport in Laser Heated Plasmas*, **Phys. Plasmas, 5**, 2742 (1998).

J. Myatt, W. Rozmus, V. Yu. Bychenkov, and V. T. Tikhonchuk, *Thomson Scattering from Ion Acoustic Waves in Laser Plasmas*, **Phys. Rev. E, 57**, 3383, (1998).

V. Eliseev, I. Ourdev, W. Rozmus, V. Tikhonchuk, C. Capjack, and P. Young, *Ion Wave Response to Intense Laser Beams in Underdense Plasmas*, **Phys. Plasmas 4**, 4333 (1997).

## Affiliated Institutes

University of Alberta, Canada; UC Davis

# Fluctuations and Nonlinear Waves in Laser Produced Plasmas

Thomson scattering (TS) from stable electron density fluctuations is a powerful diagnostic used to measure local plasma parameters, distribution functions and transport processes. In laser produced plasmas TS has become a standard technique for studying enhanced fluctuations and related instabilities. The TS cross section is determined by the dynamical form factor for electron density fluctuations $S(\mathbf{k}, \omega)$. The evaluation of the dynamical form factor requires the solution of equations of motion for the density fluctuations in the plasma.

In this project we have developed a theoretical framework, which combines calculations of $S(\mathbf{k}, \omega)$ with hydrodynamic evolution of laser-produced plasmas and accounts for experimental resolutions of measuring devices. Our theory leads to accurate predictions for the TS cross-section, which after comparison with experimentally measured scattered power has elucidated new kinetic processes in high-Z gold plasmas. Studies of high-Z plasmas improve our understanding of radiative properties of hot dense matter and find many applications in inertial confinement fusion, laboratory astrophysics or x-ray lasers.

The phase space fluctuation density, i.e. the quantity from which all other macroscopic fluctuating quantities are derived, obeys the exact linearization of the kinetic equations for the single particle distribution function. This observation has lead us to formulate a nonlocal hydrodynamic theory for $S(\mathbf{k}, \omega)$ [1], that is based on the solution to the linearized kinetic equation for the fluctuating quantities [2] that is not restricted by the usual validity conditions for hydrodynamics, namely small wavenumber and frequency. The resulting expression for $S(\mathbf{k}, \omega)$ is dependent on the frequency and wavenumber dependent ion viscosity and electron transport coefficients. This theory has been applied to the interpretation of TS data in gold plasmas [3]. In this experiment for the first time ion acoustic and Langmuir wave fluctuation spectra have been simultaneously observed. This allowed accurate measurements of plasma parameters and in particular an average ionization stage.

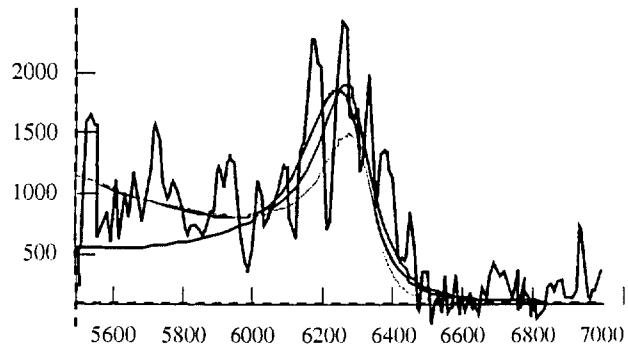


*Comparison between calculated TS spectra and experimental results [3] using different electron distribution functions.*

The Langmuir fluctuations have been measured at relatively large values of the wavenumber making the spectra very sensitive to the form of the electron distribution function (EDF). In addition, the Thomson probe has reached high intensity values giving values for the parameter $Z(v_o/v_e)^2$ up to four ($v_0$ is the electron quiver velocity, $v_e$ stands for the thermal velocity). Under such conditions the EDF assumes a non-Maxwellian form [4]. The comparisons with the measured Langmuir wave spectrum resulted in the first "almost" direct observation of the non-Maxwellian features of the EDF. However, in addition to super-Gaussian [4] form at low electron velocities we have observed Maxwellian-like tails of superthermal electrons in the EDF.

## References

[1] J. Myatt, W. Rozmus, V. Yu. Bychenkov, and V.T. Tikhonchuk, *Thomson Scattering from Ion Acoustic Waves in Laser Plasmas*, **Phys. Rev. E, 57**, 3383, (1998).

[2] V. Yu. Bychenkov, W. Rozmus, V.T. Tikhonchuk, and A.V. Brantov, *Nonlocal Electron Transport in a Plasma*, **Phys. Rev. Lett., 75**, 4405 (1995).

[3] S.H. Glenzer, W. Rozmus, B.J. MacGowan, K.G. Estabrook, J.D. De Groot, G.B. Zimmerman, H.A. Baldis, B.A. Hammel, J.A. Harte, R.W. Lee, E.A. Williams and B.G. Wilson, *Thomson Scattering From High-Z Laser-produced Plasmas*, **Phys. Rev. Lett., 82**, 97, (1999).

[4] A.B. Langdon, **Phys. Rev. Lett.**, **44**, 575 (1980).

## Contact Information

Wojciech Rozmus
Phone: (780) 492-2375
E-mail: rozmus@space.ualberta.ca

PROJECTS

# Compton Scattering

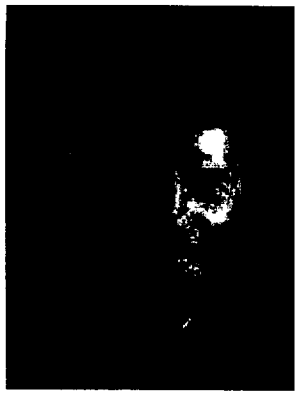


Frederic Hartemann, Principal Investigator, UC Davis

***Co PI:***

*Hector Baldis – LLNL and UC Davis*

***Collaborator:***

*Neville Luhmann, Jr., Jonathan Heritage – UC Davis*

*Bernard Rupp – LLNL and University of Vienna*

*Claudio Pellegrini – UC Los Angeles*

*Arthur Kerman – Massachusetts Institute of Technology*

***Students:***

*Eric Landahl, David Gibson, Anthony Troha, Fabian Strong, James Van Meter – UC Davis*

*Arnold Le Foll – Ecole Polytechnique, France*


The central theme of our research program is the detailed theoretical and experimental study of the interaction of relativistic electrons and coherent photon fields in vacuum. Electrons are the lightest of the charged leptons and they are point-like particles, which means that they have no internal structure. Photons are the quanta of the electromagnetic field; a laser pulse is a good example of a coherent photon field: its spectrum (color content) is well-defined, and a simple mathematical expression encapsulates all of its characteristics. Despite its apparent simplicity, this field of research contains a wealth of exciting phenomena: ultra-high-intensity laser pulses can coherently accelerate electrons in vacuum with very high gradients (which means that the electrons gain a lot of energy, thousands of volts, over a short distance, measured in microns); the same laser pulses can also be used in a collision with the relativistic electrons to produce amazing x-ray flashes by Compton scattering. One of the most exciting applications of our research is x-ray protein crystallography, which has provided, together with recombinant DNA technology, a new paradigm for drug design and synthesis

*Fred, Fabian, Anthony, Devon and Elson*

## Recent Publications


F.V. Hartemann, E.C. Landahl, D.J. Gibson, A.L. Troha, J.R. Van Meter, J.P. Heritage, H.A. Baldis, N.C. Luhmann, Jr., C.H. Ho, T.T. Yang, M.J. Horhy, J.Y. Hwang, W.K. Lau, and M.S. Yeh, *RF Characterization of a Tunable, High-Gradient, X-Band Photoinjector*, **IEEE Trans. Plasma Phys. 28**, 898 (2000).

F.V. Hartemann, H.A. Baldis, R.R. Freeman, A.K. Kerman, et al., *The Chirped-pulse Inverse Free-electron Laser: A High-gradient Vacuum Laser Accelerator*, **Physics of Plasmas, 6,** 4104 (1999).

A.L. Troha, J.R. Van Meter, E.C. Landahl, R.M. Alvis, et al., *Vacuum Electron Acceleration by Coherent Dipole Radiation*, **Physical Review E, 60,** 926 (1999).

F.V. Hartemann, J.R. Van Meter, A.L. Troha, E.C. Landahl, et al., *Three-dimensional Relativistic Electron Scattering in an Ultrahigh-intensity Laser Focus*, **Physical Review E, 58,** 5001 (1998).


## Affiliated Institutes

UC Davis; Stanford Linear Accelerator Center (SLAC); Massachusetts Institute of Technology (MIT); UC Los Angeles

Remarkable advances in ultrashort pulse laser technology based on chirped-pulse amplification, and the recent development of high-brightness, relativistic electron sources allow the design of novel, compact, monochromatic, tunable, femtosecond x-ray sources using Compton scattering. Such new light sources are expected to have a major impact in a number of important fields of research, including the study of fast structural dynamics, advanced biomedical imaging, and x-ray protein crystallography; however, the quality of both the electron and laser beams is of paramount importance in achieving the peak and average x-ray spectral brightness required for such applications. Therefore, one of the primary purposes of our work is to establish a theoretical formalism capable of fully describing the three-dimensional nature of the interaction, as well as the influence of the electron and laser beam phase-space topologies upon the x-ray spectral brightness. This is the first detailed analysis of its kind; furthermore, the new radiation theorem that is demonstrated and used in this work is of a general nature, and is hoped to represent a useful contribution to the field of classical electrodynamics; finally, new analytical expressions of the x-ray spectral brightness including the effects of emittance and energy spread are obtained in the one-dimensional limit.

The aforementioned technical breakthroughs in the fields of solid-state lasers and high-brightness electron accelerators provide a unique opportunity to develop an entirely new class of advanced x-ray sources, with characteristics approaching those of third-generation light sources, in a much more compact and inexpensive package. This, in turn, offers the possibility of an important spin-off of ultra-short pulse laser technology into the field of molecular biology, which is currently growing at an exponential rate: following the completion of the Human Genome Project, the systematic study of protein structure and function is expected to dominate biophysics in the first half of the 21st Century. In addition, a new paradigm for rational drug design has now emerged, using both recombinant DNA technology and x-ray protein crystallography. New classes of drugs, as recently exemplified by the development of HIV protease inhibitors, successfully reduced the viral load of AIDS patients below the detection threshold of enzyme-linked immuno-sorbent assays.

In protein crystallography, recombinant DNA technology is used to produce large quantities of a given protein by splicing the corresponding coding DNA sequence into the genetic material of a bacterium. The transfected bacteria are cultivated and upon induction overexpress large quantities of the selected protein, which is then isolated, purified, and crystallized. Diffraction data are routinely collected at LN2 temperature, and the experimental phase measurements necessary for the reconstruction of the electron density are primarily determined by the multi-wavelength anomalous diffraction (MAD) method. Finally, a molecular model of the structure is built into the reconstructed three-dimensional electron density map.

The key characteristics of an x-ray source useful for protein crystallography are its small size, low angular divergence, good transverse coherence, and high average spectral brightness. In turn, these requirements determine the necessary electron and laser beam quality; this forms one of the main lines of research performed by our group. We are planning to start an important research program in 2001, where a compact, high-quality, integrated electron linac will be used in conjunction with a tabletop terawatt laser to produce high-brightness x-ray flashes at a repetition rate of 10 Hz. This system will demonstrate proof-of-principle Compton x-ray generation, and will also allow the detailed benchmarking of our three-dimensional x-ray code; scalability to higher repetition rates will also be an important component of this program. Prospective graduate students interested by our research are strongly encouraged to contact the P.I., or one of the contact persons.

## References

F.V. Hartemann, H.A. Baldis, R.R. Freeman, A.K. Kerman, et al., *The Chirped-pulse Inverse Free-electron Laser: A High-gradient Vacuum Laser Accelerator,* **Physics of Plasmas, 6,** 4104 (1999).

A.L. Troha, J.R. Van Meter, E.C. Landahl, R.M. Alvis, et al., *Vacuum Electron Acceleration by Coherent Dipole Radiation,* **Physical Review E, 60,** 926 (1999).

F.V. Hartemann, J.R. Van Meter, A.L. Troha, E.C. Landahl, et al., *Three-dimensional Relativistic Electron Scattering in an Ultrahigh-intensity Laser Focus,* **Physical Review E, 58,** 5001 (1998).

## Contact Information

Frederic V. Hartemann
Ph: (925) 423- 3398
Email: hartemann1@llnl.gov

# X-Ray Protein Crystallography and Compton Source Development

Frederic Hartemann, Principal Investigator, LLNL

*Co PIs:*
*Bernard Rupp - LLNL*
*Hector Baldis – LLNL and UC Davis*

ILSA is currently developing a unique, monochromatic, tunable, 1 Å x-ray microfocus source based on Compton scattering between a high-brightness, relativistic electron beam and a terawatt-class, femtosecond laser pulse produced by chirped-pulse amplification (CPA). LLNL has applied for a patent describing a particular configuration, capable of generating x-ray flashes with extremely high average brightness, and called the ReFLEX (Ring Femtosecond Laser-Electron X-ray) source concept.

## Motivation

One extremely important application identified and targeted for the 1 Å Compton x-ray source is protein crystallography, where recombinant DNA technology can be used to produce large quantities of a given protein by introducing the corresponding coding DNA sequence into the genetic material of a bacterium. Overexpression of large quantities of the protein is induced, and the protein is extracted and purified. Single crystals of the protein are grown in solution, and diffraction data (intensities of lattice reflections) are collected at cryogenic temperatures to minimize radiation damage. To reconstruct the three-dimensional electron density of the molecule by Fourier methods, two terms per reflection are needed: the structure factor amplitudes, which are readily measured as the square root of the reflection intensities, and the phase angle for each reflection, which is not directly obtainable from protein data (the "phase problem" in crystallography). The most powerful method to solve the phase problem is MAD phasing, where experimental phase information is obtained from dispersive differences between and anomalous (Bijvoet) differences within data sets collected at different wavelengths around the absorption edge of anomalously scattering atoms introduced into the protein.

This approach, first demonstrated at dedicated synchrotron beamlines, has proven extremely successful, for example, to provide the structural information crucial for the ab initio design of inhibitor molecules targeting specific binding sites on proteins such as the HIV protease, thus providing a paradigm for systematic drug design and development. As synchrotrons are large and expensive facilities, our goal is to develop compact, tunable, x-ray sources with nearly comparable characteristics at a fraction of the cost. Laser-driven Compton scattering allows one to use much lower electron beam energies (tens of MeV's instead of GeV's), while retaining the tunability distinguishing synchrotrons from conventional x-ray sources. The combination of a tabletop,

## Recent Publications

F.V. Hartemann, H.A. Baldis, A.K. Kerman, A. Le Foll, N.C. Luhmann, Jr., and B. Rupp, *Three-Dimensional Theory Of Emittance In Compton Scattering and X-Ray Protein Crystallography*, Physical Review E, **64**, 016501 (2001).

F. V. Hartemann, *Stochastic Electron Gas Theory Of Coherence In Laser-Driven Synchrotron Radiation*, Physical Review E, **61**, 1 (2000).

J. R. Van Meter, A. K. Kerman, P. Chen, and F. V. Hartemann, *Radiative Corrections In Symmetrized Classical Electrodynamics*, Physical Review E, 62, 6 (2000).

## Affiliated Institutes

University of California, Los Angeles; Massachusetts Institute of Technology; Columbia University

terawatt-class laser with an integrated, high-brightness, relativistic photoelectron source will result in such a compact x-ray source.

In recent years, molecular biology has yielded tremendous advances in our understanding of the basic mechanisms underlying the biology of multi-cellular organisms, as exemplified by the Human Genome Project and the emergence of recombinant DNA technology. These advances have resulted in novel approaches to the systematic diagnosis and treatment of an broad range of illnesses: for example, a detailed understanding of the expression of proto-oncogenes might lead to highly efficient new strategies to fight cancer. With the HGP nearing full completion, the attention of the biomedical research community is rapidly shifting to the fundamental problem of protein structure and function, or structural genomics. We also note that in FY 1998, the R&D budget of the pharmaceutical industry reached $21B, 82% of which was spent domestically. Finally, the understanding of the causes of cancer at the molecular level is one of the top research priorities set by the National Institutes of Health (NIH).

Within this context, x-ray protein crystallography is one of the foremost tools to study the three-dimensional structure of proteins. As recently demonstrated by the development of HIV protease inhibitors, x-ray protein crystallography is a key enabling technology for rational drug design and development.

## What are Proteins?

Proteins are highly structured and complex polymers of L-amino (left-handed) acids, linked together by peptide bonds. Three-dimensional, structured proteins are produced from their linear DNA templates in a complex transcription and subsequent ribosomal translation process. The importance of structural knowledge cannot be overemphasized as the molecular structure of proteins determines an extremely wide variety of functions: enzymes catalyze biochemical reactions; membrane receptor proteins signal to the cell interior when a ligand binds; transport and storage proteins, such as hemoglobin and ferritin, distribute metal ions or chemicals throughout the body; structural proteins, including collagen and keratin, and muscle fibers, such as actin and myosin, play an important role in the architecture of multi-cellular organisms; nutritional proteins provide amino acids for growth (e.g. casein and ovalbumin); antibody proteins are essential components of the immune system; finally, regulatory proteins such as transcription factors, bind to and modulate the transcription of DNA. Human DNA contains approximately 3 x 109 base pairs, which are estimated to code for over one hundred thousand different proteins.

## HIV Protease Inhibitors: A New Paradigm for Structure-Based Drug Design

One of the most dramatic illustrations of the power of x-ray protein crystallography and MAD is the recent development of completely new classes of anti-viral drugs, as exemplified by HIV protease inhibitors. The recent development of such powerful anti-viral drugs to fight HIV has demonstrated the efficiency of x-ray protein crystallography as a powerful tool to help design new drugs ab initio, in sharp contrast with the previous trial-and-error approach. For example, the first generation of anti-HIV drugs include such molecules as AZT (azidothymidine), a molecule analogous to the nucleoside thymidine; the reverse transcriptase enzyme of the virus is thus misled into using AZT instead of thymidine, which is normally paired with adenosine on the RNA chain to be transcribed. However, because of its relatively poor specificity, AZT also inhibits the cellular polymerase of mitochondria, which produce adenosine tri-phosphate (ATP); this explains the serious side effects of this drug, including severe muscle fatigue and anemia. 36 Similarly, other reverse transcriptase inhibitors have been synthesized and administered to AIDS patients, including ddI (a precursor to ddA, an analogue to deoxyadenosine), and ddC (an analogue to deoxycytosine); both are toxic, causing neurological problems, including polyneuritis. More recently, equally active and somewhat less toxic drugs have been introduced, such as 3TC, an analogue of cytosine, d4T, an analogue of thymidine, and non-nucleoside analogues, such as TIBO inhibitors. Combining such drugs, at lower doses, helps minimize the aforementioned side effects; however, the most dramatic improvements have been obtained after the HIV protease structure has been determined by x-ray crystallography: with the knowledge of atomic details within the catalytic site of the HIV protease, a novel family of small molecular drugs, called protease inhibitors, has been designed and synthesized ab initio, with high specificity to the aspartyl binding sites of the HIV protease. These new drugs have been very successful, especially when used in conjunction with the aforementioned reverse transcriptase and integrase inhibitors (the so-called "triple therapy"), in reducing the viral load in some patients below the detection threshold of enzyme-linked immuno-sorbent assays.

## X-Ray Protein Crystallography and Compton Source Development

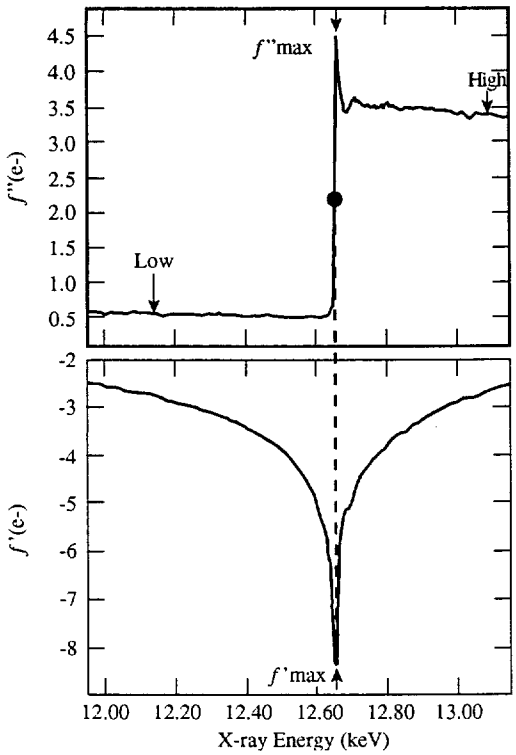


*Figure 1. Selenium K-edge.*

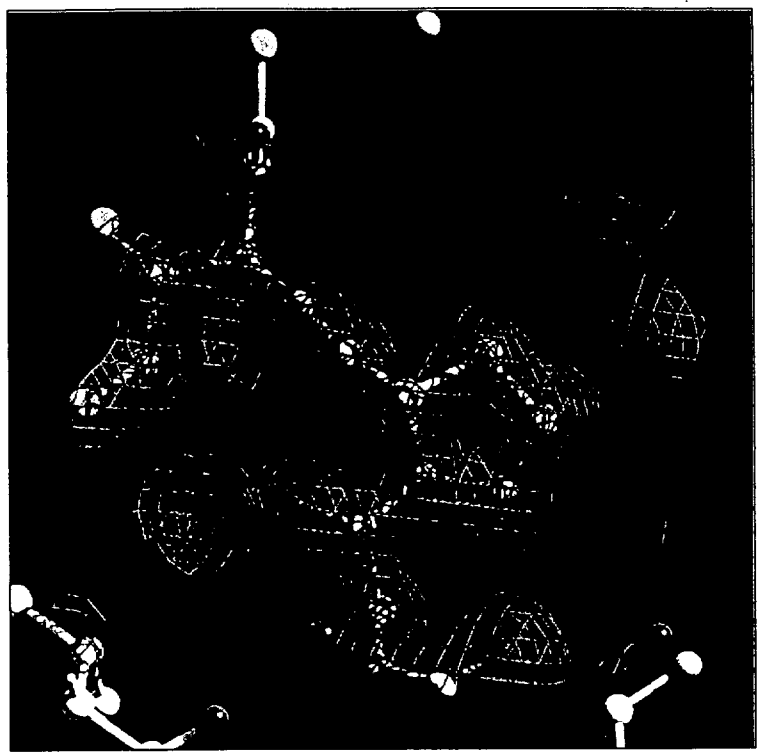

*Figure 2: Example of atomic-resolution, three-dimensional electron density map obtained using MAD phasing. A chemical model is also shown for illustration.*

### How Does MAD (Multi-Wavelength Anomalous Diffraction) Work?

The basic elements behind MAD phasing are presented below; here, we note that before the introduction of MAD, the isomorphous replacement method was successfully used to obtain the structure of complex proteins; for example urease was studied by Jabri et al., with 40 heavy atom compounds screened to find five sufficiently isomorphous derivatives of the crystal: $HOHgC_6H_4CO_2Na$, $EuCl_2$, $Hg_2(CH_3COO)_2$, $C(HgOOCCH_3)_4$, and $(CH_3)_3Pb(CH_3COO)$. This example indicates the level of complexity and uncertainty involved in the search for multiple isomorphous heavy metal derivatives, and why MAD has quickly become the preferred method for phase determination for complex macromolecular crystals, as explained above.

One of the key challenges in protein crystallography is the determination of the phase of the diffracted waves, which is determined by the absolute spatial position of each diffracting atom in the lattice. The electron density in the crystallized protein is obtained by performing the Fourier summation:

$$\rho(x,y,z)=\frac{1}{V}\sum_{h=-\infty}^{+\infty}\sum_{k=-\infty}^{+\infty}\sum_{l=-\infty}^{+\infty}\left|F(h,k,l)\right|\exp$$

$$\left\{-2\pi i\left[hx+ky+lz-\varphi(h,k,l)\right]\right\},$$

where $|F(h,k,l)|$ is the structure factor amplitude of reflection $(h,k,l)$, including the temperature factor, and $\varphi(h,k,l)$ (is the phase angle to be determined. The X-ray detector measures the diffracted intensity, $I(h,k,l)\propto|F(h,k,l)|^2$; therefore, additional information is required to determine the phase, in order to perform the three dimensional Fourier summation in the equation above.

In the case where a crystal contains anomalous scatters (either as heavy atoms soaked into the protein crystals or introduced into the protein as Se-Methionine), one can exploit the differences in intensity between Bijvoet pairs within a data set, and dispersive differences between data sets recorded at different wavelengths, to determine the

reflection phase angles. In MAD, the strong wavelength dependence of the anomalous scattering around an x-ray absorption edge is used: typical spectral widths for well-defined K or L-edges are of the order of a few eV. The wavelengths must be correspondingly carefully chosen to optimize the anomalous and dispersive signal (see Figure 1). Many high-Z elements, which can be incorporated into proteins, give rise to sufficiently strong anomalous signals. Hendrickson showed that the presence of a single Se atom in a protein of up to approximately 150 amino acid residues is sufficient to determine phases via MAD. A single heavy atom like Au or Hg can have the power to phase 300 or more residues. Several anomalous scatterers present in a single crystal allow the phase determination of correspondingly larger structures. The results of a MAD phasing experiments are presented in Figure 2, where the electron density map is shown with atomic precision.

## The μMAD Concept

A unique characteristic of the Compton source is the very small size of the x-ray source, which essentially matches that of the laser focal spot size; for imaging applications, this translates into increased contrast and better resolution. This also has important implications for micro-crystals, which are more easily produced and often are of better quality (i.e., diffracting to higher resolution with smaller mosaicity), than larger ones. Cooling also becomes less problematic in smaller crystals due to the lower amount of heat generated and the more advantageous surface to volume ratios. Therefore, the Compton x-ray source seems almost ideally suited for the development of a compact, user-friendly, tunable x-ray source, with an average brightness comparing well with that of rotating anode sources, and the capability of using MAD on micro-crystals; this is the idea underlying the micro-MAD (μMAD) concept currrently being evaluated at LLNL.

## References

http://www-structure.llnl.gov/
http://www-structure.llnl.gov TB Structural Genomics Consortium
http://www.doe-mbi.ucla.edu/TB
http://www.doe-mbi.ucla.edu/TB EU Mirror
http://www.ccp14.ac.uk/ccp/web-mirrors/llnl.rupp/
http://www.ccp14.ac.uk/ccp/web-mirrors/llnlripp/

## Contact Information

Frederic V. Hartemann
Ph: (925) 423- 3398
Email: hartemann1@llnl.gov

Bernard Rupp
Ph: (925) 423-3273
Email: br@llnl.gov

PROJECTS

# Inverse Free Electron Laser


Frederic Hartemann, Principal Investigator, UC Davis

***Co PI:***
*Hector Baldis – LLNL and UC Davis*

***Collaborators:***
*Neville Luhmann, Jr. – UC Davis*
*Arthur Kerman – Massachussetts Institute of Technology*

***Students:***
*Eric Landahl, David Gibson, Anthony Troha, James R. Van Meter – UC Davis*


Our group has proposed a new accelerating concept, the chirped-pulse inverse free-electron laser (CPIFEL). We are studying the inverse free-electron laser (IFEL) interaction both theoretically and computationally in the case where the drive-laser intensity approaches the relativistic regime, and the pulse duration is only a few optical cycles long. The IFEL concept has already been experimentally demonstrated as a viable vacuum laser acceleration process; we have shown that by using an ultra-short, ultra-high-intensity drive laser pulse, the IFEL interaction bandwidth and accelerating gradient are increased considerably, thus yielding large energy gains. Using a chirped pulse and negative dispersion focusing optics will allow us to take further advantage of the laser optical bandwidth and produce a chromatic line focus maximizing the gradient. The combination of these novel ideas results in a compact vacuum laser accelerator capable of accelerating picosecond electron bunches with a high gradient (GeV/m) and very low energy spread.

## Recent Publications


F.V. Hartemann, A.L. Troha, H.A. Baldis, A. Gupta, A.K. Kerman, E.C. Landahl, N.C. Luhmann, Jr., and J.R. Van Meter, *High-Intensity Scattering Processes of Relativistic Electrons in Vacuum and Their Relevance to High-Energy Astrophysics*, **The Astrophysical Journal Supplement Series, 127,** 347 (2000).

F.V. Hartemann, *Stochastic Electron Gas Theory of Coherence in Laser-driven Synchrotron Radiation*, 972 (2000).

F.V. Hartemann, H.A. Baldis, R.R. Freeman, A.K. Kerman, et al., *The Chirped-pulse Inverse Free-electron Laser: A High-gradient Vacuum Laser Accelerator*, **Physics of Plasmas, 6,** 4104 (1999).

A.L. Troha, J.R. Van Meter, E.C. Landahl, R.M. Alvis, et al., *Vacuum Electron Acceleration by Coherent Dipole Radiation*, **Physical Review E, 60,** 926 (1999).

F.V. Hartemann, J.R. Van Meter, A.L. Troha, E.C. Landahl, et al., *Three-dimensional Relativistic Electron Scattering in an Ultrahigh-intensity Laser Focus*, **Physical Review E, 58,** 5001 (1998).

F.V. Hartemann, *High-intensity Scattering Processes of Relativistic Electrons in Vacuum*, **Physics of Plasmas, 5,** 2037 (1998).


## Affiliated Institutes

UC Davis; Stanford Linear Accelerator Center (SLAC); Massachusetts Institute of Technology (MIT), and UC Los Angeles

## Inverse Free Electron Laser

The inverse free-electron laser (IFEL) interaction has been proposed as a viable vacuum laser acceleration process. IFEL acceleration was first demonstrated experimentally at Columbia University, followed by experiments at Brookhaven National Laboratory (BNL) using a nanosecond-duration, gigawatt (GW) $CO_2$ laser. The IFEL is attractive for laser acceleration because the interaction occurs in a vacuum, away from boundary conditions, thus allowing for a relatively large interaction region; since a plasma is not employed as the accelerating medium, this resolves a number of potential problems, including plasma instabilities, nonlinear laser propagation, shot-to-shot reproducibility of the plasma, and the extremely small accelerating potential well, or "bucket", which characterizes laser-plasma acceleration schemes. Also, the IFEL wiggler is suitable to provide good focusing and electron-beam optics and transport, thus offering the potential for producing the high-quality electron beams required for advanced light sources, biomedical applications, and the Next Linear Collider.

However, one of the fundamental limitations of this acceleration scheme is the dephasing of the trapped electron with respect to the drive-laser wave: As the electron energy increases, the free-electron laser (FEL) resonance condition can no longer be maintained, and the electron reaches a maximum energy given by the FEL interaction bandwidth. This problem can be solved in two different ways: either the wiggler period and/or amplitude can be tapered, as successfully demonstrated in a high-efficiency FEL, or, equivalently, the drive laser pulse can be chirped. Up to now, IFEL gradients have been comparable to those possible with high-frequency rf systems (roughly up to 100 MeV/m). By contrast, the main focus of our work is the preliminary theoretical and computational study of the IFEL interaction in a different regime, where we consider ultra-short, TW-class drive laser pulses which are now routinely generated by tabletop systems using chirped pulse amplification (CPA). For such femtosecond (fs) laser pulses, the IFEL interaction bandwidth is considerably wider than in the case of lower-intensity drive pulses with durations in the picosecond to nanosecond range: Basically, the FEL resonance condition indicates that when the electron slips over one laser optical cycle, it also propagates over one wiggler period; thus, for femtosecond pulses, the wiggler interaction region is extremely short, and the IFEL resonance bandwidth is correspondingly wide. This directly translates into the fact that the electron energy can now vary significantly before the IFEL interaction detunes and saturates; additionally, the ultra-high laser pulse intensity yields a high accelerating gradient. Thus, the IFEL interaction physics is expected to change dramatically for broadband (femtosecond) drive laser pulses near the so-called "relativistic intensity regime" ($>10^{17}$ W/cm$^2$ for optical wavelengths).

We have determined how the use of a chirped laser pulse allows the FEL resonance condition to be maintained beyond the conventional dephasing limit, thus further improving the electron energy gain. It has also been shown that the ultra-short, high-intensity laser pulses generated by the CPA technique make it possible to design an IFEL with very high accelerating gradients (>1 GeV/m), in contrast with the longer pulse approaches previously considered.

Another practical limitation of IFEL accelerators is the diffraction of the drive laser pulse. This can be alleviated by taking advantage of the ultra-wide optical bandwidth of the chirped laser pulse: Negative dispersion focusing optics can be used to produce a chromatic line focus, where long wavelengths are focused first, while the shorter wavelengths required to maintain the FEL resonance condition at higher energies are focused further along the interaction region. We have demonstrated numerically that the accelerating IFEL bucket is very wide compared to plasma-based laser acceleration schemes: For a 1 ps FWHM (full width at half-maximum) Gaussian electron bunch, and a 1 cm period wiggler, the IFEL energy spread is <0.9%. This is extremely advantageous for a practical laser accelerator, as the device could be driven by a conventional rf photoinjector. Prospective graduate students interested by our research are strongly encouraged to contact the P.I., or one of the contact persons

### Contact Information

Frederic V. Hartemann
Ph: (925) 423- 3398
Email: hartemann1@llnl.gov

PROJECTS

# Plasma Focusing of 30 GeV Electrons


Pisin Chen, Principal Investigator, Stanford Linear Accelerator Center

***Co PI's:***
*Hector A. Baldis – LLNL and UC Davis; Dave Cline – UC Los Angeles*

***Collaborators:***

*J.S.T. Ng*
*W. Craddock, F.J. Decker*
*R.C. Field, R. Iverson*
*F. King, R.E. Kirby*
*T. Kotseroglou, P. Raimondi*
*D. Walz – SLAC*
*P. Bolton – LLNL*
*Y. Fukui, V. Kumar – UCLA*
*C. Crawford, R. Noble – FNAL*
*K. Nakajima – KEK*
*A. Ogata – Hiroshima University*
*A.W. Weidemann – University of Tennessee*


The plasma lens was proposed as a final focusing mechanism to achieve high luminosity for future high energy linear colliders [1]. Previous experiments to test this concept were carried out with low energy density electron beams [2]. Recently, the E-150 collaboration working at the Stanford Linear Accelerator Center has obtained data on plasma focusing of high energy density electron and, for the first time, positron beams.

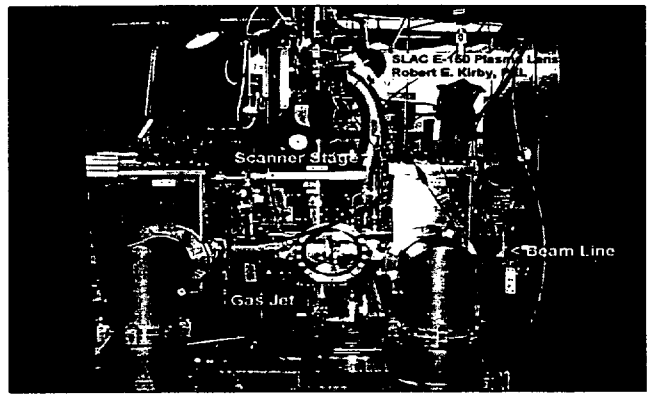


*Plasma chamber installed in the Final Focus Test Beam line.*

## Recent Publications


J.S.T. Ng, et al., *Proceedings of the 9th Workshop on Advanced Accelerator Concepts*, Santa Fe, NM, June 2000, P.Colestock ed.

J.S.T. Ng, et al., *Proceedings of the 20th International Linac Conference*, Monterey, CA, August 2000, A.Chao ed.


## Affiliated Institutes

UC Davis; Fermi National Accelerator Laboratory; Hiroshima University; KEK National Laboratory for High Energy Physics; Lawrence Berkeley National Laboratory; Lawrence Livermore National Laboratory; Stanford Linear Accelerator Center; University of California at Los Angeles; University of Southern California; University of Tennessee

# Plasma Focusing of 30 GeV Electrons

The experiment was carried out at the SLAC Final Focus Test Beam facility (FFTB). The nominal positron beam energy was 30 GeV, with 1.5E10 positrons per beam pulse. The plasma lens was produced by laser and beam ionization of a neutral nitrogen gas-jet injected into the plasma chamber by a fast-pulsing nozzle. The beam size was measured using a carbon fiber wire scanner system.

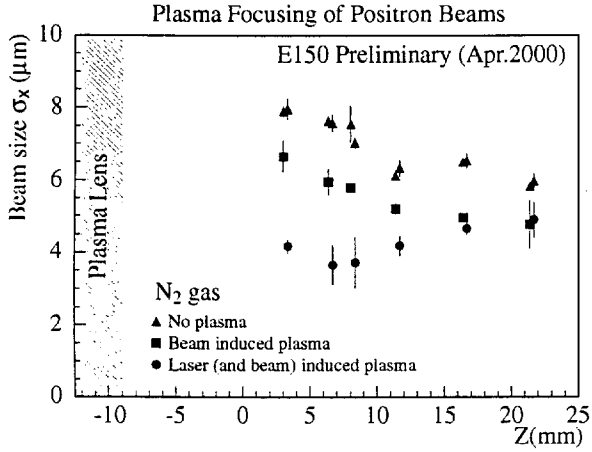


*Plasma focusing of positron beams*

The results for laser (and beam) ionization plasma focusing of positron beams are shown in the figure.The measured transverse beam size is shown as a function of the distance (Z) between the wire scanner and the plasma lens. The axis of the gas-jet is at Z = -10.5 mm. The beam envelope is shown converging without plasma focusing (triangle points); while with laser (and beam) induced plasma focusing (filled circles), the beam envelope is shown converging towards a reduced waist and then diverging because of the strong focusing. Focusing is also observed for beam-induced plasma with the laser turned off.

## References

[1] P. Chen, Part. Accel., vol. 20, 171 (1987)

[2] J.B. Rosenzweig, et al., **Phys. Fluids B, 2,** 1376 (1990); H. Nakanishi, et al., **Phys. Rev. Lett, 66,** 1870 (1991); G. Hairapetian, et al., **Phys. Rev. Lett. 72,** 2403 (1994); R. Govil, et al., **Phys. Rev. Lett, 83,** 3202 (1999).

## Contact Information

Pisin Chen
Phone (650) 926-3384
*Email:* chen@SLAC.Stanford.edu

Hector A. Baldis
Ph: (925) 422-0101
Email: baldis1@llnl.gov

PROJECTS

# Development of Picosecond X-ray Laser Sources

James Dunn, Principal Investigator, LLNL

***Co PI's:***

*Joseph Nilsen, Albert Osterheld – LLNL*

*Vyacheslav Shlyaptsev – UC Davis*

***Collaborators:***

*Anatoly Faenov – VNIIFTRI, Mendeleevo, Russia*

*Tania Pikuz; Henryk Fiedorowicz, Andrzej Bartnik – Institute of Optoelectronics, Military University of Technology, Poland*

***Post Doc:***

*Yuelin Li – LLNL*

We are exploring the use of tabletop picosecond lasers as compact drivers for short wavelength collisional excitation x-ray lasers. The gain medium for amplifying the x-ray laser is produced from a highly ionized plasma column created by focusing a 600 ps laser beam onto a polished metal target. The population inversion is generated by the rapid heating of this plasma with a second, high intensity ~1 ps pulse. This two step process allows higher efficiency and higher repetition rate x-ray lasers using low ~5 J laser driver energies.

By optimizing the plasma conditions, x-ray lasers in the 11.9 – 32.6 nm wavelength range have been generated from Ni-like and Ne-like closed-shell ions. We have recently achieved optimum extraction efficiency by driving these x-ray lasers into saturation. Various characterization experiments to measure the gain region inside the plasma and study the effect of line focus uniformity have been successfully completed. Initial studies are also underway to investigate the use of gas puff targets to create more uniform and efficient x-ray lasers at shorter wavelengths. Several applications using the x-ray laser beam are being planned for the near future including the study of material properties and the characterization of high density plasmas.

*Yuelin Li aligns x-ray laser target in COMET laser target chamber*

## Recent Publications

J. Dunn, Y.Li, A.L. Osterheld, J. Nilsen, J.R. Hunter, and V.N. Shlyaptsev, *Gain Saturation Regime For Laser-Driven Tabletop, Transient Ni-like Ion X-ray Lasers*, **Phys. Rev. Lett. 84**, 4834 (2000).

J. Nilsen, J. Dunn, A.L. Osterheld, and Y. Li, *Lasing on the Self Photopumped Ni-like $4f\,^1P_1 - 4d\,^1P_1$ X-ray Transition*, **Phys. Rev. A 60**, R2677 (1999).

J. Dunn, J. Nilsen, A.L. Osterheld, Y. Li, and V.N. Shlyaptsev, *Demonstration of Transient Gain X-ray Lasers Near 20 nm for Nickellike Y, Zr, Nb, and Mo*, **Opt. Lett. 24**, 101 (1999).

J. Dunn, A.L. Osterheld, Y. Li, J. Nilsen, and V.N. Shlyaptsev, *Transient Collisional Excitation Lasers with 1-ps Tabletop Drivers*, in Short Wavelength Lasers and Applications, ed. J.G. Eden and J.J. Rocca, **IEEE Journal of Selected Topics in Quantum Electronics 5(6)**, 1441 (1999).

J. Dunn, A.L. Osterheld, R. Shepherd, W.E. White, V.N. Shlyaptsev, and R.E. Stewart, *Demonstration of X-ray Amplification in Transient Gain Nickel-like Palladium Scheme*, **Phys. Rev. Lett. 80** (13), 2825 (1998).

Y. Li, J. Nilsen, J.Dunn, A.L. Osterheld, A. Ryabtsev, and S. Churilov, *Wavelengths of the Ni-like $4d\,^1S_0 - 4p\,^1P_1$ X-ray Laser Line*, **Phys. Rev. A 58**, R2668 (1998).

## Affiliated Institutes

UC Davis; VNIIFTRI, Mendeleevo, Russia; Institute of Optoelectronics, Military University of Technology, Poland

# Development of Picosecond X-ray Laser Source

Gain saturation is the desired operating regime for x-ray lasers if the maximum extraction efficiency of energy from the plasma gain medium is to be attained. The main challenge to improving x-ray lasers has been taking a tabletop scheme and succesfully driving it into saturation. Towards this goal, substantial improvement has been made in the reduction of the laser drive energy required to generate the inversion by collisional excitation. The pre-pulse technique, proposed by Nilsen [1], has achieved gain saturation when using 75 ps pulses with 30 to 150 J energy on various Ni-like 4d $\rightarrow$ 4p J=0 $\rightarrow$ 1 transitions from 140 Å to 59 Å for Ag and Dy in the last 3 years [2, 3].

Progress towards a tabletop x-ray laser has advanced in parallel because the advantages of reduced size, low cost and high repetition rate are important for future development of applications. The fast capillary discharge plasma operating at 469 Å for Ne-like Ar has been shown to achieve gain saturation [4]. The transient collisional excitation scheme has been proposed by Shlyaptsev and demonstrated experimentally on Ne-like Ti at 326 Å for laser-driven tabletop schemes [5]. This utilizes two laser pulses where a ns pulse generates the plasma and creates the required Ne-like or Ni-like ionization conditions. After a delay to allow for plasma cooling and expansion which is desirable for both optimum pumping and ray propagation along the plasma column, a 1 ps laser pulse generates a transient population inversion. This fast heating timescale allows efficient pumping without perturbing the ionization. Very high x-ray laser gains greater than 100 $cm^{-1}$ are predicted and so saturation for target lengths of less than 1 cm is possible.

The experiments were performed on the Compact Multipulse Terawatt (COMET) laser system at LLNL. This laser, operating at 1054 nm wavelength, utilizes the technique of CPA to produce two beams of nominally 500 fs and 600 ps (FWHM) pulse duration with a repetition rate of 1 shot/4 minutes. The short pulse was lengthened to 1.2 ps with 5 J energy while the long pulse energy was typically less than 2 J. The peak-to-peak delay between the laser pulses was 700 ps with the short pulse arriving after the long pulse. The line focus length of 1.1 cm was achieved with a cylindrical lens and an on-axis paraboloid. The on axis x-ray laser output was observed with a 1200 line $mm^{-1}$ variable-spaced flat-field grating spectrometer with a back-thinned 1024 × 1024 charge-coupled device (CCD). Filters giving attenuation between 10 – 30 × were used to prevent the x-ray laser saturating the CCD. A major change from our previous x-ray laser campaigns [6] was to introduce a traveling wave scheme to mitigate against the reduced amplification at longer target lengths. This effect results from the short-lived transient gain lifetime. A simple reflection echelon technique was adopted consisting of five flat mirror segments placed before the focusing optics. Each segment was offset by 0.12 cm to introduce a traveling wave towards the spectrometer with a delay of 7.7 ps per step. This matches the 1 ps laser excitation to the propagation of the x-ray laser in the gain region. For non-traveling wave excitation the reflection echelon was replaced with a flat mirror.

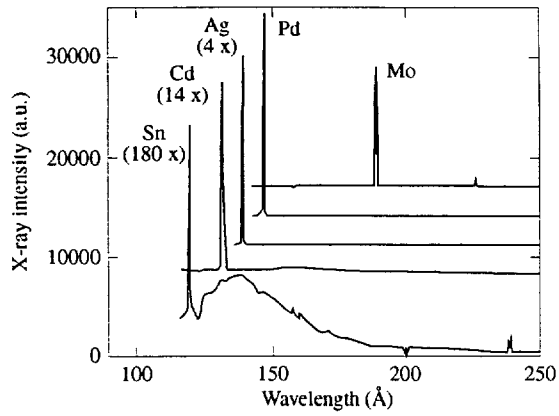


*Figure 1. Single shot spectra from the Ni-like ion sequence from Mo to Sn*

Figure 1 shows the spectra of Ni-like ion sequence for 0.9 cm targets of Mo, Pd, Ag, Cd and Sn irradiated with the two laser pulses pulse with the traveling wave optic. The 4d $\rightarrow$ 4p x-ray laser transitions are dominant in each spectrum with the highest intensity observed for the 188.9 Å, 146.8 Å and 138.9 Å lines of Mo, Pd, and Ag, respectively. Our recent gain measurements for Mo together with spatial imaging of the gain region indicate that the gain length product is 16.8 ± 0.6 and that the laser intensity is several times above the saturation regime. Overall, the Pd x-ray laser has the highest intensity.

Figure 2 shows the intensity versus length of the Pd x-ray laser with and without the traveling wave. Nominal energy in the line focus is 2 J in 600 ps and 5 J in 1.2 ps. The small signal gain is determined to be 41 $cm^{-1}$ using the Linford formula. The laser output smoothly increases to achieve an overall gain length product of 18.1. With no traveling wave, the x-ray laser output flattens out for targets above 0.4 cm. In contrast the traveling wave data shows continued increase in output to between 20 to 100 times higher at 0.9 cm. Our analysis using the RADEX simulation code concludes that the rolloff in the x-ray laser output without the traveling wave excitation is determined primarily by the short transient gain lifetime in the plasma

# Development of Picosecond X-ray Laser Source

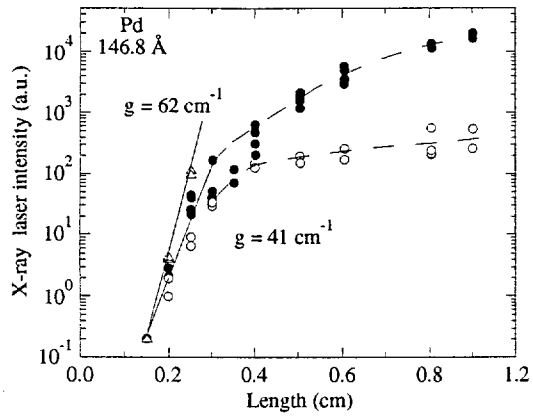


*Figure 2. Intensity versus length plot for Ni-like Pd 4d → 4p x-ray laser line.*

column and secondly by refraction issues related to density gradients. The transient gain lifetime was estimated to have an exponential decay constant of ~ 7 ps which corresponds to 0.2 cm photon transit path. The traveling wave excitation scheme substantially reduces the transient gain effect hence leaving plasma refraction as the most important effect.

The predicted saturation intensity $L_{sat}$ of the Pd x-ray laser line is estimated to be $3.7 \times 10^9$ W cm$^{-2}$. The experimental 146 Å Pd x-ray laser intensity, $I_{exp}$, can be also estimated. The output energy was determined to be 12 μJ. The gain region of 80 μm × 50 μm and x-ray laser pulse duration of ~7 ps, estimated from previous analysis yield an experimental Pd x-ray laser intensity of $I_{exp} = 4 \pm 2 \times 10^{10}$ W cm$^{-2}$ which is ~10 times higher than $I_{sat}$. Due to high small-signal gain the laser output is still increasing nonlinearly with length at the longest targets while the laser is operating in the saturation regime. The output is smoothly increasing at a continually decreasing rate and it should be possible to extract more energy with a few additional millimeters of target under the present irradiation conditions or by driving the plasma harder. More significantly, this demonstrates the strong robustness of this concept where driving table-top x-ray lasers into sub -100 Å wavelength range will be of primary importance in the future.

## References

[1] J. Nilsen et al., **Phys. Rev. A 48,** 4682 (1993).

[2] J. Zhang et al., **Phys. Rev. Lett. 78**(20), 3856 (1997); R. Smith, et al., **Phys. Rev. A 59,** R47 (1999).

[3] R. Tommasini, F. Löwenthal, and J.E. Balmer, **Phys. Rev. A 59**, 1577 (1999).

[4] J.J. Rocca, et al., **Phys. Rev. Lett. 77,** 1476 (1996); B.R. Benware, et al., ibid. 81, 5804 (1998).

[5] V.N. Shlyaptsev, et al., **Proc. SPIE Int. Soc. Opt. Eng. 2012,** 111 (1993); P.V. Nickles, et al., **Phys. Rev. Lett. 78**, 2748 (1997).

[6] J. Dunn, et al., **Phys. Rev. Lett. 80,** 2825 (1998).

## Contact Information

Jim Dunn
Ph: (925) 423-1557
Email: dunn6@llnl.gov

# Inner Shell X-ray Laser Development

Luiz Da Silva, Principal Investigator, LLNL

***Co PI's:***
*Peter Celliers, Franz Weber, James Dunn, Joseph Nilsen – LLNL*

***Students:***
*Nicholas Matlis – University of Texas at Austin*
*Tommy Ao – University of British Columbia*

Historically, x-ray lasers have been produced with large and expensive multi-kilojoule laser systems significantly limiting their availability for research and applications. The goal of this project is to develop the next generation of soft x-ray lasers that can achieve high brightness at short wavelengths yet require small table top optical pumping lasers. In order, to achieve this we have focused on the development of an inner-shell x-ray laser. This scheme uses x-rays produced by an ultrashort pulse (<50 fs) optical laser to produce K-shell vacancies and inversion in a low density carbon foam. Although yet to be demonstrated, inner-shell x-ray lasers have the potential for improved efficiency and can be scaled to very short wavelengths. We have designed the target and hope in the near future to perform the first experiments to demonstrate an inner-shell carbon x-ray laser operating at 45 Å.

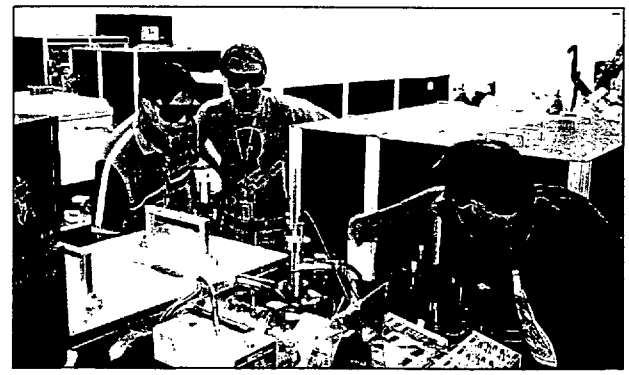

*Franz Weber (LLNL) and graduate students Nicholas Matlis (UT Austin) and Tommy Ao (UBC) aligning an interferometer used in the inner-shell XRL experiment on the Falcon Laser*

## Recent Publications

K. Takahashi, R. Kodama, K.A. Tanaka, H. Hashimoto, Y. Kato, K. Mima, F.A. Weber, T.W. Barbee Jr., L.B. Da Silva, *Laser-Hole Boring Into Overdense Plasmas Measured with Soft X-ray Laser Probing*, **Phys. Rev. Lett. 84**, 2405 (2000).

R. Kodama, K. Takahashi, K.A. Tanaka, Y. Kato, K. Murai, F. Weber, T.W. Barbee Jr., L.B. Da Silva, *Measurements of Las[illegible]-hole Boring Into Overdense Plasmas Using X-ray Laser Refractometry*, **Rev. Sci. Instrum. 70**, 543 (1999).

A.S. Wan, T.W. Barbee Jr., R. Cauble, P. Celliers, L.B. Da Silva, J.C. Moreno, P.W. Rambo, G.F. Stone, J.E. Trebes, and F. Weber, *A Soft X-Ray Laser Interferogram of a High-Density Colliding*, Plasma **IEEE Transactions on Plasma Science, 27**, 120 (1999).

## Affiliated Institutes

Colorado State University; ILE, Osaka University, Japan; University of Texas at Austin; University of British Columbia

## Inner Shell X-ray Laser Development

A long standing goal of laboratory x-ray laser research is the realization of x-ray lasers working at wavelengths close to or even below the water window (26-44 Å) with a table-top energy source. Although a number of table-top sized schemes have been recently demonstrated, they work at wavelengths beyond 100 Å and are difficult to scale to shorter wavelengths. In this project we have adopted an alternative approach to short wavelength x-ray lasers, which is the inner-shell photo-ionization (ISPI) scheme. The laser transition is pumped by an incoherent x-ray source. Using carbon for the lasant material as an example, the underlying concept is based on the fact that the photo-ionization cross section is much larger for the tightly bound inner shell electrons (i.e., the 1s electrons) than for the more loosely bound outer shell electrons (i.e., the 2p and 2s electrons). This requires photon energies at least high enough to photo-ionize the K-shell, ~286 eV, in the case of carbon. As a consequence of the higher cross section, the inner-shell are "selectively" knocked out, leaving a hole state $1s2s^22p^2$ in the singly charged carbon ion. This generates a population inversion to the radiatively connected state $1s^22s^22p$ in $C^+$, leading to gain on the 1s-2p transition at 45 Å. The resonant character of the lasing transition in the single ionization state intrinsically allows much higher quantum efficiency.

Competing processes that deplete the population inversion include auto-ionization, Auger decay, and in particular collisional ionization of the outer-shell electrons by electrons generated during photo-ionization. These competing processes rapidly quench the gain. Consequently, the pump method must be capable of populating the inversion at a rate faster than the competing processes. This can be achieved by an ultra-fast, high intensity laser that is able to generate an ultra-fast, bright x-ray source. Our calculations to date indicate that for the C 2p-1s lasing transition an ultra-fast x-ray burst (on the order of 40 fs) is needed to generate gain of ~10 $cm^{-1}$ with a duration of 50 fs. Although the basic concept of the ISPI laser was proposed over 30 years ago by Duguay and Rentzepis, it has never been demonstrated because the necessary pumping sources have not been available. With the advent of advanced chirped-pulse amplification techniques we now have available ultrashort pulse lasers with the necessary pulse width and energy. The Falcon laser at LLNL is one such laser.

During the past year we optimized the x-ray converter/filter assembly to maximize the x-ray output above the carbon K absorption edge (286 eV). The converter comprises a layer of 200 Å of gold on top of 1 kÅ of titanium. The ionization velocity in the absorber material ensures that the thin gold layer is completely ionized at the end of the ~ 40 fs optical pump pulse. The realized x-ray source is incoherent and insensitive to heating of the filter material. Other advantages of this target design include the lack of toxic constituent materials and a simple and inexpensive fabrication process. The thin titanium filter prevents soft x-rays from ionizing L-shell electrons in the carbon lasant.

Using an x-ray spectrometer and CCD we measured the time integrated x-ray flux as a function of laser intensity. At a laser intensity of $6.9 \times 10^{17}$ W/$cm^2$ the conversion efficiency into useful x-rays that radiate through the filter and have enough energy to ionize the K-shell was $10^{-4}$. In order, to be able to pump a 2 mm long gain medium will require a 2-5J laser, this is three orders of magnitude lower total energy than used to demonstrate the Ni-like Tantalum x-ray laser on the NOVA laser.

Before attempting a demonstration of an ISPI x-ray laser several challenges remain: making a time resolved measurement of the x-ray emission and producing an effective traveling wave pumping scheme. Time resolution of conventional x-ray diagnostics is insufficient to resolve a 40 fs rise time x-ray pulse. We are planning a series of experiments that will use optical reflectivity to probe the change in the carrier density induced in a thin diamond sample. By using an ultrashort probe we expect to achieve 20-30 fs temporal resolution of the x-ray emission. The second challenge that needs to be overcome is to develop an effective technique for producing a traveling wave pump. Traveling wave pumping requires that the optical laser generates x-rays along the x-ray laser axis synchronized to the propagation of the x-ray laser photons. This is necessary because the gain duration is expected to be 10-20 fs whereas the time for x-rays to travel 3 mm is 10 ps.

The successful demonstration of a table top inner-shell x-ray laser will not only validate our fundamental understanding of the atomic and plasma physics relevant in this regime, but also make available to a wide community a new and exciting x-ray source. Using the Falcon laser system at LLNL we hope within the coming year to perform the first ISPI x-ray laser tests.

Contact Information
Luiz Da Silva
Ph: (925) 423-9867
Email: dasilva1@llnl.gov

# Thomson Scattering with X-ray Lasers

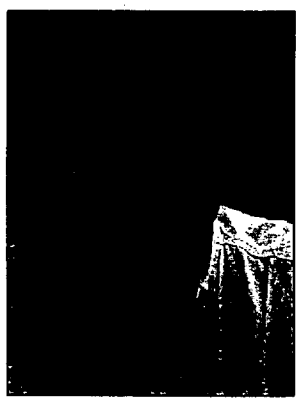

Hector A. Baldis, Principal Investigator, LLNL and UC Davis

***Co PI's:***
*W. Rozmus – University of Alberta*
*J. Dunn, M. Foord, R. Shepherd – LLNL*

***Student:***
*C. Andersen – UC Davis*

There has been much progress recently reported on laser-driven soft x-ray laser systems capable of producing megawatts of stimulated emission in the range of 100Å - 200Å from Ni-like collisional excitation schemes [1-2]. This opens the door to many exciting opportunities for many applications including microscopy, x-radiography, and for use in probing high-density plasmas [3] with lower energy x-ray laser pump sources. Longer wavelength lasers are typically employed for many plasma diagnostic applications such as interferometry, Thomson scattering (TS) and Faraday rotation, but are limited to lower densities, typically in the range 1020 – 1021 $cm^{-3}$ for visible-UV light. X-ray lasers therefore offer the exciting possibility of probing orders of magnitude higher densities than previously reached.

Thomson scattering from stable density fluctuations is a powerful diagnostic used to measure local plasma parameters, distribution functions and transport process [4]. In this work we demonstrate through calculations and theoretical analysis the first application of an existing x-ray laser for probing high-density plasmas. We find necessary conditions for the probe intensity, spectral resolution of the spectrometer and sensitivity of the scattered x-ray detection system for the measurement of electron temperature in short pulse laser-produced plasmas.

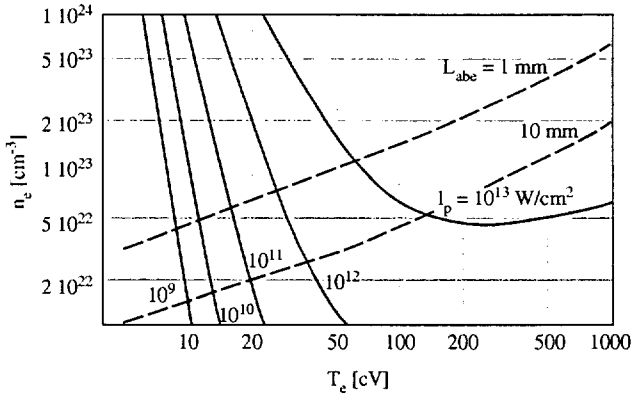


*The electron density vs temperature plane. The curves show threshold values of the Thomson probe at necessary to overcome thermal emission levels at the wavelength of the probe.*

## Recent Publications

H.A. Baldis, J. Dunn, M. Foord, W. Rozmus, C. Andersen, and R. Shepherd, *X-Ray Thomson Scattering: Towards Diagnostics for Solid Density Plasmas*, **Comments Plasma Phys. Contr. Fusion**, (in press) (2001).

## Affiliated Institutes

UC Davis; Theoretical Physics Institute, University of Alberta

# Thomson Scattering with X-ray Lasers

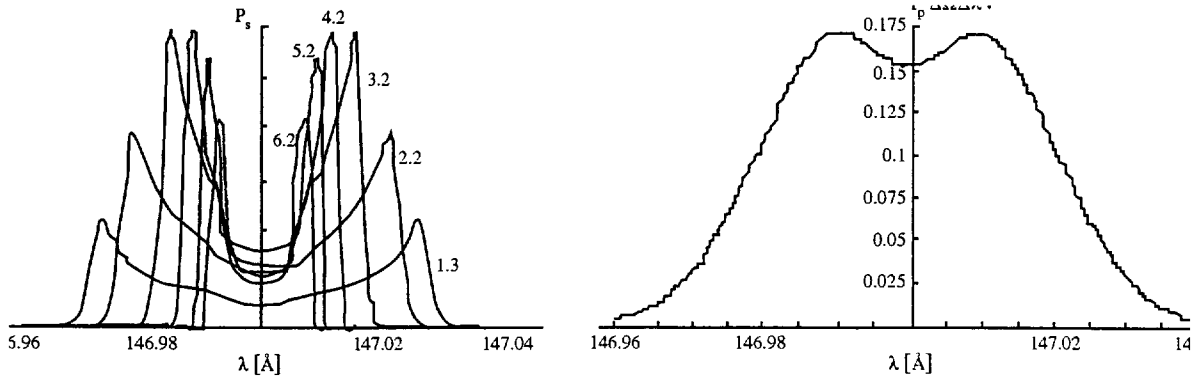


*(a) Thomson scattered power calculated at different moments in time (b) Time averaged Thomson scattered power convoluted with the instrumental width.*

We discuss the general application of Thomson Scattering (TS) as a probe of hot dense plasmas. Usually limiting the electron density $n_e$ to 0.1 of the critical density, $n_c$, eliminates refraction and strong absorption. For the x-ray laser wavelength of 147 Å, $n_c = 4.4\ 10^{24}\ cm^{-3}$. The goal of this discussion is to demonstrate the feasibility of such a measurement with an existing x-ray laser as well as to illustrate several general issues related to the applications of TS as plasma diagnostic at high particle densities. Furthermore, TS of the x-ray laser beam allow a direct insight into a dynamical electron density correlation function. The novelty of our study is in the examination of this function for plasma conditions previously inaccessible to TS experiments.

Consider a geometry of the measurement where θ is the angle between the direction of the probe propagation, along $k_0$ and the direction of the scattered light detection, parallel to k1. The angle θ defines the $k$-vector in a plasma, $k = |k_o - k_1|\ [k = 2k_o \sin(\phi/2)]$, of the spectral component of an electron density correlation function contributing to the TS cross-section. The probed $k$-vector and parameter $\alpha = 1/k\lambda_D$ define two regimes of the incoherent TS: collective for $\alpha > 1$, where the cross-section is dominated by electrostatic plasma mode resonance and single particle for $\alpha > 1$, where single particle distribution function defines form of the electron density correlation's. The range of plasma parameters in the planned experiment ($T_e$~50eV,$n_e \geq 10^{23}$ $cm^{-3}$) and the wavelength of the Thomson probe ($\lambda$ = 147 Å) lead to values of α larger than one ($\alpha > 1$) for all scattering angles θ, thus allowing us to limit the discussion to a case of the collective TS.

High electron density allows examination of the plasma response under conditions, which have been inaccessible in the past to the TS experiments. For example, conditions of the planned experiment lead to $k\lambda_{ei}$~0.11, where $\lambda_{ei}$ is the electron-ion mean-free-path. For this value of the wave-vector $k$, the dynamical form factor $S(k,\omega)$ [5] must be derived from the kinetic theory including weak collisional effects [6].

In view of the limited power output of the x-ray laser, it is important to first apply the TS cross-section in threshold calculations, where by comparison with plasma thermal emission levels we find the necessary intensity of the x-ray probe, $I_p$. For this threshold value of $I_p$ Thomson scattered signal equals to bremsstrahlung emission. Results of threshold calculations are displayed in the figure, showing several intensity curves on the plane of electron density and temperature. The relevant range of plasma parameters must be located above the threshold intensity curve.

## References

[1] J. Zhang, A.G. MacPhee, J. Nilsen, et al., **Phys. Rev. Lett. 78,** 3856 (1997).

[2] C.L.S. Lewis, R. Keenan, A.G. MacPhee, et al., **Proc. SPIE - Int. Soc. Opt. Eng. 3776,** 292 (1999).

[3] R. Cauble, L.B. Da Silva, T.W. Barbee, Jr., et al., **Phys. Rev. Lett. 74,** 3816 (1995).

[4] B. La Fontaine, H.A. Baldis, D. M. Villeneuve, et al., **Phys. Plasmas 1,** 2329 (1994).

[5] J. Sheffield, **Plasma Scattering of Electromagnetic Radiation** (New York, Academic, 1975).

[6] J.F. Myatt, W. Rozmus, V. Yu. Bychenkov, and V.T. Tikhonchuk, **Phys. Rev. E 57,** 3383 (1998).

[7] **Plasma Diagnostics Techniques,** R.H. Huddlestone and S.L. Leonard, editors, 627 (New York, Academic, 1965).

## Contact Information

Hector A. Baldis
Ph: (925) 422-0101
Email: baldis1@llnl.gov

# Theoretical Study of Table-top X-ray Lasers

Yvacheslav N. Shlyaptsev, Principal Investigator, UC Davis

***Co PI's:***
*Mark Eckart, James Dunn, Albert Osterheld, Art Toor – LLNL*
*Hector A. Baldis – LLNL and UC Davis*

The project we are working together with LLNL has been related to detailed modeling of a new kind of short wavelength laser and its applications.

Our recent theoretical and experimental investigations were accomplished with the building of table-top X-ray lasers, which are many-fold smaller and cheaper than those which were first developed at LLNL 15 years ago. Improved physical models of these lasers, obtained due to close interaction with the experiment, will represent the basis for efficient and compact X-ray lasers of the next generation and further shortening of generated wavelengths.

The second problem which we discovered theoretically and plan its realization experimentally, is related to new kinds of X-ray optics and other applications for free-electron laser light sources. The optical methods based on original plasma refracting lenses, and special configuration mirrors, promise to achieve very tight X-ray laser beam spots size and extremely high fluxes.

## Recent Publications

K.B. Fournier, D. Stutman, R. Vero, V. Soukhanovskii, M. Finkenthal, M.J. May, V.N. Shlyaptsev, W.H. Goldstein, *Measurement of Population Inversion For FUV Transitions in Kr-like Y IV In a High-Current Reflex Discharge*, **Physica Scripta**, 301, (2000).

M.C. Marconi, C.H. Moreno, J.J. Rocca, V.N. Shlyaptsev, A.L. Osterheld, *Dynamics of a Microcapillary Discharge Plasma Using a Soft X-ray Laser Backlighter*, **Physical Review E**, 7209 (2000).

J. Dunn, A. L. Osterheld, V. N. Shlyaptsev, *Demonstration of X-Ray Amplification in Transient Gain Nickel-like Palladium Scheme*, **Phys.Rev.Lett., 80**, 13, 2825 (1998).

J. Dunn, Y. Li, A.L. Osterheld, J. Nilsen, J.R. Hunter, and V.N. Shlyaptsev, *Gain Saturation Regime for Transient Ni-like Ion X-ray Lasers*, **Phys. Rev. Lett.** (in press).

P. Kalachnikov, P. V. Nickles, M. Schnurer, W. Sandner, V. N. Shlyaptsev, C. Danson, D. Neely, E. Wolfrum, J. Zhang, A. Behjat, A. Demir, G.J. Tallents, P.J. Warwick, and C.L.S. Lewis, *Saturated Operation of a Transient Collisional X-ray Laser*, **Phys.Rev.A, 57**, 5, 4378, (1998).

C.H. Moreno, M.C. Marconi, V.N. Shlyaptsev, B.R. Benware, C.D. Macchietto, J.J..A. Chilla, J.J. Rocca, and A.L. Osterheld, *Two-dimensional Near-field and Far-field Imaging of a Ne-like Ar Capillary Discharge Table-top Soft X-ray Laser*, **Phys Rev A**, (1998).

C. H. Moreno, M. C. Marconi, V. N. Shlyaptsev, and J. J. Rocca, *Shadowgrams of a Dense Micro-Capillary Plasma Obtained with a Table-top Soft X-ray Laser*, **IEEE Trans on Plasma Sci.**, (1998).

## Affiliated Institutes

UC Davis

# Theoretical Study of Table-top X-ray Lasers

## Gain Saturation on Tabletop Laser-Driven Ni-like Ion X-ray Lasers

The compact table-top X-ray lasers we have been working on are called transient collisional excitation X-ray lasers. These short pulse ~1-10 ps devices operate in 100-300 A region with the power comparable to generation Nova-based lasers. Due to its unique parameters, it was possible dramatically scale down laser size and cost. It currently occupies 1-2 optical tables.

In theory, the way this advanced type of lasers operate is based on selective excitation of highly charged ions with the speed exceeding interatomic times [1]. Since these times for high-Z ions are in picosecond and shorter range the new powerful short-pulse lasers, so-called Chirp-Pulse Amplification (CPA) lasers, are used to prepare the plasma. Preliminary calculations suggested incredible parameters not seen before in X-ray lasers.

Our goal consisted in creating detailed numerical models to understand the underlying physics of kinetics of ions under fast excitation, the hydrodynamics of plasma formation with short laser pulses and the amplification properties for prediction and reproduction of all data obtained in real experimental conditions. The numerical codes we successfully continued to develop allowed us to look inside of these plasma objects and reliably describe their behavior.

Transient collisional excitation X-ray lasers were reproduced in many laboratories in the world which actively continue working in this field.

These codes, which include magnetic hydrodynamics effects, were also successfully used for development in several other types of X-ray lasers based on electric current plasma formation. This work was done in collaboration with several groups in USA and abroad.

The problem that we started to investigate recently is related to development of applications for next generation light sources. The free-electron X-ray laser (called LINAC Coherent Light Source, LCLS) is based here on electron acceleration technique and whole experimental setup in this case is of course very large and expensive. But X-ray laser itself has extremely high brightness parameter and operates in 1.5 A range. Its power is so high that it is hard to transport and focus the output because most materials do not sustain the overheating.

Applying finding in X-ray lasers plasmas hydrodynamics based on electrical discharge in gas-filled tubes (called capillaries) we are considering to use the optical elements based on capillary plasma. Refractive medium here has been formed due to ablation of the wall material, heating of plasma with electric current and strong thermal conduction to the capillary walls. Because the medium in this case is relatively rear and already enough hot (plasma), it can easily sustain high X-ray fluxes. Focal spot size ~1000nm and high fluxes $10^{18}$-$10^{19}$ W/cm$^2$ are expected to achieve with this lens. Several other designs of X-ray optical elements also are under consideration which allow to achieve even shorter focal spot size of ~10 nm in diameter with enormous flux densities ~$10^{23}$ W/cm$^2$.

## Reference

[1] Y.V. Afanasiev and V.N. Shlyaptsev, *Formation of a Population Inversion of Transitions in Ne-like Ions in Steady-State and Transient Plasmas,* **Sov. J. Quant. Electronics, 19,** 1606 (1989).

Contact Information

V. Shlyaptsev
Ph: (925) 423-3456
Email: slava@llnl.gov

# Short-pulse Ultra-intense Laser Plasma Interactions

Pravesh Patel, Principal Investigator, LLNL

***Co PI's:***
*Dwight Price, Jim Bonlie, Frank Patterson, Andy Mackinnon, Paul Springer – LLNL*

The field of short-pulse ultra-high intensity laser interactions has seen an explosion in recent years in terms of both advances in laser technology and in our understanding of the physics of laser-plasma interactions and the plasma state. Critical to the growth of this field has been the continuous development of laser systems around the world capable of reaching ever-increasing focal intensities (the focal intensity of a laser is defined as the incident laser energy per unit time, per unit area at the laser focus). The largest strides in achieving increased intensities have been made through reducing the temporal length of the pulse; thus whilst a decade ago nanosecond ($10^{-9}$s) pulses were regarded as short, today laser systems with 30 femtoseconds ($30 \times 10^{-15}$s) pulses are relatively common. These pulse durations are fast approaching the duration of a single optical cycle of the laser light (1 μm wavelength light has an optical cycle of 3.3 femtoseconds). This rapid development in ultra-intense lasers has enabled experimenters to access hitherto unexplored extreme states of hot dense matter, and in doing so has created a wholly new field of relativistic laser-plasma interactions.

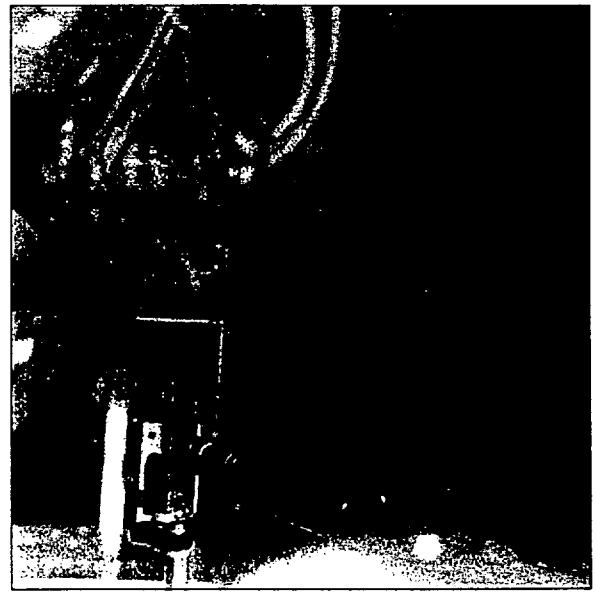

*Pravesh Patel aligning a target inside the interaction chamber.*

## Recent Publications

P.K. Patel, E. Wolfrum, O. Renner, A. Loveridge, R. Allott, D. Neely, S.J. Rose, and J.S. Wark, *X-ray Line Reabsorption In a Rapidly Expanding Plasma*, **Journal of Quantitative Spectroscopy and Radiative Transfer, 65,** 429 (2000).

M.E. Beer, P.K. Patel, S.J. Rose, and J.S. Wark, *Calculations of the Modal Photon Densities and Gain In a K/Cl Resonantly Photopumped X-ray Laser*, **Journal of Quantitative Spectroscopy and Radiative Transfer, 65,** 71 (2000).

P.K. Patel, *Initial Experiments on the JanUSP Laser at Focal Intensities* > $10^{21}$ *Wcm*$^{-2}$, **29th Annual Anomalous Absorption Conference,** Pacific Grove, June 13-18 1999.

## Affiliated Institutes

UC Davis

# Short-pulse Ultra-intense Laser Plasma Interactions

At LLNL we have recently completed the construction of a new 200 TeraWatt (1 TW = $10^{12}$ Watts), 100 femtosecond laser, the JanUSP laser, capable of producing a focussed intensity in excess of $10^{21}$ Watts/cm$^2$ – the highest recorded laser intensity in the world. At these light intensities the primary absorption mechanism, or process through which the laser interacts and transfers energy to a target material, is through direct acceleration of electrons by the electric field of the laser. Since the electric field of the laser is oscillating rapidly in time, the accelerated electrons describe an oscillatory motion in the direction of the electric field. The mean energy associated with this motion is termed the 'quiver energy' and it scales with the square root of the laser intensity. In the long pulse regime (typically pulselengths > 100 ps and intensities < $10^{16}$ Wcm$^{-2}$) this quiver energy is of the order of 10's of keV (NB. 1 keV of energy is equivalent to a temperature of 11.6 million degrees Celsius). However, in the picosecond and femtosecond regime far higher intensities can be attained. At an intensity of 5 x $10^{18}$ Wcm$^{-2}$ the quiver energy exceeds 511 keV (0.511 MeV) – the rest mass of the electron. This means that the electrons in the plasma are being accelerated to near relativistic velocities. At the peak intensity of the JanUSP laser the quiver energy is several MeV, and the electrons become highly relativistic. The resulting plasmas exhibit a wide range of interesting phenomena, many of which are traditionally home to the field of high energy particle physics such as strong gamma ray production, electron-positron pair creation, and photo- and particle-induced nuclear reactions.

Our initial experiments on the laser have focussed on characterising the high energy electron, gamma, ion production from the plasma. One of the techniques we employ is to utilize the fact that many of these particles have kinetic energies sufficient to induce nuclear reactions in the atoms with which they collide. Threshold energies for these reactions are typically in the above MeV range. An example is the (gamma, neutron) reaction in Au-197 (where 197 is the nuclear mass number). Its peak cross-section lies from approximately 12 to 16 MeV. On collision of the gamma ray with a Au-197 atom a neutron is emitted leaving behind a nucleus of Au-196. Au-196 is an unstable isotope with a half-life of six days and its decay to Pt-196 is easily measured. Hence, by measuring the number of decays in the sample and convolving with the cross-section for the reaction one can deduce the number of gamma rays between 12 and 16 MeV which must emitted from the plasma. Furthermore, since the primary mechanism for gamma production is through the bremsstrahlung emission of energetic electrons travelling through the solid target, one can infer the total number of electrons in the target with energies exceeding 12 MeV (since a single gamma ray of say 12 MeV can be produced by an electron with any energy greater than or equal to 12 MeV). Using this technique we have measured a conversion of several percent of the incident laser energy into relativistic multi-MeV electrons.

Recently we have used a similar method to measure the number and energy distribution of protons emitted from the target. This was done by placing a stack of 75 μm thick titanium foils behind the target. Protons having a minimum threshold energy of 4.8 MeV are able to induce (proton, neutron) reactions in atoms of Ti-48, converting the nuclei to V-48. Each foil in the stack acts both as a detector and as an energy degrader. For instance, a proton which penetrates the first 75 μm thick foil will lose a certain fraction of its initial energy in doing so (through multiple inelastic collisions with atoms in the foil). To induce a reaction of the type (proton, neutron) in the second foil the incident proton must still have a remaining kinetic energy of at least 4.8 MeV. The rate of energy loss is well-known and so we can calculate that to activate an atom in the second layer the proton would need to possess an initial energy of at least 6.4 MeV. Likewise, protons detected in further layers correspond to higher energies. This enables us to extract the energy distribution of the protons. These and other ongoing experiments are performed to help improve our basic understanding of the physics governing ultra-intense laser-plasma interactions.

## Contact Information

Pravesh Patel
Ph: (925) 423-7450
Email: patel9@llnl.gov

# Laser Astrophysics

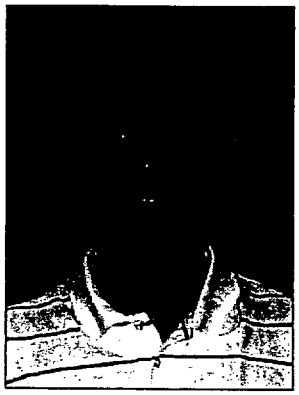

Jave Kane, Bruce Remington, Principal Investigators, LLNL

*Co PI's:*
*Dave Arnet – University of Arizona*
*Dick McCray – University of Colorado-Boulder*
*R. Paul Drake – University of Michigan*
*Edison Liang – Rice University*

The field of astrophysics contains spectacular displays of plasma physics. An impressive example is the recent supernova (SN) of 1987 in the Large Magellanic Cloud (SN1987A), a nearby galaxy at a distance of ~50 kpc. Hydrodynamic instabilities such as the Rayleigh-Taylor (RT) instability allowed the Ni-Co core to rapidly penetrate out to the surface, as illustrated in Fig. 1 from results of a two-dimensional (2D) simulation by Muller, Fryxell, and Arnett (Ref. 1). Fingers of denser He, C, and O (yellow) penetrate radially outwards through the surrounding lower density H envelope, while bubbles of the lower density H (dark blue-black) "rise" radially inward into the higher density core. Experiments on the Nova laser (Ref. 2) at Lawrence Livermore National Laboratory (LLNL) are being developed to examine the differences between RT growth in 2D (Ref. 3,4) versus 3D (Ref. 5) to address the limitation that supernovae are 3D, whereas exploding star simulations can only be done in 2D.

*Simulation of Core Mixing: Density distribution at a time of 3.6 hr. after the supernova explosion from a 2D simulation of the hydrodynamic mixing of SN 1987 A.*

## Recent Publications

K.S. Budil, B.A. Remington, D.M. Gold, K. Estabrook, R. Lerche, P. Bell, and J. Kane, *A Shock Breakout Diagnostic For The PetaWatt Laser System*, **Rev. Sci. Instrum, 70**, 806 (1999).

J. Kane, R.P. Drake, and B.A. Remington, *An Evaluation Of The Richtmyer-Meshkov Instability In Supernova Remnant Formation*, **Ap. J. 511**, 335 (1999).

J. Kane, D. Arnett, B.A. Remington, S.G. Glendinning, G. Bazan, R.P. Drake, and B.A. Fryxell, *Scaling Supernova Hydrodynamics To The Laboratory*, **Physics of Plasmas, 6**, 2065 (1999).

## Affiliated Institutes

University of Arizona; University of Colorado-Boulder; University of Michigan; Rice University

## Laser Astrophysics

The Center for Laboratory Astrophysics in ILSA is using the Omega laser at the University of Rochester to study hydrodynamics (the flow of gases or fluids) in supernovae (SNe). Supernovae, the explosion of massive stars, shape the evolution and chemical composition of our galaxy, solar system, and Earth. However, puzzling observations of radioactive material ejected from the famous SN 1987A suggest that large-scale hydrodynamic mixing of the star's material occurred during that explosion. Hydrodynamic mixing is similar in SNe and in laser fusion experiments to be done at the National Ignition Facility at LLNL, making SN experiments of interest to both LLNL workers and university astrophysicists.

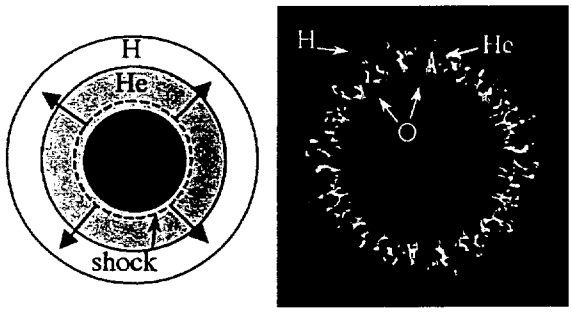


*Supernova explosion. Schematic of shock expanding through structure of initial star. Hydrodynamic mixing in computer simulation of SN 1987A using PROMETHEUS code.*

At left panel, the initial star has several layers of material: a very dense iron core (Fe), a less dense oxygen layer (O), a still less dense Helium layer (He), and a tenuous hydrogen envelope (H). In the explosion, a strong shock emerges from the core and expands outward through the star. Because the shock front is distorted by the misshapen core and by dense clumps in the O layer, it oscillates and can trigger hydrodynamic mixing as it crosses the O-He and He-H interfaces. The right panel shows such mixing, from a computer simulation of SN 1987A using the astrophysics code. At the O-He interface, 'spikes' of dense O penetrate well into the He layer, while 'bubbles' of the lighter He move into the O layer. Similar, spikes of He and bubbles of H appear at the He-H interface.

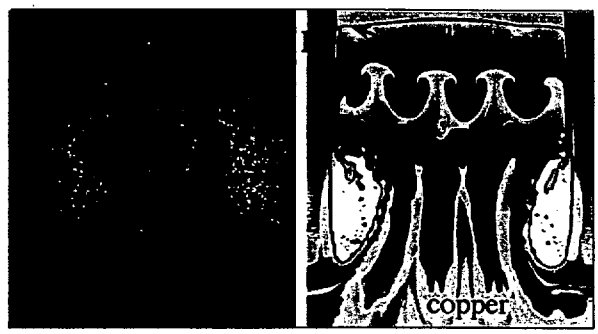


*Data and computer simulation using CALE code of an astrophysical hydrodynamics experiment at the Omega laser. Long fingers of dense Cu penetrate a less dense plastic layer, while shorter fingers of plastic penetrate a low-density foam layer.*

This figure shows results of the laser experiment at Omega. The left panel shows an x-ray photograph of the target after it was hit by the laser beams. The right panel shows a computer simulation of the experiment using the LLNL Code CALE. The target has three layers of material: dense copper (Cu), less dense plastic, and low-density foam. A beryllium shock tube (Be) encloses the target; it is transparent in the data but is shown in the simulation. The laser beams heat the Cu, sending a strong shock through the target from top to bottom in the data. The shock turns the target into hot star-like plasma and triggers hydrodynamic mixing at the copper-plastic and plastic-foam interfaces. The long dark fingers are spikes of Cu penetrating the plastic; the short gray fingers are spikes of plastic penetrating the foam. The plastic spikes line up with the plastic bubbles at the Cu-plastic interface and not with the Cu spikes. This happens by design because the shock crosses a carefully machined ripple at the Cu-plastic interface, making it oscillate once before hitting the plastic-foam interface where it imprints an 'inverted' ripple. The data produced clear evidence that an oscillating shock was present and that such shocks can produce significant hydrodynamic mixing in multiple-layer plasmas, a result of interest to fusion and SN researchers.

### Contact Information

Bruce Remington
Ph: (925) 423-2712
Email: remington2@llnl.gov

# High Energy Density Plasmas

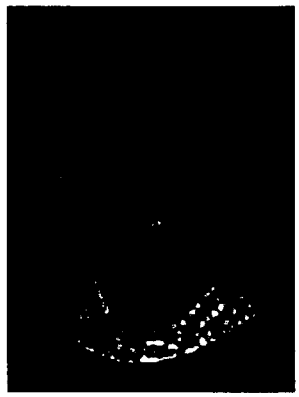

Richard Lee, Principal Investigator, LLNL

***Co PI's:***
*T. Missalla, J. K. Nash, C. A. Back, S. Libby – LLNL*
*L. Klein – Howard University*
*H. Nishimura, K. Fujita, H. Nagatomo – ILE Osaka, Japan*
*R. Mancini – University of Nevada, Reno*
*N. Woolsey – York University*
*A. Calisti, R. Stamm, B. Talin – Université de Provence*

The development of a set of stable implosions using indirectly driven plastic microspheres with argon (01.atm) doped deuterium (50 atm) has provided a unique test bed for testing the plasma spectroscopy of the high energy density imploded core. The core reaches electron densities of > $10^{24}$ $cm^{-3}$ with temperatures of ~ 1 keV and has been shown to be reproducible on a shot to shot basis. Moreover, we have shown that not only the peak temperature and density are consistent, but that the temporal evolution of the mean temperature and density of the final phase of the implosion is also reproducible. Therefore these imploding cores provide a unique opportunity to test aspects of plasma spectroscopy that are difficult to study in other plasmas. The ionization depression, the possible shift of energy levels, and the shape of the spectral features can all be studied. We will report on these investigations.

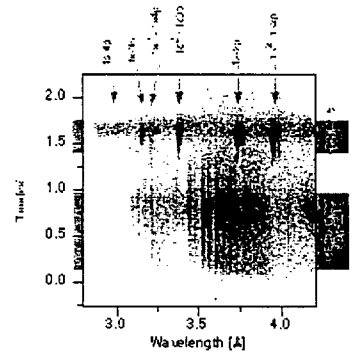


*The streak camera image of the emission from a Au hohlraum. The time increase upward and the spectra are dispersed in the horizontal direction. Note that the Ar emission occurs at a distinct time from the Au emission.*

## Recent Publications

L. Godbert-Mouret, T. Meftah, A. Calisti, R. Stamm, B. Talin, M. Gigosos, V. Cardenoso, S. Alexiou, R.W. Lee, and L. Klein, *Accuracy of Stark Broadening Calculations for Ionic Emitters*, **Phys. Rev. Lett, 81,** 5568 (1998).

N.C. Woolsey, B.A. Hammel, C.J. Keane, C.A. Back, J.C. Moreno, J.K. Nash, A. Calisti, C. Mose, R. Stamm, B. Talin, A. Asfaw, L.S. Klein, and R.W. Lee, *Competing Effects of Collisional Ionization and Radiative Cooling in Inertially Confined Plasmas*, **Phys. Rev. E, 57,** 4650 (1998).

N.C. Woolsey, B.A. Hammel, C.J. Keane, A. Asfaw, C.A. Back, J.C. Moreno, J.K. Nash, A. Calisti, C. Mosse, R. Stamm, B. Talin, L. Klein, and R.W. Lee, *Evolution of Electron Temperature and Electron Density in Indirectly Driven Spherical Implosions*, **Phys. Rev. E, 56,** 2314 (1997).

N.C. Woolsey, B.A. Hammel, C.J. Keane, C.A. Back, J.C. Moreno, J.K. Nash, A. Calisti, C. Mosse, L. Godbert, R. Stamm, B. Talin, C.F. Hooper, A. Asfaw, L.S. Klein, and R.W. Lee, *Spectroscopic Line Shape Measurements at High Densities*, **JQSRT, 58,** 975 (1997).

N.C. Woolsey, A. Asfaw, K.B. Hammel, C. Keane, C.A. Back, A. Calisti, C. Mosse, R. Stamm, B. Talin, J.S. Wark, R.W. Lee, and L. Klein, *Spectroscopy of Compressed High Energy Density Matter*, **Phys. Rev E 53,** 6396 (1996).

## Affiliated Institutes

Department of Physics and Astronomy, Howard University, Washington, DC 20059, USA; Institute of Laser Engineering, Osaka University 2-6 Yamada-oka, Suita, Osaka, 565-0871, Japan; Department of Physics, University of Nevada Reno, NV 89557, USA; Department of Physics, York University, York, England; PIIM, CNRS UMR 6633, Université de Provence, Centre St. Jérôme, Case232 13397 Marseille cedex 20, France

## High Energy Density Plasmas

In addition to the plasma spectroscopic observations it has been noted that there is the potential to go beyond the measurement of mean temperature and density measurement as a function of time, extending the techniques to a time dependent measure of the gradient in the emitting core. To achieve this one needs to work on the development of three aspects of the problem. First, we need to design and field a spectrometer that is capable of providing time resolved monochromatic images with spatial resolution. There are two unique solutions to this instrument development; one has a slit assembly on the target imaged with a crystal onto a streak camera, and the other is based on multiple crystals focusing images onto a gated MCP. Second, we need to develop an algorithmic approach in order to extract from the monochromatic images information on the temperature and density gradients. The difficulty resides in the fact that the images are directly related to the emissivity of the core not to the plasma parameters. To unfold the relationship we rely on the guidance of hydrodynamic simulations that have been coupled to radiation transport calculations and self consistently solved with the kinetics equations for the level populations of the argon ions. These calculations together with the hydrodynamics model provide the necessary information to develop the data reduction algorithms. Third, we need to ensure that the gradients are consistent with the observed spectra and for this purpose we required detailed line shape calculations. These calculations must include the standard effects of quasi-static ion and impact electrons broadening the bound-bound transitions of interest. However, these calculations must also be capable of bracketing the residual effects due to dynamic ions, quasi-static electrons, and effects due to double excited states.

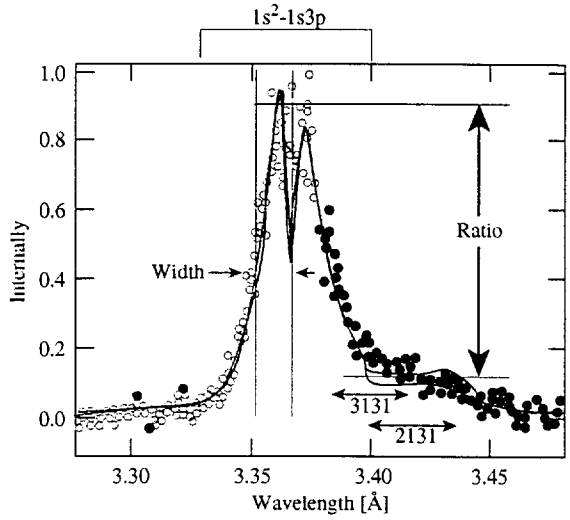


*A trace at one time along the wavelength axis through the Ar $1s^2$-$1s3p$ line profile can be matched to a calculation to determine the $n_e$ and $T_e$.*

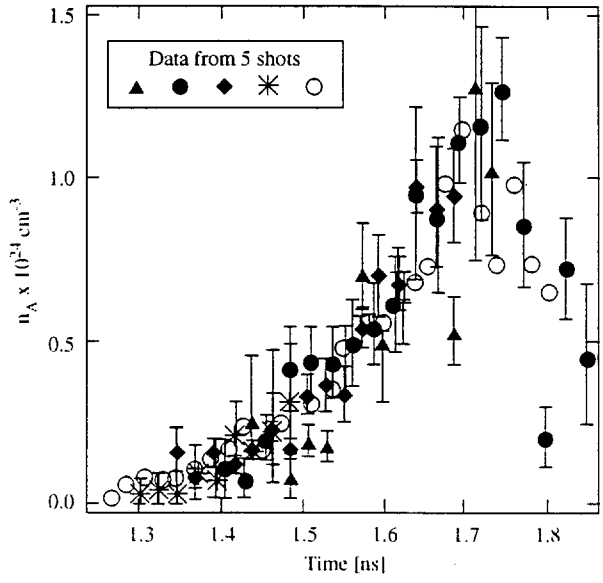


*The time history of $n_e$ determined from the line profile. Note the consistency of the data over several shots.*

Contact Information
R. W. Lee
Ph: (925) 422-7209
Email: dicklee@llnl.gov

# X-ray Studies of Laser Warmed Solids

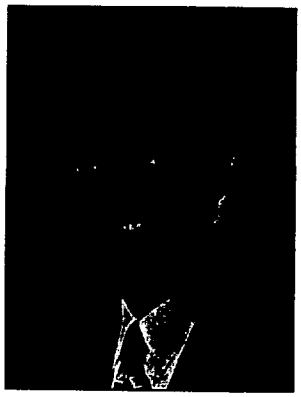

Roger Falcone, Principal Investigator, UC Berkeley

***Co PI:***
*Richard Lee, LLNL*

***Collaborator:***
*Phil Heimann, LBNL*

***PostDoc:***
*Inuk Kang*

***Graduate students:***
*Aaron Lindenberg, Steve Johnson*

We study dynamics of materials on the fundamental timescale of the vibrational period of atoms in a solid. Experiments involve the excitation of a solid by an ultrashort pulse laser, followed by a probe of x-ray radiation that is scattered or diffracted by atoms in the solid. The pattern of the scattered x-ray light and the absorption of x-ray radiation changes as materials change structure.

Our laser produces a 100 femtosecond duration pulse. Probe x-rays are produced at the Advanced Light Source Synchrotron at Lawrence Berkeley National Laboratory. Temporal resolution is determined by a novel high-speed x-ray detector, a streak camera that records changes on a picosecond time scale.

Experiments range from fundamental studies of non-equilibrium states of materials, to the measurement of properties of warm-dense-matter. We are particularly interested in the physics of matter that is too warm for conventional solid state physics models, and too cold for conventional plasma physics models.

*Roger Falcone (professor), Aaron Lindenberg (grad student), Steve Johnson (grad student), Inuk Kang (postdoc), Phil Heimann (LBNL Scientist).*

## Recent Publications

A. Lindenberg, et al, *Time Resolved X-Ray Diffraction from Coherent Phonons During a Laser-Induced Phase Transition*, **Phys. Rev. Lett. 84**, 111 (2000).

## Affiliated Institutes

University of California, Berkeley; Lawrence Berkeley National Laboratory; Lund Institute of Technology, Oxford University

# X-ray Studies of Laser Warmed Solids

Developments in time-resolved x-ray diffraction have led to the capability of directly observing structural phase transitions, the motion of complex molecules, and biological and chemical reactions, on picosecond time scales. We have recently observed x-ray diffraction from laser-induced coherent acoustic phonons at frequencies up to 0.1 THz. The results are in agreement with simulations based on dynamical diffraction theory, and consistent with an interpretation based on the excitation of coherent phonon states by a short pulse of laser light. For sufficiently high laser fluences, we observe a reversible, optically induced phase transition which develops on a time scale equal to one-half of a phonon period. We conclude that the approach to disorder (laser induced melting) is through the excitation of large-amplitude, coherent lattice motion.

The experimental setup includes a bending magnet beam line at the Advanced Light Source synchrotron, which produces light in a broad spectrum up to photon energies of 15 keV. A Si (111) monochromator crystal selects a single wavelength of 2.4 Å. The diffracted beam is then directed onto an InSb crystal. We use a titanium-sapphire–based, 150 fs, 1 kHz, 800 nm laser, synchronized to individual electron bunches within the synchrotron ring with jitter less than 5 ps. The laser is also incident on the InSb crystal and overlapped in both space and time with a single x-ray pulse. The time-resolved x-ray diffracted intensity following laser excitation is measured using the streak camera detector triggered by a GaAs photoconductive switch. A CCD camera records the x-ray streak projected onto a phosphor screen. The resulting temporal resolution of the camera is 3 ps.

The time history of the diffracted signal following laser excitation is measured at once. Coherent phonons are manifested as oscillatory signals in time-resolved x-ray diffraction, as shown below.

Impulsive excitation of a solid on a time scale shorter than the material's hydrodynamic response time generates coherent acoustic phonons across a range of wave vectors near the Brillouin zone center and peaked at a wave vector of order one inverse laser penetration depth. A phonon of wave vector q induces an extra time-dependent periodicity to the lattice. This gives rise to sidebands centered on the Bragg peak. In our experiment, since the phonons are coherently excited, the sidebands oscillate at the phonon frequency and we resolve this coherent time-dependent

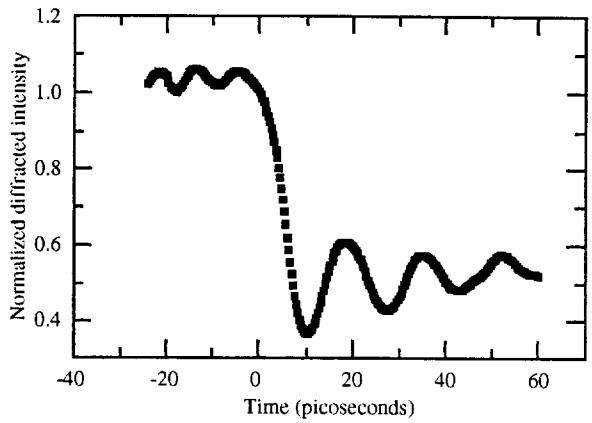


*Time history of the diffracted signal following laser excitation.*

atomic motion At these relatively low fluences, impulsive excitation of the solid induces small-amplitude, coherent atomic motion about equilibrium lattice positions.

Above a critical laser fluence of 13 mJ/cm2, the lattice no longer coherently oscillates about this equilibrium value, but instead is driven into a disordered state. This occurs on a time scale set by one-half of a phonon period, at which point the average atomic displacement is maximum for a given mode, in analogy with the Lindemann criterion. Since the diffracted x-ray intensity does not oscillate, this is indicative of a state for which atomic motion with long-range coherence does not exist. Loss of coherence on fast time scales is an indication of disorder on fast time scales. Since an observed 3 ps drop in the diffracted intensity occurs faster than the thermal coupling time, we conclude that the first step in the observed laser-induced disordering transition at high laser fluence is the initial excitation of hot carriers which subsequently drive large-amplitude, coherent vibrational motion, a transition essentially nonthermal in nature.

In conclusion, we have shown that time-resolved x-ray diffraction is a useful tool in phonon spectroscopy and a sensitive probe of electron-phonon coupling strengths. For low laser fluences we measure oscillations in the x-ray diffraction efficiency corresponding to coherent phonons at frequencies up to 0.1 THz. At higher fluences a reversible phase transition has been observed, driven by large amplitude, correlated atomic motion, the first step in the approach towards disorder.

Contact Information
Roger Falcone
Ph: (510) 642-8916
Email: rwf@physics.berkeley.edu

# Waveguide Lasers and Devices

Denise Krol, Principal Investigator, UC Davis

***Co PI's:***
*Eric Honea, Steve Payne, Subhash Risbud – LLNL*

***Students:***
*Falgun Patel – UC Davis Department of Applied Sciences, graduated*
*James Chan – UC Davis Department of Chemical Engineering and Material Sciences*
*Prissana Thamboon, UC Davis Department of Applied Sciences*

Our research program is involved with new lasers and optical devices that are based on waveguide technology. Such devices, which include waveguide lasers and amplifiers, Bragg gratings, and nonlinear optical switches, have applications in the communications, sensor and laser industry. For certain applications waveguide structures may be preferred over fibers because of their compactness and the ability to integrate different optical components such as splitters, couplers and laser amplifiers or signal sources on a single substrate.

We are working on rare-earth doped phosphate glasses, in which channel waveguides are fabricated using photolithography and electric-field assisted Ag ion diffusion. We have demonstrated a diode-pumped Nd-phosphate channel waveguide laser and are currently studying other lasant ions such as Yb.

We are also investigating the possible fabrication of other optical elements such as Bragg gratings or electro-optic modulators in these new waveguide materials. Our objective is to integrate these different functionalities into novel optical laser devices.

**Integrated Waveguide Device**

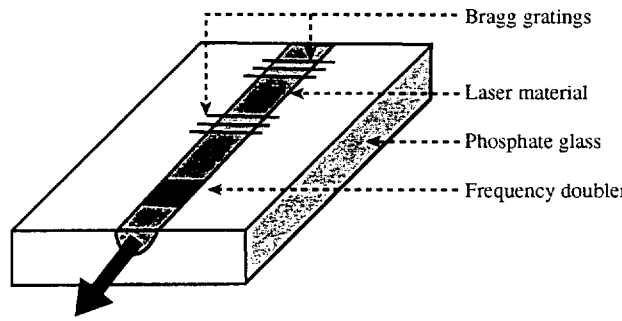


*Our integrated waveguide devices consist of laser material — rare earth-doped phosphate glasses, Bragg gratings as cavity mirrors, and frequency doubler via thermal poling*

## Recent Publications

R.R. Patel, H.E. Garrett, M.A. Emanuel, M.C. Larson, M.D. Pocha, D.M. Krol, R.J. Deri, and M.E. Lowry, *WDM Filter Modules In Compact, Low-Cost Plastic Packages For Byte-Wide Multimode Fibre Ribbon Cable Data Links*, **Electronics Lett. 35**, 840 (1999).

J.J. Adams, C. Bibeau, R.H. Page, D.M. Krol, L.H. Furu, S.A. Payne, *4.0-4.5- mu m Lasing of Fe:ZnSe Below 180 K, a New Mid-Infrared Laser Material*, **Optics Letters, 24,** 1720 (1999).

F. D. Patel, E.C. Honea, D. Krol, S.A. Payne, J.S. Hayden, *Waveguide Fabrication in $Nd^{3+}$ and $Yb^{3+}$ Doped Phosphate Glasses*, **OSA TOPS 19, Advanced Solid State Lasers,** Walter R. Bosenberg and Martin M. Fejer (eds.), 446 (1998).

F. D. Patel, E.C. Honea, D. Krol, S. A. Payne, J. S. Hayden, *$Nd^{3+}$ and $Yb^{3+}$ Doped Phosphate Glass Waveguides Fabricated Using Electric Field Assisted $Ag^{+}$ Diffusion*, **Proc. of the 18th International Congress on Glass,** July 5-10, 1998, San Francisco, CA.

## Affiliated Institutes

UC Davis

# Fabrication and Characterization of Optical Waveguides in $Nd^{3+}$ and $Yb^{3+}$ Phosphate Glasses for Applications in Waveguide Lasers.

## $Nd^{3+}$: Phosphate Glass Waveguide Laser

Fabrication of optical waveguides by ion exchange or ion diffusion in glasses is a mature technology [1-3]. A common method, employed in our experiments, is electric field assisted solid film diffusion, schematically shown in Figure 2.

The substrates used for our experiments were phosphate glasses obtained from Schott Glass Technologies, Inc. The glasses, designated IOG-1 (Integrated Optic Glass;1 for phosphate), were specifically designed for the ion exchange/diffusion process. The composition of the glass is devoid of refining agents typically added to optical glass to remove bubbles and to increase the durability of the glass. These refining agents are believed to be responsible for a redox interaction in which electrons are donated to $Ag^+$ ions, thus reducing them to metallic Ag colloids. These metal clusters serve as loss centers, increasing the loss of the waveguide by scattering and/or absorbing the guiding beam.

Systematic experiments were conducted to understand the process parameters of fabricating waveguides in $Nd^{3+}$ and $Yb^{3+}$ doped phosphate (IOG-1) glasses. The impact of the diffusion time, temperature, applied voltage, and post process annealing are reported [4, 5]. Planar waveguides were characterized by the prism coupling technique and the graded refractive index profile of our waveguides was best characterized by a gaussian.

Channel waveguides were fabricated with standard photolithography methods See Figures 2 and 3). The smallest waveguide had cross-sectional dimensions of ~ 28 x 9 $\mu m^2$. Laser performance of the $Nd^{3+}$ phosphate glass channel waveguides was studied for various size channels and for three different output coupler reflectivities. The resonator was set up in a Fabry-Perot configuration and loss values at the laser wavelength (1053 nm) were calculated

**I. Stripes pf Ag are created by a photolithographic process**

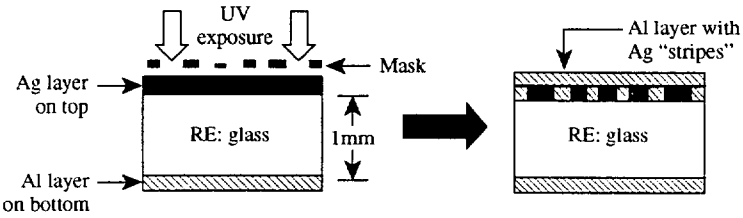


**II. Electric field assisted $Ag^+$ diffusion to form channel waveguides**

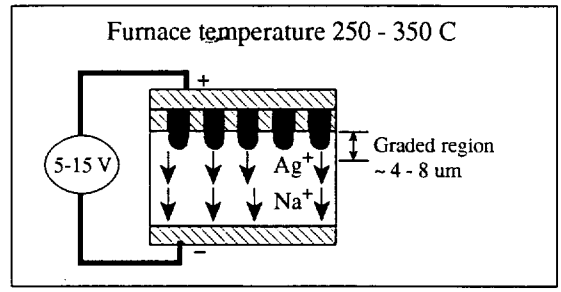


*Figure 2. Schematic diagram of waveguide fabrication process.*

*Figure 3. Channel waveguide in a Nd:doped phosphate glass. The waveguide is made by ion exchange and made visible by scattering of a He-Ne laser propagating through the channel.*

based on measured slope efficiencies. The best laser performance was achieved in a channel waveguide with dimensions of ~ 50 x 9 $\mu m^2$, with an incident pump power threshold of 44 mW and a slope efficiency of 15% with respect to incident pump power. Losses as low as 0.2 dB/cm were determined from slope efficiency measurements in several size channels lasing for three different output coupler reflectivities (67%, 82%, 97%) [6].

While $Nd^{3+}$ has been studied extensively over the years as a laser ion, $Yb^{3+}$ has only recently been utilized. The main emission bands are approximately the same (~ 1050 nm for $Nd^{3+}$ and ~ 1000 nm for $Yb^{3+}$); however, the laser dynamics are quite different (4-level for $Nd^{3+}$ and quasi 3-level for $Yb^{3+}$).

### $Yb^{3+}$: Phosphate Glass Spectroscopy

The $Yb^{3+}$ ion has gained in prominence as a laser ion since the availability of diode laser pump sources, which allow direct pumping of the absorption band (~ 900-975 nm). The electronic structure of $Yb^{3+}$ is composed of only two manifolds in the 4f shell. With the $^2F_{5/2}$ and $^2F_{7/2}$ manifolds separated by ~ 10,000 $cm^{-1}$, the absorption and emission features near 1 mm overlap to a large degree. The measurement of the spectroscopic parameters is impacted by reabsorption processes and is further enhanced by radiation trapping effects. Radiation trapping is dependent on the sample size and geometry, whereby a fraction of the emitted radiation from $Yb^{3+}$ ions is reflected back into the sample by total internal reflection at the substrate to air interface, upon which the cycle of emission and absorption starts again.

A process to isolate these effects and to measure intrinsic fluorescence lifetimes, absorption and emission cross-sections of $Yb^{3+}$ doped phosphate, silicate, and silica glasses was described. Laser performance modeling of channel waveguides was also presented, where the quasi-three level laser dynamics of $Yb^{3+}$ were included. The modeling showed that in order to overcome the losses (~ 5%/cm) for the waveguides and the reabsorption losses at the laser wavelength, small feature sizes for the channel waveguides were very important. Combined with the inherent losses in the substrate, insertion losses also were important. Coupling the pump beam into the asymmetric waveguide was not ideal for our experiments and could possibly have benefited from the addition of an extra lens to provide more flexibility in the matching the pump mode to the waveguide mode. Also important in these experiments is the optomechanical design of the mounts, which must provide for submicron precision and mechanical stability to mitigate

## References

[1] N.V. Nikonorov, and G.T. Petrovskii, *Ion-Exchanged Glasses in Integrated Optics: The Current State of Research and Prospects (A Review),* **Glass Physics and Chemistry, 25,** 16 (1999).

[2] R.V. Ramaswamy and R. Srivastava, *Ion-Exchanged Glass Waveguides: A Review,* **J. Lightwave Technol., 6,** 984 (1988).

[3] T. Findakly, *Glass Waveguides by Ion Exchange: A Review,* **Opt. Engineering, 24,** 244 (1985).

[4] F.D. Patel, E.C. Honea, D. Krol, S.A. Payne, and J.S. Hayden, *Waveguide Fabrication in $Nd^{3+}$ and $Yb^{3+}$ Doped Phosphate Glasses,* **OSA Trends in Optics and Photonics on Advanced Solid-State Lasers,** Walter R. Bosenberg and Martin M. Fejer (eds.), **19,** 446 (1998).

[5] F.D. Patel, E.C. Honea, D. Krol, S.A. Payne, and J.S. Hayden, *$Nd^{3+}$ and $Yb^{3+}$ Doped Phosphate Glass Wave Guides Fabricated Using Electric Field Assisted $Ag^+$ Diffusion,* **Proc. VIII Int. Congress on Glass,** San Francisco: Am. Ceram. Soc. (1998).

## Contact Information

Denise Krol
Ph: 925-424-29
Email: krol@oasis.llnl.gov

# Optical Laser Damage

Stavros Demos, Principal Investigator, LLNL

***Post Doc:***
*Feng Chen – Cal. State University, Northridge*

***Students:***
*Christopher W. Carr – UC Davis, Physics Department*
*Nelson Garces – West Virginia University*

The aim of this research program is to study the photo-physical processes associated with excessive light absorption by an optical material leading to irreversible catastrophic processes. Major part of this effort is devoted to KDP crystals and fused silica, the key optical materials for NIF. The fundamental mechanisms for the coupling of laser energy into the host material leading to damage as well as subsequent to laser damage leading to damage growth are questions of great importance for both technological applications and basic science. Various spectroscopic tools are employed in this study. Fluorescence microscopy is used to image material defects. Micro-Raman provides a way to study material modifications. Time resolved and pump-and-probe spectroscopy provides the means to study the dynamics of the damage-related process. Finally, theoretical modeling is used to complement the experimental work and better understand material defects.

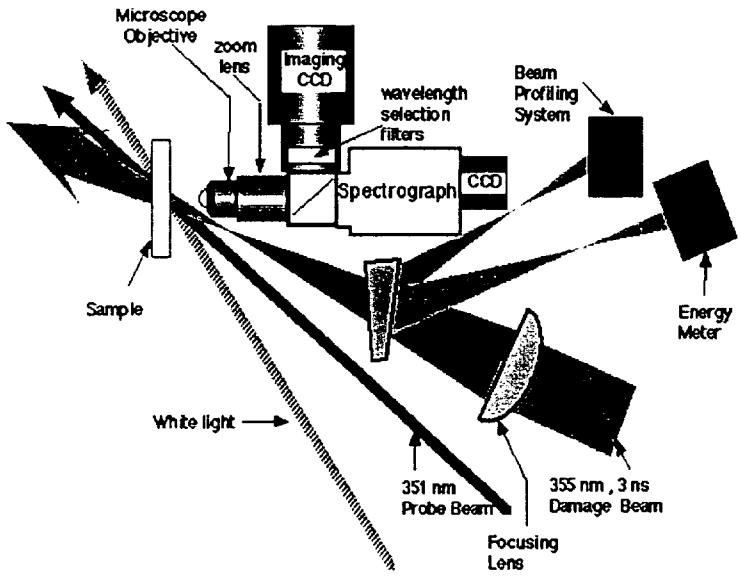


*Imaging CCD camera for optical laser damage photo*

## Recent Publications

S.G. Demos, A. Burnham, P. Wegner, M. Norton, L. Zeller, M. Runkel, M.R. Kozlowski, M. Staggs, H.B. Radousky, *Surface Defect Generation in Optical Materials Under High Fluence Laser Irradiation in Vacuum*, **Electronics Letters, 36**, 566 (2000).

S.G. Demos, H.B. Radousky, and R.R. Alfano, *Deep Subsurface Imaging in Tissues using Spectral and Polarization Filtering*, **Optics Express, 7**, 23 (2000).

S.G. Demos, D.M. Calistru, S. Owen, V. Petricevic, and R.R. Alfano, *Resonance Between a Phonon and Local Mode Pair Promotes Participation in the Nonradiative Relaxation*, **Phys. Rev. Lett., 82**, 2556 (1999).

S.G. Demos, M. Staggs, M. Yan, H.B. Radousky, and J.J. De Yoreo, *Investigation of Optically Active Defect Clusters in KH2PO4 Under Laser Photoexcitation*, **J. of Appl. Phys., 85**, 3988 (1999).

S.G. Demos, M. Yan, H.B. Radousky, and J.J. De Yoreo, *Raman Scattering Investigation of KDP Subsequent to High Fluence Laser Irradiation*, **Appl. Phys. Lett., 72**, 2367 (1998).

## Affiliated Institutes

UC Davis, Physics Dept.; California State University Northridge; West Virginia University

## Optical Laser Damage

Although the problem of laser induced damage has existed since the invention of the laser, the initiation mechanism and its evolution still largely defies a fundamental understanding despite more than three decades of research. While the damage thresholds in optical materials have improved over time, primarily in response to better filtration of growth solutions, purer raw materials, and improvement in the polishing and growth processes, they are still far below what is expected from their band structure. Exposure of a transparent optical material to an intense laser pulse at optical wavelengths can lead to energy deposition only if the interaction first transforms this material into an absorber. Early attempts to understand the intrinsic absorption of energy by nominally transparent solids from an intense laser pulse adopted the electron avalanche model. This primary process involves the generation of free charge carriers (i.e., electrons in the conduction band) [1-5]. These free charge carriers can be efficient at absorbing photons and via collisions with phonons, they can transfer their energy into the crystal lattice.

Point defects or defect clusters at which absorption of light can occur at wavelengths longer than the fundamental absorption edge can provide the initiation mechanism for the cascade processes leading to plasma formation [3,4]. Nonabsorbing defects such as cracks and voids cause dielectric discontinuities that enhance the local electric field of an optical wave and/or serve as positive or negative lenses for the incident laser light and thus, initiating the mechanism leading to damage at lower average fluences [1,6]. Finally, foreign particles or nonstoicheiomenthic materials that may be incorporated in the bulk of the material during growth or into its surface during polishing must be avoided because they may initiate excessive absorption of laser light that can lead to damage.

The overall research strategy for this project is the following:

1) Perform a time-resolved tudy of plasma formation with picosecond time resolution. Time resolved spectroscopy will allow the investigation of the spectral characteristics of the light emitted during damage and provide information regarding the starting time of plasma formation and its evolution under 355 nm, 3 ns high-power laser irradiation with time resolution that will reflect 10-nm spatial resolution during plasma expansion.

   We will also obtain information regarding how fast plasma expands, its temperature and density, and its dynamic behavior. The comparative study of plasma formation in the bulk of a crystal (KDP and/or DKDP) as well as at the surface of the same material in air and in vacuum and its comparison with plasma formation, a spectroscopic investigation of plasma emission as a function of the irradiation (damage pulse) wavelength will provide key information to understand the underlying physics of laser damage.

2) Investigation of the wavelength dependence of damage threshold in NIF optical materials.

   Information on the damage-correlated absorption spectra of the material will provide important information on the electronic processes leading to laser induced damage. If damage is initiated by a nanoparticle, the peak temperature grows as the square of particle size in wavelength units ($a/\lambda$) implying a similar behavior of the damage threshold [6]. In addition, models for the wavelength dependence of the threshold for breakdown by avalanche ionization and multiphoton ionization exist in the literature and may be used in our investigation [1,3]. On the other hand, the measurements of the wavelength dependence of plasma (damage) initiation can reveal the absorption spectrum of the responsible contaminants.

3) Spectroscopic detection and characterization of crystalline band-zone electronic defect structures as a possible plasma initiation mechanism and/or consequence to plasma formation.

   Laser interaction with optically active defect formations prior and following high power laser irradiation and/or plasma formation can be responsible for damage initiation or damage growth. Optically active electronic defect clusters were imaged for the first time in the bulk of a dielectric material in KDP crystals. The experiments were carried out using a specially designed fluorescence microscope having spatial resolution of 1 μm. The experimental results show that the concentration of these clusters is $10_4$-$10_6$ per $mm^3$, depending on the crystal growth method, speed of growth and crystal sector. It was also observed that under subdamage threshold laser irradiation the cluster concentration decreases logarithmically with respect to the number of pulses while they remain unaf-

fected under thermal conditioning. Spectroscopic analysis of the defect clusters has been carried out showing similarity with defect formations resulting from localized laser induced damage. To test the correlation of preexisting defect formations to damage initiation, we have built an in-situ damage testing micro-spectroscopy imaging system which can obtain light scattering, fluorescence and plasma images of the same site with incorporated capability to measure the emission spectra of features of interest (see figure). Defect formations are also studied using various optical spectroscopy methods as well as with EPR spectroscopy.

We have also developed capabilities for theoretical modeling of electronic states of defect formations through our University collaboration.

We plan to expand this investigation to other materials such as laser crystals and alkali halides.

## References

[1] N. Bloembergen, Laser Induced Electric Breakdown in Solids, **IEEE J. of Quantum Electr., 10,** 375 (1974).

[2] W.L. Smith, Laser Induced Breakdown in Optical Materials, **Optic. Eng. 17,** 489 (1978).

[3] S.C. Jones, P. Braunlich, R.T. Casper, X.A. Shen, Recent Progress on Laser-induced Modifications and Intrinsic Bulk Damage of Wide-gap Optical Materials, **Optic. Eng. 28,** 1039 (1989).

[4] L.L. Chase, Laser Ablation and Optical Surface Damage, **Springer Series in Material Science, 28,** Laser Ablation, J.C. Miller, Ed., Springer-Verlag, Berlin (1994).

[5] B.C Stuart, M.D. Feit, A.M. Rubenchik, B.W. Shore, and M.D. Perry, Nanosecond-to-femto Second Laser Induced Breakdown in Dielectrics., **Phys. Rev. B., 53,** 1749 (1996).

[6] M.D. Feit, and A.M. Rubenchik, Laser Intensity Modulation by Nonabsorbing Defects, **SPIE Proceedings, 2966**, 475 (1996).

## Contact Information

S. Demos
Ph: (925) 423-3388
Email: demos1@llnl.gov

# Silicon Micromachined Scanner for OCT

Jonathan Heritage, Principal Investigator, UC Davis

***Co PI's:***
*Olav Solgaard – EL Ginzton Laboratory, Stanford University*
*Matt Everett – Medical Technology Program, LLNL*

***Graduate Student:***
*Kimberly T. Cornett – UC Davis*

We report the first experimental integration of a rotary scanning micromirror into a compact rapid scanning optical delay line. The delay line is a special case of femtosecond pulse shaping. Introduction of a micromirror has allowed for the delay line to be geometrically minimized to a compact optical length of 5.3 cm, ~ 4 to 5 times smaller than pulse shapers used today in common practice. A 40 ps delay range, a linear delay of 1.2 cm in air, is demonstrated at a scanning rate of 12.7 m/s with 25 nm full bandwidth pulses. The pulse width is maintained very closely to the 100 fs pulsed laser source. Scaling laws establish how compact a scanner can be made for Optical Coherence Tomography applications.

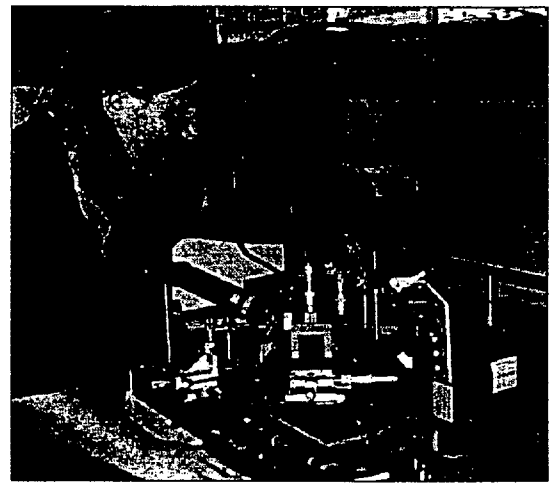

*Graduate student Kimberly T. Cornett*

## Recent Publications

K.T. Cornett, P.M. Hagelin, J.P. Heritage, O. Solgaard, and M. Everett, *Miniature Variable Optical Delay Using Silicon Micromachined Scanning Mirrors*, **CLEO 2000,** San Francisco, CA, 383 (2000).

K.T. Cornett, J.P. Heritage, and O. Solgaard, *Compact Optical Delay Line Based on Scanning Surface Micromachined Polysilicon Mirrors*, **2000 IEEE/LEOS International Conference on Optical MEMS,** Kauai, HI, 15 (2000).

## Affiliated Institutes

UC Davis; Berkeley Sensors and Actuators Center (BSAC) at UC Berkeley; Lawrence Livermore National Laboratory; Stanford University

# Silicon Micromachined Scanner for OCT

## Introduction

Optical Coherence Tomography (OCT) is a cross-sectional optical technique for high-resolution clinical imaging of microstructure in biological systems [1]. OCT performs spatially localized imaging by combining coherent signal acquisition and joint time frequency analysis of wide-band near IR radiation in a white light interferometer. The technique requires a rapid (~ 1-2 kHz) scanning optical delay (RSOD) in order to construct images at 4-8 Hz [2]. Quasi-real time OCT imaging with a delay line of ~3mm [3] has been demonstrated using scanners based on technology originally developed for femtosecond optical pulse diagnostics [2], [4]. We report the development of compact RSOD scanners that use, for the first time, silicon micromachined scanning mirrors. The use of dynamic micro-optical components lends itself to compact geometry systems and allows for lower scanning vibration and higher overall speed. We investigate the design trades-off of a RSOD optimized for the stringent requirements of OCT, namely, large optical bandwidth and long linearly scanned delay range.

The core of the system is the tilt-up scanning micromirror, shown in Figure 1. In 1993, work on tilt-up micromirrors by Kiang et al. [5,6] demonstrated the use of resonant micromirrors for one-dimensional (1-D) barcode scanning. In-plane (not tilt-up) micromachined mirrors are already available commercially in display systems, first demonstrated by Texas Instruments in 1994 based on digital micromirror device (DMD) technology. In the past few years, micromirrors continue to be commerically demonstrated with the introduction of all-optical switching technology. In February 1999, Bell Labs, the research and development arm of Lucent Technologies, demonstrated the seesaw switch.

Optical microelectromechanical systems (MEMS), also referred to as MOEMS, are fabricated by bulk and surface micromachining, a fabrication process based on silicon integrated circuit (IC) technology. MOEMS are positioned at the intersection of micromechanics, microoptics, and microelectronics. Evident by this junction, optical MEMS are another stage of the silicon revolution [7]. The beginning of the silicon revolution is marked by the demonstration of the first integrated circuit (IC) in 1958 by Jack Kilby of Texas Instruments and Robert Noyce of Fairchild Semiconductor Corporation. Between 1970 and 1980 bulk micromachining was developed as an extension of IC technology for fabrication of three-dimensional (3-D) structures [8]. MEMS fabrication technology integrates optical components on-chip with movable structures, microactuators, and microelectronics. Utilizing semiconductor fabrication technology, IC-compatible microfabrication of optical MEMS satisfies a demand for low-cost mass-produced free-space optical systems that are compatible with standard silicon microelectronics.

Our scanning micromirror is integrated into a modified Michelson interferometer (Figure 2), referred to as a μMichelson interferometer [9]. In an RSOD, the traditional translating mirror of a Michelson interferometer is replaced by a scanning mirror with a rotation angle of a few degrees. The μMichelson interferometer consists of a RSOD based on scanning surface micromachined polysilicon mirrors. The RSOD, which is based on femtosecond pulse shaping technology [4], was developed to overcome the speed limitations of traditional approaches

Adjustable optical delay lines are important functional elements in ultrafast optical science and interferometry. Ultrafast optical time resolved measurements are performed using pairs of interfering laser pulses; a probe pulse propagating

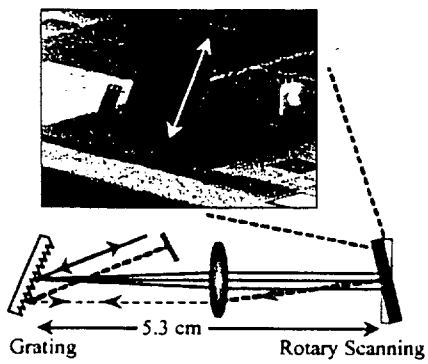


*Figure 1. Schematic of double pass rapid scanning optical delay line with a silicon micromachined rotary scanning mirror.*

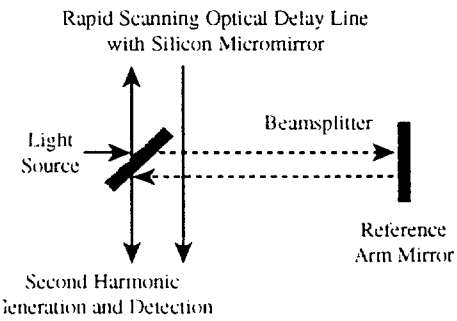


*Figure 2. Schematic of optical delay line in a μMichelson interferometer configuration.*

along a variable-length path, and a reference pulse propagating along a fixed-length path. A commonly used method for creating variable optical time delays involves mechanically moving a retro-reflecting mirror along the pulse propagation direction using a lateral translation stage. This method offers excellent accuracy when precision lead screws are employed. However, scans are inherently slow owing to substantial mechanical inertia. OCT requires scan rates exceeding 1 kHz [10].

## System design

Our RSOD is based on our surface micromachined tilt-up mirror (Figure 1). The polysilicon mirror is connected to a supporting frame with torsional polysilicon beams and is dynamically driven by an electrostatic comb-drive actuator. The rectangular mirror face is 760 μm by 500 μm, with a resonant frequency of 1060 Hz and a measured range of deflection of 16 degrees optical. The challenges of introducing a micromachined scanning mirror into the delay line include the static buckling of the mirror face due to stress gradients in the fabrication process [11,12] as well as surface roughness and dynamic deformation of the mirror while scanning [13]. The residual stress gradients give our micromirror a measured convex radius of curvature of 34 cm. Figures 3 and 4 show the frequency and deflection characteristics of the micromirror. These electrostatic mirrors have been demonstrated in a 2D raster scanning system [14] and most recently in a scalable fiber-optic switch [15].

The final challenge is the scaling of bulk systems to include and maximize for the introduction of micro-optical components. The resolution of our system on the micromirror is defined by the ratio of the spectral spread to the spot size of one spectral frequency. Therefore, we designed for the largest reasonable spot size of our input beam at the grating, subject to the constraint that the beam radius must be small enough to allow adequate translation motion across the lens. This is accomplished by defining our input Rayleigh range to be 10 times the focal length of our achromatic lens. By this conservative rule of thumb, we still attain a tight 23 mm spot size at the focal plane of the lens. Once this is established we decide upon the grating groove spacing, d. The grating spectral dispersion then dictates the minimum dimension of the scanning mirror face, Δx. Our system inputs a 835 nm central wavelength with 25 nm total bandwidth from a modelocked Ti:sapphire laser. With the use of a micromirror, the RSOD has an optical length of 5.3 cm, ~ 4 to 5 times smaller than pulse shapers used today in common practice. The 600 lines/mm grating and 2.54 cm focal length (f/2 achromatic) contribute to the compact size. Experimentally, the spectral spread slightly overfills the mirror face. Spectral narrowing contributes a broadening of about 25%, in addition to the residual uncompensated phase of the pulse.

The grating dispersion is defined by $\Delta\theta/\Delta\lambda = m/(d\cos\theta_d)$, where $\Delta\theta$ is the dispersion spread, $\Delta\lambda$ is the full spectral bandwidth, m is the diffraction order (or spectral order), and $\theta_d$ is the diffraction angle. The spatial extent of the spectral spread is then $\Delta x = f\tan\Delta\theta$, where f is the focal length of the lens. We define a usable lateral motion across the lens as $D_l = a^{*}\Delta x$, where $a=f\tan(2\delta)$ is the motion of the beam center, $D_l$ is 70% of the diameter of the lens, and $\delta$ is the mechanical angle of the mirror. With all the scaling guidelines met, the time delay is given by:

$$t_{delay} = \Delta L_{path} / c = 2\left(2\int \lambda_0 \delta\right) / \left(cd\cos\phi_d\right)$$

where $\lambda_0$ is the central wavelength. We collected a time window of 40 psec, while maintaining the pulsewidth on the same order as the 100 fsec pulsed laser source shown in Figures 5 and 6. Residual broadening and asymmetry are a result of modest spectral clipping, noted above, as well as mild mirror imperfections including apparent third order ("S" shape) curvature of the mirror.

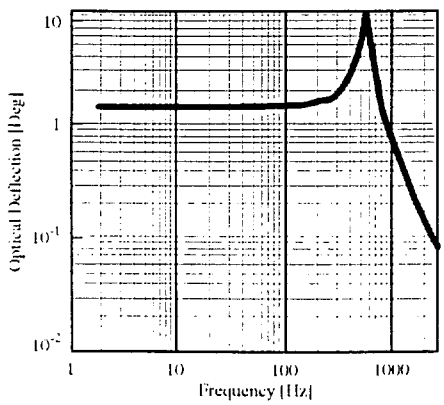


*Figure 3. Static micromirror deflection.*

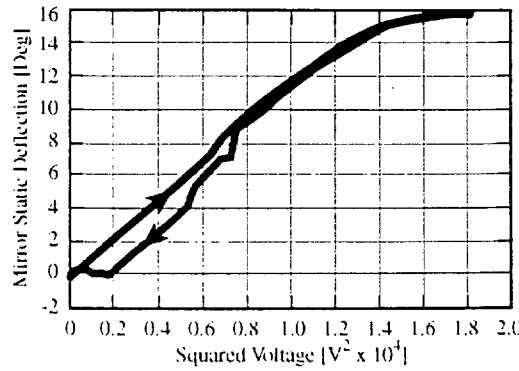


*Fig. 4 Static micromirror deflection*

# Silicon Micromachined Scanner for OCT

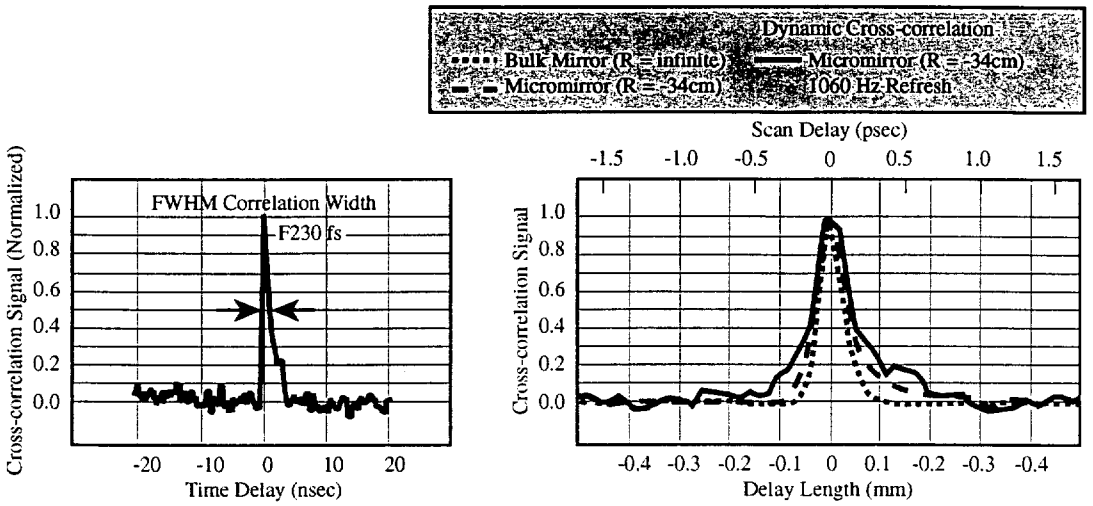


*Figure 5. Dynamic cross-correlation measurement, refresh rate 1060 Hz.*

*Figure 6. Precision cross-correlation measurement.*

Successful integration of scanning micromirrors into the μMichelson interferometer configuration demonstrates the potential of MEMS technology for the creation of hand-held portable optical devices. With the added benefits of microdevices, including speed and reduced vibration of mechanical components, the potential is also evident for use of this configuration in systems such as Optical Coherence Tomography (OCT) and Fourier transform infrared spectroscopy (FTIR).

## References


[1] G.J. Tearney, M.E. Brezinski, B.E. Bouma, S.A. Boppart, C. Pitris, J.F. Southern, and J.G. Fujimoto, **SCIENCE 276,** 2037 (1997).

[2] K.F. Kwong, D. Yankelevich, K.C. Chu, J.P. Heritage, and A. Dienes, **Optics Letters 18,** 558 (1993).

[3] G.J. Tearney, B.E. Bouma, and J.G. Fujimoto, **Optics Letters 22,** 1811 (1997).

[4] J.P. Heritage, A.M. Weiner, and R.N. Thurston, **Optics Letters 10,** 609 (1985).

[5] M-H. Kiang, O. Solgaard, K.Y. Lau, and R.S. Muller, **IEEE J. of MicroElectroMechanical Sys(JMEMS), 7,** 1, 27 (1998).

[6] M.-H. Kiang, O. Solgaard, K.Y. Lau, and R.S. Muller, **IEEE Photonics Technology Let, 8,** 12, 1707 (1996).

[7] P. McWhorter, http://www.mdl.sandia.gov/micromachine/vision.html

[8] K.E. Petersen, **Proceedings of the IEEE, 70,** 5, 420 (1982).

[9] K.T. Cornett, J.P. Heritage, and O. Solgaard, **2000 IEEE/LEOS Int'l Conf. on Optical MEMS,** Kauai, HI, 15 (2000).

[10] J.M. Schmitt, **IEEE J. of Selected Topics in Quantum Electronics 5,** 1205 (1999).

[11] M.R. Hart, R.A. Conant, K.Y. Lau, and R.S. Muller, **Transducers '99**, Sendai, Japan, 470 (1999).

[12] J.T. Nee, R.A. Conant, R.S. Muller, and K.Y. Lau, **2000 IEEE/LEOS International Conference on Optical MEMS,** Kauai, HI, 9 (2000).

[13] R.A. Conant, J.T. Nee, K.Y. Lau, and R.S. Muller, **2000 IEEE/LEOS International Conference on Optical MEMS,** Kauai, HI, 49 (2000).

[14] P.M. Hagelin, K. Cornett, and O. Solgaard, 1998 **IEEE/LEOS Summer Topical Meeting,** Monterey, CA, 109 (1998).

[15] P.M. Hagelin, U. Krishnamoorthy, C.M. Arft, and O. Solgaard, **Transducers '99,** June 1999, Sendai, Japan, 782 (1999).


## Contact Information


Jonathan Heritage
Ph: (530) 752-2455
Email: heritage@ece.ucdavis.edu

# Endoscopic Subsurface Optical Imaging for Cancer Detection

Stavros Demos, Principal Investigator, LLNL

***Co PI's:***
*Ralph W. deVere White, MD – Professor and Chair, Dept. of Urology, Director, UC Davis Cancer Center*

*Regina Gandour-Edwards, MD – Assistant Professor, UCDavis, Anatomic and Clinical Pathology Residency at UCDMC*

*Harry B. Radousky – LLNL*

This research project represents an effort to develop novel instrumentation to be employed in the continuous effort to fight cancer. More specifically, this project involves the development of endoscopic subsurface imaging technology that can be used as a minimally invasive early cancer detection/screening and diagnostic tool. The images obtained will be able to provide information of different tissue structures on the surface and below the surface at different depth zones. The utilization of this technology can be incorporated into different types of existing endoscopes allowing for subsurface imaging inside the human body. This imaging technology provides fast image acquisition, involves no expensive equipment or expertise and can be utilized in a doctor's office or in the field.

The physical basis of this subsurface imaging method for cancer detection originates in the differences in the interaction of light with cancer and normal tissue arising from their differences in the cellular level (size of the cells, density, cell makeup and biochemical composition). Two main techniques are explored based on imaging using light scattering and autofluorescence under laser excitation. The images attained using the light scattering method represent differences in absorption by blood or other chemical substance and scattering due to the presence of different types of tissue at different depths. Photon discrimination methods using polarization and light scattering spectral filtering followed by image processing allow for effective removal of the image information of the outer layers of the tissue and enhancement of the contrast and image quality of subsurface tissue structures. Biochemical fluorophores activated by laser excitation are used in the second method for tissue imaging and characterization. As part of this research effort, we have undertaken the task of building an endoscopic system for subsurface imaging inside the human body and test it in a clinically relevant environment. This imaging system incorporated existing technology that has been developed for medical endoscopes with the appropriate modifications to accommodate the proposed subsurface imaging technology. This "endoscope" type system will be able to perform the measurements utilizing low cost off-the-self components, will be user friendly requiring no particular specialization nor exposure of the operator to any harmful radiation and will be minimally invasive for the patient. The possible applications will involve cancer detection at early stages in the skin, bladder, lung, bronchus, uterus, cervix, GI track, prostate and kidney. In addition, this imaging technology may find application in providing minimally invasive monitoring of the tumor's response to various stages of treatments and in assisting during surgery by providing information on the depth of penetration of the tumor.

Human and animal tissue samples are studied in order to optimize and test the optical imaging modality's ability to address a number of clinical situations. This is achieved using prototype instumentation that has been built at LLNL and used at the UC Davis Medical Center. The key parameters such as illumination wavelength and source, imaging depth and resolution, ability to distinguish between normal tissue and maligned or benign tumors in various body parts are the focus of our effort. The application of this technology for the detection of cancer in bladder, colon, prostate and kidney is our initial objective.

## Affiliated Institutes

*UC Davis* Medical School

# Endoscopic Subsurface Optical Imaging for Cancer Detection

## Introduction

The promise that optical techniques may offer new medical diagnostic tools has stimulated a great deal of research over the past decade. Optical imaging and optical biopsy are two of the research areas where rapid progress has been achieved indicating that photonic technologies can be particularly suitable in a clinical environment. In the field of optical imaging, there are a number of subsurface imaging techniques such as optical coherence tomography [1], linear and nonlinear emission and harmonic generation imaging [2,3], and confocal microscopy [4] which are currently under development for clinical evaluation. These techniques provide high resolution images of subsurface structures with the drawback that the imaging depth is very small (i.e., 1 millimeter or less). This problem is caused by the fact that the image arises from photons that have undergone no scattering until and after they reach their target. As the imaging depth increases, the number of photons that reach the specific depth without scattering decreases exponentially. In order to provide larger imaging depths, other techniques need to be explored.

## Goal

The goal of this research effort is to develop an endoscopic subsurface optical imaging system that can offer deep subsurface imaging of the order of 1-cm using the spectral and polarization imaging technique (SPDI)5. The images obtained using this subsurface imaging technique delineate the differences in depolarized backscattering light between different tissue types (e.g. normal and cancer tissues) arising from differences in the cellular level. These differences include size and concentration of cells and light scattering centers within and between cells, and their absorption properties. In addition, tissue autofluorescence is explored as a secondary method tissue imaging for the detection of superficial cancer lesions. This second methods aims in probing differences in the biochemical constituents of cancer tissues as a result of its different metabolism.

## The SPDI technique

The SPDI technique is realized using the following steps:

1. Illuminate the sample with different wavelengths ($\lambda 1$, $\lambda 2$) in order to reach different mean penetration depths;
2. Record the perpendicular image for every illuminating wavelength in order to avoid the image information from the surface;
3. Determine the times of exposure t($\lambda$ so that the image information arising from the outer tissue layers for each pair of wavelengths is normalized (nearly equal intensity).
4. Subtract the perpendicular images obtained under different illuminating wavelengths to obtain a new image containing structures underneath the surface.
5. Select the appropriate illuminating wavelengths to effectively reach different "depth zones" inside the tissue.

The improvement of the contrast in the images obtained using the SPD imaging technique is the result of the removal of a large segment of the image information that is not relevant to the target. In an ordinary imaging arrangement, photons that are backscattered at the surface and just below the surface dominate an image. The information regarding an object located below the surface, which is transported by photons that have reached this depth, is hidden in a strong "background" making its identification difficult. By recording only the cross polarized image component in this imaging method, the photons that are backscattered at the surface of the host tissue (specular reflection) are rejected. In addition, subtraction of the two images obtained for different illumination wavelengths cancels out most of the image information arising from photons that were backscattered before reaching the depth where the object of interest is located. This process enhances the relative intensity of the image of objects located below the surface of the host tissue.

As part of this effort, we have built appropriate instrumentation to test, in a clinical environment, the basic concepts for endoscopic imaging and cancer detection. A first prototype instrument has been built and is currently used to collect data from human samples at the UC Davis Medical Center while other designs are under development. The experimental layout is shown in the figure on page 55.

# Endoscopic Subsurface Optical Imaging for Cancer Detection

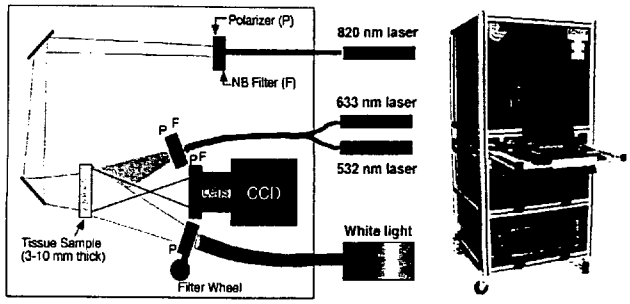


*Experimental layout prototype instrument.*

To test the first concept (light scattering approach) using this prototype instrumentation, a white light source is used to illuminate the sample at different wavelengths selected by optical filters and the two polarization image components in the backscattering geometry are recorded. The experimental results obtained using human tissue samples will reveal differences between normal and cancerous tissue components and provide information on the applicability of the subsurface imaging technique to address the problem of early cancer detection.

## Second Concept

The second concept we are examining involves imaging of various tissue types using the near infrared emitted light under red (633 nm) and green (532 nm) laser excitation. The experiments are performed by incorporating polarization selection to enhance the volume of information. These measurements are designed to reveal differences between normal and cancerous tissue components by comparing the intensity of the NIR emission images, the totally polarized NIR emission images and the degree of polarization of the emission images.

The experiments so far are extremely encouraging, suggesting that all of the approaches that we are exploring may be proven fruitful. More specifically, the polarized light scattering method appears to be a promising approach for surface as well as for subsurface imaging of cancer lesions. In addition, experiments involving imaging using tissue autofluorescence under laser excitation suggest that this method may also be proven useful for cancer imaging. While the human tissue investigation is in progress, we are developing at LLNL the endoscopes that will incorporate, in a final stage, the most successful approaches for cancer detection under investigation using the prototype instrumentation.

## References

[1] D. Huang, E.A.Swanson, C.P. Lin, J.S. Schuman, W.G. Stinson, W. Chang, M.R. Hee, T. Flotte, K. Gregory, C., C.A. Puliafito, and J. Fujimoto, **Science 254,** 1178 (1991).

[2] W. Denk, J.H. Strickler, and W.W. Webb, **Science, 248,** 73 (1990).

[3] Y.C. Guo, P.P. Ho, H. Savage, D. Harris, P. Sacks, S. Schantz, F. Liu, N. Zhadin, R.R. Alfano, **Opt. Lett., 22,** 1323 (1997).

[4] B.R. Masters, A. Kriete, and J. Kukulies, **Appl. Opt., 32,** 592 (1993).

[5] S.G. Demos and RR. Alfano, **Appl. Optics, 36,** 150 (1997).

## Contact Information

Stavros Demos
Ph: 925-423-3388
Email: demos1@.llnl.gov

PROJECTS

# Mercury: Next Generation Laser for High Energy Density

Camille Bibeau, Principal Investigator, LLNL

***Co PI's:***
*Jean Christophe Chanteloup – LULI, France*
*Hitoshi Nakano – Kinki University, Japan*

***Students:***
*A.J. Bayramian – UC Davis*

We are now building the "Mercury" laser system as the first in a series of new generation diode-pumped solid-state lasers for inertial fusion research. Mercury will be the first integrated demonstration of scalable laser architecture compatible with numerous advanced high energy density physics applications. The laser design is predicated upon employing three technological advances: efficient and reliable diodes operating at 900 nm, Ytterbiumb-doped crystals that offer longer storage lifetimes than the traditional Neodymium-doped materials, and active cooling with near-sonic helium gas flow across the crystalline laser slabs for rep-rated operation. The system layout incorporates an oscillator, pre-amplifiers, and two power amplifiers. The gas-cooled power amplifiers are four-passed in an angular multiplexing scheme. An adaptive optic in the beamline will be used to correct for wavefront distortions incurred during amplification. We have completed an analysis of the laser system's performance. For a nominal operating pump pulse width of 1 ms the predicted energy output is over 100 J with an optical to optical efficiency of 24%. Primary performance goals include 10% electrical efficiencies at 10 Hz with a 2-10 ns pulse length and 1.047 um energy of 100 J.

## Recent Publications

A.J. Bayramian, C. Bibeau, K.I. Schaffers, et. al., *Gain Saturation Measurements of Ytterbium-doped $Sr_5(PO_4)_3F$*, **Applied Optics, 39**, 982, 2000.

A.J. Bayramian, C. Bibeau, R.J Beach, et al., *Consideration of Stimulated Raman Scattering in Yb:S-FAP Laser Amplifiers*, **Applied Optics, 39**, 3746, 2000.

C. Bibeau, R.J. Beach A. Bayramian, et al., *Mercury and Beyond: Diode Pumped Solid-state Lasers for Inertial Fusion Energy*, Invited paper, **Proc. of SPIE, High-Power Lasers in Energy Engineering, 3886**, 57, 2000.

A.J. Bayramian, C. Bibeau, K.I. Schaffers, et al., *Development of Ytterbium-doped $Sr_5(PO_4)_3F$ for the Mercury Laser Project*, **OSA Trends in Optics and Photonics Series, 26**, 635, 1999.

C. Orth, R. Beach, C. Bibeau, et al., *Design Modeling of the 100-J Diode Pumped Solid-state Laser for Project Mercury*, **Proceedings SPIE,**

## Affiliated Institutes

Commissariat a l'energie Atomique (CEA), France; Centre National de la Recherche Scientifique, LULI, France; Kinki University and Osaka University, Japan; UC Davis, Department of Applied Science.

# Mercury: Next Generation Laser for High Energy Density

## Introduction

The ultimate goal of inertial confinement fusion (ICF) is to build a power plant based on laser fusion. The top-level requirements for the inertial fusion energy driver (IFE) driver itself are:

- Efficiency, > 5 %
- Reliability, availability and maintainability, >109 shots
- Cost, < $1.5 B
- Beam smoothness for direct drive, < 1% on-target for < 1 nsec
- Wavelength, < 0.4 μm

The efficiency of the driver is important, since together with the target gain and costs, it determines the recycled power needed for the driver. The reliability and cost requirements follow from the need to produce commercially attractive electric power with a minimum 30-year plant lifetime.

Gas-cooled, diode-pumped, Yb:crystal lasers are envisioned to be the next-generation ICF solid state laser system producing high energy per pulse at modest rep-rates. The diode-pumped solid state laser (DPSSL) approach builds on the last two decades of solid state laser development but also adds several imposing challenges — repetition rate, reliability, and cost. Innovative solutions for building ICF lasers with high repetition rate and efficiency include:

- Trading the flashlamps for large, low-cost laser diode arrays
- Using Yb:crystals for greater energy storage and thermal conductivity than Nd:glass
- Employing near-sonic helium for cooling of the laser slabs

The Mercury Laser is the first step in integrating these new approaches, and in producing new capabilities for irradiating ICF targets. The primary performance goals for the Mercury Laser are to build a 100 J laser with 10% efficiency that operates at 10Hz-repetition rate.

### Laser Architecture

The Mercury laser design (Figure 1) is predicated upon employing three key technological advances: efficient and reliable diodes operating at 900 nm, Yb-doped crystals that offer 2-3x longer storage lifetimes than the traditional Nd-doped materials, and active cooling with near-sonic (Mach 0.1) helium gas flow across the crystalline laser slabs for 10 Hz rep-rated operation. The two gas-cooled power amplifiers are four-passed in an angular multiplexing scheme. Adaptive optics will be used to correct for wavefront distortions incurred during amplification. Both amplifier heads will be optically pumped from both sides. This dual-ended, longitudinal pumping design allows for more uniform pumping and thermal loading on the crystals than traditional side pumping schemes.

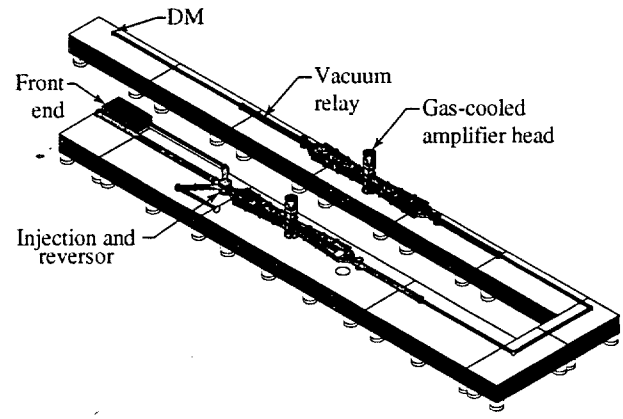


*Figure 1. Mercury laser schematic.*

We have begun fabricating and assembling the hardware surrounding one of the amplifier heads. In order to begin testing the pump delivery design and gas flow dynamics in the amplifier, we will use surrogate gain media (Nd:glass) in the amplifier head. Once the Yb:S-FAP crystals are ready, we can easily switch the surrogate slabs with the crystals. This approach will allow us to test the key elements in parallel with our efforts to develop adequately large crystals. We plan to have one half of the system built by early next year.

# Mercury: Next Generation Laser for High Energy Density

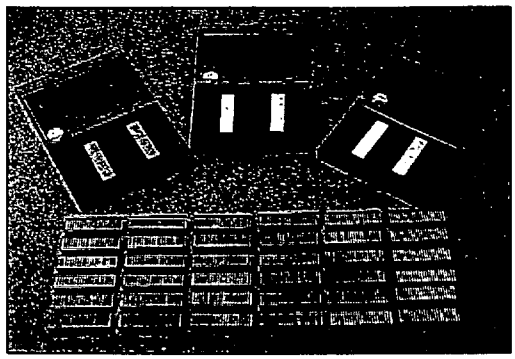

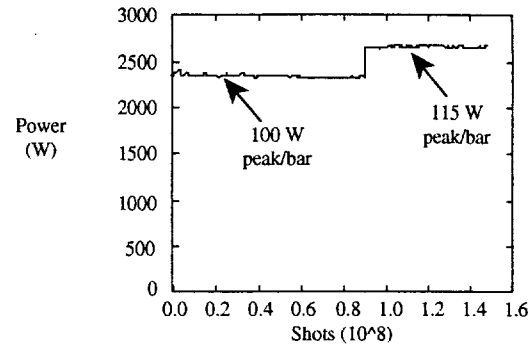


*Figure 2. (a) 23-bar diode packages which operate at over 23 kW of peak power. (b) Lifetest data for 900nm diode material under the Mercury conditions: 750 μs, 10 Hz operation. The power per bar is noted on the plot.*

## Diodes

A critical technology for realizing inertial fusion energy is in the cost and efficiency of laser diode arrays. Existing diode technical performance specifications do not currently meet the demanding requirements of IFE. In addition, the manufacturing costs will have to be reduced by approximately two orders of magnitude to make IFE economically viable. Together with an industrial partner, Coherent-Tutcore, we made significant progress on the development of aluminum-free 900 nm laser diode bars. We packaged, characterized and life-tested many arrays of 900nm laser bars using this diode material as shown in Figure 2.

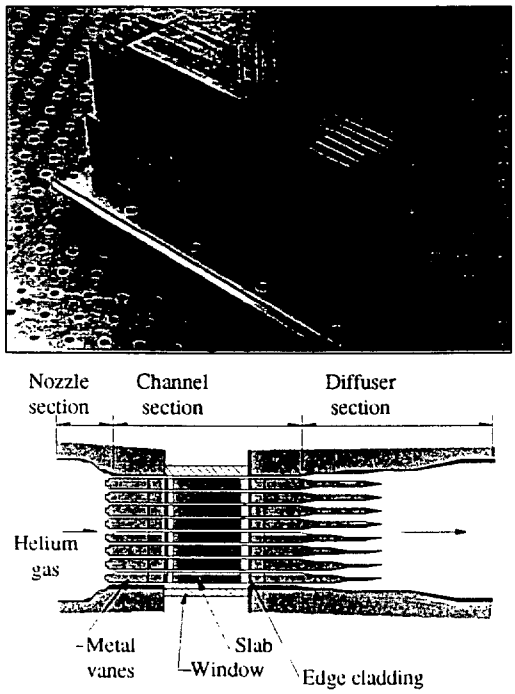


*Figure 3. (a) Actual vanes in assembly. (b) A schematic cross-section through the amplifier head, showing the cooling passages between vanes.*

## Amplifier Head

The Mercury laser amplifier head and gas cooled architecture has been designed in a modular and scalable fashion, with the laser slabs mounted in an aerodynamic vane element as depicted in Figure 3a. The vane elements are then stacked in a manner that forms a cooling channel between pairs of vanes, as depicted in Figure 3b. Gas flows over the faces of the laser slabs, in the cooling channel, to remove the waste heat generated during the lasing process [2,3]. The assembled slab and vane cassette is then inserted into the amplifier head. Flow tests were performed and demonstrated that high flow can be achieved without inducing mechanical vibrations.

## Crystal Growth

Significant progress has been made in understanding the growth characteristics and defect chemistry of Yb:S-FAP [$Yb^{3+}$:$Sr_5(PO_4)_3F$] crystals. The Mercury laser requires crystalline slabs of dimension 4 x 6 x 0.75 cm. The growth of full size crystals has been a challenge due to a number of defects, including: cloudiness, bubbles in the core or center of the crystal, index of reflection variations, and cracking in large diameter boules. An effort is underway to eliminate

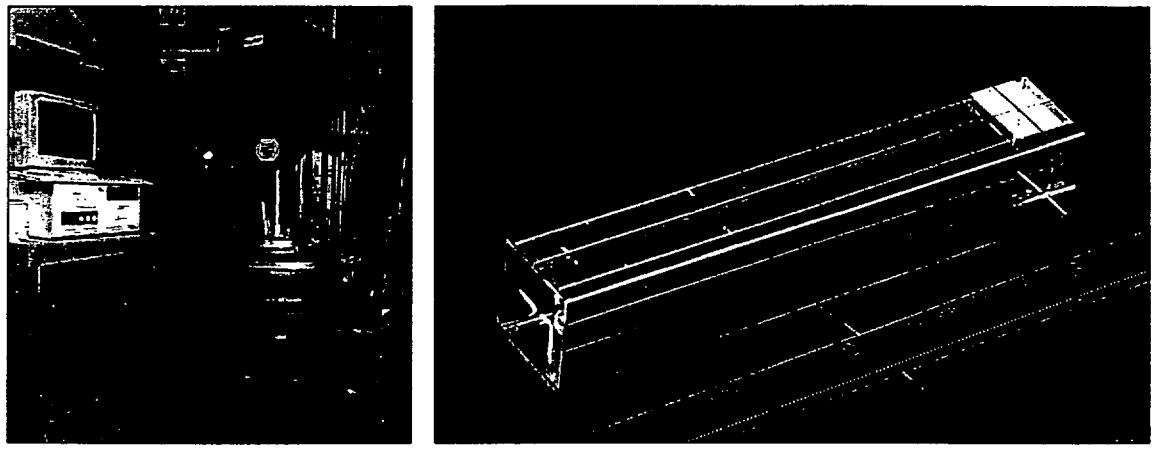

*Figure 4. (a) Crystal growth furnace (b) Yb:S-FAP crystal.*

all of these defects and determine a reproducible growth. In working closely with Litton Airtron we have produced 1/3 size crystals that meet the Mercury specifications. We plan to scale up to half size crystals and bond them together to make full size crystal slabs for Mercury.

## Summary

When completed Mercury will be the highest energy/pulse diode-pumped laser ever built by an order of magnitude that offers the dimension of high repetition rate (~10 Hz). It will motivate the development of rep-rated targets and diagnostic capabilities. In addition, a major objective of the Mercury laser relates to establishing the readiness of the Mercury DPSSL driver to proceed to the next stage and beyond for fusion energy [1].

## References

[1] W.J. Hogan, ed., *Energy from Inertial Fusion* **International Atomic Energy Agency**, Vienna, (1995).

[2] S.B. Sutton and G.F. Albrecht, **J. Appl. Phys. 69**, 1183 (1991).

[3] G.F. Albrecht, et al., **Appl. Opt. 29**, 3079 (1990).

## Contact Information

Camille Bibeau
Ph: 925-422-7798
Email: bibeau1@llnl.gov

# UNIVERSITY COLLABORATIVE RESEARCH PROJECTS

*1998 – 2000*

# UCRP 1998

UNIVERSITY COLLABORATIVE RESEARCH PROGRAM

# Advanced X-Ray Diagnostics

## LS98-001

Roger Falcone, Principal Investigator, UC Berkeley
Richard Lee, Co-Principal Investigator, LLNL

*ILSA/LLNL Collaborator:*
Thomas Missalla
*Lawrence Berkeley National Laboratory Collaborators:*
Phil Heimann, Howard Padmore
*University of Michigan Collaborators:*
Henry Kapteyn, Margaret Murnane, Zenghu Chang
*University of Oxford Collaborator:*
Justin Wark
*UC Berkeley Students:*
Aaron Lindenberg, Steve Johnson
*UC Berkeley Postdocs:*
Jorgen Larsson, Inuk Kang

During the reporting period we made excellent progress in establishing a functioning pump/probe x-ray beamline at the Advanced Light Source at Lawrence Berkeley National Laboratory. The beamline includes a pulsed laser system (1 mJ at 1 KI-Iz; 100 mJ at 10 Hz) that is synchronized with x-ray (100 eV to 15 KeV) pulses from the ALS synchrotron. Studies utilize the lasers to heat materials, and synchrotron x-ray pulses to probe the resulting high-energy-density matter. We have implemented two detector systems. One is an avalanche diode system, capable of single photon detection and allowing 50 ps temporal resolution due to the pulse length of the synchrotron pulses. The second is an ultrafast streak camera system with demonstrated resolution of < 1 ps single shot detection, or 2 ps resolution in an averaging mode. The beamline has an associated test chamber equipped with monochromators and goniometers for precise angular alignment of samples for diffraction, absorption, and scattering studies.

## Scientific Goals

Science on the beam-line has involved the study of laser-heated materials using time-resolved x-ray diffraction and absorption. In particular, we have examined systems including (1) ultrafast-laser-heated InSb crystals and (2) laser-heated silicon thin films. We have measured time-resolved x-ray Bragg diffraction from the laser illuminated materials, in an effort aimed at determining the mechanism of ultrafast laser induced melting and regrowth. We have also studied time-resolved absorption edge changes in laser heated material, in an effort to understand rapid structural and electronic changes in warm condensed matter.

The effort involves one faculty member at UC Berkeley (Falcone), two graduate students at UC Berkeley (Lindenberg and Johnson), two post doctoral students at- UC Berkeley (Larsson and Kang), two scientists at LBNL (Heimann and Padmore), two scientists at LLNL (Lee and Missalla), and a professor at Oxford (Wark). Additional resources have been obtained from DOE/DP, LBNL, and NSF for this beamline.

## Progress and Conclusions

The scientific efforts have resulted in two publications:

1) Larsson, et al, Opt. Lett. 2, 1012 (1997) which describes the beamline and detectors;
2) Larsson, et al, Appl. Phys. A 66, 587 (1998), an invited paper describing the measurement of ultrafast structural changes using time-resolved x-ray diffraction.

Several invited talks have been given on this work, accepted contributed papers will be given at the QELS Meeting and the APS Centennial Meeting Spring 1999, a invited plenary talk on this work will be given at the Conference on Laser Ablation Summer 1999, and an invited talk on this work will be given at the Nonlinear Optics Gordon Conference Summer 1999. Our effort has high visibility in the synchrotron community. Related efforts have now been established at the European Synchrotron (ESRF) and at the Advanced Photon Source synchrotron at Argonne National Lab (involving our group).

Efforts so far have resulted in the important observation of coherent lattice excitation and ultimate disordering and regrowth of laser heated solids. Currently we are focusing our efforts on both theory (with collaborators in H-division at LLNL) and experiments for the study of warm condensed matter through measurement of opacity changes in laser heated silicon and other thin films; our data is challenging condensed matter theorists. Additionally, we are examining the diffuse x-ray scattering from warmed materials on the 100 fs, ultrafast timescale, in an attempted to separate rapid material strain from similarly rapid disordering, following heating. We have established that laser induced structural changes in materials occur on time scales of $< 10$ ps, and now we need to separate out the contributing processes of thermal and pure electronic disorder.

UNIVERSITY COLLABORATIVE RESEARCH PROGRAM

# Critical Surface Interaction Plasma Physics Experiments

## LS98-004

Peter Y. Cheung, Principal Investigator, UC Los Angeles
Peter Young, Co-Principal Investigator, LLNL

## Introduction

Similarities abound between interactions and instabilities in laser plasmas and ionospheric plasmas. Although the actual physical parameters of laser and ionospheric plasmas are very different (Table 1), the scaled or normalize parameters are actually very similar as listed in Table 2. Common interests also exist in the study of these interactions in both communities. Two such examples are the study of critical layer turbulence and the use of Thomson scattering as a key diagnostic.

*Table 1: Comparison of physical parameters of laser and ionospheric plasmas.*

| Parameters | Ionosphere | Laser Plasma |
|---|---|---|
| Pump frequency, *fo* | 5 MHz | 300 THz |
| Pump wavelength, λ | 60 m | 1 μm |
| Pump field, Eo | < 5 V/m | 3 x $10^{10}$ V/m |
| Pump intensity, Io | < 3 x $10^{-7}$ W/ $cm^2$ | < 1 x 1014 W/ $cm^2$ |
| Critical density, ηc | 3 x $10^5$ $cm^{-3}$ | 1 x 1021 $cm^{-3}$ |
| Scale length, L | 60 km | 1000 μm |
| Electron temp.,Te | 0.2 eV | 1 keV |
| Ion temp., Ti | 0.1 eV | 0.3 keV |
| Average charge, Z | 1 | 4 - 50 |
| Average mass, M | 20 | 6 - 200 |
| Debye length, λD | 0.5 cm | 0.007 μm |
| Radar frequency, *f*T | 430 MHz | < 1200 THz |
| Radar wavelength, λT | 35 cm | > 0.25 μm |

In close collaboration with the LLNL co-PI, Dr. Peter Young, a survey of the key critical layer physics issues deemed common to both laser plasma and ionospheric plasma interactions were identified. Ionospheric experiments were then planned and performed accordingly. Research progress and preliminary results in performing these experiments are described in this report. In particular, progress has been made in two ionospheric experiments where key critical layer physics issues have been studied. The first experiment involves the study of stimulated backscattered radiation near the fundamental of the pump frequency and the second experiment involves the study of Langmuir wave turbulence via Thomson scattering. In the remainder of this report, details of research progress in each experiment are summarized, titles of published article and conference poster presentations are listed.

*Table 2: Comparison of scaled parameters of laser and ionospheric plasmas.*

| Parameters | Ionosphere | Laser Plasma |
|---|---|---|
| Scale length, $L/\lambda$ | 1000 | ≤ 1000 |
| Scattered wavenumber, $2k_i\lambda_D$ | ≤ 0.2 | ≤0.35 |
| Temperature ratio, $ZT_e/T_i$ | 2 | ~ 10 |
| Jitter velocity, $v_{osc}/c$ | < $10^{-5}$ | 1.6 x $10^{-4}$ |
| Pump intensity, $E^2/4\pi\eta T_e$ | < 0.01 | ~ 0.04 |
| Electron damping rate,$v_i/\omega_i$ | ~ $10^{-5}$ | ~ $10^{-3}$ |
| Ion damping rate, $v_i/\omega_i$ | < 0.1 | ≤ 0.4 |
| Ion wave frequency, $\omega_i/\omega_o$ | 0.003 | 0.003 |

## Stimulated Electromagnetic Radiation

Experiments have been performed in the investigation of stimulated backward radiation near the fundamental of the pump frequency at the HIPAS Observatory. In particular, the experiments focused on the generation mechanism of electromagnetic radiation inside filaments or density striations. In laser plasma interaction, such filaments can occur due to either ponderomotive or thermal self-focusing instabilities. In the ionosphere, the density striations are predominantly aligned with the ambient magnetic field and develop on a thermal time scale. Preliminary results indicate that once these density striations are formed, trapped electrostatic upper hybrid eigenmodes are excited via conversion of electromagnetic pump wave off the density striations. The parametric decay of these eigenmodes leads to the generation of electromagnetic radiation. The end result is that these trapped modes inside the striations act as very efficient radiators and the threshold for exciting the decay instability of these trapped modes is much lower than normal decay instability. The partial support from the UCRP/LLNL grant on this research results in the completion of a short article titled "Controlled ionospheric preconditioning

and stimulated electromagnetic radiation", published in Phys. Rev. Lett. [Phys. Rev. Lett. 80, 489] (1998).

## Thomson Scattering Experiment

Experiments have been performed in the study of Langmuir wave turbulence and parametric decay instability near the critical layer at Arecibo with the newly upgraded HF transmitters. Detailed temporally and spatially resolved wave measurements using the Thomson scattering radar have been made. The combination of recent results from Thomson scattering experiments and numerical simulations have led to a much improved understanding of critical layer phenomena involving parametric decay instabilities and strong Langmuir turbulence in the ionosphere. A comparison of the Thomson scattering capabilities for laser and ionospheric experiments is listed in Table 3.

*Table 3: Comparison of Thomson scattering diagnostic capabilities*

| Parameters | Ionosphere | Laser Plasma |
|---|---|---|
| Spectral resolution | $\sim 10^{-3}$ | $\sim 10^{-3}$ |
| Temporal resolution | $\sim 10^{4}$ cycles | $\sim 10^{4}$ cycles |
| Spatial resolution | 150 m | 30 μm |
| Spatial resolution | ~ 0.3% L | ≥ 3% L |
| Spectrum vs position | routine | possible |
| Detected range of k | very limited | very flexible |
| Spectrum vs $k_{T\,D}$ | limited | routine |
| Other challenges | natural variation | plasma production |

## Initial Development of Turbulence

The onset of plasma wave turbulence is first detected from two well distinct layers along the plasma density profile. Near the critical layer or the first Airy maximum of the pump profile where the pump frequency, $\omega_o$, is near the local plasma frequency, $\omega_p$, the wave spectrum is dominated by strong Langmuir turbulence characterized by a broad, diffuse "caviton" continuum near $\omega_o$, and an upshifted spectral line called the "free mode". This is illustrated in times 2 - 4 (T:2 to T:4) in the figure above. Such an unique spectrum has been predicted from numerical modeling based on the Zakhar equations. Further down the density gradient, a second layer occurs where

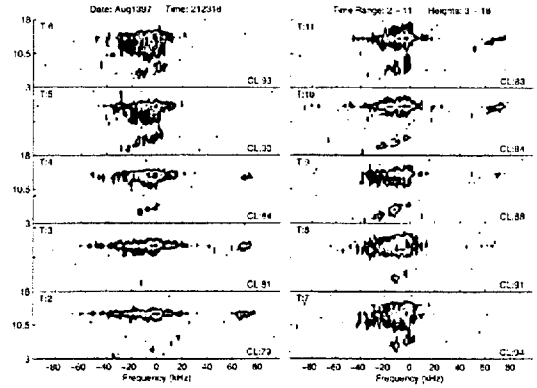

*Contour plots of plasma line data for 10 consecutive times (T:2 - T:11) in milliseconds. The pump is turned on just before T:2 and is turned off after T:11. Each plot covers 16 heights of 150 m resolution or a total distance of 2,400 m.*

strong scattered signal are also observed (T:4 in figure). This layer is generally called the "matching height" where $\omega_o$, matches that of the scattering wave frequency $\omega$, occurs. In this region the wave spectrum is dominated by parametric decay instabilities characterized by discrete frequency lines that matches the decay wave frequency and wave number. Theoretically, this region is called the coexistence regime where both strong and weak Langmuir turbulence coexist.

## Saturated State of Turbulence

As the highly nonlinear process continues (T ¿ 5), the initial thin layer of turbulence near the reflection height gradually spreads to lower range heights, possibly overlapping several Airy maxima. The continuum or the caviton part of the spectrum now consists significant upshifted components while the free mode appears to have broadened. The spectrum at the highest range height, however, generally contains only the continuum but not the free mode. Further down near the matching height, new scattered signals from successive parametric decay or cascading processes, called the so-called 1, 3, and 5 lines for historical reasons, now occur at successive lower matching heights (T:4 - T:6). The local density scale length can be inferred from the systematic frequency shift of free modes and decay lines at successive height ranges.

# Critical Surface Interaction Plasma Physics Experiments

## Publications, Poster and Invited Talks

Under the partial support from the UCRP/LLNL grant, one article has been submitted and has been accepted for publication. Separately, a poster and an invited talk have also been given in a workshop.

P.Y. Cheung et al., *Controlled Ionospheric Preconditioning and Stimulated Electromagnetic Radiation*, **Phys. Rev. Lett. 80**, 4891 (1998).

*Early Time Radar Observations of HF-induced Langmuir Turbulence at Arecibo*, poster presented at the RF Ionospheric Interactions Workshop, Santa Fe (1998).

SEE, *Langmuir Turbulence, Striations, and Upper Hybrid Turbulence*, invited talk presented at the RF Ionospheric Interactions Workshop, Santa Fe (1998).

*The Study of Critical Layer Turbulence in the Ionosphere*, poster presented at the APDDPP meeting, New Orleans (1998).

*Controlled Ionospheric Pre-conditioning and Stimulated Electromagnetic Radiation*, poster presented at the APDDPP meeting, New Orleans (1998).

# Preparation and Characterization of Glasses for Fiber Bragg Gratings

**LS98-006**

Subhash Risbud, Principal Investigator, UC Davis
Denise Krol, Co-Principal Investigator, LLNL

***Student:***
James Chan, UC Davis

Phosphate glasses are of interest as materials for waveguide lasers and other fiber and waveguide devices. Since fiber Bragg gratings are rapidly being incorporated into such optical systems, it is important to study the formation of optically induced Bragg gratings in these rare earth doped phosphate glasses and to characterize these glasses both before and after the writing of the refractive index gratings. The rare earth dopants are used to increase photosensitivity of the glass material for producing larger refractive index changes. Characterization techniques include absorption and luminescence spectroscopy.

## Glass Synthesis Progress

Lanthanum phosphate glasses doped with various concentrations of thulium were synthesized. Table 1 lists the compositions in mole % of the glass sample.

*Table 1. Glass compositions.*

| | Composition (mole %) | | |
|---|---|---|---|
| Sample | $La_2O_3$ | $Tm_2O_3$ | $P_2O_5$ |
| 1 | 0.18 | 0.02 | 0.8 |
| 2 | 0.198 | 0.002 | 0.8 |
| 3 | 0.1998 | 0.0002 | 0.8 |
| 4 | 0.19998 | 0.00002 | 0.8 |

Sample 1 was prepared by mixing the appropriate amounts of $Tm_2O_3$, $LaPO_4$, and $P_2O_5$ to give the final compositions of $La_2O_3$, $Tm_2O_3$, and $P_2O_5$ (mole %) listed in Table 1. The powders were mixed thoroughly and as quickly as possible to minimize the exposure time to air since the materials are hygroscopic. The mixture was put in a platinum crucible and melted in air at 1400° C using a Deltech Model DT-31 Mode C furnace. After roughly 1 to 1-1/2 hours, the melt was removed from the furnace and quenched by pouring it on a brass plate at room temperature. The glass sample was annealed in a Lindberg oven held at 300° C for roughly 1 hour, then kept in the oven to cool overnight.

The samples with lower concentrations of $Tm_2O_3$ were prepared by taking the higher $Tm_2O_3$ concentration mixtures and diluting them with the appropriate amounts of $LaPO_4$, and $P_2O_5$ powders to achieve the final desired concentrations as listed in Table 1. The melting, quenching, and annealing of the samples were the same as described above.

The glass samples were polished and cut. The sizes of the cut glass samples are roughly 15 mm x 5 mm x 5 mm. Striations, which are present in the final polished glass samples, may pose a problem when attempting to run optical experiments on them. Modifications still need to be made in the synthesis of the glasses.

## Characterization

Both X-ray Fluorescence (XRF) spectrometry and absorption spectroscopy have been used to characterize the glass samples. These techniques were used to detect the presence of thulium in the phosphate glass and to compare the thulium concentrations in the glass samples. From the XRF spectrum for the 0.002 $Tm_2O_3$ glass (mole %), the Tm peak height indicated the amount of Tm to be in the range of 5-50 ppm. An exact number on the amount of Tm was difficult to determine because a standard was not available. The XRF spectrum for the 0.0002 $Tm_2O_3$ sample (mole %) showed much smaller Tm peaks. Although exact amounts of Tm were not able to be determined, a comparison of the Tm peak heights for the two glass samples showed that the relative abundance of Tm in the two samples were different by an order of magnitude consistent with the difference between the two Tm concentrations. The height of the Ge peak in the spectra gives an indication of the amount of sample present while that of the Tm peak indicates how much Tm is present. The ratio of the Ge peak to the Tm peak was 21.75 for the 0.0002 $Tm_2O_3$ (mole %) sample while that for the 0.002 $Tm_2O_3$ (mole %) sample was an order of magnitude less at 2.89.

Absorption data were taken of the glass samples. The absorption peaks correspond to the transitions

## Preparation and Characterization of Glasses for Fiber Bragg Gratings

within the 4f ñ multiplet of the Tm3+ ion (360, 470, 685, 790, 1210, 1720 nm). The absorption spectrum for the 0.002 $Tm_2O_3$ (mole %) glass shows that the absorbance decreases compared to that of the 0.002 $Tm_2O_3$ glass with an order of magnitude consistent with the change in the thulium concentration in the glass.

# Three Dimensional Particle-in-Cell Simulations of Intense Lasers Propagating in Underdense Plasma Near Quarter Critical Density

**LS98-008**

Warren B. Mori, Principal Investigator, UC Los Angeles
Chris Decker, Co-Principal Investigator, LLNL

***Students, UCLA:***
Brian Duda, Roy Hemker

We have partially supported the development of a three dimensional particle-in-cell (PIC) code and we have developed a variational principle formalism for analyzing the evolution of finite width laser pulses propagating in underdense plasmas. This new formalism was used to describe new long wavelength hosing, new long wavelength spot size modulation, and new asymmetric spot-size modulation instabilities. One limit of asymmetric spot size modulation is asymmetric self-focusing. A draft of a manuscript was submitted to *Physical Review Letters* and abstracts presented at the 1998 Anomalous Absorption Conference. We summarize these results below:

## Code Development

During the first few months of this period, Roy Hemker was partially supported on this award to develop an object oriented parallelized 3-D PIC code. Subsequently, the code development has been funded from other sources. Currently, we have a working 2D slab geometry object oriented PIC code that has a moving window algorithm and runs on several parallel computer platforms. We also have a working 3D algorithm. We expect these 3D algorithms and several others to be incorporated into the object oriented code within the next four weeks. This code will be used to study the coupled two-plasma decay and Raman scattering instabilities as well as relativistic self-focusing.

## A Variational Principle Approach to Laser Plasma Interactions

During the past year, Brian Duda has developed a variational principle formalism for describing the evolution of short-pulse lasers propagating in underdense plasmas. This approach extends the work of Anderson and Bonneda [1] to include Raman scattering and self-phase modulational type instabilities. The starting point are the well established model equations for describing the evolution of short pulse lasers in plasmas

$$\left[\nabla_\perp^2 - \frac{1}{c}\frac{\partial^2}{\partial_\psi \partial_\tau} - 2i\frac{\omega_0}{c}\partial_\tau\right]a = \frac{\omega_{p^2}}{c^2}(1-\phi)a$$

$$\left[\frac{\partial^2}{\partial_\psi{}^2} + \omega_{p^2}\right]\phi = \omega_{p^2}\frac{|a|^2}{4}$$

where a is the normalized complex envelope of the laser, $\phi$ is the scalor potential, and

$\psi = t - \frac{x}{c}, \tau = \frac{x}{c}$ are the speed of light frame variables.

These equations can be obtained from requiring that the action, $S = \int dx_\perp d\psi d\tau L$ be stationary, where

$$L(a,a^*,\phi) = \nabla_\perp a \cdot \nabla_\perp a^* - i\frac{\omega_0}{c}\left(a\partial_\tau a^* - a^*\partial_\tau a\right)$$

$$-\frac{2}{c}\left(\partial_\psi \phi\right)^2 + 2\frac{\omega_{p^2}}{c^2}\phi^2 - \frac{\omega_{p^2}}{c^2}(\phi - 1)|a|^2$$

In the variational approach, carefully chosen trial functions, which have slowly varying parameters such as a spot size, a transverse centroid, a radius of curvature, and a complex amplitude, are substituted into S and the $d\vec{x}_\perp$ integration is performed. Requiring that the resulting reduced action be stationary results in coupled envelope equations for the slowly varying parameters.

## Long Wavelength Hosing

By linearizing the coupled envelope equations obtained from the variational principle of formalism, we have identified new long wavelength hosing and spot size modulations instabilities. These instabilities grow as

$$\exp\left[\left(\frac{P}{P_c}\right)\left(kc/\omega p\right)^{1/2}\left(\tau/\tau_R\right)\right]$$

where $P/P_c$ is the laser power normalized to the critical

# Three Dimensional Particle-in-Cell Simulations of Intense Lasers Propagating in Underdense Plasma Near Quarter Critical Density

power for relativistic self focusing, k is the wave number of the unstable perturbation, and $\tau_R$ is the Rayleigh or defraction time. These instabilities can occur above the quarter critical density, $n_c/4$ and they are the whole beam analogs to self-phase modulation and filamentation. We have performed large-scale parallel PIC simulations which clearly show the importance of these instabilities.

## LASNEX Simulations

We have carried out preliminary LASNEX simulations to find the scalelengths of exploding foils when the peak density falls through $n_c/4$. This work was done by the LLNL Collaborator, Dr. Chris Decker. The simulations show that irradiating a 1 μm thick tungsten foil with a 5 x $10^{14}$ W/cm$^2$, 1ns pulse gives a 50-60 μm long flat top density regions which lasts for about 50ps.

## Reference

[1] P. Anderson and M. Bonnedal, Phys. Fluids, 22, 105 (1979)

# Short Pulsed Laser Vaporization of Metals

## LS98-010

Ted Bennett, Principal Investigator, UC Santa Barbara

Mark Havstad, Co-Principal Investigator, LLNL

There is a growing body of experimental evidence showing that the kinetics of nascent vapor produced during pulsed laser heating of metals cannot always be ascribed to the surface thermal conditions. Some investigations have proposed that the discharge of energetic (nonthermal) atoms from metals can involve light coupling to surface plasmons. This requires that surface roughness facilitate wavevector matching of laser light with surface electromagnetic excitation modes. If true, superthermal vaporization kinetics should disappear from time-of-flight measurements when an optically smooth surface is sued. Unfortunately, maintaining such an ideal surface is infeasible on a solid target because each laser pulse introduces nanometer sized roughness through the process of melting and resolidification. We have investigated the nature of vaporization from a liquid Hg surface using a nanosecond laser emitting 5 eV photons. Surface tension of the liquid provides an optically smooth surface for this experiment. Nevertheless, we observe superthermal vaporization kinetics from liquid Hg. The shape of the energy distribution is Boltzmann (the thermal expectation), however, and the energy distribution does not demonstrate any quanta characteristic of vaporization mediated by an electronic excitation.

## Introduction

Over the past few years, there has been active research concerning short pulsed laser vaporization of metals (Kim and Helvajian 1991; Hoheisel et al. 1993; Lee et al. 1993; Shea and Compton 1993; Bennett et al. 1996; Elam and Levy 1997). The recent interest stems from observations of superthermal vaporization kinetics. Because important applications frequently operate in a plasma regime, the nascent character of vaporization went unexplored for many years after pulsed laser processing of metals became technologically important. Since a plasma is heated directly by the laser, subsequent vapor kinetics can no longer reflect the surface desorption process in this regime. However, when sub-plasma conditions were eventually investigated high translational energies were observed. In the initial attention given to this departure from expectation, it was often argued that collisional effects in the plume could explain these experimental results. This line of reasoning was made popular by a number of theoretical papers (Kelly and Dreyfus 1998; Kelly and Dreyfus 1988) devoted to the effect of Knudsen layer formation on time-of-flight (TOF) measurements. The Knudsen layer is region adjacent to the surface in which the nascent velocity distribution acquires a stream velocity. In the simplest idealization, the velocity distribution past the Knudsen layer is fully Maxwell-Boltzmann, in a coordinate system moving with the stream velocity. In contrast, the nascent velocity distribution is half Maxwell-Boltzmann, with zero stream velocity. When the "vapor-pressure" generated by the peak thermal conditions of the target is small, collisional effects are unimportant to the translational energy distribution of the vapor.

The energy (or velocity) distribution can be determined from the time it takes atomic material liberated from the target surface to translate to a detector in a TOF measurement. Given a sufficient number of vapor-phase collisions, the mot probable flight time will shift to a higher value. However, if the nascent velocity distribution remains half Maxwell-Boltzmann, the average translational energy is related to the most probable flight time $t^*$ by $\overline{E} = m\left(L/t^*\right)^2/2$, where $m$ and $L$ are the atomic mass and flight distance, respectively. In turn, the mean translational energy should be related to the surface temperature by:

$$\overline{E} = 2k_B T. \qquad (1)$$

The formation of a Knudsen layer is significant to the interpretation of raw TOF measurements. However, an important point, frequently overlooked, is that the shift in the most probable flight time does not reflect a change in the mean translational energy, since energy is conserved. Development of a non-zero flow velocity results from the transfer of internal energy to translational energy of the center-of-mass. This can result in smaller value of internal energy ("temperature") than the total translational energy of the vapor. However, the temperature of the vapor is no longer related simply to the surface thermal conditions. An adiabatic expansion of an ideal monatomic gas offers at most an order $k_B T$ increase in center-of-mass translational energy (or decrease in internal energy). Flow velocities exceeding this value cannot be explained by energy provided by the surface thermal conditions alone.

The difficulty in quantifying plasma and collisional effects in experiments generating relatively large vapor pressure of target material has made it difficult to resolve, in many cases, whether vaporization kinetics are indeed

# Short Pulsed Laser Vaporization of Metals

superthermal. Interestingly, the observation of superthermal vaporization kinetics has also been encountered from the other limiting condition of low vapor pressure in experiments where the surface temperature does not rise above the melting point (Kim and Helvajian 1991); Hoheisel et al. 1993, Lee et al. 1993; Shea and Compton 1993). Here, the influence of vapor-phase phenomena can be ruled out, and TOF measurements unambiguously probe the nascent energetics of the vaporization process. So, where does this extra energy come from?

A proposed explanation involves energy coupling of surface plasmons to be vaporization process (Kim and Helvajian 1991; Hoheisel et al. 1993; Lee et al. 1993; Shea and Compton 1993). A plasmon is the energy quanta of the collective wave-motion of free electrons in a metal (Pines 1956). Plasmon energies in many metals range from 3 to 16 eV. Consequently, if the plasmon energy is given to a desorption process, when a plasmon is annihilated in a collision with a phonon, then the desorbing atom could have energies far exceeding the thermal conditions of the surface (Richie et al. 1994). However, several issues arise with adopting this explanation. First, simultaneous energy and momentum conservation require some qualification of conditions under which surface plasmons can be excited with laser light. In traditional optical-plasmon interaction studies, light is introduced to the backside of a metal film that plates the surface of a prism. Under geometries of frustrated total internal reflection, the evanescent light wave at the interface can couple to surface plasmons in the film (Lemberg et al. 1974). This is not similar to typical conditions used in pulsed laser vaporization. However, conversion of photon energy to surface plasmon energy can also be facilitated by surface roughness, where the reciprocal space of the roughness augments the plasmon wavevector to permit momentum and energy matching with the incident photon. Therefore, it is argued that either intentionally placed or inherent surface roughness can facilitate light coupling to surface plasmons that subsequently participate in the super.ıermal desorption of atoms.

To test this hypothesis, one would like to be able to control the process by which surface plasmons are excited to demonstrate whether there exists a correlation with superthermal vaporization kinetics. However, development of surface roughness, having scales between nanometers to micrometers, is intrinsic to the process of nanosecond pulsed laser melting of metal surfaces. The development of high frequency roughness is due to asynchronous resolidification of the surface. Low frequency surface roughness is due to hydrodynamic instabilities in the molten surface. To avoid these effects in the present study, we have investigated a liquid Hg system. In the liquid state, surface tension provides and maintains an optically smooth surface throughout the experiment. Since light coupling to surface plasmons is prohibited when the smooth surface is irradiated from vacuum, the proposed liquid Hg system should be free from possible effects of surface plasmons. In this paper, we report measurements of the vaporization kinetics of liquid Hg using 16 ns pulsed ultra-violet laser light.

## Experiment and Results

The laser, vacuum chamber, and detector are shown schematically in Figure 1. The detector, used to measure atomic material liberated from the target by the laser, is a fixed appendage to the chamber. The detector placement requires the sample to be held vertically in the vacuum chamber, which poses a significant problem for investigating liquid samples. We have resolved this problem with a specially designed crucible that raises a liquid film of metal to the vertical position. Figure 2 shows schematically this crucible. We chose to study liquid Hg metal to alleviate the need to heat the crucible. The crucible contains a center cylinder (0.75 cm diameter and 1.0 cm length) that is free to rotate within the body. The lower portion of the cylinder rotates through a pool of liquid that wets the surface of the cylinder. The front of the crucible is open, exposing the cylinder to the incident laser beam and providing an

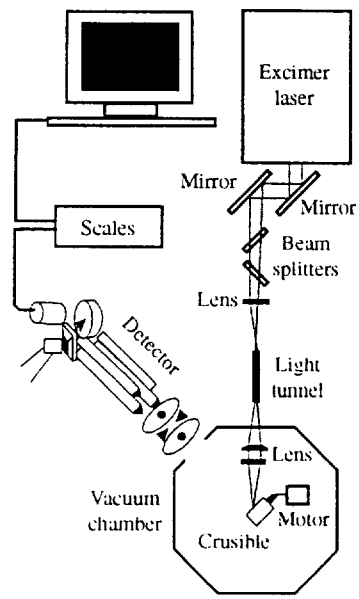


*Figure 1. Schematic of the major components in the TOF measurement system.*

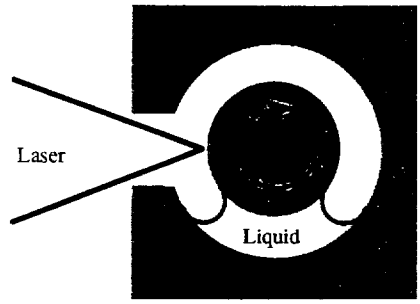


*Figure 2. Illustration of the liquid Hg crucible used in TOF measurements.*

unobstructed view of the sample surface for the detector. The cylinder is coupled to a small dc motor using stranded wire. The cylinder is rotated at approximately 5 rpm during measurements.

The laser is a Luminonics Excimer operated with a KrF gas fill for 248 nm light. The output of the laser is shaped into a uniform top-hat profile using a light tunnel. The intensity of the top-hat is uniform to better than 10% over the nominal spot area. At the target surface, the irradiated area is nominally 0.7mm x 1mm. To achieve the low fluences required in the following experiment beamsplitters were used to attenuate the beam. Pairs of beamsplitters having 10% and 30% or 10% and 50% nominal transmittance (at 450 angle of incidence) were used. Although the light leaving the cavity of the laser is unpolarized, the beamsplitters transmit preferentially p-polarized light. From the manufacturer's specifications, it was calculated that the 10-30% and 10-50% beamsplitter combinations transmit 91% and 87% p-polarized light, respectively. Pulse energies are measured in situ with a joulemeter measuring a portion of the beam energy split from the main beam before entering the light tunnel. The joulemeter is cross-calibrated with a calorimeter measurement used to determine the fluence delivered to the target surface.

The detector is differentially pumped to a base pressure of $10^{-10}$ torr. The detector has three stages. The first stage ionizes a fraction of the vapor plume entering the detector with an electron beam. Ions then pass through a quadrapole mass filter, the second stage, that is used to block the transmission of species not having the charge to mass ratio of $Hg^+$ transmission efficiency. Since Hg has a large atomic weight relative to the residual background gases in the chamber, the resolution of the quadrapole can be set relatively low to obtain a high $Hg^+$ transmission efficiency. In the third stage, transmitted ions are detected by accelerating them into an organic scintillation pad with a 25 kV field. The pad emits a photon burst at each collision event, which is detected with a photomultiplier tube and relayed to a digital scaler. The scaler is used to count the number of pulses arriving in consecutive 6 μs time "bins" over a period of 6000 μs after the laser fires. From this information TOF measurements are obtained. The measured temporal distribution is offset by the "ion flight time" between stage one and stage three of the detector. The ion flight time is largely established by the electric fields in the detector, with a small correction accounting for the velocities of neutrals entering the detector.

The laser is operated at 10 Hz during TOF measurements. The detector signal is averaged over 100 laser pulses to obtain good signal to noise. To minimize the potential effect of surface oxides, an initial 5 pulse sequence of "clean-up" laser pulses are used immediately before the TOF measurement. The surface of Hg will oxidize in the presence of background gases ($10^{-6}$ torr) in the chamber. During the measurement, new surface area is continuously introduced into the irradiated area by the rotation of the cylinder. However, the fraction of new surface area to the total area irradiated is always small because of the low rotational speed used.

Typical raw TOF measurements are shown in Fig. 3. The temporal distribution is converted into an energy distribution using the following factors: At time $t$, the detector signal $N(t)$ can be related to the value of $P(E)$ *at* $E = (m/2)(L/t)^2$. The $N(t)$ signal is proportional to the transient number density of neutrals in stage one of the detector. Consequently, the total flux of atoms passing through the detector in a time interval dt is proportional to $n(t) \sim N(t)/t$, and conservation of flux requires that $n(t)dt = P(E)dE$ be satisfied. Since $dE \sim dt \cdot t^3$, the following relationship holds between the raw TOF signal and the energy distribution:

$$N(t) \sim P(E)/t^4 \qquad (2)$$

Using equation 2, the raw TOF measurements shown in Figure 3, are converted to energy distributions, shown in Figure 4. The mean translational energy can be determined directly from the measured energy distribution. A normalized Boltzmann distribution is plotted over the experimental data in Figure 4 using only the measured mean translational energy to establish the distribution. No stream velocity is used to fit the experimental data. As can be seen from Figure 4., the experimental energy distribution is well described by a Boltzmann fit. The mean translational energies for the distribution shown range from 0.31 eV, corresponding to the low fluence, to

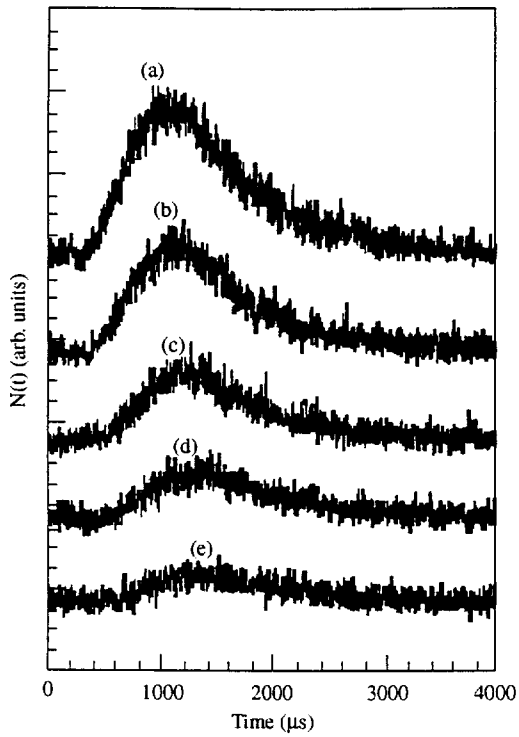


*Figure 3. Raw time-of-flights from Liquid Hg. Distributions reflect 100-shot measurements. The five cases shown are for laser fluences of (a) 0.211, (b) 0.193, (c) 0.176, (d) 0.155, and (e) 0.135 J/cm².*

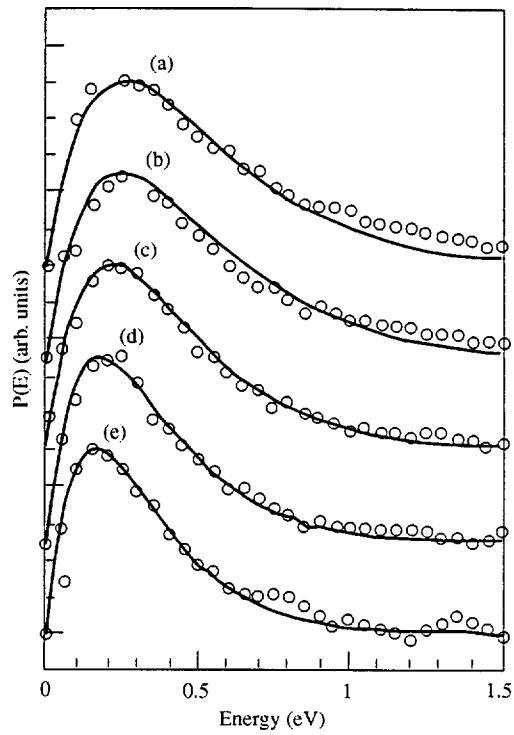


*Figure 4. Energy distributions of Hg corresponding to TOF measurements in Figure 3. The distributions reflect the experimental measurements (o) as well as Boltzmann fits (—).*

0.54 eV at the high fluence. If the energetics of vaporization can be ascribed to the thermal conditions of the surface, then, from equation (1) the peak surface temperatures of the target should fall between 1,800 K to 3,100 K for our experimental conditions. To assess how reasonable these temperatures are, we have numerically modeled the thermal conditions generated during a laser pulse. The code used for our calculations has been described in detail elsewhere (Bennett and Krajnovich 1997) and the principles only are highlighted below.

## Numerical Model

The peak temperature rise at the target surface is calculated considering the transient heating provided by the laser, competing with heat dissipation through diffusion. In the present work, the fact that phase-change is not present greatly simplifies the calculation. The problem is further simplified with the observation that heat transfer can be assumed one-dimensional, since the diffusion depth is three orders of magnitude smaller than the lateral extent of the heated area. Volumetric laser heating of the target is model using Beer's law weighted by the temporal profile of the laser pulse:

$$g(z,t) = \phi(1 - \Re) \cdot I(t) \cdot \zeta e^{-\zeta z}$$

Where $\zeta = 4\pi n_{im} / \lambda$. $n_{im}$ is the imaginary part of the surface index of refraction, $\Re$ is the surface reflectance, and $I(t)$ is the normalized temporal profile of the laser pulse. $I(t)$ has been measured experimentally, and is well described by a triangular shape, with a pulse length $t_b$ = 28 ns at the base and having a maximum intensity occurring at $t_p$ = 7 ns. The surface reflectance depends on the polarization state of the light incident off-normal to the target surface. The general Fresnel formulas for light polarized normal (⊥) or parallel (∥) to the plane of incident are:

$$\Re_{\parallel} = \left| \frac{\tan(\vartheta_i - \vartheta_t)}{\tan(\vartheta_i - \vartheta_t)} \right|^2 \qquad (4)$$

$$\Re_{\perp} = \left| \frac{\sin(\vartheta_i - \vartheta_t)}{\sin(\vartheta_i - \vartheta_t)} \right|^2 .$$

where $\vartheta_i$ is the (real) angle of incidence with respect to the surface normal and $\vartheta_t$ is the complex angle of refraction in the absorbing medium. The angles $\vartheta_i$ and $\vartheta_t$ are related by Snell's law:

$$\sin\vartheta_t = \frac{\sin\vartheta_i}{n_{re} - in_{im}} \tag{5}$$

For partially p-polarized light, with degree of polarization $V_{\|}$, the surface reflectance is:

$$\Re = \left(1 - V_{\|}\right)\left(\Re_{\perp} + \Re_{\|}\right)/2 + V_{\|}\,\Re_{\|} \cdot \tag{6}$$

Experimental measurements are made with the laser beam incident at 450 to the target surface normal. Due to the beamsplitters, the light is approximately 90% p-polarized for our experimental conditions. Using the optical properties in Table I, the surface reflectance at the wavelength of the laser is 62%. In contract, if the light were unpolarized, or if the laser beam was incident perpendicular to the target, the surface reflectance of liquid Hg would be 69%.

The principal difficulty in accurately calculating the thermal conditions during the laser pulse are: 1) obtaining the correct temperature dependent thermophysical properties; 2) obtaining accurate optical constants for the surface at the wavelength of the laser; and 3) correct numerical treatment of thermophysical conditions at the target. The importance of the first two points is self-evident. Temperature dependent thermophysical properties for Hg are available from references: Touloukian 1970; Touloukian 1970; Touloukian 1970; Choyke et al. 1971; Zinov'yev and Itkin 1990; Iida and Guthrie 1993, and have been summarized in Table I. However, using temperature dependent properties will not improve the results without performing the solution on a Lagrangian mesh to account for thermal expansion. Expansion of the mesh is calculated from a linear elastic hydrostatic model of the liquid (Bennett and Krajnovich 1997). Because the timescale for sound propagation in the liquid is much shorter than that of the propagation of heat, the thermal expansion is nearly quasistatic. The coupled problems of heat transfer and thermal expansion are solved using a finite element code. The heat diffusion equation is solved with a heat generation source near the surface of the Hg specified by Equation 3. A domain 16 μm into the surface is modeled, the back surface is held at the ambient temperature. The linear elastic equations of motion of the hydrostatic fluid are solved with a free surface boundary condition applied to the surface. The lower boundary is constrained.

Figure 5 illustrates the thermal physical conditions near the liquid Hg surface at the peak of a thermal cycle

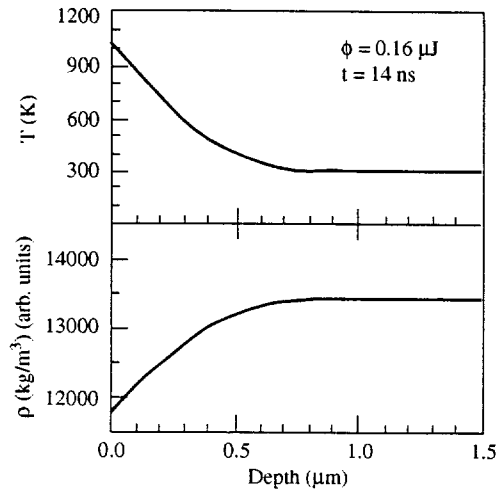


*Figure 5. Thermal physical conditions near the liquid Hg surface at the peak of the thermal cycle. Left panel the temperature distribution; right panel the density as a function of depth.*

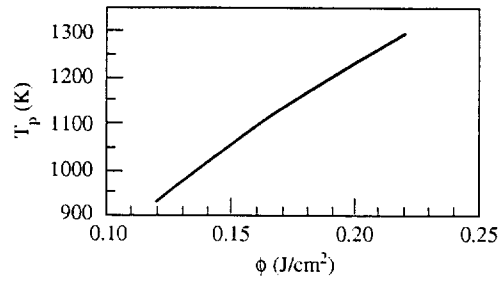


*Figure 6. Peak surface temperature as a function of pulse fluence.*

generated with a 0.16 J/cm² pulse. The top panel shows the temperature distribution below the surface of the liquid Hg. The bottom panel shows the density as a function of depth. Local values of density are determined by contrasting the current element volume with the initial value, of known density. In the calculations, densities oscillate within a few percent of value dictated by the local temperature, because of sound wave propagating through the numerical domain. Figure 6 summaries the peak surface temperature as a function of pulse fluence.

## Discussion

Using the calculated surface temperatures, the mean translational energies of distributions shown in Figure 7 are contrasted with the classical thermal expectation of

## Short Pulsed Laser Vaporization of Metals

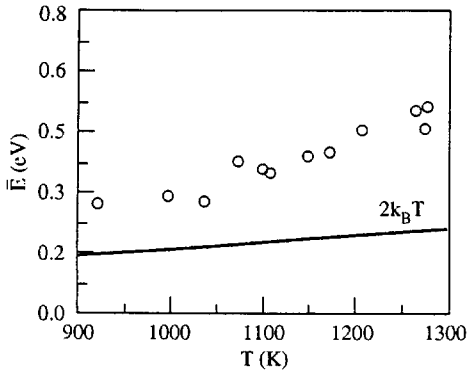


*Figure 7. Summary of measured mean translational energies versus calculated peak surface temperatures. The theoretical $2k_BT$ relation for mean translational energy is plotted as a reference.*

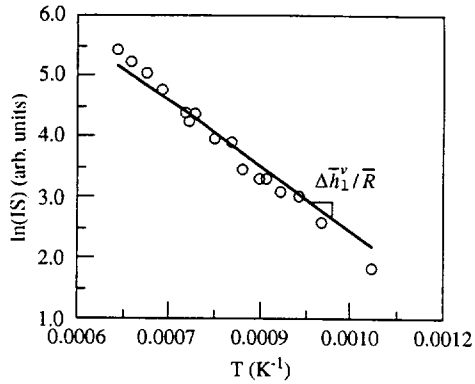


*Figure 8. Natural log of integrated TOF signal versus the reciprocal of calculated peak surface temperature. The solid lines corresponds to the anticipated slope of $-\Delta\bar{h}_\ell^v/\bar{R}$ for a thermal mediated process with $-\Delta\bar{h}_\ell^v$ = 59.1 kJ/mol for Hg.*

$\bar{E} = 2k_BT$ plotted as a line. There are two striking results. The first is that the measured translational energy of Hg significantly exceeds values for a thermal process. Measured translational energies are higher than classical expectation by about a factor of 2. The second observation is that the mean translational energies do not exhibit a $2k_B$ slope with respect to the peak surface temperature. Instead, the measured slope exceeds the classical expectation by about a factor of two. These results show clearly the inadequacy of describing vaporization kinetics using purely classical theory. The measured energies correspond to surface temperatures ranging from 1,800 K to 3,100 K, while the calculated temperatures are between 900 and 1,300 K. The critical temperature of Hg is about 1500°C, lower than any of the experimentally measured "translational-temperatures." The kinetics of vaporization might be reconciled with thermal expectation if vapor-phase heating occurs through a plasma. However, plasmas require extensive ionization of the plume, such that inverse Bremsstrahlung absorption of laser light by free electrons can occur. Since the near threshold conditions used in the TOF measurements reported here introduce many orders of magnitude fewer ions than neutrals into the plume. It is difficult to conceive that a plasma is responsible for significant heating of neutrals.

As mentioned in the introduction, another possible source for misinterpreting the vaporization energetics is collisional effects, which can change the "most-probable" flight time. However, we have determined mean translational energies from the energy distribution, and not the most probable flight time. Interatomic collisions cannot change the mean energy of the vapor plume (unless a substantial amount of vapor recondenses back to the surface of the target), and consequently cannot provide an explanation for the high observed mean translational energies. Therefore, these results provide some important facts with which to reevaluate the nature of pulsed laser vaporization of metals, and the potential role of surface plasmons. We have created experimental condition that should prohibit surface plasmon excitations but still yield superthermal vaporization kinetics. The energy distribution does not demonstrate any signature quanta characteristic of the surface plasmons energy; the shape of the energy distribution is Boltzmann (the thermal expectation) despite the fact that the energetics of vaporization is inconsistent with the surface thermal conditions.

The TOF integrated signal (IS) is a measure of the vapor-pressure generated by the laser pulse. This quantity provides another measure with which the vaporization process can be evaluated. Using the equilibrium vapor-pressure, the integrated signal can be related to temperature by:

$$ln(IS) \sim -\Delta\bar{h}_\ell^v/\bar{R}T + const. \qquad (7)$$

Equation (7) predicts that plotting $ln(IS)$ against $1/T$ will result in a straight line having slope of $-\Delta\bar{h}_\ell^v/\bar{R}$ if the vaporization process is thermally mediated. Since the vapor-pressure depends exponentially on temperature, the integrated signal is heavily weighted by peak temperature of the thermal cycle. Figure 8 plots the natural log of the integrated TOF signal against the reciprocal calculated peak surface temperature. The solid lines appearing in this figure correspond to the slope of $-\Delta\bar{h}_\ell^v/\bar{R}$ using the literature value of $-\Delta\bar{h}_\ell^v$ for Hg. The best linear fit of the experimental data in Figure 8 yields a value of 69.8 kJ/mol for the latent

heat of vaporization of Hg, 18% higher than the literature value. Within experimental errors, the vaporization yield suggests that the vaporization process is thermally mediated. In other words, the energy "bath" driving the vaporization process is the thermal energy of the surface.

Targets of Ag have been used extensively to study surface plasmons, and in several investigations to study the role of surface plasmons in non-thermal desorption (Kim and Helvajian 1991; Lee et al. 1993; Shea and Compton 1993). We have performed TOF measurements of pulse laser vaporization of Ag from a solid surface to establish whether the kinetics are distinct from what we have observed on the liquid Hg surface. The Ag surface is prepared in a manner similar to our previous study of Au (Bennett et al., 1996), in which we found, despite our best efforts to product a smooth surface, the kinetics of vaporization were superthermal. Time-of-flight measurements were made on a single-crystal Ag target held at an initial temperature of 900 K. At low initial target temperatures, measurements on Ag are contaminated by a substantial number of ions in the plume. This is due principally to the higher occurrence of vapor phase ionization resulting from a high laser intensity. Consequently, the TOF measurements on Ag have been performed holding the target at a high initial temperature, so that a lower laser fluence can be used to reach the same peak surface temperature. Measurements at this temperature have the added advantage that Ag oxide is thermodynamically unstable at 900 K. The Ag target surface was polished but not etched. Instead of etching, the selvage layer was removed with the laser in the course of taking sets of 10-shot TOF measurements. The initial TOF measurements on a previously unirradiated spot exhibited a fast contamination signal that disappeared in 10-40 laser pulses.

Figure 9 shows the N(t) distributions taken from the 5th set of consecutive 10-shot TOF measurements. The laser fluence ranges between 0.39 and 0.70 J/cm$^2$, and fluences are given explicitly in the figure caption. Figure 10 shows energy distributions corresponding to the TOF

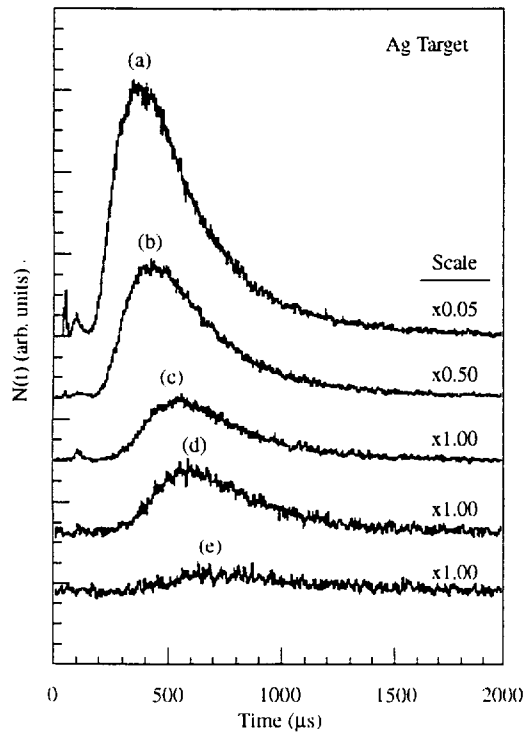


*Figure 9. Time-of-flights from the single crystal Ag target held at $T_o$=900 K. Distributions reflect the 5th set of 10-shot consecutive measurements. The five cases shown are for laser fluences of (a) 0.39, (B) 0.46, (C) 0.53, (D) 0.60 AND (E) 0.70 J/cm$^2$.*

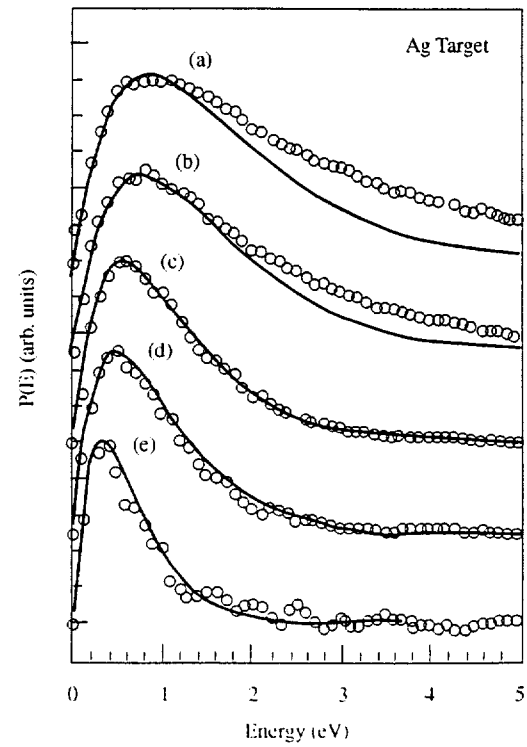


*Figure 10. Energy distributions of Ag corresponding to TOF measurements in Fig. 9. The distributions reflect the experimental measurement (o) as well as a Boltzmann fit (—) to the slow body of the distribution.*

## Short Pulsed Laser Vaporization of Metals

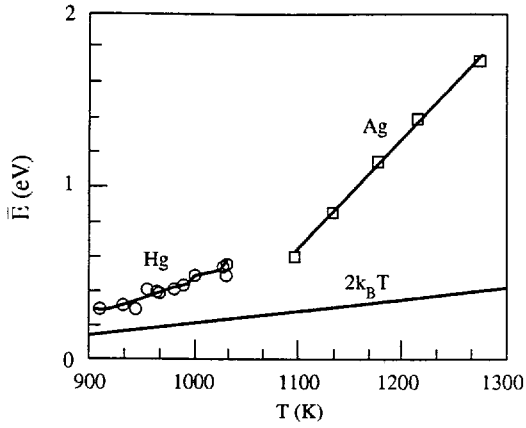


*Figure 11. Summary of measured mean translational energies versus calculated peak surface temperatures. The theoretical $2k_BT$ relation for mean translational energy is plotted as a reference.*

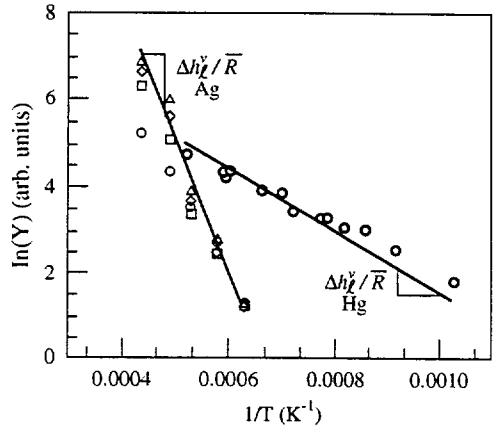


*Figure 12. Natural log of integrated TOF signal versus reciprocal of the calculated peak surface temperature. The solid lines corresponds to the anticipated slope for a thermal mediated process, where $-\Delta h_\ell^v$ = 258 kJ/mol for Ag and $-\Delta h_\ell^v$ = 59.1 kJ/mol for Hg.*

measurements shown in Figure 9. At high fluences, shown in measurements (a) and (b), the P(E) exhibits a high energy tail which may reflect the influence of laser heated ions in the vapor-phase. The reported mean energies reflect Boltzmann fits to the rising (slow) edge of measured energy distributions.

Using the calculated surface temperatures, the TOF information shown in Figures 9 and 10 can be presented in terms of peak surface temperatures generated with the laser. This is done in Figure 11, which summarizes the results of the measured translational energies for both the Ag and Hg targets. The measured translational energy of Ag substantially exceeds the thermal expectation. Measured Ag energies are a factor of 2 to 4 times the classical theory. Also, like the Hg target, the mean translational energy of Ag has a steep temperature dependence that is about $20k_B$, much greater than the classical expectation of $2k_B$. These results show clearly the inadequacy of describing vaporization kinetics using purely classical theory for Ag, but are qualitatively similar to the Hg system where the role of surface plasmons has been ruled out. For the Ag data, the actual surface temperatures would need to be between 3,500 K and 10,000 K to reconcile the measured translational energy with thermal expectation. This is in contrast to the numerically calculated peak temperatures between 1,600 and 2,300 K. While the difference between classical expectation and our measurements of Hg translational energies is not as large, the discrepancy is still significant.

The energetics of Ag vaporization is inconsistent with the surface thermal conditions. However, like Hg, the vaporization yields of Ag is consistent with a thermal process. Figure 12 plots the natural log of the integrated TOF signal against the reciprocal calculated peak surface temperature. The solid lines appearing in these figures correspond to the theoretical slope of $-\Delta h_\ell^v / R$, which is close to the experimental value.

## Conclusion

The nascent mean translational energy of vapor released in pulse laser heating fails to produce the classical $\bar{E} = 2k_BT$ expectation on liquid Hg. The observed superthermal translational energy is strong evidence that pulsed laser vaporization relies on pooling energy from the electronic structure of a metal. However, the nascent Boltzmann energy distribution and the dependence of mean translational energy on fluence do not appear to be consistent with previous views of a surface plasmon assisted desorption process. Furthermore, light coupling to surface plasmons should be prohibited for the optically smooth surface of the liquid. The measured Hg translational energies are a factor of 2 higher than classical theory, with an apparent temperature dependence that is a factor of 2 steeper than the classical expectation. However, the dependence of yield on surface temperature appears indicative of a thermal process, despite the irreconcilably high mean translational energy of the vapor. This suggests that the measured superthermal translational energy is not available

for overcoming the latent heat of vaporization, but is acquired at some point in the process of atoms leaving the surface.

Comparing the results of the Ag and Hg system, we conclude that the basic dichotomy of thermal versus non-thermal nature of vaporization is common to both systems. The basic features of vaporization appear similar in these two systems. Therefore, since the possibility of surface plasmons playing a role in vaporization in the liquid Hg system is excluded a priori, we are led to the conclusion that surface plasmons are not responsible for the superthermal character in vaporization of the Ag target.

## References

[1] T.D. Bennett, and D.J. Krajnovich, **ASME Proceedings of the 32nd National Heat Transfer Conference: Presented at the 32nd National Heat Transfer Conference,** Baltimore, Maryland, August 87-12, 1997, Baltimore, Md., ASME (1997).

[2] T.D., Bennett, D.J. Krajnovich, and C.P. Grigoropoulos, **Physical Review Letters 76**, 10, 1659 (1996).

[3] W.J. Choyke, S.H. Vosko, and T.W. O'Keeffe, **Solid State Communications 9,** 6, 361 (1971).

[4] J.W. Elam,and D.H. Levy, **J. of Appl. Phys. 81**, 1, 539 (1997).

[5] W. Hoheisel, M. Vollmer, and F. Trager, **Phys. Rev. B-Condensed Matter 48**, 23, 17463 (1993).

[6] T. Iida, and R.I.L. Guthrie, **The Physical Properties of Liquid Metals**, Oxford, Clarendon (1993).

[7] R. Kelly, and R.W. Dreyfus, **Surface Sci. 198,** 1-2, 263 (1988a).

[8] R. Kelly, and R.W. Dreyfus, **Nuclear Instruments & Methods in Physics Research, B, B32**, 1-4, 341 (1988b).

[9] H.S. Kim, and H. Helvajian, **J. of Phys. Chem. 95**, 17, 6623 (1991).

[10] I. Lee, T.A. Callcott, and E.T. Arakawa, **Phys. Rev. B-Condensed Matter 47,** 11, 6661 (1993).

[11] H.L. Lemberg, S.A. Rice, and D. Guidotti, **Phys. Rev. B (Solid State) 10**, 10, 4079 (1974).

[12] D. Pines, **Rev. of Modern Phys. 28,** 3, 184 (1956).

[13] R.H. Ritchie, J.R. Manson, and P.M. Echenique, **Phys. Rev. B-Condensed Matter 49,** 4, 2963 (1994).

[14] J.J. Shea, and R.N. Compton, **Phys. Rev. B-Condensed Matter 47,** 15, 9967 (1993).

[15] Y.S. Touloukian, **Specific Heat: Metallic Elements and Alloys,** New York, IFI/Plenum (1970).

[16] Y.S. Touloukian, **Thermal Conductivity: Metallic Elements and Alloys,** New York, IFI/Plenum (1970).

[17] Y.S. Touloukian, **Thermal Expansion: Metallic Elements and Alloys,** New York, IFI/Plenum (1970).

[18] V.E. Zinov'yev, and V.P. Itkin, **Metals at High Temperatures: Standard Handbook of Properties**, New York, Hemisphere Publishing Corp (1990).

# UCRP 1999

UNIVERSITY COLLABORATIVE RESEARCH PROGRAM

# Plasma Compression of Chirped Electromagnetic Pulses

## LS99-001

Peter Y. Cheung, Principal Investigator, UC Los Angeles
Peter Young, Co-Principal Investigator, LLNL

*Collaborators:*
D.F. DuBois and D.A. Russell, Lodestar Research Corp., Boulder, CO;
M.P. Sulzer, Arecibo Observatory, Arecibo, PR.

## Introduction

This report summarizes research progress in data analysis, in preparation and performing field experiments, and in numerical and feasible studies. The research effort involves the PI and one graduate student, Alex Ryutov.

The original proposed pulse compression experiment in laser produced plasma was not carried out under this research period. New calculations indicated that the original calculation used in the proposal contained significant errors resulting in overly optimistic estimates of experimental parameters. After careful consideration and discussion between the PIs, it is concluded that such an laboratory experiment on pulse compression would not be feasible within the proposed time period, budget, and manpower. As a result, the objectives of the research program was revised with a set of research tasks:

1. Continuation and completion of data analysis of critical layer ionospheric experiments previously funded by UCRP.
2. Implementation of testing of pulse compression concept in ionospheric experiments.
3. Perform numerical and ray-tracing calculation in support of pulse compression experiment.

## Data Analysis of Critical Layer Experiments

The study of the onset of Langmuir turbulence near the critical layer has been studies in detail. In particular, results from recent experiments at Arecibo has been analyzed. Significant progress has been made in the understanding of electrostatic turbulence driven by a high power electromagnetic wave. The diagnostic used here is the Thomson scattering radar. Several distinct and unique features of the backscattered spectra are shown in Figure 1 and can be summarized:

1. At early time, there is a separation of altitudes or "layering" of where plasma line signals originate from. The signals can be categorized as to initiate from near the reflection altitude where $\omega_{hf} = \omega_p$, from the lower matching altitudes where $\omega_{hf} \sim \omega_p$, and from intermediate altitude bounded by the two altitudes. The spectral features are very different at the different altitudes.

2. Near the reflection altitude or the first Airy maximum, the plasma line spectrum resembles that of the theoretically predicted caviton spectrum. It consists of the downshifted broad frequency continuum and the upshifted isolated free model peak. The width of the continuum is proportional to the strength of the pump. The altitude extension of the caviton continuum is generally restricted to several altitude bins (*sim* 450 m) but does tend to expand to lower altitudes as heating continues. This is illustrated by following the evolution of the spectra from T:2 to T:6. At T:6, the caviton continuum is observed to extend to lower altitudes overlapping apparently what appears to be the first and second Airy maxima.

3. Near the matching altitude, a weak signal is usually observed near but less than the pump frequency. This is the well known "decay line". As heating continues, the decay line signal can easily be masked by the stronger signal from the reflection altitude due to the cluttering effect. Secondary and tertiary decay lines are rarely seen at early times (within the first 2 ms) during cold start. However, as will be discussed later, they are commonly observed after the heater is turned off.

4. In the intermediate altitude between the reflection altitude and the matching altitude, the caviton continuum is weak but isolated free modes are commonly observed. The free mode peaks become more prominent with

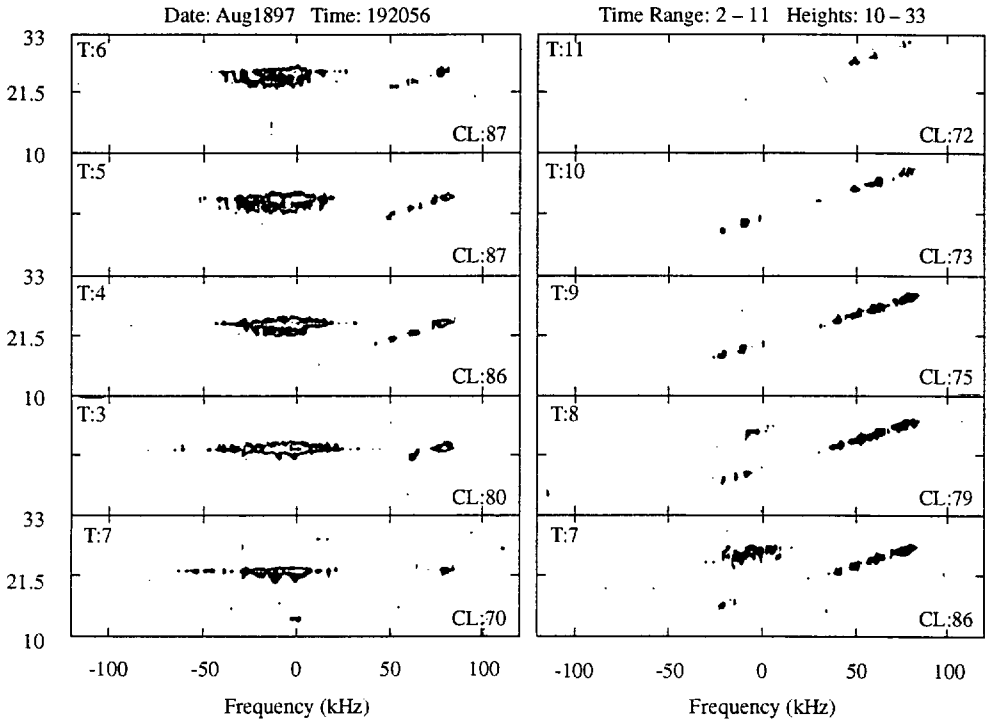


*Figure 1: Temporal and spatial evolution of Upshifted plasma line spectra.*

respect to the caviton continuum at successive lower altitudes, with correspondingly less positive frequency shifts due to the gradual decrease in local plasma density. As a result, this change in frequency versus altitude can be used to determine the local density scale length. For this set of data, the scale length is estimated to be $L \sim 42$ km.

5. The spectra unambiguously demonstrate that successive decay lines have larger frequency shifts and occur at successive lower altitudes. This is in agreement with theoretical predictions and that the turbulence occurs under cold start conditions.

As a result of this work, a manuscript is now in preparation.

## Ionospheric Experiment on Pulse Compression

A field experiment was planned for March 1999 HAARP campaign on pulse compression (a schematic of the physics of pulse compression was previously shown in our proposal). To physically implement such a experiment, the transmitter has to be programmed to launch a pulse with the frequency chirping.

$$\omega(t) = \omega\left[1 + \frac{1}{4}\frac{c^2}{l_n}(t - t_o)^2\right] \qquad (1)$$

and intensity modulation

$$I(t) = I_o \exp\left[-\frac{\omega}{\Delta\omega}\frac{1}{2}\frac{c^2}{l_n}(t - t_o)^2\right] \qquad (2)$$

where $t_o$ is a constant. Such a transmitter has to be wideband and for HAARP, a frequency sweep of over $\pm$100 kHz at the pump frequency of about 6 MHz is required. Equation (1) also shows that this frequency sweep must be achieved in about 100 μs. This chirp rate has never been attempted before until during the campaign. Significant effort was spent before and during the campaign interacting with the HAARP engineers in implementing such a scheme. In the end, the experiment was canceled at the last minute due to concern of damage to the HAARP transmitter as this is the first full power operation. The experiment has now been rescheduled for the next campaign scheduled in March, 2000.

# Plasma Compression of Chirped Electromagnetic Pulses

## Numerical and Ray Tracing Studies

In preparation for the pulse compression experiment, a numerical code has been developed to perform ray tracing study of wavepacket in magnetized, inhomogeneous plasma. Alex Ryutov, a graduate student, has made significant progress in developing such a code. This research is necessary for the planning of the experiments and the interpretation of data. A fully functioning 3D ray tracing computer code with full cold plasma dielectrics has been developed at UCLA by Crowley and Ryutov and partially funded by this grant. Future experimental research will rely heavily on the use of this computer code and the analysis of its results. Depending on its frequency and its launching angle from ground, the propagation path of a radio wave can be quite complex and can lead to unexpected results. The ray trajectory of the wave, or the direction of its group velocity, is influenced by refractive and reflective effects. In particular, the refraction and reflection of a bundle of obliquely launched rays of a given wave can lead to the formation of the so-called "caustics" where rays are horizontal and focusing of the wave energy can occur. This can lead to enhanced heating effects.

# Silicon Micromachined Scanner for Optical Coherence Tomography

**LS99-004**

Jonathan P. Heritage, Principal Investigator, UC Davis
Matt Everett, Co-Principal Investigator, LLNL
***Collaborators:***
Olav Solgaard, UC Davis
***Students:***
Kimberly T. Cornett, Paul M. Hagelin, UC Davis

A femtosecond pulse shaper employs a silicon micromachined scanning mirror (mirror width ~ 700 microns, 2 degrees angular deviation) to obtain 10 ps temporally scanned delay at ~ 100 Hz for 10 nm spectral bandwidth in a compact geometry only 5 cm long. Scaling laws establish that a compact scanner can be made for Optical Coherence Tomography applications provided methods to fabricate wider, flatter mirrors can be developed. Curvature of the scanning mirror due to residual stress in the gold-coated polysilicon mirror acts as an undesirable dispersive filter that broadens the optical pulses to 3.35 ps. The addition of a convex achromatic lens adjacent to the scanning micromirror will compensate for the mirror's measured –3 cm focal length. In addition, new mirror designs that should allow for wider and flatter scanning mirrors has been submitted to the MUMPS process for fabrication.

## Introduction and Goals

This work focuses on experimental and theoretical investigation of a Rapid Scanning Optical Delay line (RSOD) based on femtosecond pulse shaping technology[1]. We build and demonstrate a RSOD in the most compact arrangement yet presented using small conventional bulk optics combined with micromachined scanning silicon mirrors. Our objective is to evaluate the compact RSOD as a potential scanner for Optical Coherence Tomography. Optical Coherence Tomography (OCT) is a cross-sectional optical technique for high-resolution clinical imaging of microstructure in biological systems[2]. OCT performs spatially localized imaging by combining coherent signal acquisition and joint time frequency analysis of wide-band near IR radiation in a white light interferometer. The technique requires a rapid (~1-2 kHz) scanning optical delay (RSOD) in order to construct images at 4-8 Hz. The MIT group[3] introduced scanners based on femtosecond pulse shaping technology that were originally developed for femtosecond optical pulse diagnostics[1, 4] and have demonstrated quasi-real time OCT imaging with a delay length of ~3 mm.

We report here the development of compact RSOD scanners that use, for the first time, silicon micromachined scanning mirrors. Use of a micromirror opens the potential for a high speed, very compact, low mechanical vibration RSOD.

Micro-Electro-Mechanical-Systems (MEMS) is the name that describes the application and development of useful miniature machines fashioned from Silicon wafers. These devices are typically smaller than 1 mm in scale but considerable larger than the gate length of a state-of-the-art MOSFET. One example of a micromachine that can perform useful work is the electrostatically movable micromirror. For example a mirror, or arrays of mirrors, can be configured to deflect an optical beam or introduce a phase shift or bulk time delay along an optical path. Our long-term objectives are to investigate new and useful ways of controlling optical beams with micromachines for applications in biomedicine, optical switching for communications, dynamic adaptive optics, control of femtosecond optical spectrum, dynamic diffractive optics and a whole host of yet to be invented devices.

This ILSA work focused on a compact scanner built from a 600 lines/mm grating, a 2.54 cm focal length achromatic lens and the micromirror as depicted in Figure 1. We investigated this scanner's potential for use in OCT by employing ~20 nm bandwidth femtosecond pulses from a KLM modelocked Ti:Sapphire laser, operating at 840 nm. Actual operation as an OCT scanner would use a broadband superluminescent diode with as much as four times this bandwidth. The use of the narrower bandwidth from the modelocked laser is useful for developing the scanner and for establishing scaling laws.

## Compact Rapid Scanning Optical Delay Line Design

Our compact scanner uses a 600 lines/mm grating, 835 nm central wavelength with 25 nm bandwidth from a modelocked Ti:Sapphire laser. The 2.54 cm focal length (f/2 achromatic) determines the compact size shown in

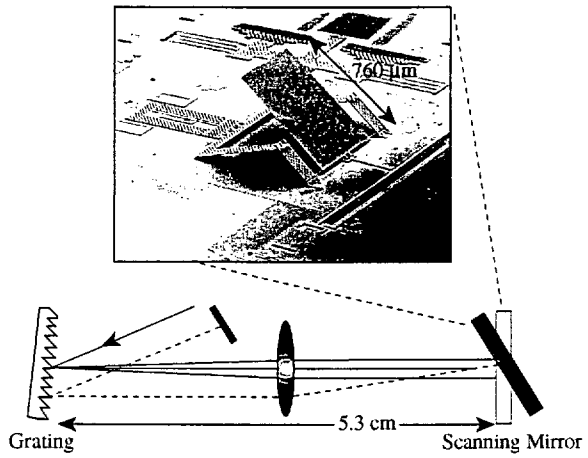


*Figure 1. Schematic of double pass rapid scanning optical delay line (DP-RSOD) with a silicon micromachined scanning mirror.*

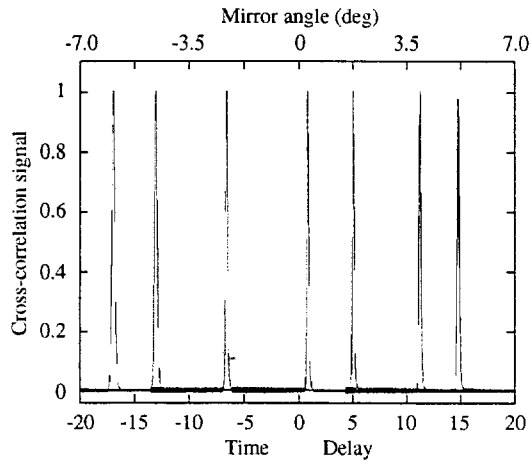


*Figure 2. 30 ps measured time delay window with bulk galvanometric mirror of a 180 fs wide correlation.*

Figure 1. The small size (765 μm width) of the scanning micromirror forces the choice of a short focal length lens to ensure that the spatially spread spectrum does not overfill the scanning mirror. This produces a small scanner but limits the temporal range of the scan. For a given set of grating parameters, the largest possible time scan is obtained when the lens is the maximum diameter. The achievable time delay can be seen from Figure 1 to arise from path-length differences at the grating as the beam is moved laterally. As expected, small f-number lenses are desired. Additional requirements are that the beam spot size on the grating be much smaller than the lens diameter. This requirement is well satisfied when the confocal range is comparable to the total path length within the pulse shaper.

Under the above conditions the time delay, is given by:

$$t_{delay} = \Delta L_{path} / c = 2\frac{2f\lambda_0\delta}{cd\cos\theta_d} \qquad (1)$$

where f is the lens focal length, $\delta$ is the mirror deflection angle, d is the grating groove spacing, and $\theta_d$ is the diffraction angle. Where the mirror width, w, must be at least as large as:

$$w = f\,\Delta\lambda / d\cos\theta_d, \qquad (2)$$

where $\Delta\lambda$ is the *full* spectral bandwidth. For the case of applying micromirrors to an OCT scanner the spectral bandwidth is very large and therefore a short focal length is required. This in turn obligates a large mirror scan angle and the necessity for a large diameter lens.

## Experimental Results with Bulk Galvo-scanning Mirror

We assess the performance of the compact RSOD optical system using a conventional optical quality, large diameter (~5 mm) mirror driven by a commercial bulk galvonometer. Figure 2 shows a 30 psec measured time window. The time window was measured by collecting the intensity autocorrelation traces at various mirror angles. Each angular trace directly corresponds to a different time delay. The seven 180 fsec FWHM intensity correlations show a delay length of 9 mm over a mirror angular scan range, $\Delta\delta$, of 14°. Some lens aberration induced broadening begins to become evident when the spectrum approaches the lens edge.

## Introduction of a Silicon Micromachined Mirror

The surface micromachined mirror used in this system is tilted out-of-plane on polysilicon hinges and is connected to the supporting frame with torsional polysilicon beams. These electrostatic mirrors have been demonstrated in a 2D raster scanning system [5] and most recently in a scalable fiber-optic switch [6]. The micromirror used in this system is rectangular with an optical surface 765 μm by 500 μm with a 50 nm aluminum coating. This micromirror has a

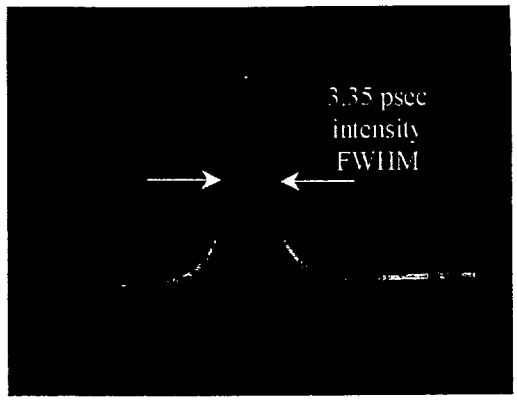


*Figure 3. Intensity autocorrelation trace of laser pulse after passing through RSOD with silicon micromachined mirror.*

resonant frequency of 550 Hz and a measured range of deflection of 16 degrees optical. Due to material-strain gradients the micromirror has a measured convex radius of curvature of 3 cm. This severe curvature imparts on the optical field spectrum a quadratic phase variation. The result is broadening of the temporal pulse upon exit from the DP-RSOD. Figure 3, shows a 3.35 psec FWHM intensity, quasi-realtime autocorrelation display, operating at 200 Hz. This result was collected without corrective optics. The micromirror was operated in its flatband region through a scan range, $\Delta\delta$ of 2° and a total time delay of 10 ps was obtained. We expect substantial improvements to the pulse width, by correcting for the curvature of the micromirror, and to the time window by operating the micromirror at its resonant frequency to achieve a scan angle closer to that of the bulk. Greater spectral bandwidth can be achieved by moving to mirrors closer to 2 mm in width.

Microphotonics, the application of MEMS technology to optics, is still in still in its infancy. This investigation has benefited microphotonics by subjecting the MEMS based RSOD performance to the scrutiny and rigorous demands of an advanced optical technology such as OCT. Mirror optical quality; e.g. flatness, reflectivity, dynamic rigidity, all must pass muster.

In the case of OCT it is quite possible that small moving mirror galvanometers will be available in a package that would make a more compact scanner viable in the near future. Integration of a MEMS scanning device into a single silicon bench remains a challenge. An abstract on this work has been submitted to the Conference on Lasers and Electro-optics (CLEO) 2000.

## References

[1] J.P. Heritage, A.M. Weiner, and R.N. Thurston, **Optics Letters 10,** 609-611 (1985).

[2] G.J. Tearney, M.E. Brezinski, B.E. Bouma, S.A. Bopart, C. Pitris, J.F. Southern, and J.G. Fujimoto, **SCIENCE 276,** 2037-2039 (1997).

[3] G.J. Tearney, B.E. Bouma, and J.G. Fujimoto, **Optics Letters 22,** 1811-1813 (1997).

[4] K.F. Kwong, D. Yankelevich, K.C. Chu, J.P. Heritage, and A. Dienes, **Optics Letters 18,** 558-560 (1993).

[5] P.M. Hagelin, K. Cornett, and O. Solgaard, **1998 IEEE LEOS Summer Topical Meeting,** Monterey, CA, 109-110 (1998).

[6] P.M. Hagelin, U. Krishnamoorthy, C.M. Arft, and O. Solgaard, **Transducers '99,** June 1999, Sendai, Japan, 782-785 (1999).

UNIVERSITY COLLABORATIVE RESEARCH PROGRAM

# Optically Induced Bragg Gratings in Phosphate Glasses

## LS99-005

Subhash H. Risbud, Principal Investigator, UC Davis
Denise M. Krol, Co-Principal Investigator, LLNL

*Student:*
Amith Murali, UC Davis

## Introduction

Rare earth doped glasses have long been of interest in the field of optics as materials for optical device fabrication. Incorporation of the rare earth ions into the glass matrix produces energy levels that make the glass optically active to laser light. Interaction between the material and laser light occurs through transitions in the energy levels of the rare earth ion. Photosensitivity of rare earth (e.g. $Eu^{2+}$, $Ce^{3+}$) doped glasses have been studied extensively, with emphasis on holographically writing Bragg gratings in glass fibers and other waveguide devices using laser light. Bragg gratings may function as filters, wavelength-selective switches, and mirrors in laser waveguide devices. Mechanisms to explain the refractive index change include local structural modification of the glass caused by localized heating as a result of excitation and nonradiative relaxation of the rare earth ion, production of color centers due to trapping of freed electrons, and densification of the glass material.

There have been several reports on photodarkening observed when thulium doped ZBLAN and aluminosilicate glass fibers were exposed to 1120 nm and 1064 nm laser light respectively. This optical attenuation in the glass is believed to be caused by a multiphoton (four or five photons) excitation scheme from the ground state of the thulium ion. It is unclear whether the production of color center defects in the glass results from complete photoionization of the ion or the absorption by the glass of UV photons from the relaxation of the excited thulium ion. Color center production results in an induced absorption change in the UV region. According to the Kramers-Kronig relations, a concomitant refractive index change can be associated with the induced absorption change in the fiber. This suggests that photodarkening may be a viable process for writing gratings in thulium doped glass materials.

Phosphate glasses possess many features that make them ideal optical materials. They are transparent over a wide range of wavelengths. Furthermore, they can readily incorporate large quantities and varieties of rare earth ion modifiers into the glass matrix, allowing for a wide range of allowed glass compositions. The flexibility in choosing the type and quantity of rare earth enables one to tailor the material to fit specific physical, chemical, and optical requirements. Phosphate glasses are currently being used in high power lasers.

In our research, we did synthesis and characterization of thulium doped lanthanum phosphate glasses and initial optical attenuation experiments to test the photosensitivity of these materials. Characterization techniques used include electron microprobe analysis (EMA), x-ray fluorescence spectroscopy (XRF), absorption spectroscopy, and $^{31}P$ magic angle spinning nuclear magnetic resonance spectroscopy ($^{31}P$ MAS NMR) to determine the chemical, structural, and optical properties of the materials. Photodarkening experiments were performed on the bulk glass samples to achieve absorption changes in the material and to determine any associated refractive index changes

## Experimental Procedure

Thulium doped lanthanum phosphate glasses were prepared using similar techniques described elsewhere on the production of lanthanum phosphate glasses. Powders of $P_2O_5$, $La_2O_3$, and $Tm_2O_3$ of 99.99% purity were mixed together in desired proportions (80% $P_2O_5$, 20 (1-x)% $La_2O_3$, 20(x)% $Tm_2O_3$ (x = 0. 0.1. 0.01, 0.001, 0.0001)) and preheated at 700° C for 1 hour in a platinum crucible. The batch mixture was then melted under atmospheric conditions and held at 1300° C for 5 hours. The temperature was reduced to 1250° C prior to pouring the melt onto a brass plate. The samples were annealed at 560° C for 1 hour and allowed to cool slowly. Each sample was cut and polished to achieve flat and parallel surfaces.

Glass compositions were determined using electron microprobe analysis (EMA) and x-ray fluorescence spectroscopy (XRF). Absorption spectra of the glasses were taken using a Perkin-Elmer Lambda 9 UV/VIS/NIR spectrometer to elucidate the energy transitions pertaining to the thulium ion. Structural characterization on the glass samples was performed using solid state NMR spectroscopy to determine the local structure of the phosphate glass. The

glass was coarsely ground in a clean mortar and pestle and passed through a 40 mesh size sieve. $^{31}P$ MAS NMR spectra were collected on a Chemagnetics CMX 400 spectrometer at 162 MHz with spinning rates of 12 kHz.

Optical attenuation experiments were conducted on 4 mm thick polished bulk samples using a Quanta Ray DCR Nd:YAG laser emitting 5 ns pulses of 1064 nm light at a 10 Hz repetition rate. Pulse energies of 25 mJ were used. The beam was focused into the glass samples using a lens with a 20 cm focal length, with the samples placed roughly 18-19 cm from the lens. The diameter of the focused spot is estimated to be roughly 1 mm. The experiment was run continuously for 3 hours. Absorption spectra of the glasses were taken before and after the experiment.

## Results and Discussion

### Chemical Characterization

Table 1 lists the theoretically calculated and experimental values as determined by EMA for the two glasses with the highest thulium concentrations (samples 4 and 5) as well as for the pure lanthanum phosphate glass (sample 1). The values agree reasonably well within experimental uncertainties. It should be noted that the phosphorus content is lower than what is theoretically expected for all samples due to volatilization losses of $P_2O_5$ during the melting process.

The concentrations of thulium in two of the glasses (samples 2 and 3) were too low to be accurately detected and measured using EMA, due to the detection limits of this technique. X-ray fluorescence spectrsocopy (XRF) is more sensitive to the presence of rare earth elements than EMA. However, it does not give absolute values of concentrations; only approximate amounts can be determined. Peak heights obtained in the spectra corresponding to specific elements are indicative of the amount of those elements present in the sample. The intensity of a peak produced by a Ge target indicates the amount of overall sample present. Comparing the ratio of the Tm and Ge peaks for various samples can give a good estimate of the relative abundance of thulium in these samples.

### Structural Characterization

NMR spectra of the highest thulium-doped glass (sample 5) and undoped glass (sample 1) showed chemical shifts for the undoped and doped glasses at -35.7 and –35.4 ppm respectively. Full width at half maximum (FWHM) values are 16.3 and 42 ppm respectively. The chemical shift values are the same within experimental uncertainties, leading to the conclusion that the phosphate structure does not change with the substitution of thulium ions for lanthanum ions. These values indicate the glass has chain-like $Q^2$ phosphate groups. The broadening of the peaks in the thulium-doped glass is due to the paramagnetic interaction with thulium. It can be concluded that the other glasses with lower thulium concentrations have the same structure as well.

### Optical Attenuation Results

Absorption spectra for samples 1 and 5, indicated that photodarkening in both glasses have occurred in the spectral region from the UV to ~1000 nm. The change in this spectral region is similar to previous published reports on photodarkening in thulium doped fibers. The magnitude of the absorption coefficient change is 1.24 $cm^{-1}$ at 400 nm. This corresponds to a transmission of 63.2% of incident light.

Previous published data showed induced absorption coefficient changes of 0.092 $cm^{-1}$ at 400 nm corresponding to 15.8% transmission. The higher transmission loss in their

*Table 1. Theoretically calculated and experimental values as determined by EMA for the two glasses with the highest thulium concentrations (samples 4 and 5) as well as for the pure lanthanum phosphate glass (sample 1).*

| | | P (atom %) | O (atom %) | La (atom %) | Tm (atom %) |
|---|---|---|---|---|---|
| Sample 1 | Theoretical | 24.24 | 69.70 | 6.06 | 0.00 |
| | EMA | 23.64 | 69.41 | 6.95 | 0.00 |
| Sample 4 | Theoretical | 24.24 | 69.70 | 6.00 | 0.06 |
| | EMA | 23.51 | 69.40 | 7.00 | 0.09 |
| Sample 5 | Theoretical | 24.24 | 69.70 | 5.45 | 0.61 |
| | EMA | 23.34 | 69.34 | 6.50 | 0.82 |

experiment despite a smaller induced absorption change is due to their use of a 40 cm long fiber.

Based upon the results for both the doped and undoped phosphate glasses, the presence of thulium is not essential for inducing absorption changes. A plausible explanation may be that the repetition rate of the laser is not fast enough to induce the multiphoton excitation process. Lifetimes of the $^3H_4$ and $^3F_4$ levels are 1.12 ms and 6.5 ms respectively (for a fluoride glass). Excited state absorption (ESA) from these levels is required for the photodarkening process. Due to the slow repetition rate of the laser, decay from these levels may occur before the laser can excite the ion upward from these levels.

Multiphoton ionization may be responsible for the observed absorption changes in both glass samples. Due to the tightly focused laser beam, the high intensity spot at the sample may allow nonlinear optical processes such as multiphoton absorption to occur. The gap between the valence and conduction band may be bridged this way. (The unfocused laser beam did not induce any absorption changes in our experiments). In fact, work has been done on focusing infrared femtosecond laser pulses inside bulk glasses to write waveguides. Production of long period fiber gratings has also been achieved using this technique.

## Summary

Thulium doped lanthanum phosphate glasses have been synthesized and chemically, optically, and structurally characterized. Photodarkening of the thulium doped and undoped glasses has been achieved, with an absorption coefficient change of 1.24 $cm^{-1}$ at 400 nm. The presence of thulium has no role on the induced changes for our experiments. A proposed multiphoton ionization due to the high intensity laser pulse may explain the changes in the absorption spectra.

UNIVERSITY COLLABORATIVE RESEARCH PROGRAM

# Computational and Experimental Development of a Compton X-ray Source

## LS99-006

Neville C. Luhmann, Jr., Principal Investigator, UC Davis
Fred V. Hartemann, Co-Principal Investigator, UC Davis

*Collaborators:*

T. Ditmire, LLNL; A. Kerman, MIT; C. Pellegrini, UC Los Angeles

*Students:*

Eric C. Landahl, James R. Van Meter, UC Davis

Compton scattering and high-gradient vacuum laser acceleration are studied theoretically and experimentally. The main thrust of this research program is the development of a laser-driven, tabletop Compton X-ray source for advanced biomedical applications. Our main results in FY99 include the demonstration of a new technique for the precise rf tuning of a 5 MeV, X-band rf gun; the development and benchmarking of a three-dimensional laser focus code; the demonstration of vacuum laser acceleration by coherent dipole radiation; the stochastic electron gas theory of coherence in Compton scattering; and the invention of a new concept for vacuum laser acceleration: the chirped-pulse inverse free-electron laser (IFEL).

We are currently conducting an in-depth theoretical and experimental analysis of the interaction between high-brightness, relativistic electron beams, and femtosecond, ultrahigh-intensity laser pulses. The two most important geometrical configurations under investigation correspond to Compton backscattering and high gradient, vacuum laser acceleration.

The motivation behind this research program is two-fold: first, tabletop, laser-based light sources hold the promise to radically transform advanced biomedical applications, including innovative cancer research; e.g., 33.1 keV X-rays are used for high-contrast angiography by imaging the K-edge of Iodine; at 1 Angstrom (12 keV), protein crystallography is revolutionizing the pharmaceutical industry by allowing the design of new drugs, as exemplified by the protease inhibitors used to decrease the viral load in HIV patients; in addition, a Compton light source based on 200 MeV electrons can create 4 MeV gamma-rays, reaching the threshold for pair-production gamma absorption; these gamma-rays penetrate deeply into high-Z materials and are extremely useful for defect imaging of manufactured components, and high-resolution flash radiography; second, compact, high-brightness electron accelerators are needed for a wide variety of applications, ranging from coherent THz radiation to the Next Linear Collider.

Within this context, we are developing two X-band (8.548 GHz) rf photoinjectors, capable of producing high-quality, relativistic electron beams, with extremely low emittance and very high peak currents (typically, 1 nC of charge generated within 1 ps, producing 1 kA of peak current). The first rf gun produces 5 MeV beams, which can generate water-window photons via Compton backscattering, while the second system, a plane-wave transformer (PWT) linac, generates 25 MeV electrons, capable of producing 1 Angstrom radiation. One of the most important experimental results achieved during FY99 is the precise, controlled tuning of the 5 MeV rf structure, using a novel rf circuit; with this technique, we have simultaneously achieved balanced pi-mode operation of the gun, which is crucial for producing high-quality beams, and critical coupling (with a reflection coefficient smaller than 1/10,000,000).

The development of a laser oscillator specifically designed to meet the stringent requirements of ultrahigh-intensity Compton backscattering, including extremely low timing jitter (< 100 fs), and excellent spatial and temporal beam quality and control, has resulted in the demonstration of a quantum-well AlGaAs semiconductor laser producing pulses with 7 nm of optical bandwidth, at repetition rates ranging between 0.595 GHz and 1.462 GHz, and externally mode-locked to the rf gun fields. We have also commissioned a 10 fs Titanium:Sapphire laser oscillator, and are currently working on the laser pre-amplified, which will produce 1 mJ at a repetition rate of 1 kHz.

Our main theoretical results include the development and benchmarking of a three-dimensional laser focus code; the demonstration of vacuum laser acceleration by coherent dipole radiation, thus clearly defining the domain of validity of the lawson-Woodward Theorem; the demonstration of vacuum ponderomotive scattering by a three-dimensional electromagnetic field distribution exactly satisfying the Lorentz-Coulomb gauge condition; the description of coherence in Compton scattering in terms of a stochastic electron gas model; the invention of a new concept for vacuum laser acceleration: the chirped-pulse inverse free-electron laser (IFEL). This last innovation is being pat-

# Computational and Experimental Development of a Compton X-ray Source

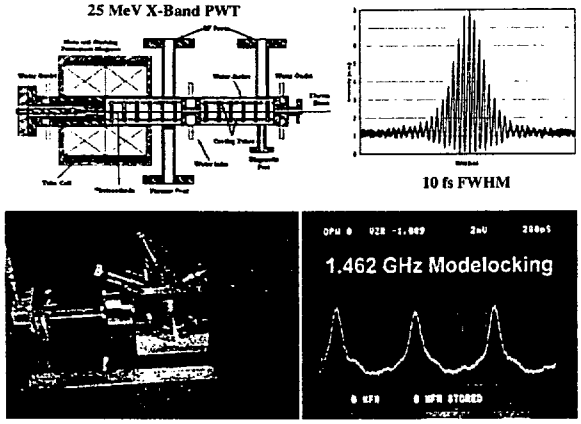


*Figure 1. Clockwise from upper left corner: 25 McV X-band PWT; 10 fs Titanium:Sapphire oscillator, 2nd-harmonic autocorrelation; 1.462 GHz QW laser modelocking; 5 MeV X-band rf gun.*

ented, and we have published a paper on this subject. The main ideas behind the chirped-pulse IFEL are the following: first, the use of an ultrashort drive laser pulse enchances the interaction bandwidth and efficiency; second, the ultrahigh intensity increases the gradient to > 1 GeV/m; finally, the chirp maintains the IFEL resonance, resulting in a high energy gain.

## References

[1] E.C.Landahl and F.V. Hartemann, **Chirped Pulse Compton Backscattering at Relativistic Intensities,** UCRL 132047.

[2] A.L. Troha, et al., UCRL 132048, **Phys. Rev. E60,** 926 (1999).

[3] F.V. Hartemannn, UCRL 133229, accepted for publication in **Phys. Rev. E.**

[4] F.V. Hartemann, et al., **High-field Electron-photon Interactions,** UCRL 133349.

[5] F.V. Hartemann, et al., UCRL 134073, **Phys. Plasmas 6,** 4104 (1999).

[6] J.R. Van meter, et al., **Reflection pf Plane Waves in Rindler Space,** UCRL 134497.

[7] F.V. Hartemann, et al., **Rf Characterization of a Tunable, High-gradient, X-band Photoinjector,** UCRL 134498.

[8] F.V. Hartemann, et al., **Ultrahigh-intensity Holographic Electron Beam Modulation and Coherent Harmonic Generation,** UCRL 134907.

[9] F.V. Hartemann and J.R. Van Meter, **Vacuum Propagation of a Near-critical Electromagnetic Wave,** UCRL 135083.

[10] J.R. Van Meter, et al., **Radiative Corrections in Symmetrized Classical Electrodynamics,** UCRL 135844.

UNIVERSITY COLLABORATIVE RESEARCH PROGRAM

# Advanced X-ray Diagnostics

## LS99-007

*Roger Falcone, Principal Investigator, UC Berkeley*
*Richard Lee, Co-Principal Investigator, LLNL*
***Collaborators:***
*Dr. Phil Heimann (ALS, LBNL)*
*Dr. Howard Padmore (ALS, LBNL)*
*Dr. Thomas Missala (ILSA, LLNL)*
*Prof. Justin Wark (Oxford)*
*Dr. Zenghu Chang (University of Michigan)*
*Prof. Henry Kapteyn (University of Michigan)*
*Prof. Margaret Murnane (University of Michigan)*
***Students:***
*Inuk Kang, Jorgen Larsson, Aaron Lindenberg, Steve Johnson, UC Berkeley*

## Abstract

Time-resolved x-ray scattering has been used toharacterize rapidly evolving material structures. Ultrafast detector technology was developed and implemented on a synchrotron beam line. We studied melting of ultrashort-pulse-laser-illuminated materials. Coherent phonons and bond breaking were measured.

## Goals

Recent developments in time-resolved x-ray diffraction, using both synchrotron and laser-plasma based sources, have led to the capability of directly observing structural phase transitions, the motion of complex molecules, and chemical reactions, on picosecond time scales. This has resulted in a number of novel experiments, including the investigation of short-pulse-laser irradiation of organic films and ultrafast laser-induced phase transitions in semiconductors. In our program, we investigate x-ray diffraction from laser-induced structural changes in materials. A bending magnet beam line at the Advanced Light Source synchrotron produces light in a broad spectrum up to photon energies of 10 keV. A Si (111) monochromator crystal selects a single wavelength with a spectral bandwidth of 1 mÅ. The diffracted beam is then directed onto a sample oriented near the Bragg angle. We use a $Ti:Al^{2}O^{3}$-based 150 fs, 1 KHz, 800 nm laser, synchronized to the individual electron bunches within the synchrotron ring with jitter less than 5 ps. The laser is incident on the sample and overlapped in both space and time with a single x-ray pulse. The time-resolved x-ray diffracted intensity following laser excitation is then measured using a streak camera detector triggered by a GaAs photoconductive switch. A CCD camera records the x-ray streak projected onto a phosphor screen. All recorded data are averaged for a period of about 1 min which corresponds to 60,000 shots. The resulting temporal resolution of the camera is 3 ps; this is monitored using an ultraviolet femtosecond pulse split off from the main pump laser.

The entire time history of the diffracted signal following laser excitation is measured at once, in contrast to more typical pump-probe geometries.

## Progress and Conclusions

At low laser fluences, impulsive excitation of a solid (in our case, InSb) induces small-amplitude, coherent atomic motion about equilibrium lattice positions. Above a critical fluence, the lattice no longer coherently oscillates about this equilibrium value, but instead is coherently driven into a disordered state. This occurs on a time scale set by one-half of a phonon period, at which point the average atomic displacement is maximum for a given mode, in analogy with the Lindemann criterion. Since the diffracted x-ray intensity does not oscillate, this is indicative of a state for which atomic motion with long-range coherence does not exist. In other words, loss of coherence on fast time scales is an indication of disorder on fast time scales. As the crystal angle is varied relative to the Bragg peak, phonons of differing wave vectors q are probed; equivalently, different length scales are being probed. Thus disorder develops over shorter length scales (large q) in less time than longer length scales (small q). One may observe a change in the diffracted intensity on arbitrarily fast time scales by tuning the crystal angle sufficiently far from the Bragg peak, presumably limited by the time scale on which the lattice stress develops.

In InSb, we observed a 3 ps drop in the diffracted intensity, faster than the thermal coupling time, and so we conclude that the first step in the observed disordering

transition at high laser fluence is the initial excitation of hot carriers which subsequently drive large-amplitude, coherent vibrational motion, a transition essentially nonthermal in nature.

In this work, we have shown that time-resolved x-ray diffraction is a useful tool in phonon spectroscopy and a sensitive probe of electron-phonon coupling strengths. For low laser fluences we measure oscillations in the x-ray diffraction efficiency corresponding to coherent phonons at frequencies up to 0.1 THz. At higher fluences a reversible phase transition has been observed, driven by large amplitude, correlated atomic motion, the first step in the approach towards disorder.

## Paper Published

A.M. Lindenberg, et al, *Time-Resolved X-Ray Diffraction from Coherent Phonons during a Laser-Induced Phase Transition,* **Phys. Rev. Lett. 84,** 111 (2000).

## Seminars and Conference Talks

R. Falcone, Seminar at LLNL, November 1999.
R. Falcone, Seminar at Princeton University, November 1999.
R. Falcone, Seminar at Harvard University, October 1999.

UNIVERSITY COLLABORATIVE RESEARCH PROGRAM

# Development of RF Photoinjector Physics and Technology

## LS99-008

James Rosenzweig, Principal Investigator, UC Los Angeles
Greg Le Sage, Co-Principal Investigator, LLNL
*Students:*
Scott Anderson, Salime Boucher, Xiadong Ding, Matt Thompson, UC Los Angeles

## Abstract

This grant supported a variety of activities aimed at development of a high brightness rf photoinjector facility Livermore to be used in tandem with the Falcon petawatt-class laser system and an existing linac. The purposes of this facility are to investigate ultra-short, mono-chromatic x-ray production using Compton scattering, and development of advanced acceleration techniques which use sub-picosecond high power lasers, electron beams, and plasma. The main research accomplished during the grant period centered on construction, characterization and commissioning of a high gradient rf photocathode gun, with associated magnetic optics components. Secondary goals dealt with emittance measurements on space-charge dominated, picosecond electron beams, and the synchronization of short electron and laser pulses.

## Scientific Goals

The primary goals of this grant were (a) to construct, and prepare for implementation and measure-ment, a state-of-the-art high-field rf photocathode gun, and (b) construct associated magnetic optics for this device. Subsequent goals intended for completion after the primary goals have been achieved were to (c) study physics issues associated with ultra-high current, low emittance electron beams, (d) study physics and technology issues concerning integration of rf photoinjectors and sub-picosecond lasers in the context of Compton scattering and laser acceleration experiments, and (e) design, and begin construction, of a bypass system which will allow the coexistence of the photoinjector source and the present thermionic electron source in the Falcon-linac facility.

## Progress Report

Considerable progress was made on this project in the past year. Most significantly, a high power, 1.625 cell S-band rf photocathode gun was constructed and commissioned. The gun design was based on the "standard" UCLA/SLAC/BNL gun which UCLA has now produced eight variants of, with a ninth in production. What sets this gun apart was the use of hot-isostatic pressure (HIP) processed copper, which allows removal of the boundaries between copper crystal grains. The gun parts were machined at UCLA at the Physics machine shop, which has considerable expertise in copper machining of rf components. The rf cold test measurements and tuning cuts on the partially-brased structure were performed by LLNL PI Greg Le Sage and UCLA collaborators at UCLA using existing UCLA equipment and a new network analyzer acquired for the project. The brazing was performed at a private company. The resulting gun was tuned for high Q, field balance and external coupling as well

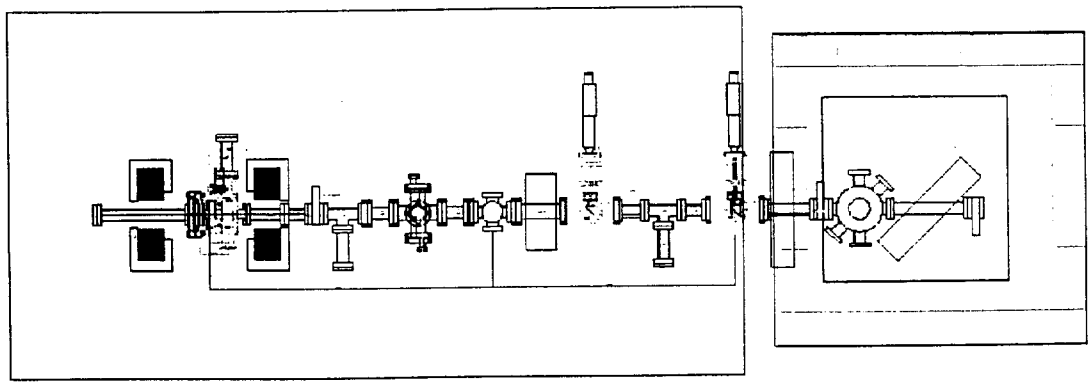

*Figure 1. Experimental arrangement for rf gun commissioning and initial Compton scattering measurements.*

or better than all previous versions of rf gun at produced UCLA. The gun has been installed at the Falcon-linac facility, and conditioned to full power (>6 MW). Initial bunches of photo-electrons have been emitted from the gun and observed on optical diagnostics.

The yoke for the magnetic focusing solenoid at gun exit was also manufactured in the UCLA shop and delivered to LLNL. Steering magnets and focusing quadrupoles for initial commissioning experiments at LLNL are presently being shipped from UCLA. A drawing of the experimental arrangement for the commissioning measurements is shown in Figure 1.

The emittance measurements in these commissioning experiments will be performed in two ways. The first is to use the emittance slit mask technique pioneered at UCLA, in which the space-charge dominate beam is sliced up into narrow, emittance-dominated beamlets by a slit array, and analyzed downstream to give a shot-by-shot reconstruction of the transverse phase space. A copy of the UCLA hardware has been purchased and assembled at LLNL by Greg Le Sage. The Labview software written at UCLA for analyzing the data in this experiment has been installed on a LLNL data acquisition computer.

The second emittance measurement technique to be used in characterizing the beam after the rf gun is the quadrupole scan. We plan to compare the results of the quad scan and slit techniques, both of which have peculiar challenges due to the strength of the "polluting" space charge forces at low energy (~5 MeV). In the case of the quad scan, we plan to show that the emittance measurement actually only produces information about the beam plasma frequency, not the phase space density. The emittance measurements will be performed with the aid of UCLA student Scott Anderson — the results will form a component of his PhD thesis.

The design of the Compton scattering experiment, as well as the bypass and matching optics that will allow the integration of the rf gun into the positron production linac at the Falcon facility, is now proceeding at LLNL and UCLA. Details of the timing issues associated with colliding sub-picosecond laser and electron pulses at this facility were examined, written up, and submitted for publication. Mechanisms for synchronization of such pulses based on chicane compressors for electrons and a newly proposed analogous path-length adjustment device have been identified in this work.

## Papers

J. B. Rosenzweig and G. Le Sage, *Synchronization of Subpicosecond Electron and Laser Pulses*, to be published in the **Proceedings of the 1998 Advanced Accelerator Concepts Workshop**.

# Thomson Scattering Measurements of Non-Maxwellian Distributions in Laser Heated Plasmas

**LS99-009**

John S. De Groot, Principal Investigator, UC Davis
Siegfried Glenzer, Co-Principal Investigator, LLNL
***Collaborators:***
Wojtek Rozmus, University of Alberta, Canada
K.G. Estabrook, LLNL
Hector Baldis, ILSA and UC Davis
Mark Foord, LLNL
***Student:***
Christian Andersen, UC Davis

The objectives of this research program which has been supported by the ILSA grant include theoretical and computational studies related to incoherent Thomson scattering (TS) experiments. Specific research objectives are:

- Theory of Thomson scattering cross-section in high-Z plasmas accounting for plasma inhomogeneity, non-Maxwellian distribution functions.
- TS as a diagnostic of the heat conductivity in classical and nonlocal regime.
- Feasibility study of x-ray Thomson scattering in dense plasmas.

The progress that has been made in meeting each of the above research objectives is detailed below.

## Theory of Thomson Scattering Spectra in High-Z Plasmas

Thomson scattering has recently been introduced as a fundamental diagnostic of plasma conditions and basic physical processes in dense, inertial confinement fusion plasmas. Experiments at the Nova laser facility have demonstrated accurate temporally and spatially resolved characterization of densities, electron temperatures, and average ionization levels by simultaneously observing Thomson scattered light from ion acoustic and electron plasma (Langmuir) fluctuations.

A high temperature plasma corona was produced by a single 3ω Nova beam which irradiated a gold disk target. A high energy 2ω TS probe was used to produce scattering signal from ion acoustic and electron plasma fluctuations. In addition, a low energy 4ω TS probe was used to characterize the coronal temperature and flow gradients of the plasma which is critical to validate cross-section calculations for the analysis of Thomson scattering spectra. During the heating of the Au disk we find an electron temperature gradient with a scale length of $L_T$ = 800 - 1800 μm. At the end of the heating the corona quickly becomes isothermal. The flow gradients are in the range of $L_v$ = 400 - 800 μm [1,2].

Detailed scattering spectra have been reproduced using generalized TS cross section for the scattered power, $P_s$, into a solid angle $d\Omega$ per frequency range $d\omega$ [3],

$$\frac{dP_s}{d\Omega d\omega} = \frac{\hat{\eta}_1 \cdot \hat{\eta}_2}{2\pi} r_0^2 \int dx S(\mathbf{k},\omega;x) n_e(x) \int d^2 r_\perp \frac{cE_0^2(r)}{8\pi},$$

where $\hat{\eta}_i (i = 1,2)$ are polarization vectors defining the directions of the Thomson probe electric field $E_0$ and of the scattered light detection; $r_0 = e^2/m_e c^2$. The dynamical form factor, $S(k,\omega;x)$ has been calculated locally to account for the spatial variations of $n_e$, $T_e$, and $V$ along the direction $x$, normal to the disk. It further includes collisional effects [4], super-Gaussian electron velocity distribution functions, and Spitzer-Harm electron transport. Ion-ion collisions are a dominant mechanism of ion wave damping in these high-Z plasmas. The width of ion acoustic resonances is due to flow and temperature inhomogeneities which are consistent with 4ω probe measurements

Using Eq. (1) in the analysis of Langmuir and ion-wave spectra we have found the averaged charge number Z with high spatial and temporal resolution. Our analysis have clearly demonstrated the importance of dielectronic recombination in these cooling high-Z plasmas. These results are important to understand the x-ray drive in inertial confinement fusion hohlraum plasmas where radiation-hydrodynamic modeling using an averaged atom model overestimates the radiation production at late times when the heater beam turns off.

UNIVERSITY COLLABORATIVE RESEARCH PROGRAM

# Thomson Scattering Measurements of Non-Maxwellian Distributions in Laser Heated Plasmas

Theoretical model of the TS data has been applied in studies of aluminium x-ray spectra [5] and in benchmarking of plasma radiation-hydrodynamical modeling [6].

## Heat Flux Measurements Using Incoherent Thomson Scattering

Experimental TS spectra often show a peak asymmetry in the ion feature corresponding to ion acoustic fluctuations propagating in the opposite directions. One possible source of this asymmetry is a presence of a heat flux. A current free plasma carrying a heat flux will have a skewed "return current" distribution in velocity space. The sound waves propagating in the direction of the temperature gradient (and opposite to the direction of the heat flux) will have a reduced Landau damping and can become even unstable for large enough heat fluxes $q \approx n_e T_e C_s$.

We have first developed the TS cross section theory for the nonequilibrium plasma where electrons are described by the perturbed Maxwellian distribution function. The deviation from a Maxwellian corresponds to the heat flux carried by electrons at velocities $\upsilon \approx 3.5\upsilon_{the}$ and to the return current of slow electrons. This distribution function has been obtained from the perturbative solution to the kinetic equation in the approximation equivalent to Spitzer-Harm transport theory and therefore it is valid for very long temperature gradient scale length $L_T, \lambda_{ei} \le 0.01 L_T$, where $\lambda_{ei}$ is an electron-ion mean-free-path. Calculations of ion acoustic fluctuation levels in such a plasma include ion-ion collisions and lead to good agreement with measured TS spectra [1].

Often in laser heated plasmas the gradient scale length is approaching values comparable with particle collision mean-free-path. In particular this is the case of gold plasmas described in Ref. [1] later in time when the main heater beam is switched off and the intense 2-ω Thomson probe starts to heat the plasma. We have used results of the nonlocal transport theory [7] to derive perturbed electron distribution function describing heat flow and the return current of electrons in this regime. By limiting a heat flux the nonlocal transport theory decreases return current of cold electrons and reduces an asymmetry of ion acoustic peaks in the TS spectrum. This also results in the higher threshold for the return current instability as compared to Spitzer-Harm transport predictions.

Using this theory we have identified the threshold for the return current instability due to localized heating from the changes of the ion acoustic peak asymmetry with probe intensity in the TS spectra. Such an instability may produce level of fluctuations which could explain an enhanced absorption of the laser light observed in recent experiments. Preliminary data from this ongoing project have been presented at the IFSA99 conference in Bordeaux.

## X-ray Thomson Scattering from Dense Plasmas

We have shown that x-ray Thomson scattering (TS) utilizing an existing table top x-ray laser [8] as a probe can be a useful and feasible diagnostic of dense hot plasmas. Feasibility of the TS experiment from the plasma produced by an ultra short laser pulse is analyzed. Plasma parameters are modelled using Lasnex code. They are used in detailed calculations of the TS cross-sections which are compared with bremsstrahlung emission levels. Necessary instrumental resolutions and sensitivities are defined for measurements of electron temperature and density fluctuations. This research was partly conducted as a summer project of Christian Andersen in collaboration with H. Baldis, M. Foord, and J. Dunn.

## References


[1] S.H. Glenzer, W. Rozmus, B.J. MacGowan, K.G. Estabrook, J.D. DeGroot, G.B. Zimmerman, H.A. Baldis, B.A. Hammel, J.A. Harte, R.W. Lee, E.A. Williams, and B. G. Wilson, **Phys. Rev. Lett., 82,** 97 (1999).

[2] S.H. Glenzer, W.E. Alley, K.G. Estabrook, J.D. De Groot, M. Haines, J.A. Hammer, J-P. Jadaud, B.J. MacGowan, J. Moody, W. Rozmus, and L.J. Suter, **Phys. Plasmas, 6,** 2117 (1999).

[3] W. Rozmus, S.H. Glenzer, K.G. Estabrook, H.A. Baldis, and B.J. MacGowan, **Modeling of Thomson Scattering Spectra in High-Z, Laser-produced Plasmas, ApJS,** in print.

[4] J. Myatt, W. Rozmus, V. Yu. Bychenkov, and V.T. Tikhonchuk, **Phys. Rev. E,** 57, 3383 (1998).

[5] L. Aschke, S. Depierreux, K.G. Estabrook, K.B. Fournier, J. Fuchs, S.H. Glenzer, R.W. Lee, W. Rozmus, R.S. Thoe, and P.E. Young, **Towards an Experimental Benchmark for Aluminum X-ray Spectra, JQSRT,** in press, (1999).

[6] S.H. Glenzer, K.G. Estabrook, R.W. Lee, B.J. MacGowan, and W. Rozmus, **Detailed Characterization of Laser Plasmas for Benchmarking of Radiation-hydrodynamic Modeling, JQSRT,** in press (1999).

[7] A.V. Brantov, V. Yu. Bychenkov, V.T. Tikhonchuk, and W. Rozmus, **Phys. Plasmas, 5**, 2742 (1998).
[8] J. Dunn, et al., **Phys. Rev. Lett., 80,** 225 (1998).

UNIVERSITY COLLABORATIVE RESEARCH PROGRAM

# Three Dimensional Particle-in-Cell Simulations of Intense Lasers Propagating in Underdense Plasma Near Quarter Critical Density

## LS99-010


Warren B. Mori, Principal Investigator, UC Los Angeles
Chris Decker, Co-Principal Investigator, LLNL

***Collaborators:***

C. Ren, UC Los Angeles
E. Esarey, LBNL

***Student:***

Brian Duda, UC Los Angeles


During the past year, we have begun to test a new three dimensional particle-in-cell (PIC) code, we have continued to develop a variational principle formalism for analyzing the evolution of finite width short-pulse lasers propagating in underdense plasmas, we have extended the variational principle to describe the evolution of single speckles of longer pulse lasers, and we have initiated PIC simulations of the coupled $2w_p$ and Raman scattering instability for short-pulses. The new code appears to be working and we have another 3D PIC code to compare results against. The variational formalism was extended to include dispersive terms and the full nonlinearities for short-pulse lasers. The long wavelength hosing described last year was published in Phys. Rev. Lett. and a long paper describing the details of the variational principle has been accepted in Phys. Rev. E.

## Code Development

Roy Hemker has continued his development of an object oriented parallelized 3D PIC code. He has been supported on another contract. The code is currently working and Brian Duda has begun to learn how to run the code. During the past six months we have begun to study the coupled two-plasma decay and Raman scattering instabilities as well as relativistic self-focusing.

## A Variational Principle Approach to Laser-Plasma Interactions

During the last year, Brian Duda developed a variational principle formalism for describing the evolution of short-pulse lasers propagating in underdense plasmas. This approach extends the work of Anderson and Bonnedal [1] to include Raman scattering and self-phase modulational type instabilities. The starting point are the by now well established model equations for describing the evolution of short-pulse lasers in plasmas,

$$\left[\nabla_\perp^2 - \frac{1}{c}\frac{\partial^2}{\partial_\psi \partial_\tau} - 2i\frac{\omega_o}{c}\partial_\tau\right]a = \frac{\omega_p^2}{c^2}(1-\phi)a$$

$$\left[\frac{\partial^2}{\partial\psi^2} + \omega_p{}^2\right]\phi = \omega_p^2\frac{|a|^2}{4}$$

where a is the normalized complex envelope of the laser, f is the scalar potential, and $\psi = t - \frac{x}{c}, \tau = \frac{x}{c}$ are the speed of the light frame variables. These equations can be obtained from the requirement that the action, $S = \int dx_\perp d\psi d\tau L$ be stationary, where

$$L(a,a^*,\phi) = \nabla_\perp a\cdot\nabla_\perp a^* - i\frac{\omega_0}{c}\left(a\partial_\tau a^* - a^*\partial_\tau a\right)$$

$$-\frac{2}{c}\left(\partial_\psi\phi\right)^2 + 2\frac{\omega_p^2}{c^2}\phi^2 - \frac{\omega_p^2}{c^2}(\phi-1)|a|^2$$

In the variational approach, carefully chosen trial functions, which have slowly varying parameters such as a spot size, a transverse centroid, a radius of curvature, and a complex amplitude, are substituted into S and the $d\vec{r}_\perp$ integration is performed. Requiring that the resulting reduced action be stationary results in coupled envelope equations for the slowly varying parameters. Last year, the above Lagrangian density was used to investigate whole beam instabilities such as hosing and spot-size self-modulation.

During the past year, the effects of dispersion were included into the variational formulation, and the work was extended to include fully nonlinear effects. The Lagrangiann density with dispersion is

$$L(a,a^*,\phi) = \nabla_\perp a\cdot\nabla_\perp a - \frac{1}{2}\left(\partial_\psi a\partial_\tau a^* + \partial_\psi a^*\partial_\tau a\right)$$

$$-i\frac{\omega_o}{c}\left(a\partial_\tau a^* - a^*\partial_\tau a\right) - \frac{2}{c}\left(\partial_\psi\phi\right)^2 + 2\frac{\omega_p^2}{c^2}\phi^2$$

$$-\frac{\omega_p^2}{c^2}(\phi-1)|a|^2$$

# Three Dimensional Particle-in-Cell Simulations of Intense Lasers Propagating in Underdense Plasma Near Quarter Critical Density

The growth rates and dispersion relations for hosing, symmetric envelope self-modulation, and asymmetric envelope self-modulation were calculated.

It was found that symmetric envelope self-modulation couples to traditional 1D forward Raman scattering, while the other two instabilities do not. The effects of this coupling were examined for a range of spot-sized, extending from the fully 3D regime, to the large spot size regime. It was found that as the initial spot size approaches infinity, the changes to laser intensity due to changes in the power are comparable to the changes caused by modulations to the spot size. We are currently trying to understand this result, as it disagrees with what we expected; that is, that the spot size modulation would asymptote to 0, as the spot size is increased. The work on dispersion is currently being written up for publication.

In addition, a variational principle for the fully nonlinear cold-plasma equations was derived which is amenable to the use of trial functions. The use of trial functions simplifies the analysis when the integrations can be carried out in the transverse coordinates. In order to carry out the transverse integrations, it is desirable that the action be written in a form that contains no square roots, or rational forms, i.e., it should be a polynominal. It is possible to construct such an action when working with the proper density, $\eta_p = \eta/\lambda$. The appropriate action is

$$S = \int d^4x \left[ \frac{1}{2}\left( \left(\vec{\nabla}\vec{a}\right)^2 - \left(\partial_\tau \vec{a}\right)^2 - \left(\vec{\nabla}\phi\right)^2 \right) + \phi + \vec{a}\cdot\vec{\nabla}\frac{\partial\phi}{\partial\tau} - \frac{\eta_p}{2}\left( \left(\phi + 1 - \frac{\partial_X}{\partial\tau}\right)^2 - \left(\vec{a} + \vec{\nabla}_X\right)^2 - 1 \right) \right]$$

Here ηp is the proper density, and $\vec{p}_c = \vec{\nabla}_X$ is the canonical meomentum. A multiple-time scale analysis was performed on this Lagrangian, and it was shown to reduce to our previous Lagrangian in the appropriate limit. This calculation was also carried out in coordinates moving with the group velocity of the pulse, which allows one to optimally include the dispersive effects for short pulses, and also allows for analytic progress to be made toward soliton and stable 3D solutions. We are still working to identify appropriate parameters for 3D PIC simulations for these effects.

## Long Wavelength Hosing

Last year we described how by linearing the coupled envelope equations obtained from the variational principle of formalism, we identified new long wavelength hosing and spot size modulation instabilities. During the first part of this year, we finished writing up these results and submitted the paper to *Physical Review Letters.* The paper has now been published [2].

## 2wp Simulations

Last year we carried out LASNEX simulations to find the scalelengths of exploding foils when the peak density falls through $n_c/4$. This work was done by the LLNL Collaborator, Dr. Chris Decker. The simulations show that irradiating a 1 μm thick tungsten foil with a 5 x $10^{14}$W/cm$^2$, 1 ns pulse gives a 50-60 μm long flat top density regions which lasts for about 50ps. We have begun to carry out 3D PIC simulations of $2\omega_p$ for appropriate scalelengths.

## Forward SBS and Self-Focusing

We have applied the variational principle formalism to the coupled forward Brillouin scattering/ponderomotive self-focusing instability. In particular, we have studied the stability of a single speckle of an ICF type of beam. We find that such a speckle is susceptible to various spot-size self-modulation and hosing instabilities with longitudinal wavelengths longer than the spreckle length. Therefore these instabilities will provide a means of interaction between speckles.

The starting equations for this problem are

$$\left(\nabla_\perp - 2i\frac{\omega_0}{c}\partial_\tau\right)a = \left(\nabla_\perp{}^2\phi\right)a$$

$$\nabla_\perp{}^2\left[\partial_\psi{}^2\phi - c_s{}^2\nabla_\perp{}^2\phi - \frac{|a|^2}{4}\right] = 0$$

where $c_s$ is the sound speed and $\nabla_\perp{}^2\phi = n_i$ is the ion density These equations can be derived from the following Lagrangian density,

$$L = \nabla_\perp a\cdot\nabla_\perp a^* + i\omega_o\left(a\partial_\tau a^* - a^*\partial_\tau a\right) - \nabla_\perp\phi\cdot\nabla_\perp aa^* - 2\left(\nabla_\perp\partial_\psi\phi\right)^2 + 2c_s{}^2\left(\nabla_\perp{}^2\phi\right)^2$$

As before, we can derive envelope equations for the spot-sizes and amplitudes of the ion wave and the laser by substituting in appropriate trial functions in $L$ and integrating in the transverse coordinates.

## Three Dimensional Particle-in-Cell Simulations of Intense Lasers Propagating in Underdense Plasma Near Quarter Critical Density

We find two distinct instabilities. One is completely analogous to the short-pulse hosing instability and it is described by the following equations

$$\partial_\tau{}^2 \chi_{a1} + \frac{P}{P_c}\frac{1}{\chi_{\Re^2}}\chi_{a1} = \frac{P}{P_c}\frac{1}{\chi_{\Re^2}}\chi_{\phi 1}$$

$$\partial_\psi{}^2 \chi_{\phi 1} + \frac{4c_s{}^2}{\omega_{0^2}}\chi_{\phi 1} = \frac{4c_s{}^2}{\omega_0{}^2}\chi_{a1}$$

where $\frac{P}{P_c} \equiv \frac{27}{1024}\frac{a^2\omega_0{}^2}{c_s{}^2}$ is the power normalized to the critical power for ponderomotive self-focusing.

The other is analgous to the short-pulse spot-size self-modulational instability and it is described by the following three coupled equations:

$$\partial_\tau{}^2 \omega_{a1} + \frac{3}{\chi_{\Re^2}}\left[1 - \frac{1}{6}\frac{P}{P_c}\right]\omega_{a1} = \frac{5}{2}\frac{P}{P_c}\frac{1}{\chi_{\Re^2}}\omega_{\phi 1}$$

$$\partial_\psi{}^2 \omega_{\phi 1} + \frac{10}{3}\frac{c_s{}^2}{\omega_{02}}\omega_{\phi 1} = \frac{\sqrt{3}}{2}\frac{c_s{}^2}{\omega_{02}}\left(\frac{1}{P/P_c}\right)\phi_1$$

$$+\frac{10}{3}\frac{c_s{}^2}{\omega_{02}\omega_{a1}}\partial_\psi{}^2\phi_1 + \frac{8}{3}\frac{c_s{}^2}{\omega_{02}}\phi_1 = \frac{\sqrt{3}}{16}\frac{P}{P}\frac{c_s{}^2}{\omega_{02}}\left[\omega_{\phi 1} - \omega_{a1}\right]$$

There are other 3D instabilities which are analogous to the short-pulse asymmetric spot size self-modulational instabilities.

## References

[1] P. Anderson and M. Bonnedal, **Phys. Fluids, 22,** 105 (1979).

[2] B.J. Duda, et al., **Phys. Rev. Lett. 83,** 1978 (1999).

# Quasi-static Investigations of High-pressure and High Temperature Dynamic Experiments

## LS99-011

Raymond Jeanloz, Principal Investigator, UC Berkeley
Robert Cauble, Co-Principal Investigator, LLNL
***Student***
Sofia Akber, UC Berkeley

We have carried out exploratory studies of the thermal equation of state, crystallographic and melting transitions, and electrical conductivity of $H_2O$ at high pressures and temperatures ($10^{10}$-$10^{11}$ Pa and 300-3000 K range) in order to complement recent and ongoing measurements using laser-driven shock waves. The properties of $H_2O$ at high pressures are of wide-ranging interest across many disciplines, from chemical physics to geophysics and planetary science (e.g., Fei, et al., 1993; Loubeyre, et al., 1999).

Our approach is to use the laser-heated diamond cell, which offers the most extensive range of static measurements to help interpret the results of dynamic experiments. Chemical reactivity makes it difficult to study $H_2O$ at high P and T under static conditions, however, as the sample is found to react chemically with most anvil, gasketting and calibration materials (e.g., oxides and metals). Hence, there is an advantage to using the temperature gradients typical of the laser-heated diamond cell (Manga and Jeanloz, 1998), as

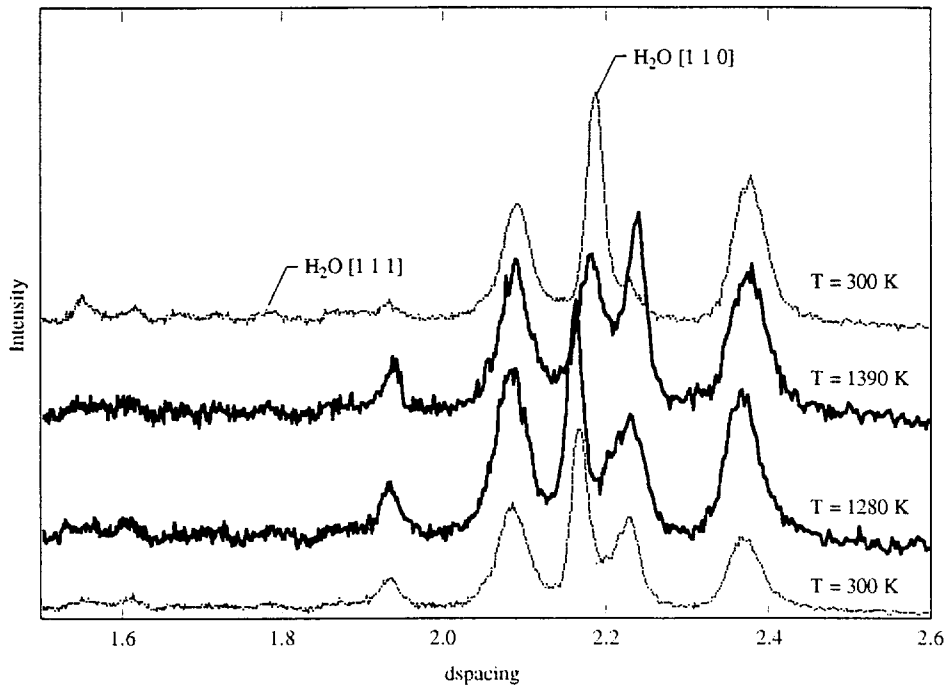


*Figure 1. X-ray diffraction patterns of $H_2O$ Ice VII at pressures between 20 and 30 GPa ([110] and [111] peaks indicated), measured in-situ with synchrotron radiation, before (dotted), during (solid) and after (dotted) heating. The data were obtained at the Advanced Photon Source (Argonne National Laboratory) using two-sided, cw YLF-laser heating, with pressures determined by an internal calibrant (Pt) and radial temperature distributions measured by spectroradiometry. Temperatures within the hottest zone exceed the melting point of $H_2O$ (middle two patterns): the crystalline (diffracting) region of the sample is at much lower temperatures (~600-750 K). The diffraction patterns confirm the identity of the crystalline phase coexisting with liquid $H_2O$ at high pressures. When properly interpreted in terms of the temperature distribution and melting temperature of the sample, these provide thermal equation of state measurements of the crystalline phase. All diffraction peaks can be explained in terms of the sample, calibrant and gasket, with no evidence of any reaction products.*

these allow the hot portion of the sample (e.g., fluid $H_2O$) to be surrounded by colder sample material, thereby minimizing the chances of spurious reactions between the sample and its surroundings.

Figure 1 shows a subset of x-ray diffraction patterns of partially molten $H_2O$ at pressures between 20 and 30 GPa, obtained in-situ (at high P and T) using synchrotron methods along with a laser-heated diamond cell. Except for the isothermal runs at 300 K (before and after heating), the quoted temperatures correspond to the hotter region within the sample, and are known to be above the melting temperature of $H_2O$. A detailed analysis of the temperature distribution makes it possible to infer the temperature of the crystalline sample (which gives the x-ray pattern) to within ±100-300 K (Manga and Jeanloz, 1998), and this is checked by varying experimental conditions. For example, heating is performed with $TEM_{00}$ (Gaussian) or $TEM_{01}$* ("doughnut") modes of the laser, and the modeling of each reveals the sample's 3-D temperature distribution and temperature-dependent thermal conductivity at high pressure (Panero, et al., 2000).

One of the key conclusions from our test runs is that it is possible to obtain measurements on $H_2O$ under static high pressures and temperatures without any evidence of contamination. The results allow us to identify the crystalline phase coexisting with fluid $H_2O$ at 20-30 GPa as being Ice VII, in good accord with previous experiments at lower pressures (Fei, et al., 1993). Furthermore, it is possible to obtain thermophysical data, with densities sufficiently well measured to obtain thermal expansion coefficients and bulk moduli as a function of pressure and temperature. A fit to the data yields a value $a \sim 25 (\pm 5) \times 10^{-5}\ K^{-1}$ for the high-temperature thermal expansion coefficient at 20-30 GPa. This is in general accord with prior results (Fei, et al., 1993), except that we infer somewhat higher melting temperatures than previously reported (as also suggested by Datchi, et al., 2000). Electrical conductivity measurements reproduce known values at low pressures, and the minimization of chemical reactions supports extending this approach to pressures in the 20-80 GPa range.

## References

[1] F. Datchi, P. Loubeyre, and R. Le Toullec, Extended and Accurate Determinations of the Melting Curves of Argon, Helium, Ice ($H_2O$) and Hydrogen, **Phys. Rev. B,** (2000).

[2] Y. Fei, H. Mao, and R.J. Hemley, Thermal Expansivity, Bulk Modulus, and Melting Curve of $H_2O$-ice VII to 20 GPa, **J. Chem. Phys., 99,** 5369 (1993).

[3] P. Loubeyre, R. Le Toullec, E. Wolanin, and D. Hausermann, Modulated Phases and Proton Centring in Ice Observed by X-ray Diffraction Up to 170 GPa, **Nature, 397,** 503 (1999).

[4] M. Manga, and R. Jeanloz, Temperature Distribution in the Laser-heated Diamond-anvil Cell, in **High-Pressure Research in Mineral Physics** (M. H. Manghnani and Y. Syono, eds.), Am. Geophys. Union, Washington, DC, 17 (1998).

[5] W. Panero, S. Morris, and R. Jeanloz, **Temperature Gradients in the Diamond Cell,** unpublished manuscript (2000).

## Presentations

L.R. Benedetti, W. Panero, and R. Jeanloz, *Structure and Density Measurements of $H_2O$ at Planetary-interior Conditions, EOS,* **Trans. Am. Geophys. Union, 80,** F629 (1999).

# UCRP 2000

UNIVERSITY COLLABORATIVE RESEARCH PROGRAM

# Advanced X-ray Diagnostics

## LS00-002


Roger Falcone, Principal Investigator, UC Berkeley
Richard Lee, Co-Principal Investigator, LLNL

***Collaborators:***

Dr. Phil Heimann (ALS, LBNL)
Dr. Howard Padmore (ALS, LBNL)
Prof. Philip Bucksbaum (University of Michigan and NSF/CUOS)
Dr. Zenghu Chang (University of Michigan and NSF/CUOS)
Prof. Margaret Murnane (University of Colorado and JILA)
Prof. Henry Kapteyn (University of Colorado and JILA)
Prof. Justin Wark (Oxford)
Dr. Jorgen Larsson (Lund Institute of Technology)

***Students:***

Aaron Lindenberg, Steve Johnson (Physics Department, UC Berkeley)

***Post Docs:***

Inuk Kang, Thomas Missalla (Physics Directorate, LLNL)



## Abstract

We implemented a new x-ray beamline at the Advanced Light Source Synchrotron at LBNL This beamline is dedicated to time-resolved x-ray scattering spectroscopies of laser-illuminated materials. Time-resolved x-ray diffraction with picosecond temporal resolution was used to observe scattering from impulsively generated coherent acoustic phonons in laser-excited InSb crystals. The observed frequencies and damping rates are in agreement with a model based on dynamical diffraction theory coupled to analytic solutions for the laser-induced strain profile. The results are consistent with a 12 ps thermal electron-acoustic phonon coupling time together with an instantaneous component from the deformation-potential interaction. Above a critical laser fluence, we show that the first step in the transition to a disordered state is the excitation of large amplitude, coherent atomic motion. Additionally we observed coherent control of laser-excited strain waves in InSb material by using a timed-array of short laser pulses. Finally, we implemented a new program in warm dense matter, and observed laser-heated Si, where we see changes in L-edge absorption features of material warmed impulsively to about 1 eV.


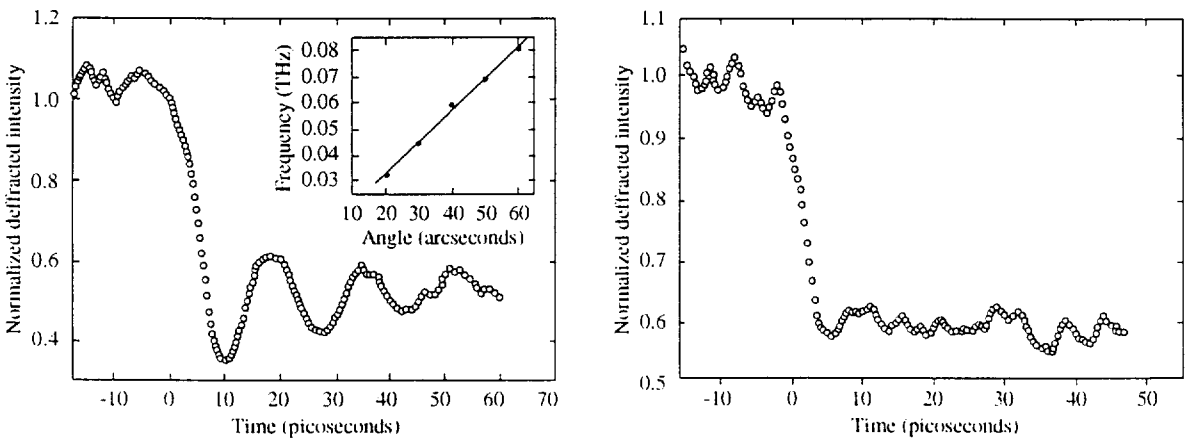


*Figure 1. (left) Sinusoidal modulation of x-ray diffraction by coherent acoustic phonons measured at 40 arcsec away from the (111) Bragg peak of InSb. The inset shows the phonon frequencies measured at different angular deviations from the Bragg peak (right). At higher fluence, rapid disordering is indicated by the prompt drop in the diffraction efficiency and absence of vibrational coherence.*

## Scientific Goals

The goals of the project were to develop the capability for time resolved x-ray scattering studies, and to study materials in the range of one-photon-absorbed per unit cell. This energy deposition leads to high-pressure, propagating strain waves, structural phase transitions, and opacity changes in the x-ray spectrum. It is the goal of our work to understand these processes and their inter-relation.

## Progress and Conclusions

A fully functional x-ray beamline was established, with a laser system synchronized to synchrotron x-ray pulses, and an x-ray streak camera detector with picosecond resolution. Experiments were performed on coherent strain wave propagation in materials, melting of materials using ultrashort pulse lasers, coherent control of strain waves in materials, and edge absorption shifts in rapidly heated materials. We observed both thermal and non-thermal components in laser-induced disorder in materials, and have shown that it is possible to control strain in materials through a multiple pulse laser pulse sequence.

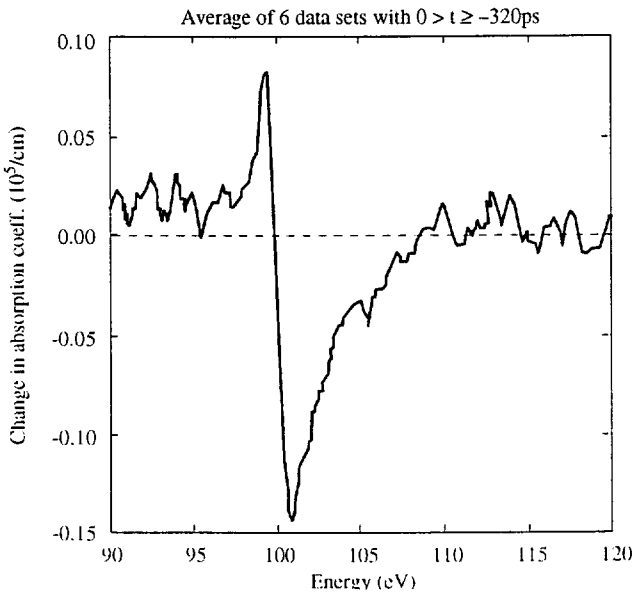


*Figure 2. Change in absorption coefficient in a heated, 100-nm thick Si foil. We are beginning to model this system, and the explanation of the first results, shown in Fig. 2 are in qualitative agreement with a model of carrier excitation above the edge and carrier depletion below the edge, upon laser-excitation.*

The major results of this study are in Phys. Rev. Lett. **84**, 11 (2000). Perhaps the most interesting results are shown in figure 1, which indicates the oscillation of x-ray diffracted signal from a particular phonon frequency associated with the intense strain wave induced by an ultrashort pulse laser incident on InSb, and then the disorder induced by the laser as the intensity was increased.

Results from the warm dense matter work are currently being written up for publication. Initially we see changes in the L-edge absorption in laser-heated Si foils at temperatures of about 1 eV. The difference in the edge absorption, over a 320 picosecond period are fairly constant, and shown in figure 2.

Papers in preparation, describing additional work on our beamline and involving the same participants, include coherent control studies and work on time-resolved x-ray measurements of polaron dynamics of charge-ordered Nd1 / 2Sr1 / 2MnO3.

## Papers Published

A.M. Lindenberg, I. Kang, S.I. Johnson, T. Missalla, P.A. Heimann, Z. Chang, J. Larsson, P.H. Bucksbaum, H.C. Kapteyn, H.A. Padmore, R.W. Lee, J.S. Wark, R.W. Falcone, *Time-Resolved X-Ray Diffraction from Coherent Phonons during a Laser-Induced Phase Transition*, Phys. Rev. Lett, **84**, 111 (2000).

## Conference Proceedings

P.A. Heimann, T. Missalla, A. Lindenberg, I. Kang, S. Johnson, Z. Chang, H.C. Kapteyn, R.W. Lee, R.W. Falcone, R.W. Schoenlein, T.E. Glover, A.A. Zholents, M.S. Zolotorev, and H.A. Padmore, *Time-resolved X-ray Photoabsorption and Diffraction on Timescales From ns to fs*, in X-ray and Inner-shell Processes, AIP conference proceedings, 506, p. 664-668.

P.A. Heimann, T. Missalla, A. Lindenberg, I. Kang, S. Johnson, Z. Chang, H.C. Kapteyn, R.W. Lee, R.W. Falcone, R.W. Schoenlein, T.E. Glover, A.A. Zholents, M.S. Zolotorev, and H.A. Padmore, *Time-resolved X-ray Photoabsorption and Diffraction on Timescales from ns to fs*, in National Synchrotron Radiation Instrumentation, Stanford, CA., October 13-15, 1999.

P.A. Heimann, A.M. Lindenberg, I. Kang, S. Johnson, T. Missalla, Z. Chang, R.W. Falcone, R.W. Schoenlein, T.E. Glover, and H.A. Padmore, *Ultrafast X-ray Diffraction of Laser-irradiated Crystals*, in Nuclear Instruments and Methods A (to be published).

# Advanced X-Ray Diagnostics

## List of Talks

*(by R. Falcone except where noted)*

Harvard University, Division of Applied Sciences Seminar, October 1999, Cambridge, MA., *Time Resolved X-Ray Scattering Studies of Materials Dynamics.*

National Synchrotron Radiation Instrumentation Conference, Stanford, CA., October 1999, *Time-resolved X-ray Photoabsorption and Diffraction on Timescales from ns to fs*, (P. Heimann).

LLNL Materials Research Institute, November 1999, Livermore, CA., *Picosecond X-Ray Scattering Studies of Materials Dynamics.*

Princeton University, Department of Mechanical and Aerospace Engineering Seminar, November 1999, Princeton, NJ., *Time-Resolved X-Ray Diffraction and Material Dynamics.*

Basic Energy Sciences Advisory Committee Review of the LBNL Advanced Light Source, February 2000, Berkeley, CA., *Coherent Phonons in Semiconductors.*

APS March Meeting, March 2000, Minneapolis, MN, "Ultrafast time-resolved x-ray measurements of polaron dynamics of charge-ordered Nd1 / 2Sr1 / 2MnO3" (I. Kang).

UC Berkeley, Physics Department Colloquium, April 2000, Berkeley, CA., *Laser-Induced Material Dynamics.*

International Workshop on Warm Dense Matter, Vancouver, Canada, May 2000, *Time-resolved X-ray Measurement of Warm Matter Using Synchrotron Radiation*, (P. Heimann).

QELS 2000, May 2000, San Francisco, CA., *Time-resolved X-ray Measurements of Polaron Dynamics of Charge-ordered Nd1 / 2Sr1 / 2MnO3*, (I. Kang).

Twelfth International Conference on Ultrafast Phenomena, July 2000, Charleston, SC, *Time-resolved X-ray Measurements of Polaron Dynamics of Charge-ordered Nd1 / 2Sr1 / 2MnO3*, (I. Kang).

7th International Conference on Synchrotron Radiation Instrumentation, Berlin, Germany, August 2000, *Ultrafast X-ray Diffraction of Laser-irradiated Crystals*, (P. Heimann).

LBNL Scientific Support Group Seminar, September 2000, Berkeley, CA., Time-Resolved Spectroscopy.

European Conference on Lasers and Electro-Optics, September 2000, Nice, France, *Time-Resolved X-Ray Scattering from Ultrashort-Pulse Laser Illuminated Materials.*

Laboratoire d'Optique Appliquee-ENSTA, September 2000, Palaiseau, France, *Time-Resolved X-Ray Scattering.*

University of Oregon, Physics Department Colloquium, October 2000, Eugene, OR., *Ultrafast Laser Induced Material Dynamics.*

Workshop on Detectors for Synchrotron Research, October 2000, Washington, D.C., *Ultrafast Dynamics in Solids.*

LBNL Advanced Light Source Users' Meeting, October 2000, Berkeley, CA., *Time-Resolved X-Ray Scattering Studies.*

3rd International Swiss Light Source Workshop, October 2000, Les Diablerets, Switzerland, *Ultrafast Time-resolved X-ray Diffraction Studies of Lattice Dynamics in Solids*, (S. Johnson).

LBNL Science Policy Board Meeting, December 2000, Berkeley, CA., *Femtosecond Science.*

## Poster Papers

Eighth International Conference on Electronic Spectroscopy & Structure, Berkeley, CA., August 2000, *Ultrafast Time-resolved X-ray Measurements of Polaron Dynamics of Change-Ordered Nd1 / 2Sr1 / 2MnO3*, (S. Johnson).

# Three Dimensional Particle-in-Cell Simulations of Intense Lasers Propagating in Underdense Plasma Near Quarter Critical Density

**LS00-003**

Warren B. Mori, Principal Investigator, UC Los Angeles
Chris Decker, Co-Principal Investigator, LLNL

***Collaborators:***

C. Ren, UC Los Angeles

***Student:***

Roy Hemker, Brian Duda UC Los Angeles

During the first six months this grant supported a student, Roy Hemker, for code development, and during the past year it has supported a new student, Brian Duda. This multi-year project will constitute a large fraction of Brian's Ph.D. research. During the first 18 months of this project, we have made considerable progress in several areas. These can be summarized by the following list of major accomplishments:

## Code Development

During the past year Roy Hemker has continued his development of an object oriented parallelized 3-D PIC code while being supported on another contract. The code is currently working and Brian Duda has begun to learn how to run the code. During the next six months, we will begin to use this multi-dimensional code study the coupled two-plasma decay and Raman scatttering instabilities, as well as relativistic self-focusing. Furthermore, we will use the PIC code to study the coupled self-modulational processes that we have discovered using the variational principle described next. The code is already being used to study the generation of single cycle pulses via photon deceleration.

## A Variational Principle Approach to Laser-Plasma Interactions

During the past year, Brian Duda developed a variational principle formalism for describing the evolution of short-pulse lasers propagating in underdense plasmas. This approach extends the work of Anderson and Bonnedal [17] to include Raman scattering and self-phase modulational type instabilities. The starting point is the by now well established model equations for describing the evolution of short-pulse lasers in plasmas,

$$\left[\nabla_\perp^2 - \frac{1}{c}\frac{\partial^2}{\partial_\psi \partial_\tau} - 2i\frac{\omega_0}{c}\partial_\tau\right]a = \frac{\omega_{p^2}}{c^2}(1-\phi)a$$

$$\left[\frac{\partial^2}{\partial_\psi{}^2} + \omega_{p^2}\right]\phi + \omega_{p^2}\frac{|a|^2}{4}$$

where a is the normalized complex envelope of the laser, $\Phi$ is the scalar potential, and $\psi = t - \frac{x}{c}, \tau = \frac{x}{c}$ are the speed of light frame variables.

These equations can be obtained from the requirement that the action, $S = \int dx_\perp d\psi d\tau L$ be stationary, where

$$L(a,a^*,\phi) = \nabla_\perp a \cdot \nabla_\perp a^* - i\frac{\omega_0}{c}\left(a\partial_\tau a^* - a^*\partial_\tau a\right)$$

$$-\frac{2}{c}\left(\partial_\psi \phi\right)^2 = +2\frac{\omega_{p^2}}{c^2}\phi^2 - \frac{\omega_{p^2}}{c^2}(\phi - 1)|a|^2$$

In the variational approach, carefully chosen trial functions, which have slowly varying parameters such as a spot size, a transverse centroid, a radius of curvature, and a complex amplitude, are substituted into S and the $d\vec{x}_\perp$ integration is performed. Requiring that the resulting reduced action be stationary results in coupled envelope equations for the slowly varying parameters. Last year, the above Lagrangian density was used to investigate whole beam instabilities such as hosing and spot-size self-modulation. Using the variational principle approach, we identified new long wavelength hosing and spot size modulation instabilities which can occur at or above quarter critical density. These instabilities grow as exp $[\{(P/P_c)(kc/w_p)\}^{1/2} z/z_R]$ where $P/P_c$ is the laser power to the critical power for self-focusing, k is the wavenumber of the instability, z is the distance the laser has propagated into the plasma, and $z_R$ is the Rayleigh length. These instabilities are whole beam analogs for relativistic self-phase modulation and filamentation. We have also studied asymmetric self-focusing and asymmetric envelope self-modulation. These results indicate that under appropriate conditions, i.e., $P/P_c > 3$, any asymmetry will be reinforced.

UNIVERSITY COLLABORATIVE RESEARCH PROGRAM

# Three Dimensional Particle-in-Cell Simulations of Intense Lasers Propagating in Underdense Plasma Near Quarter Critical Density

Recently the effects of dispersion were included into the variational formulation, and the work was extended to include fully nonlinear effects. The Lagrangian density with dispersion is

$$L(a,a^*,\phi) = \nabla_\perp a \cdot \nabla_\perp a$$
$$-\frac{1}{2}\left(a_\psi a\partial_\tau a^* + \partial_\psi a^* \partial_\tau a\right)$$
$$-i\frac{\omega_o}{c}\left(a\partial_\tau a^* - a^*\partial_\tau a\right) - \frac{2}{c}\left(\partial_\psi \phi\right)^2$$
$$+2\frac{\omega_{p^2}}{c^2}\phi^2 - \frac{\omega_{p^2}}{c^2}(\phi-1)|a|^2$$

The growth rates and dispersion relations for hosing, symmetric envelope self-modulation, and asymmetric envelope self-modulation were calculated. It was found that symmetric envelope self-modulation couples to traditional 1D forward Raman scattering, while the other two instabilities do not. The effects of this coupling were examined for a range of spot-sizes, extending from the fully 3D regime, to the large spot size regime. It was found that as the initial spot size approaches infinity, the changes to laser intensity due to changes in the power are comparable to the changes caused by modulations to the spot size. We are currently trying to understand this results, as it disagrees with what we expected, that is that the spot size modulation would asymptote to 0, as the spot size is increased. We are currently writing a paper which describes the variational principle concept.

In addition, a variational principle for the fully nonlinear cold-plasma equations was derived which is amenable to the use of trial functions. The use of trial functions simplifies the analysis when the integration can be carried out in the transverse coordinates. In order to carry out the transverse integration, it is desirable that the action be written in a form that contains no square roots, or rational forms, that is — a polynomial. It is possible to construct such an action when working with the proper density, $n_p = n/\gamma$. The appropriate action is:

$$S = \int d^4x \left[ \begin{array}{l} \frac{1}{2}\left(\left(\vec{\nabla}\vec{a}\right)^2 - \left(\partial_t \vec{a}\right)^2 - \left(\vec{\nabla}\phi\right)^2\right) + \phi + \vec{a}\cdot \\ \vec{\nabla}\frac{\partial\phi}{\partial t} - \frac{n_p}{2}\left(\left(\phi + 1 - \frac{\partial\chi}{\partial t}\right)^2 - \left(\vec{a} + \vec{\nabla}\chi\right)^2 - 1\right) \end{array} \right]$$

Here, $n_p$ is the proper density, and $\vec{p}_c = \vec{\nabla}\chi$, is the canonical momentum. A multiple-time scale analysis was performed on this Lagrangian, and it was shown to reduce to our previous Lagrangian in the appropriate limit. This calculation was also carried out in coordinates moving with the group velocity of the pulse, which allows one to optimally include the dispersive effects for short pulses, and also allows for analytic progress to be made toward soliton and stable 3D solutions. We are currently working to identify appropriate parameters for 3D PIC simulations of these effects. Portions of this work are being written up for publication.

## Long Wavelength Hosing

We have carried out large scale 2D PIC simulations of hosing for parameters of relevance to current experiments. These simulations indicate that the new long wavelength regime dominates the behavior of a short-pulse laser. During the first part of this year, we finished writing up the long wavelength hosing results and submitted the paper to Physical Review Letters.

## $2\omega_p$ Simulations

During the first 18 months, we have also carried out LASNEX simulations to find the scale lengths of exploding foils when the peak density falls through $n_c/4$. This work was done by the LLNL Collaborator, Dr. Chris Decker. The simulations show that irradiating a 1 μm thick tungsten foil with a 5 x $10^{14}$ W/cm$^2$, 1 ns pulse gives a 50-60 μm long flat top density regions which lasts for about 50ps. We have begun to carry out 2D and 3D PIC simulations of $2\omega_p$ for appropriate scale lengths.

## Mutual Attraction Between Lasers in Plasmas

During the last half year, we have been investigating the mutual interaction between two or more laser pulses in plasmas. We have concentrated on the relativistic nonlinearity, but the results can be generalized to other nonlinearities. The starting point is to describe the propagation of two by two coupled nonlinear Schrodinger equations for the envelopes each lasers' vector potential

$$\left(\nabla_\perp^2 + 2ik_0\partial_z - k_p^2\right)a_1 = -\frac{k_p^2}{4}\left(|a_1|^2 + |a_2|^2\right)a_1,$$

$$\left(\nabla_\perp^2 + 2ik_0\partial_z - k_p^2\right)a_2 = -\frac{k_p^2}{4}\left(|a_1|^2 + |a_2|^2\right)a_2.$$

# Three Dimensional Particle-in-Cell Simulations of Intense Lasers Propagating in Underdense Plasma Near Quarter Critical Density

For simplicity we assume that the two lasers are polarized in mutually orthogonal directions. Obtaining exact solutions to these two coupled equations is not possible. However, approximate and parameterized solutions which illustrate mutual attraction can be obtained using variational principle methods. The Lagrangian density for the coupled equations is

$$L=\sum_{j=1,2}\left[ik_0\left(a_j\frac{\partial a_j^*}{\partial\tau}-a_j^*\frac{\partial a_j}{\partial\tau}\right)+\nabla_\perp a_j^*\cdot\nabla_\perp a_j-k_p^2\left(\frac{a_j^2a_j^{*2}}{8}-a_ja_j^*\right)\right]-k_p^2a_1a_1^*a_2a_a^*.$$

Using this Lagrangian density and a Gaussian trial function for the laser envelopes,

$$A_je^{-i\theta_j}e^{i[k_{xj}(x-X_{cj})+k_{yj}(y-Y_{cj})]}e^{[(x-X_{cj})^2+(y-Y_{cj})^2](ik_0/2R_j-1/W_j^2)}.$$

We can integrate the Lagrangian density in the transverse (x,y) plane and obtain a reduced Lagrangian density

$$L\equiv\frac{2}{\pi}\int_{-\infty}^{\infty}dx\int_{-\infty}^{\infty}dyL$$

$$=\sum_{j=1,2}\{\frac{k_0A_j^2W_j^2}{4}[8\frac{d\theta_j}{d\tau}+\frac{2k_0W_j^2}{R_j^2}\frac{dR_j}{d\tau}-8(k_{xj}\frac{dX_{cj}}{d\tau}-+k_{yj}\frac{dY_{cj}}{d\tau})]$$

$$+\frac{A_j^2}{4}[\frac{2k_0^2W_j^4}{R_j^2}+8+4W_j^2(k_{xj}^2+k_{yj}^2)]+k_p^2W_j^4(A_j^2-\frac{A_j^4}{16})\}$$

$$-\frac{k_p^2}{4}A_1^2A_2^2\frac{W_1^2W_2^2}{W_1^2+W_2^2}e^{-2\left[\left(X_{c1}-X_{c2}\right)^2+\left(Y_{c1}-Y_{c2}\right)^2\right]/\left(W_1^2+W_2^2\right)}.$$

The Euler-Lagrange equations for this reduced Lagrangian give the equations of motion for the laser centroids (Xcj, $Y_{cj}$). The motion of the centroids turns out to be just like point mass, with the mass proportional to the beam power, moving under a mutually attractive force,

$$P_j\frac{d^2\vec{r}_j}{d\tau^2}=-\frac{\partial}{\partial\vec{r}_j}[-\frac{k_p^2}{8k_0^2}\frac{P_1P_2}{W_1^2+W_2^2}\exp(-\frac{2d^2}{W_1^2+W_2^2})],$$

$$d^2\equiv\left(\vec{r}_1-\vec{r}_2\right)^2=\left(X_{c1}-X_{c2}\right)^2+\left(Y_{c1}-Y_{c2}\right)^2,P_j\equiv A_j^2W_j^2.$$

We have verified the mutual attraction in PIC simulations using OSIRIS. We have written up this work for publication. Dr. Chuang Ren is helping with the analytical work and with the simulations.

UNIVERSITY COLLABORATIVE RESEARCH PROGRAM

# Spectroscopic Analysis of Shock Precursor Radiation from Laser Generated Blast Waves

## LS00-004

Robert J. Cattolica, Principal Investigator, UC San Diego
Todd Ditmire, Co-Principal Investigator, LLNL

Blast waves generated by a femtosecond laser (20 mJ, 30 fs @ 820 nm) were used to produce radiating cylindrical shock waves in Argon, Xenon, and Krypton pulsed free jets. Spectroscopic observations of the radial distribution of emission across the cylindrically expanding shock wave in the near uv (250 -350 nm) were obtained with 0.35 meter spectrometer with a gated imaged intensified CCD camera that provided 2ns temporal resolution. Temporally resolved spectroscopic measurements were obtained over the first 200ns in the developing radiating shock waves. Analysis of the emission spectra for the Argon data indicates the presence of Ar II, Ar III, and Ar IV. This data is currently under analysis to provide radial distribution of these ionized Argon species through the shock waves to determined there relative density distributions from which a gas temperature can be calculated. Similar data analysis is also continuing for laser generated radiating shock waves in Xenon and Krypton shock waves.

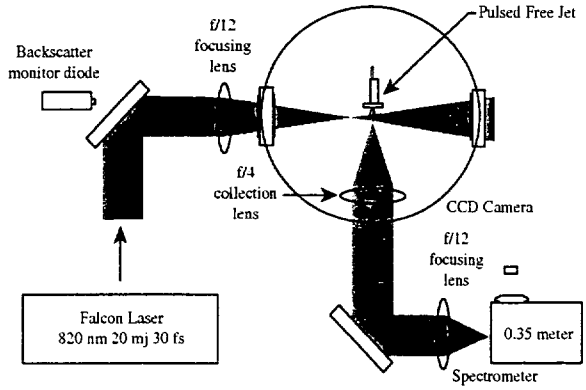


*Figure 1. Laser generated shock wave experimental setup in Falcon Laser Facility: laser beam backscatter monitor and 0.35 meter sprectrometer and gated CCD camera for temporally resolve emission measurements.*

## Scientific Goals

In the formation of interstellar shocks formed by collapsing supernova, the effects of radiation transport are important and can dramatically affect the shock dynamics. Radiation transport affects the shock dynamics in the interstellar medium in a number a ways, such as by radiative cooling and via the formation of a radiative precursor ahead of the shock front.

At Lawrence Livermore National Laboratories (LLNL) a unique laser systems provides the means to produce laboratory plasmas. These laser-generated plasmas produce shock physics with relevance to the understanding of interstellar shocks and validation of plasma codes. Using the Falcon laser system (820 nm , 20 mJ , 30 femtosecond) laser pulses were used to generate shock waves in Hydrogen, Argon, and Xenon. Of particular interest is the appearance of radiative precsor emission ahead of a Mach number 50 shock waves produced in Xenon. Comparison of these experimental results with a simulation using the LASNEX plasma simulation code also predicts radiative precursor emission. The goal of this research project is to perform experiments in which the emission spectrum from laser generated shock waves is spatially and temporally resolved to investigate the structure and mechanism of the formation of the radiative precursor emission ahead of the shocks. For this purpose an imaging spectrometer was designed and constructed and experiments conducted in Argon, Xenon, and Krypton in pulsed free jets.

## Progress and Conclusions

The basic experimental setup for the study of laser generated blast waves and the subsequent development of a hypersonic shock is illustrated in Figure 1.

The design of the optical system used in the experiment and the modification of a 0.35 meter imaging spectrograph to accommodate a gated, imaged-intensified CCD camera were accomplished in the last quarter of 1999. The new imaging spectrograph system was assembled, tested, and calibrated and installed in the Falcon laser facility during the first quarter of 2000. Preliminary experiments on Argon shock waves generated with the Falcon Laser were initiated during the second quarter of 2000. Production experiments on Argon, Xenon, and Krypton for a range of free jet source pressure were conducted during the third quarter (summer 2000).

An example of the type of emission spectra obtained from a radiating shock wave in Argon is presented in Figure 2.

# Spectroscopic Analysis of Shock Precursor Radiation from Laser Generated Blast Waves

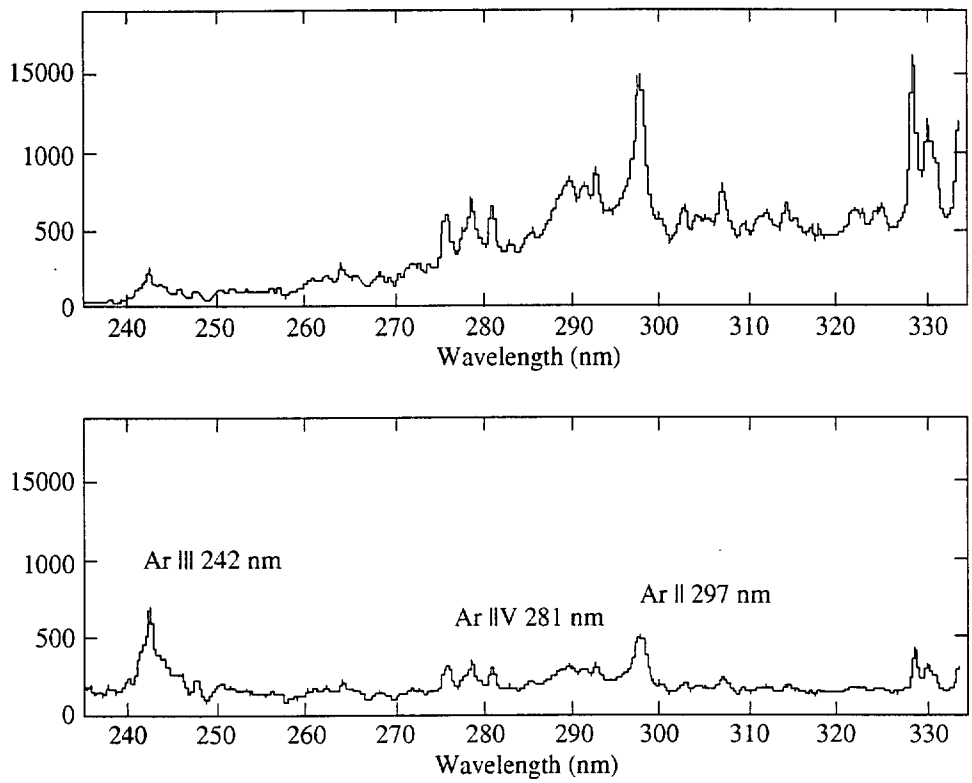


*Figure 2. Emission spectra from the centerline of a radiating Argon cylindrical shock wave 4 ns after formation. Both the original signal and the signal corrected for the spectral sensitivity of theimaging spectrometer are presented.*

In Figure 2 emission for Ar II (242 nm), Ar III (297 nm), and Ar IV (281nm) are identified in the radiating Argon shock wave formed from the laser generated blast wave. This emission spectrum was obtained from the radiation from the centerline of the cylindrical shock wave. Radial distributions of the Ar II, III, and IV emission as a function of radial coordinate across the shock can also be obtained. Since the oberserve emission is integrated across the cylindrically symmetric shock to obtain a true radial distribution of the emission and the associated number density requires a deconvolution procedure. The Argon data as well as data from Xenon and Krypton are undergoing this procedure. The deconvolved radial distribution of the emission will be used to extract a gas temperature distribution and shock location as a function of time for comparison with previous interferometric observations.

UNIVERSITY COLLABORATIVE RESEARCH PROGRAM

# Theory and Computational Modeling of Short Pulse Laser Irradiation of Atomic Clusters

## LS00-005

Alexander Rubenchick, Principal Investigator, UC Davis
Todd Ditmire, Co-Principal Investigator, LLNL
***Collaborators:***
J.C. Garrison, UC Davis
***Students:***
Aleksey Komashko (UC Davis)

## Abstract

The short pulse laser irradiation of atomic clusters can be divided into three stages: (1) Deposition of the laser energy and ionization of the atoms. (2) Expulsion of the free electrons. (3) The Coulomb explosion of the positively charged ion cluster. A study of the expansion of the ion cluster and the expulsion of high energy ions has been carried out using both fluid dynamics and kinetic theory. For the kinetic theory, a combination of symmetry and dynamical arguments was used to reduce the three-dimensional problem to a one-dimensional model. This model has been incorporated in a computer program which is in the final stages of development.

## Scientific Goals

The interaction of intense, femtosecond laser pulses with atomic or molecular clusters containing a few thousand atoms has demonstrated extremely efficient conversion of laser energy into ion kinetic energy. The subsequent explosion of the micro plasma created in the cluster expels ions at very high energies. Experiments using deuterium clusters have shown that the collision of ions from different clusters leads to fusion, with production of fusion neutrons for a pulse energy of 0.1 J. The large inertia of the ions prevents their motion during the energy deposition, ionization and expulsion of the free electrons. We have therefore concentrated on the expansion of the ion cluster after the end of the laser pulse. The objective is to study the so-called "Coulomb explosion" by using both fluid dynamics and kinetic theory descriptions of the dynamics of the ion cluster. Both treat Coulomb repulsion in a self-consistent way, but the Vlasov equation satisfied by the ion distribution function provides a more detailed description than the hydrodynamic model. Analytical results, such as scaling laws, can be derived from this treatment, but much more information can be obtained by numerical simulations. A major thrust of our program is to construct a simplified model which will allow the development of a practical computational scheme.

## Progress and Conclusions

We first used a fluid-dynamics description of the Coulomb explosion to study the expansion of the original ball of ions. The energy distribution after expansion is found to be far from Maxwellian, in fact it has a cutoff when the kinetic energy is equal to the potential energy of an ion at rest at the cluster surface.Previous calculations of neutron yields usually assumed a Maxwellian ion distribution function, therefore the estimates of fusion neutron production must be reevaluated.We assume that the laser field extracts the electrons, and that the ions subsequently expand under the effect of the self-consistent Coulomb field.The ion distribution function is proportional to $\sqrt{\ }$ E and the cutoff occurs at an energy proportional to the square of cluster radius. Since the experiment produces clusters of various sizes, the ion distribution function must be averaged over the cluster size distribution.We calculated the neutron yield using the available experimental information on cluster size distribution, and found results in good agreement with the experimental measurements[1].

We next studied the Coulomb explosion using kinetic theory. In the parameter range of interest, collisions may be neglected so that the ion distribution function is controlled by a Vlasov-type kinetic equation, in which the Coulomb force is calculated self-consistently >from the distribution function. By rewriting the kinetic equation in terms of appropriate dimensionless variables, we were able to show rigorously that the mean kinetic energy of the ions is proportional to (ZR0)2, where Z is the ionic charge and R0 is the initial radius of the cluster.

Since the expansion occurs in three spatial dimensions (3D) the corresponding phase space, defined by the position and velocity of an ion, is six dimensional (6D). Substantial simplification is achieved by assuming a simple but reason-

able model for the initial distribution. In this model the initial phase space distribution factorizes into a spatial distribution which is independent of the angular variables and a Maxwellian velocity distribution. Under this assumption the initial ion distribution is separately spherically symmetric in position and velocity. By combining this feature with the rotational invariance of the kinetic equation, we have shown that the 6D phase space is reduced to a 3D space defined by the radial coordinate, the magnitude of the velocity, and the angle between the position and velocity vectors. Thus the original 3D expansion has been reduced to 1.5D. This poses a problem which is computationally practicable, but still difficult. It would therefore be better still to reduce the dimensionality further to 1D. This was achieved by again using the spherical symmetry of the initial distribution to show that the self-consistent Coulomb potential remains spherically symmetric at all times. The angular momentum of each particle is therefore conserved. The initial angular momenta are small, due to the very small initial velocities, and the velocities and radius vectors both increase rapidly during the expansion; therefore conservation of angular momentum requires the angle between them to become small. The ion distribution must therefore quickly become confined to the region of the 3D phase space in which the angle between radius vector and velocity is close to zero. This behavior was explicitly verified in the simpler case of free streaming expansion, for which the kinetic equations can be solved analytically. Integrating the 3D kinetic equation over this angle and making use of the sharply peaked nature of the distribution in angle then leads to a 1D kinetic equation for the reduced distribution function depending only on the radial coordinate and the magnitude of the velocity.

The 1D kinetic equation resulting from the arguments sketched above retains a vestige of the original 3D geometry because of the restriction that the radial coordinate r and the velocity magnitude v are both positive. This feature can be hidden from view by the expedient of extending r and v to negative values with the assumption that the distribution function is even in both r and v. This trick also facilitates the use of fast Fourier transforms which are needed in the interpolation steps of the integration scheme we have chosen. Even in the 1D case the Vlasov equation presents notorious difficulties, so considerable experimentation with different methods was required before we settled on a split-operator technique [2]. This scheme is based on the method of characteristics and is therefore initially formulated in the full 6D phase space. The distribution function at r, v, t+dt is given by the value of the distribution function at r-dr, v-dv, t, where dr and dv are calculated by integrating backwards along the characteristic from t+dt to t . The split step aspect is introduced by approximating the characteristic curve with three straight segments. The first segment from t+dt to t+dt/2, is a free-streaming step which only uses the convective term in the kinetic equation. The second segment is an 'instantaneous' step which only uses the force term. The third step is another free streaming integration from t+dt/2 to t. In each of the steps the previous value of the distribution function has to be evaluated at points which in general do not lie on the discrete coordinate mesh. These relations in the full (6D) phase space are then projected on the reduced (1D) phase space. The necessary interpolations are handled by the use of fast Fourier transforms. This scheme is second order accurate in dt and fairly easy to implement. A version of this code has been written, but it is not quite ready for comparison to experiments. There remain some questions of speed and accuracy which may require the use of a different interpolation method, e.g., cubic splines, in the second step of the integration scheme.

## References

[1] J. Zweiback, et al., *Characterization of Fusion Burn Time in Exploding Deuterium Cluster Plasmas*, **Phys. Rev. Lett. 85**, 3640 (2000).

[2] C. Z. Cheng and G. Knorr, *The integration of the Vlasov equation in configuration space*, **J. Comp. Phys. 22**, 330 (1976).

UNIVERSITY COLLABORATIVE RESEARCH PROGRAM

# Time-Resolved Imaging Study of Material Modification and Crack Formation During Laser Damage

## LS00-006

Harry W. K. Tom, Principal Investigator, UC Riverside
Michael D. Feit, Co-Principal Investigator, LLNL
***Collaborators:***
Hongbing Jiang, Postdoctoral Researcher, UC Riverside

A series of nanosecond time-resolved images have been obtained during Q-switched Nd:YAG laser-induced damage events near the surface of DKDP crystals. The images show that catastrophic damage of the front surface occurs by nucleation of subsurface bulk damage and subsequent propagation of cracks to the surfacce.. Front-surface-nucleated damage produces a plasma mirror that prevents additional laser absorption and bulk damage. In contrast, back-surface-nucleated damage reflects incident radiation back into the bulk and leads to catastrophic bulk damage and subsequent cracking to the surface.

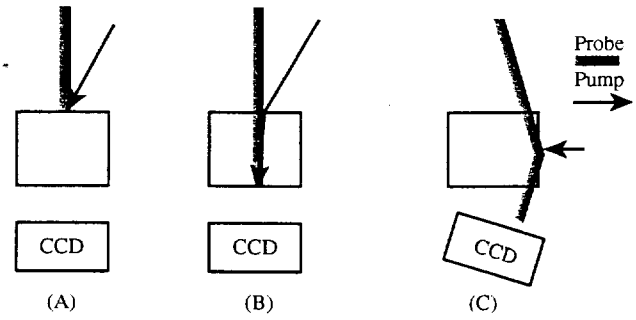


*Figure 1. Pump-probe optical arrangement. A) pump damages on front face, probe image obtained in transmission, B) pump damages on back face, probe image obtained in transmission, C) pump damages on front face, probe image is obtained in geometry of total internal reflection.*

*Figure 1a.*

## Scientific Goals

In previous work we developed a novel time-resolved imaging system that allows a series of 3 nanosecond time-resolved images to be obtained for a single laser-induced event. We initially used this technique to study melt-front propagation, plastic deformation, and cracking dynamics in bulk DKDP during the first 100 ns after a 10 ns pulse above the bulk damage threshold. In this work, we wanted to study several issues related to surface damage. First we wanted to study the difference between bulk and surface damage. Second, we wanted to study the evolution of surface damage to see whether it was bulk-nucleated or surface-nucleated.

## Progress and Conclusions

The experimental setup consists of a nanosecond Q-switched Nd:YAG pump laser from which the pump and 3 probe beams are obtained. The pump was at 1.06 μm wavelength and focussed to fluences ~40-60 J/cm$^2$ which is at the lower end of the "S" curve for bulk damage on high quality LLNL rapid-grown DKDP. The 3 probe beams are generated using Stimulated Raman scattering in a 1 meter long cell of CH4 and are time-delayed with respect to the pump with delay lines. The pump is focussed onto the front (1A, 1C) or back surface (1B) of the sample as shown below at an (internal) angle of 130 with respect to the DKDP z-axis. The probe beam is either propagated along the z-axis normal to the surface (1A, 1B or at glancing angle in reflection inside the crystal (1C).

In entrance face damage (geometry of Figure 1A), we have observed direct evidence of "plasma shielding", an effect well known in laser-processing of materials. The early part of the laser pulse ablates material and the low density plasma acts as a mirror, shielding the solid from substantial energy absorption during the rest of the laser pulse. The figure was obtained at 60 ns delay.

The ring is due to a sound wave in air. DKDP plasma was generated outside the crystal and this tells us that damage was nucleated at the surface. The diffuse bright spot in the center is from fluorescence from the plasma in the air above the sample. After the fact, however, no

# Time-Resolved Imaging Study of Material Modification and Crack Formation During Laser Damage

damage spot is visible by direct optical imaging of the surface. We can imagine the surface damage spot only in diffraction so we know the size of this damage spot must be sub-micron. Each pixel in the image corresponds to 1.17 x 1.17 $\mu m^2$ and the image shown is 748 x 561 $\mu m^2$. At intensities at or slightly above the damage threshold of the bulk, damage that is nucleated at the surface does not lead to substantial damage. It is likely that damage tests that use scatter from the after-the-fact spot do NOT detect this damage so the damage threshold of the entrance surface would appear much higher than it really is.

On the entrance face, catastrophic damage is always nucleated in the bulk below the surface. We don't see the sound wave in air characteristic of a plasma expansion at the surface. In Figure 2, we observe these dynamics in "side view" in the geometry of Figure 1C. The images have a mirror plane because of total internal reflection. The 4 images below are taken at 15 ns, 30 ns, 45 ns and 2 s delay (from left to right). The images are obtained with the pump propagating along the x-axis, and the probe image showing the nominal x-z plane with x-horizontal and z-vertical. We see that a melt region is created ~45 μm below the surface and that initially the melt-front and cracks propagate as expected for bulk. The cracks that appear diagonal in the image propagate along the equivalent [1,1,1.5] crystal directions and form the edges of a 4-sided pyramid with the base at the surface. The whole pyramid volume as well as a ~5 μm thick layer at the surface are "missing" after the event is over (fourth image on right). There are very important dynamics after 100 ns but we did not measure them. The resolidification process plays an important role in the final morphology. From previous bulk studies we know that the surrounding crystalline material is plastically deformed and is compressed compared to the equilibrium structure. A relatively large volume around the damage nucleus may be under permanent compression and this region may contract back from the nominal surface plane as the liquid region cools. In contrast, plastic deformation and cracking in the bulk are essentially over by 50-80 ns.

At the exit face, catastrophic damage appears to be initiated directly on the exit surface. We always see a sound wave in air characteristic of plasma formation and ablation of material from the surface. The same plasma mirror that "saves" the solid on the front face, now traps the incoming laser energy at the surface depositing more of the laser energy than one would expect. As this occurs, the absorption front moves toward the laser. This is the first experimental evidence of either "laser supported detonation wave" (LSDW) or a "laser supported combusion wave". The former is supersonic, the later sonic, and we have not yet measured the wave speeds. In the images in Figure 3, we see that the dark region occupied by the liquid is concentrated just a few microns off center (below) from the source of the sound wave at the surface. The liquid is formed where the most energy is absorbed and this appears to be a short distance away from the surface and along the $13^0$ angle of the incident pump. In the 60 ns image, the irregularly shaped ring is probably due to ablated DKDP liquid which travels more slowly outward into the air than the sound wave propagates in air. The shape is probably due to the anisotropic melting and strain propagation of the surface as well as the crack anisotropy of the underlying bulk. Since we do not see this in the entrance face surface damage images, the exit face damage is much more severe creating a much hotter and larger volume of ablated material than in the front face damage case. Many investigators have found that exit face damage thresholds are lower than entrance face damage thresholds for many optical materials. This effect is always explained by self-focussing, that the laser beam is simply more intense at the back face. Here

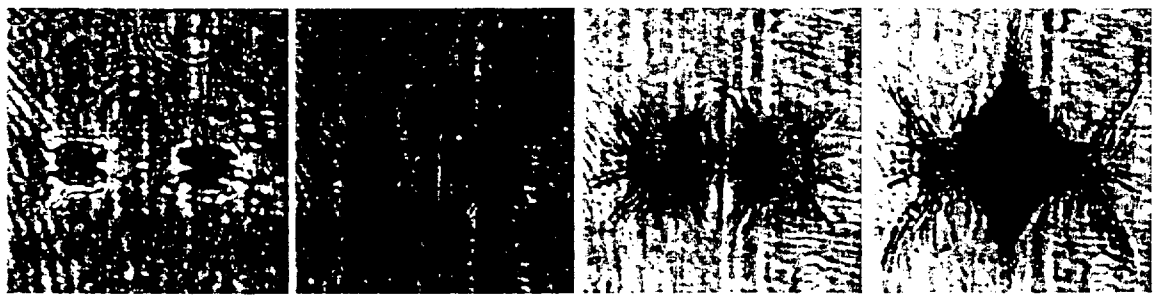

*Figure 2. Time-sequenced image of laser damage in DKDP. The image is obtained in total internal reflection geometry as in Figure 1C and therefore has a vertical mirror plane. Delay times from top left to right are 15 ns, 30 ns, 45 ns, and 2 s after the pump pulse. The image size is 195 x 202 $\mu m^2$.*

UNIVERSITY COLLABORATIVE RESEARCH PROGRAM

## Time-Resolved Imaging Study of Material Modification and Crack Formation During Laser Damage

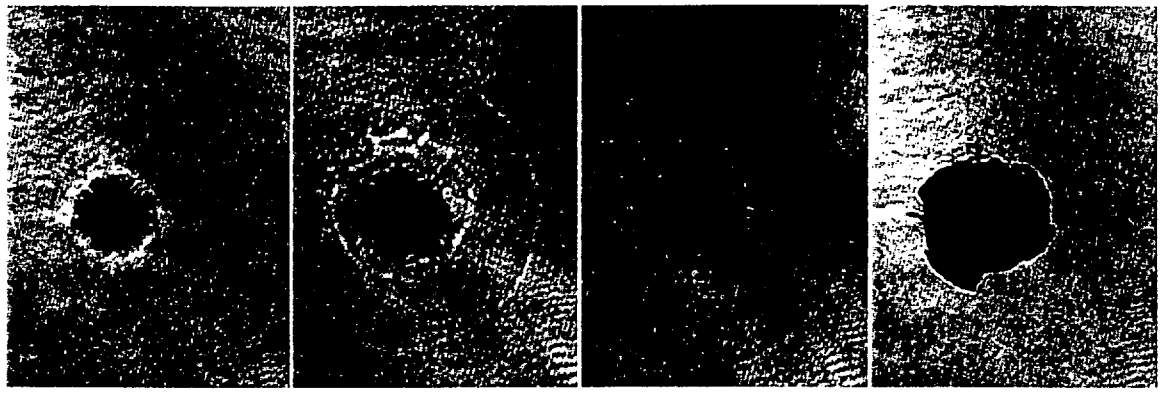

*Figure 3. Time-sequenced images from damage on exit face of DKDP. Delay times from top left to right are 30 ns, 60 ns, 90 ns, and 2 s. Size: 456 x 608 $\mu m^2$. Images are rotated $90^0$ with respect to geometry shown in Figure 1B.*

we show that the plasma behavior at the rear face leads to dramatically different laser absorption efficiency than the entrance face. We also note that surface cracking occurs along the x and y directions. This is completely different from the bulk which prefers the [1,1,1.5] and [1,1,$\beta$] where $\beta<0.3$.

The experimental work was conducted at UC Riverside by Hongbing Jiang, a postdoctoral researcher, under the direction of UC PI H. Tom. These results are preliminary as we did not have enough samples to do additional studies over varying conditions such as pump intensity, images in different planes, etc. No publications or talks on this topic have been submitted yet. The LLNL PI is Michael Feit who has studied these results in the context of laser supported detonation wave and laser supported combustion wave dynamics.

# Electric-Field Poling of Phosphate Glasses for Nonlinear Optical Waveguide Devices

**LS00-007**

D.M. Krol, Principal Investigator, UC Davis
E. Honea, Co-Principal Investigator, LLNL
*Student:*
Prissana Thamboon, UC Davis

The introduction of a second-order nonlinearity, $\chi^{(2)}$, in a glass enables the integration of glass waveguide lasers with EO modulators and/or frequency doublers. Such devices have applications in optical communications as well as sensor and medical technology. Although glasses normally do not possess a $\chi^{(2)}$, one can be introduced through a separate processing step. The most effective way to do this is through electric field poling. This process has been shown to work in silica glass. The focus of this project was to study electric field poling in phosphate glasses, which have hitherto not been explored for this purpose. We have built and tested an experimental set-up to induce and characterize second-order optical nonlinearities in phosphate glass samples.

## Scientific Goals

This project had the following specific goals:

- Build an electric field poling apparatus with the capability of studying the effects of elevated temperature and field strength on the induced $\chi^{(2)}$ in the glass.
- Build an optical set-up to measure the second harmonic signal strength using the Maker fringe technique in order to characterize the induced $\chi^{(2)}$ profile in the glass. Testing of this set-up using a quartz crystal.
- Use the electric-field apparatus to induce $\chi^{(2)}$ nonlinearities in phosphate glasses and measure their SH response.

## Progress and Conclusions

In the first part of this project we have built the experimental facilities needed to pole and characterize our glass samples.

First we built an apparatus in which glass samples can be subjected to very high (1-20 kV) DC electric fields at elevated temperatures (up to 500 C). A schematic diagram of this poling apparatus is shown in Figure 1. The set-up consists of a Bertan high-voltage power supply and an electric furnace, both of which are computer controlled. This allows us to program a specific temperature-voltage-time profile in order to study the effects of poling voltage and poling time on the induced optical nonlinearity.

Secondly, we built an experimental set-up to characterize the induced $\chi^{(2)}$ profile using the SHG Maker fringe technique. A schematic diagram is shown in Figure 2. Since the typical SH power at 532 nm, generated in our samples, is on the order of <10–8 of the incident 1064 nm power, extreme care had to be taken to filter out any 1064 nm light as well as any stray light from other sources in the room.

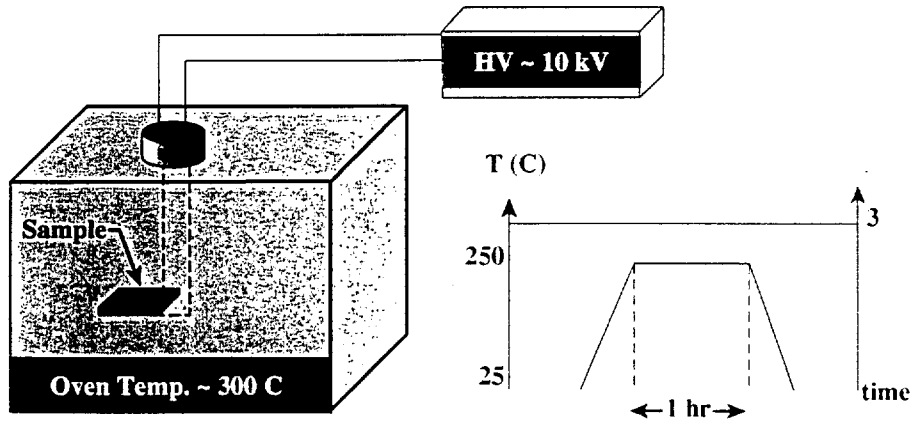


*Figure 1. Schematic diagram of the poling set-up used to induce second-order nonlinearities in glass. A typical voltage-temperature-time program is shown.*

# Electric-Field Poling of Phosphate Glasses for Nonlinear Optical Waveguide Devices

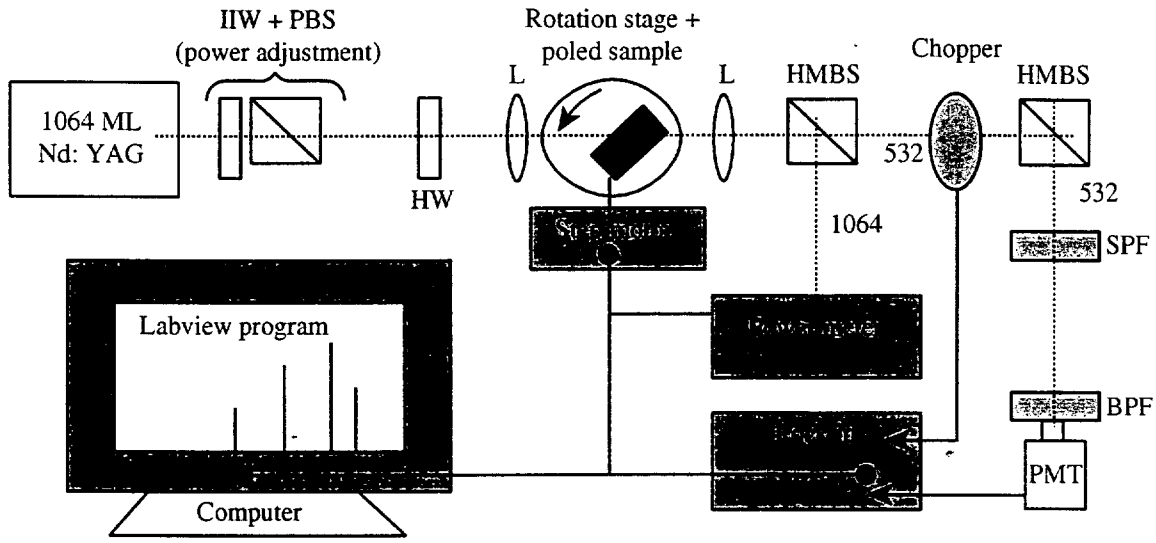


*Figure 2. Schematic diagram of the experimental set-up used to measure SH Maker fringes in poled glass samples. HW= half wave plate; PBS = polarization beam splitter; L = lens; HMBS= harmonic beam splitter; SPF= short pass filter; BPF= band pass filter; PMT = photomultiplier tube*

In the second part of the project we tested the equipment shown in figures 1 and 2. We poled several different phosphate glasses, including IOG-1 (a commercial glass from Schott Glass) as well as glasses with molar composition 20 La2O3 80P2O5, made at UC Davis in Prof. Risbud' s group.

In order to test our optical set-up we measured Maker fringes of quartz crystals. Our initial experiments showed that we were able to measure fringes but the observed fringe patterns deviated from those that are predicted theoretically. This is most likely due to insufficient precision in our control of sample orientation and polarization of the fundamental beam. We have recently improved our set-up using different sample mounts and polarization optics. Our most recent Maker fringe measurements of quartz show good agreement with theory. We are currently measuring the SH signals from our poled glass samples.

In conclusion, we have built and tested experimental facilities to induce and characterize second-order optical nonlinearities in phosphate glass samples.

## Presentations Related to this Project

P. Thamboon and D. M. Krol, "Thermal Poling Studies of Lanthanum Phosphate Glasses", Fall 2000 Mtg of the Glass and Optical Material Division of AcerS, Corning, NY, Oct 1-4, 2000, paper GP-008-00.

## Students Involved in this Project

Prissana Thamboon is currently a 3rd year Ph. D. student in the Department of Applied Science at UC Davis. Prissana carried out all of the experimental work described in this report. In addition to her experimental work in the lab, Prissana took several courses during this funding period and she will take her Ph. D. qualifying exam in May 2001. After that, Prissana will continue her work on electric-field poling in phosphate glasses and she is expected to graduate in Summer 2002.

# Emittance and Dynamics of Space Charge Dominated Electron Beams

## LS00-009

James Rosenzweig, Principal Investigator, UC LA
Greg Le Sage, Co-Principal Investigator, LLNL
*Students:*
Scott Anderson, Salime Boucher, Joel England, Matt Thompson, UC LA

## Abstract

This grant supported a variety of activities aimed at development and physics characterization of a high brightness rf photoinjector facility at Livermore to be used with the Falcon laser system and an existing linac. The purposes of this facility are to investigate ultra-short, monochromatic x-ray production using Thomson scattering, and development of advanced beam generation and diagnostic techniques for systems using sub-picosecond intense lasers and electron beams. The main research accomplished during the grant period centered on emittance measurements on space-charge dominated, picosecond electron beams. Secondary efforts were made in the areas of design, simulation and construction of a beam switchyard for the Falcon linac, to handle injection of both the photoinjector and therminonic injector beams, and on design of a magnetic compressor to create ultra-short electron pulses, and enhance laser-electron beam phase-locking in this system.

## Scientific goals

The primary goal of this grant was to continue collaborative work on construction of a high brightness photoinjector beam system, to be used in basic beam physics experiments as well as Thomson scattering measurements. In the previous year, the photocathode rf gun was built at UCLA and commissioned at LLNL, so this year's efforts were focused on beam physics investigations of emittance behavior and the effects of space-charge in emittance measurement. In addition, a detailed beam optics study of the electron beam switchyard for the ultimate integration of the rf photocathode gun into the existing linac/injector system was needed to prepare for construction of the switchyard. These optimized beamline studies were translated into engineering design for the magnetic optics, in the system, which are now in the fabrication and installation stages. More detailed optics studies, including the effects of coherent synchrotron radiation in the intense, bending beams in the planned compressor, are underway.

## Progress Report

Considerable progress was made on this project in the past year, as it moved from a high power microwave cavity development effort to a beam physics program. Using the

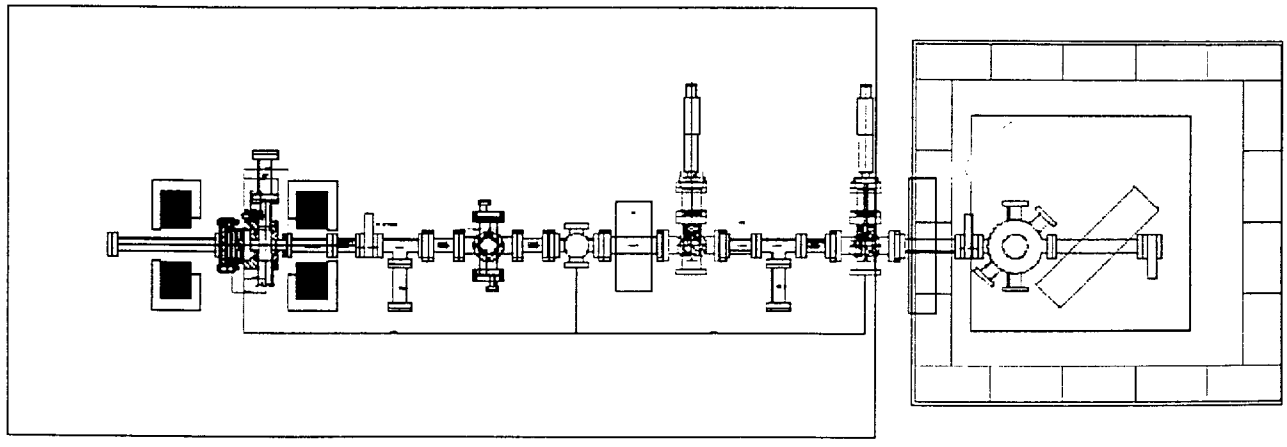

*Figure 1. Experimental arrangement for rf gun commissioning, space-charge dominated beam emittance measurements, and initial Compton scattering experiments.*

UNIVERSITY COLLABORATIVE RESEARCH PROGRAM

## Emittance and Dynamics of Space Charge Dominated Electron Beams

rf gun built by the UCLA/LLNL collaboration, and a laser pulse seeded by the Falcon system, a 5 MeV several hundred pC electron was produced for the initial experiments. A drawing of the experimental arrangement for the commissioning measurements is shown in Figure 1. The rf performance of the gun, and the quantum efficiency of the cathode were determined to be at the levels expected from similar experiments during the commissioning phase. With the commissioning phase complete, the beam was made available for experiments. While the UCLA role in the measurement of the Thomson-scattered Falcon laser photons from the photoinjector has been one of background and support, we have played the lead role in the experimental investigation of the effects of space-charge on emittance measurements in high brightness beams.

The emittance measurements in these experiments were be performed in two ways. The first involves use the emittance slit mask technique pioneered at UCLA, in which the space-charge dominate beam is sliced up into narrow, emittance-dominated beamlets by a slit array, and analyzed downstream to give a shot-by-shot reconstruction of the transverse phase space. A copy of the UCLA hardware was installed at LLNL by Livermore PI Greg Le Sage. The Labview software written at UCLA for both controlling the experiment and analyzing the data in this measurement was installed on a LLNL data acquisition computer, and an operating system was quickly achieved.

The second emittance measurement technique used in characterizing the beam after the rf gun was the quadrupole scan. In this scan we ignore, as is customary in many labs, the perturbing forces of space-charge, and analyze variations in the beam size due to quad strength changes as if the beam particle trajectories were ballistic. Again the data acquisition and analysis implementation was based on the equivalent UCLA system. We have compared the results of the quad scan and slit techniques, both of which have peculiar challenges due to the strength of the "polluting" space charge forces at low energy (~5 MeV). In the case of the quad scan, we see (Figure 2) that the emittance measurement is larger than the simulated (by the multi-particle code PARMELA), and accurate (according to dynamics analyses) slit-based results. It is strongly dependent on the beam plasma frequency $k_p \cong \sqrt{4\pi_e n_b / \gamma^3}$, as opposed the phase space density. The results of the quad scan were benchmarked against an envelope code, HOMDYN, which has a linear model of the effect of space-charge on the of beam rms moments. There was surprisingly good agreement, considering that HOMDYN has an idealized model of space-charge, and the experiment includes . These measurements and their interpretation are currently being written up for publication and will form a component of UCLA student Scott Anderson's PhD thesis.

The design of the Thomson scattering experiment, as well as the design and manufacturing of bypass and matching optics that will allow the integration of the rf gun into the positron production linac at the Falcon facility, are now proceeding at LLNL and UCLA. Completion of the integration of the rf photoinjector and linac systems should be completed in the next six months. This work is presently supported mainly by an IUT from LLNL to UCLA, and is expected to be the focus of proposed work involving ILSA in the coming year.

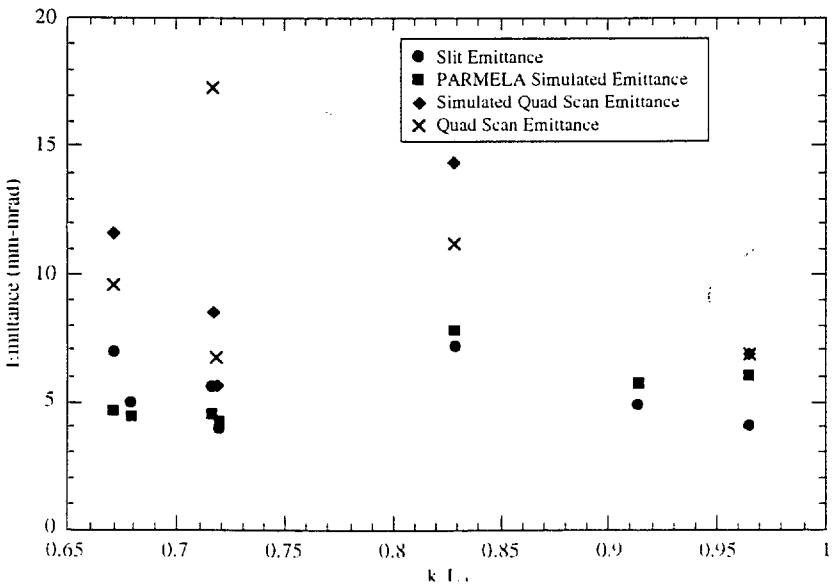


*Figure 2. Data and simulation of space-charge emittance measurements in LLNL gun experiments.*

## Papers

S.G. Anderson and J.B. Rosenzweig, *Nonequilibrium Transverse Motion and Emittance Growth in Ultrarelativistic Space-charge Dominated Beams*, **Phys. Rev.** Special Topics - Accel. and Beams, 3, 094201 (2000).

## Emittance and Dynamics of Space Charge Dominated Electron Beams

M. Thompson and J.B. Rosenzweig, *Production and Synchronization of Electron Beams from RF Photoinjector/ Compressor Systems for Ultra-fast Applications*, to be published in the Proceedings of the 2000 Advanced Accelerator Concepts Workshop.

S.G. Anderson, G. Le Sage, and J.B. Rosenzweig, Space-charge Effects on High Brightness Beam Emittance Measurements, in preparation for submission to **Phys. Rev.** Special Topics - Accel. Beams

# PUBLICATIONS

# JOURNALS


Adams, J.J., C. Bibeau, R.H. Page, D.M. Krol, L.H. Furu, S.A. Payne, *4.0-4.5- mu m lasing of Fe:ZnSe below 180 K, a new mid-infrared laser material,* **Optics Letters, 24,** 1720 (1999).

Alfano, R.R., S.G. Demos, P. Galland, S.K. Gayen, Yici Guo, P.P. Ho, X. Liang, F. Liu, L. Wang, Q.Z. Wang, and W. B. Wang, *Time-resolved and Nonlinear Optical Imaging for Medical Applications,* **The Annals of the New York Academy of Sciences, 14-2,** 838 (1999).

Beer, M.E., P.K. Patel, S.J. Rose, and J.S. Wark, *Calculations of the modal photon densities and gain in a K/Cl resonantly photopumped X-ray laser,* **Journal of Quantitative Spectroscopy & Radiative Transfer, 65,** 71 (2000).

Baldis, H.A., C. Labaune, J.D. Moody, T. Talineud, and V.T. Tikhonchuk, *Localization of Stimulated Brillouin Scattering in Random Phase Plate Speckles,* **Physical Review Letters, 80,** 1900 (1998.)

Budil, K.S., B.A. Remington, D.M. Gold, K. Estabrook, R. Lerche, P. Bell, and J. Kane, *A Shock Breakout Diagnostic for the PetaWatt Laser System,* **Review of Scientific Instruments, 70,** 806 (1999).

Chanteloup, J.-C., H.A. Baldis, A. Migus, G. Mourou, B. Loiseaux, and J.-P. Huignard, *Nearly Diffraction Limited Laser Focal Spot Obtained Using an Optically Addressed Light Valve in an Adaptive Optics Loop,* **Optics Letters, 23,** 475 (1998).

Cohen, B.I. E.B. Hooper, M.C. Spang, and C.W. Domier, *Theoretical Aspects of the Use of Pulsed Reflectometry in a Spheromak Plasma,* **Review of Scientific Instruments, 70,** 1407 (1999).

Cohen, B.I., E.B. Hooper, T.B. Kaiser, and E.A. Williams, *Modeling of Ultra-Short-Pulse Reflectometry,* **Physics of Plasmas, 6,** 1732 (1999).

Cohen, B.I., B.F. Lasinski, A.B. Langdon, E.A. Williams, H.A. Baldis, and C. Labaune, *Suppression of Stimulated Brillouin Scattering by Seeded Ion Wave Mode Coupling,* **Physics of Plasmas, 5,** 3402 (1998).

Cohen, B.I., B.F. Lasinski, A.B. Langdon, E.A. Williams, K.B. Wharton, R.K. Kirkwood, and K.G. Estabrook, *Resonant Stimulated Brillouin Interaction of Opposed Laser Beams in a Drifting Plasma,* **Physics of Plasmas, 5,** 3408 (1998).

Demos, S. G., D. M. Calistru, S. Owen, V. Petricevic, and R. R. Alfano, *Resonance Between a Phonon and Local Mode Pair Promotes Participation in the Nonradiative Relaxation,* **Physical Review Letters, 82,** 2556, (1999).

Demos, S.G., M. Staggs, M. Yan, H.B. Radousky, and J.J. De Yoreo, *Investigation of Optically Active Defect Clusters in $KH_2PO_4$ Under Laser Photoexcitation,* **Journal of Applied Physics, 85,** 3988 (1999).

Demos, S.G., M. Staggs, M. Yan, H.B. Radousky, and J.J. De Yoreo, *Microscopic Fluorescence Imaging of Bulk Defect Clusters in $KH_2PO_4$ Crystals,* **Optics Letters, 24,** 268 (1999).

Demos, S.G., M. Yan, H.B. Radousky, and J.J. De Yoreo, *Raman Scattering Investigation of KDP Subsequent to High Fluence Laser Irradiation,* **Applied Physics Letters, 72,** 2367 (1998).

Demos, S.G., W.B. Wang, and R.R. Alfano, *Imaging Object Hidden in Scattering Media Using Fluorescence Polarization Preservation of Contrast Agents,* **Applied Optics, 37,** 792 (1998).

Demos, S.G., W.B. Wang, J. Ali, and R.R. Alfano, *New Optical Approaches for Sub-surface Imaging of Tissues,* J.G. Fujimoto and M.S. Patterson, Eds., **OSA TOPS Advances in Optical Imaging & Photon Migration, 21,** 405 (1998).

Depierreux, S., C. Labaune, J. Fuchs, and H.A. Baldis, *Identification of Ion Acoustic Waves Using Thomson Scattering in Laser Produced Plasmas: Application to the Langmuir Decay Instability,* **Review of Scientific Instruments, 71,** 3391 (2000).

Depierreux, S., J. Fuchs, C. Labaune, A. Michard, H.A. Baldis, D. Pesme, S. Huller, and G. Laval, *First Observation of Ion-Acoustic Waves Produced by the Langmuir Decay Instability,* **Physical Review Letters, 84,** 2869 (2000).

Dimits, A.M., G. Bateman, M.A. Beer, B.I. Cohen, et al., *Comparisons and Physics Basis of Tokamak Transport Models and Turbulence Simulations,* **Physics of Plasmas,** 7, 969 (1999).

Drake, R.P., S.G. Glendinning, K. Estabrook, et. al., *Observation of forward and reverse shocks driven by high-energy-density plasma flow,* **Physical Review Letters, 81,** 2068 (1998).

Drake, R.P., J.J. Carroll, K. Estabrook, S.G. Glendinning, B.A. Remington, R. Wallace, and R. McCray, *Development of a laboratory environment to test models of supernova remnant formation,* **Astrophysical Journal, 500,** L157 (1998).

Dunn, J., A.L. Osterheld, Y. Li, J. Nilsen, and V.N. Shlyaptsev, *Transient Collisional Excitation Lasers with 1-ps Tabletop Drivers, in Short Wavelength Lasers and Applications,* ed. J.G. Eden and J.J. Rocca, **IEEE Journal of Selected Topics in Quantum Electronics, 5**, 1441 (1999).

Dunn, J., J. Nilsen, A.L. Osterheld, Y. Li, and V.N. Shlyaptsev, *Demonstration of Transient Gain X-ray Lasers Near 20 nm for Nickellike Y, Zr, Nb, and Mo,* **Optical Letters, 24**, 101 (1999).

Dunn, J., A.L. Osterheld, R. Shepherd, W.E. White, V.N. Shlyaptsev, and R.E. Stewart, *Demonstration of X-ray Amplification in Transient Gain Nickel-like Palladium Scheme,* **Physical Review Letters, 80**, 2825 (1998).

Edwards, J., S.G. Glendinning, L.J. Suter, B.A. Remington, O. Landen, R.E. Turner, T.J. Shepard, B. Lasinski, K. Budil, H. Robey, J. Kane, H. Louis, R. Wallace, P. Graham, M. Dunne, B.R. Thomas, *Turbulent hydrodynamics experiments using a new plasma piston,* **Physics of Plasmas, 7,** 2099 (2000).

Fournier, K.B., D. Stutman, R. Vero, V. Soukhanovski, M. Finkenthal, M.J. May, V.N. Shlyaptsev, W.H. Goldstein, *Measurement of population inversion for FUV transitions in Kr-like Y IV in a high-current reflex discharge,* **Physica Scripta,** 301, (2000).

Fuchs, J. C. Labaune, S. Depierreux, A. Michard, and H.A. Baldis, *Modification of Spatial and Temporal Gains of Stimulated Brillouin and Raman by Polarization Smoothing,* **Physical Review Letters, 84,** 3089 (2000).

Glenzer, S.H., W. Rozmus, B.J. MacGowan, K.G. Estabrook, J.D. De Groot, G.B. Zimmerman, H.A. Baldis, J.A. Harte, R.W. Lee, E.A. Williams, and B.G. Wilson, *Thomson Scattering from High-Z Laser-produced Plasmas,* **Physical Review Letters, 82**, 97 (1999).

Hartemann, F.V., *Stochastic electron gas theory of coherence in laser-driven synchrotron radiation,* **Physical Review E, 61,** 972 (2000).

Hartemann, F.V., E.C. Landahl, D.J. Gibson, A.L. Troha, J.R. Van Meter, J.P. Heritage, H.A. Baldis, N.C. Luhmann, Jr., C.H. Ho, T.T. Yang, M.J. Horhy, J.Y. Hwang, W.K. Lau, and M.S. Yeh, *RF Characterization of a Tunable, High-Gradient, X-Band Photoinjector,* **IEEE Trans. Plasma Phys., 28,** 898 (2000).

Hartemann, F.V., A.L. Troha, H.A. Baldis, A. Gupta, A.K. Kerman, E.C. Landahl, N.C. Luhmann, Jr., and J.R. Van Meter, *High-Intensity Scattering Processes of Relativistic Electrons in Vacuum and their Relevance to High-Energy Astrophysics,* **Astrophysical Journal Supplement, 127,** 347 (2000).

Harteman, F.V., E.C. Landahl, A.L. Troha, J.R. Van Meter, H,A. Baldis, R.R. Freeman, N.C. Luhmann, Jr., L. Song, A.K. Kerman, and D.L. Yu, *The Chirped-Pulse Inverse Free-Electron Laser: a High-gradient Vacuum Accelerator,* **Physics of Plasmas, 10**, 4104 (1999).

Hartemann, F.V., H.A. Baldis, R.R. Freeman, A.K. Kerman, et al., *The Chirped-pulse Inverse Free-electron Laser: A High-gradient Vacuum Laser Accelerator,* **Physics of Plasmas, 6**, 4104 (1999).

Harteman, F.V., J.R. Van Meter, A.L. Troha, E.C. Landahl, N.C. Luhmann Jr., H.A. Baldis, A. Gupta, A.K. Kerman, *Three-dimensional Relativistic Electron Scattering in an Ultrahigh-intensity Laser Focus,* **Physics Review E, 58**, 5001 (1998).

Hartemann, F.V., *High-intensity Scattering Processes of Relativistic Electrons in Vacuum,* **Physics of Plasmas, 5**, 2037 (1998).

Kalachnikov, P., P.V. Nickles, M. Schnurer, W. Sandner, V. N. Shlyaptsev, C. Danson, D. Neely, E. Wolfrum, J. Zhang, A. Behjat, A. Demir, G. J. Tallents, P. J. Warwick, and C. L. S. Lewis. *Saturated Operation of a Transient Collisional X-ray Laser,* **Physical Review Letters A, 57**, 4378 (1998).

Kane, J., D. Arnett, B.A. Remington, S.G. Glendinning, G. Bazan, E. Muller, B.A. Fryxell, R. Teyessier, *Two-dimensional versus three-dimensional supernova hydrodynamic instability growth,* **Astrophysical Journal, 528,** 989 (2000).

Kane, J., D. Arnett, B.A. Remington, S.G. Glendinning, D. Ryutov, B.A. Fryxell, R.P. Drake, K. Moore, R. Teyssier, *Scaling Supernova Hydrodynamics to the Laboratory,* **Physics of Plasmas, 6**, 2065 (1999).

# JOURNALS


Kane, J., R.P. Drake, and B.A. Remington, *An Evaluation of the Richtmyer-Meshkov Instability in Supernova Remnant Formation,* **Astrophysical Journal, 511**, 335 (1999).

Kane, J., D. Arnett, E. Mueller, B.A. Remington, S.G. Glendinning, and B.A. Fryxell, *2D vs. 3D supernova hydrodynamic instability growth,* **Astrophysical Journal Letter,** (1999).

Labaune, C., H.A. Baldis, E. Schifano, B.S. Bauer, A. Maximov, I. Ourdev, W. Rozmus, and D. Pesme, *Enhanced Forward Scattering in the case of Two Crossed Laser Beams Interacting with a Plasma,* **Physical Review Letters, 85,** 1658 (2000).

Labaune, C., H.A. Baldis, B.I. Cohen, W. Rozmus, S. Depierreux, E. Schifano, B.S. Bauer, and A. Michard, *Nonlinear Modification of Laser-Plasma Interaction Processes Under Crossed Laser Beams Irradiation,* **Physics of Plasmas, 6**, 2048 (1999).

Labaune, C., H.A. Baldis, B.S. Bauer, E. Schifano, and B.I. Cohen, *Spatial and Temporal Coexistence of Stimulated Scattering Processes under Crossed-Laser Beam Irradiation,* **Physical Review Letters, 82**, 3613 (1999).

Labaune, C., H.A. Baldis, B.I. Cohen, W. Rozmus, E. Schifano, B.S. Bauer, and A. Michard, *Non-linear Modification of Laser-plasma Interaction Processes Under Laser Beams Irradiation,* **Physics of Plasmas, 6**, 2048 (1999).

Labaune, C., H.A. Baldis, B.S. Bauer, E. Schifano, and B.I. Cohen, *Spatial and Temporal Coexistence of Stimulated Scattering Processes Under Crossed-Laser-Beam Irradiation,* **Physical Review Letters, 82**, 3613 (1999).

Labaune, C., H.A. Baldis, B.S. Bauer, V.T. Tikhonchuk, and G. Laval, *Time-resolved Measurements of Secondary Langmuir Waves Produced by the Langmuir Decay Instability,* **Physics of Plasmas, 5**, 234 (1998).

Landahl, E.C., F.V. Hartemann, G.P. Le Sage, W.E. White, et al., *Phase Noise Reduction and Photoelectron Acceleration in a High-Q RF Gun,* **IEEE Transactions on Plasma Science, 26**, 814 (1998).

Landahl, E.C., F.V. Hartmann, G.P. Le Sage, W.E. White, H.A. Baldis, C.V. Bennett, J.P. Heritage, N.C. Luhmann,Jr., and C.H. Ho, *Phase Noise Reduction and Photoelectron Acceleration in a High-Q RF Gun,* **IEEE Trans. Plasma Science, 26**, 814 (1998)

Li, Y., J. Nilsen, J.Dunn, A.L. Osterheld, A. Ryabtsev, and S. Churilov, *Wavelengths of the Ni-like 4d 1So - 4p 1P1 X-ray Laser Line,* **Physical Review Letters, 58**, R2668 (1998).

Marconi, M.C., C.H. Moreno, J.J. Rocca, V.N. Shlyaptsev, A.L. Osterheld, *Dynamics of a microcapillary discharge plasma using a soft x-ray laser backlighter,* **Physical Review E, 62,** 7209 (2000).

Moreno, C. H., M. C. Marconi, V. N. Shlyaptsev, and J. J. Rocca, *Shadowgrams of a Dense Micro-capillary Plasma Obtained with a Table-top Soft X-ray Laser,* **IEEE Trans. on Plasma Science**, (1998).

Nilsen, J., J. Dunn, A.L. Osterheld, and Y. Li, *Lasing on the Self Photopumped Ni-like 4f 1P1 – 4d 1P1 X-ray Transition,* **Physical Review Letters, 60**, R2677 (1999).

Patel, P.K., Wolfrum, E. Renner, O., A. Loveridge, R. Allott, D. Neely, S.J. Rose, and J.S. Wark, *X-ray line reabsorption in a rapidly expanding plasma,* **Journal of Quantitative Spectroscopy & Radiative Transfer, 65,** 429 (2000).

Patel, R.R. H.E. Garrett, M.A. Emanuel, M.C. Larson, M.D. Pocha, D.M. Krol, R.J. Deri, and M.E. Lowry, *WDM filter modules in compact, low-cost plastic packages for byte-wide multimode fibre ribbon cable data links,* **Electronics Lett. 35,** 840 (1999).

Remington, B.A., D. Arnett, R.P. Drake, and H. Takabe, *Modeling Astrophysical Phenomena in the Laboratory with Intense Lasers,* **Science, 284**, 1488 (1999).

Rocca, J.J., D.P. Clark, J.L.A. Chilla, and V.N. Shlyaptsev, *Energy Extraction and Achievement of the Saturation Limit in a Discharge-Pumped Table-Top Soft X-ray Amplifier,* **Physical Review Letters, 77**, 1476 (1996).

Rocca, J.J., V. Shlyaptsev, F.G. Tomasel, O.D. Cortazar, D. Hartshorn, and J.L.A. Chilla, *Demonstration of a Discharge Pumped Table-Top Soft-X-Ray Laser,* **Physical Review Letters, 73**, 2192 (1994).

Ryutov, D., R.P. Drake, J. Kane, E. Liang, B. Remington, W.M. Wood-Vasey, *Similarity criteria for the laboratory simulation of supernova hydrodynamics,* **Astrophysical Journal, 518**, 2 (1999).

Troha, A.L., J.R. Van Meter, E.C. Landahl, R.M. Alvis, et al., *Vacuum Electron Acceleration by Coherent Dipole Radiation,* **Physical Review E, 60**, 926 (1999).

Wang, W.B., S.G. Demos, J. Ali, G. Zhang, and R.R. Alfano, *Enhancement of Visibility of Fluorescent Objects Hidden in Animal Tissues Using Spectral Absorption Difference Imaging,* Eva Sevick-Muraca and Joseph Izatt, Eds., **OSA TOPS, Biomedical Optical Spectroscopy and Diagnostics, 22**, 57 (1998).

Wang, W.B., S.G. Demos, J. Ali, G. Zhang, and R.R. Alfano, *Enhancement of Visibility of Fluorescent Objects Hidden in Animal Tissues Using Spectral Fluorescence Difference Method,* **Optical Communications, 47**, 11 (1998).

Wharton, K.B., C. Joshi, R.K. Kirkwood, S.H. Glenzer, K.G. Estabrook, B.B. Afeyan, B.I. Cohen, and J.D. Moody, *Observation of Energy Transfer Between Identical-Frequency Laser Beams in Flowing Plasmas,* **Physical Review Letters, 81**, 2248 (1998).

Wharton, K.B., R.K. Kirkwood, S.H. Glenzer, K.G. Estabrook, B.B. Afeyan, B.I. Cohen, J.D. Moody, and C. Joshi, *Energy Transfer Between Identical-Frequency Laser Beams,* **Physics of Plasmas, 6**, 2144 (1999).

Zhang, G., S.G. Demos, and R.R. Alfano, *Far-red and NIR Spectral Wing Emission from Tissues under 532 nm and 632 nm Photo-excitation,* **Lasers in the Life Sciences, 9**, 1 (1999).

# CONFERENCE PROCEEDINGS

Afanasiev, Y.V., V.N. Shlyaptsev, and A.L. Osterheld, *Calculations of Capillary Z-pinch at Fusion-scale Currents,* **26th International Conference on Plasma Science,** Monterey, CA, June (1999).

Baldis, H.A., J. Dunn, M. Foord, W. Rozmus, and C. Andersen, *X-Ray Thomson Scattering as a Diagnostic of Dense Hot Plasmas,* **Proceedings of the 7th International Conference on X-ray Lasers,** Saint Malo, France (2000).

Budil, K.S., D.M. Gold, K.G. Estabrook, B.A. Remington, J. Kane, P.M. Bell, D.M. Pennington, C. Brown, S.P. Hatchett, J.A. Koch, M.H. Key, M.D. Perry, *Development of a Radiative-hydrodynamics Testbed Using the Petawatt Laser Facility,* **Astrophysical Journal Supplement Series,** 261 (2000).

Burnham, K., M. Runkel, S.G. Demos, M.R. Kozlowski, P.J. Wegner, *Effect of vacuum on the occurrence of UV-induced surface photoluminescence, transmission loss, and catastrophic surface damage,* E.W. Taylor, Ed., **SPIE, 4134,** 243 (2000).

Datskos, P.G., S.G. Demos, and S. Rajic, *A Miniature Uncooled Infrared Sensitive Detectors for in Vivo Biomedical Applications,* in **Biomedical Sensing, Imaging, and Tracking Technologies III,** R.A. Lieberman, Ed., **SPIE, 3253,** 94 (1998).

Demos, S.G., M. R. Kozlowski, *Spectroscopic investigation of Si)$_2$ surfaces of optical materials for high power lasers,* H. Helvajian, K. Sugioka, M.C. Gower, and J.J. Dubowski, Eds., **SPIE, 3933,** 316 (2000).

Demos, S.G., M. Staggs, H.B. Radousky, R.R. Alfano, *Instrumentation for subsurface imaging in a clinical environment,* R. R. Alfano, Ed., **SPIE, 3917,** 62 (2000).

Demos, S.G. A. Burnham, P. Wegner, M. Norton, L. Zeller, M. Runkel, M.R. Kozlowswki, *Properties of modified silica detected within laser-induced damage sites,* A.J. Marker, E.G. Arthurs, Eds., **SPIE, 4102,** 106 (2000).

Demos, S.G., M. Balooch, G.W. Marshall, S.J. Marshall, R.R. Gallagher, *Optical Spectroscopy study of Transparent Non-Carious Human Dentin and Dentin-Enamel Junction,* J.D. Featherstone and P. Rechmann, D. Fried, Eds., **SPIE, 3910,** 102 (1999).

Demos, S.G., H.B. Radousky, and R.R. Alfano, *Subsurface Imaging Using the Spectral Polarization Difference Technique and NIR Illumination,* **Optical Tomography and Spectroscopy of Tissue III,** B. Chance and R.R. Alfano, Eds., **SPIE, 3597,** 406 (1999).

Demos, S.G., M. Staggs, and H.B. Radousky, *Damage Induced Material Modification in the Bulk KDP Crystals,* G.J. Exarhos, A.H. Guenther, M.R. Kozlowski, K.L. Lewis, M.J. Soileau, Eds., **SPIE, 3902,** 428 (1999).

Demos, S.G., M. Staggs, M. Yan, H.B. Radousky, and J.J. De Yoreo, *Observation of Photoexcited Emission Clusters in the Bulk of KDP and Laser Conditioning Under 355 nm Irradiation,* **Optical materials for high power lasers,** A. H. Guenther, Ed., **SPIE, 3578** (1999).

Demos, S.G., M. Staggs, M. Yan, H.B. Radousky, and J.J. De Yoreo, *Investigation of Steady-state and Transient Defect Populations in $KH_2PO_4$ Subsequent to High Fluence Laser Irradiation,* **Laser Material Crystal Growth and Nonlinear Materials and Devices,** K.I. Schaffers and L.E. Myers, Eds., **SPIE, 3610,** 2 (1999).

Demos, S.G., M. Yan, M. Staggs, B.W. Woods, Z.L. Wu, H.B. Radousky, and J.J. De Yoreo, *Temperature and Spectral Investigation of Bulk KDP Below Damage using 355 nm Laser Irradiation,* in **Optical Materials for High Power Lasers,** A. H. Guenther, Ed., **SPIE, 3244,** 223 (1998).

Depierreux, S., C. Labaune, H.A. Baldis, and J. Fuchs, *Experimental Observation of the Langmuir Decay Associated with Stimulated Raman Scattering,* **ECLIM Proceedings,** Prague, Czech Republic (2000).

Depierreux, S. C. Labaune, H.A. Baldis, J. Fuchs, A. Michard, *Observation of secondary plasma waves in laser-plasma interaction experiments,* **Inertial Fusion Science and Applications (IFSA) '99 Proceedings,** Bordeaux, France (2000).

Dunn, J. A.Y. Faenov, T.A. Pikuz, A.L. Osterheld, S.J. Moon, K.B. Fournier, J. Nilsen, I.Y. Skobelev, A.I. Magunov, and V.N. Shlyaptsev, *Spectral and Imaging Characteristics of Tabletop X-ray Lasers,* **Proceedings of 7th International Conference on X-ray Lasers,** Saint Malo, France (2000).

Dunn, J., A.L. Osterheld, J. Nilsen, J.R. Hunter, Y. Li, A. Y. Faenov, T.A. Pikuz, and V.N. Shlyaptsev, *Saturated Output Tabletop X-ray Lasers,* **Proceedings of 7th International Conference on X-ray Lasers,** Saint Malo, France (2000).

Dunn, J., A.L. Osterheld, Y. Li, J. Nilsen, and V.N. Shlyaptsev, *Transient Collisional Excitation X-ray Lasers with 1 ps Tabletop Drivers*, **Journal of Selected Topics in Quantum Electronics on Short Wavelength Lasers and Applications, 5,** IEEE, 1441 (1999).

Dunn, J., A.L. Osterheld, Y. Li, J. Nilsen, and V.N. Shlyaptsev, *High Gain Table-top Transient Collisional X-ray Lasers*, **Institute for Electronics and Electrical Engineers, International Conference on Plasma Science**, Monterey, CA, June (1999).

Dunn, J., A.L. Osterheld, Y. Li, J. Nilsen, and V.N. Shlyaptsev, *Transient Inversion Collisional X-ray Lasers*, **15th Interdisciplinary Laser Science Meeting**, Santa Clara, CA, September (1999).

Dunn, J., Y. Li, A.L. Osterheld, J. Nilsen, S.J. Moon, K.B. Fournier, J.R. Hunter, A. Ya Faenov, T.A. Pikuz, and V.N. Shlyaptsev, *Table-top Transient Collisional Excitation X-ray Lasers*, in proceedings of **Soft X-ray Lasers and Applications III**, J.J. Rocca and L.B. Da Silva, eds., **SPIE Proc. 3776**, 2, Bellingham, WA (1999).

Dunn, J., Y. Li, A.L. Osterheld, J. Nilsen, S.J. Moon, K.B. Fournier, J.R. Hunter, A. Ya Faenov, T.A. Pikuz, and V.N. Shlyaptsev, *Tabletop Transient Collisional Excitation X-ray Lasers*, **International Society for Optical Engineering Conference on Soft X-Ray Lasers and Application III**, Denver, CO (1999).

Dunn, J., A.L. Osterheld, and V.N. Shlyaptsev, *Characterization of Transient Gain X-ray Lasers*, in proceedings of **6th International Conference on X-ray Lasers**, Kyoto, Japan, **159**, 131 (1998).

Dunn, J., A.L. Osterheld, V.N. Shlyaptsev, J.R. Hunter, R. Shepherd, R.E. Stewart, and W.E. White, *High Gain X-ray Lasers Pumped by Transient Collisional Excitation, Atomic Processes in Plasmas: 11th APS Topical Conference*, Auburn, AL., March 1998. E. Oks, and M.S. Pindozola, eds., **CP443**, 106 American Institute of Physics (1998).

Dunn, J., A.L. Osterheld, V.N. Shlyaptsev, Y. Li, J. Nilsen, R. Shepherd, and L.B. Da Silva, *Progress in Table-top Transient Collisional Excitation X-ray Lasers at LLNL*, in proceedings of **6th International Conference on X-ray Lasers**, Kyoto, Japan, **159**, 51 (1998).

Fiedorowicz, H., A. Bartnik, J. Kostecki, R. Rakowski, M. Szczurek, J. Dunn, J. Hunter, J. Nilsen, V.N. Shlyaptsev, and A.L. Osterheld, *Investigations on transient gain soft x-ray lasers using a laser-irradiated gas puff target*, **Proceedings of 7th International Conference on X-rayLasers,** Saint Malo, France (2000).

Fournier, K.B., D. Stutman, V. Soukhanovskii, M. Finkenthal, M.J. May, V.N. Shlyaptsev, and W.H. Goldstein, *Estimates of Population Inversion for Deep-UV Transitions in Kr-Like Y, Zr, Nb and Mo in a High Current Reflex Discharge*, in proceedings of **Soft X-ray Lasers and Applications III**, J.J. Rocca and L.B. Da Silva, eds., **SPIE 3776**, 181, Bellingham, WA (1999).

Frati, M., F.G. Tomasel, B. Bowers, J.J. Gonzalez, V.N. Shlyaptsev, and J.J. Rocca, *Generation of highly ionized cadmium plasma columns for a discharge-pumped Nickel-like Cd laser*, **Proceedings of 7th International Conference on X-ray Lasers,** Saint Malo, France (2000).

Fuchs, J., C. Labaune, S. Depierreux, H.A. Baldis, A. Michard, *Polarization smoothing in laser-plasma experiments*, **Inertial Fusion Science and Applications (IFSA) '99 Proceedings,** Bordeaux, France (2000).

Glendinning, S.G., K.S. Budil, C. Cherfils, R.P. Drake, D. Farley, D.H. Kalantar, J. Kane, M.M. Marinak, B.A. Remington, A. Richard, D. Ryutov, J. Stone, R.J. Wallace, S.V. Weber, *Experimental measurements of hydrodynamic Instabilities on Nova*, **Astrophysical Journal Supplement Series, 325** (2000).

Gonzalez, J.J., J. Frati, M. Rocca, and V.N., Shlyaptsev, *Generation of Plasma Columns for Shorter Wavelength Capillary Discharge Soft X-ray Lasers Utilizing a High-power Blumlein Generator*, Proceedings of the SPIE - The International Society for Optical Engineering, **3776. Soft X-Ray Lasers and Applications III**, Denver, CO, **159.** (1999).

Hartemann, F.V., H.A. Baldis, D.J. Gibson, J.P. Heritage, E.C. Landahl, A.L. Troha, and N.C. Luhmann, Jr., *Development of Tabletop Compton X-Ray Sources for Advanced Biomedical Applications*, **Proceedings of the 7th International Conference on X-ray Lasers,** Saint Malo, France (2000).

Hartemann, F.V., A. Le Foll, A.K. Kerman, B. Rupp, D.J. Gibson, E.C. Landahl, A.L. Troha, N.C. Luhmann, Jr., and

# CONFERENCE PROCEEDINGS

H.A. Baldis, *Three-Dimensional Theory of Emittance in Compton Scattering,* **Proceedings of the Advanced Accelerators Concepts 2000,** Santa Fe, NM (2000).

Hartemann, F.V., E.C. Landahl, A.L. Troha, J.P. Heritage, et al., *Decoherence in a Chirped-pulse Free-electron Laser,* **26th IEEE International Conference** on Plasma Science, Piscataway, NJ, **185** (1999).

Hartemann, F.V., H.A. Baldis, A.K. Kerman, E.C. Landahl, et al., *High-field Electron-photon Interactions,* **Proceedings of the International Conference on LASERS'98**, V.J. Corcoranm and T.A. Goldman, eds., **888** (1999).

Hartemann, F.V., H.A. Baldis, A.K. Kerman, E.C. Landhal, N.C. Luhmann Jr., A.L. Troha, and J.R. Van Meter, *High-Field Electron-Photon Interactions,* **Proceedings of the International Conference on Lasers**, Tucson, AZ (1999).

Hartemann, F.V., H.A. Baldis, E.C. Landahl, N.C. Luhmann, Jr., T. Tajima, A.L. Troha, J.R. Van Meter, and A.K. Kerman, *Nonlinear Vacuum Electron-photon Interactions at Relativistic Intensities,* **JIFT Proceedings: Workshop on High Field Science**, Plenum, (1999).

Hartemann, F.V., J.R. Van Meter, A.L. Troha, H.A. Baldis, N.C. Luhmann, A. Gupta, and A.K. Kerman, *Classical Theory of Ultrahigh-Intensity Relativistic Scattering of Electrons and Photons in Vacuum,* **Advanced ICFA Beam Dynamics Workshop on "Quantum Aspects of Beam Physics**, Monterey, CA (1998).

Janulewicz, K.A., F. Bortolotto, P.J. Warwick, M.P. Kalachnikov, V.N. Shlyaptsev, W. Sandner, J.J. Rocca, and P.V. Nickles, *Studies of a Sulfur Capillary Discharge Irradiated by a ps-laser Pulse: A New Way Towards Collisionally Pumped Table-top X-ray Lasers,* **Proceedings of the SPIE - The International Society for Optical Engineering 3776**, 37. **Soft X-Ray Lasers and Applications III**, Denver, CO (1999).

Jiang, H., H.W.K. Tom, M. Yan, H.B. Radousky, J. DeYoreo, and S. Demos, *Time-resolved Studies of Laser Damage Processes in DKDP Crystals,* G. J. Exarhos, A. H. Guenther, M. R. Kozlowski, K. L. Lewis, M. J. Soileau, Eds., **SPIE, 3902**, 294 (1999).

Kane, J. D. Arnett, B.A. Remington, S.G. Glendinning, G. Bazan, R.P. Drake, B.A. Fryxell, *Supernova experiments on the Nova laser,* **Astrophysical Journal Supplement Series,** 365 (2000).

Kanizay, K., M.C. Marconi, C.H. Moreno, J.J. Rocca, V.N. Shlyaptsev, Y.A. Uspenskii, A.V. Vinogradov, and Y.P. Pershin, *Plasma Diagnostics Using a Tabletop Soft X-ray Laser: Demonstration of Shadowgraphy and Interferometry Using a Lloyd's Mirror,* **Proceeding of the SPIE - The International Society for Optical Engineering, 3776**, 212, **Soft X-Ray Lasers and Applications III**, Denver, CO (1999).

Keilty, K., E. Liang, B. Remington, R. London, K. Estabrook, J. Kane, *Numerical simulations of blast waves generated by an impulsive temperature source,* **Astrophysical Journal Supplement Series, 375** (2000).

Kozlowski, M. R., C.L. Battersby, and S.G. Demos, *Luminescence Investigation of $SiO_2$ Surfaces Damaged by 0.35 mm Laser Illumination*, G.J. Exarhos, A.H. Guenther, M.R. Kozlowski, K.L. Lewis, M.J. Soileau, eds., **SPIE**, **3902**, 138 (1999).

Labaune, C. J. Fuchs, S. Perierreux, A. Michard, H.A. Baldis, B. Cohen, P.E. Young, S. Glenzer, *Laser-Plasma Interaction Physics at LULI,* **Inertial Fusion Science and Applications (IFSA) '99 Proceedings,** Bordeaux, France (2000).

Labaune, C., H.A. Baldis, B.S. Bauer, E. Schifano, and A. Michard, *Effect of Crossed Beams Irradiation on Stimulated Brillouin and Raman Scattering,* **(Invited) Proceedings de la 25th European Conference on Laser Interaction with Matter**, Fornia, Italy (1998).

Landahl, E.C., R.M. Albis, A.L. Troha, F.V. Hartemann, G.P. Le Sage, W.E. White, H.A. Baldis, C.V. Bennett, K. Li, J.P. Heritage, C.H. Ho, and N.C. Luhmann, Jr., *X-band Photoinjector for a Chirped-pulse FEL,* **High Energy Density Microwaves,** R.M. Phillips, ed. (1999).

Landahl, E.C., R.M. Alvis, A.L. Troha, F.V. Hartemann, et al., *X-band Photoinjector for a Chirped-pulse FEL,* **AIP Conference Proceedings**, **474**, 433 (1999).

Langdon, A.B., R.L. Berger, B.I. Cohen, C.D. Decker, D.E. Hinkel, R.K. Kirkwood, C.H. Still, and E.A. Williams,

*Power Transfer Between Smoothed Laser Beams*, **Bull. Amer. Phys. Soc. 45**, 328 (2000).

Li, Y., J. Dunn, J. Nilsen, A. Osterheld, T.W. Barbee, Jr., and V.N. Shlyaptsev, *Saturated Plasma X-ray Laser at 19 nm*, **Free Electron Laser Conference 2000,** Durham, NC,(2000).

Li, Y., J. Dunn, J. Nilsen, A.L. Osterheld, and V.N. Shlyaptsev, *Near Field Imaging of a Saturated Table Top X-Ray Laser*, **Society of Photo-Optical Instrumentation Engineers 44th Annual Meeting of the International Symposium on Optical Science, Engineering and Instrumentation**, **3776**, 45 (1999).

Li, Y., J. Dunn, J. Nilsen, A.L. Osterheld, L.B. Da Silva, and V.N. Shlyaptsev, *Two-dimensional Near-field Images of the Table-top 18.9 nm Nickellike Molybdenum Soft X-ray Laser Pumped by 1 ps Laser Pulses*, **44th Annual Meeting of the International Symposium on Optical Science, Engineering and Instrumentation**, Denver, CO (1999).

Li, Y., J. Dunn, J. Nilsen, T.W. Barbee Jr., L.B. Da Silva, A.L. Osterheld, and V.N. Shlyaptsev, *Near-field Imaging of a Saturated Table-top X-ray Laser*, in proceedings of **Soft X-ray Lasers and Applications III**, J.J. Rocca and L.B. Da Silva, eds., SPIE proc. **3776**, 45 (1999).

Moon, S. J., J. Dunn, A. Faenov, T. Pikuz, K.B. Fournier, A.L. Osterheld, V.N. Shlyaptsev, Y. Li, and J. Nilsen, *Characterization of a High-Gain Ne-like Fe Transient X-Ray Laser*, **International Symposium on Optical Science, Engineering, and Instrumentation**, Denver, CO (1999).

Moon, S.J., J. Dunn, A. Ya Faenov, T.A. Pikuz, K.B. Fournier, A.L. Osterheld, V.N. Shlyaptsev, Y. Li, and J. Nilsen, *Characterization of a High-Gain Ne-like Fe Transient X-ray Laser*, in proceedings of **Soft X-ray Lasers and Applications III**, J.J. Rocca and L.B. Da Silva, eds., **SPIE proc. 3776**, 9 (1999).

Moon, S.J., J.Dunn, A.L.Osterheld, V.N.Shlyaptsev, Y. Li, and J. Nilsen, *Investigation of Time Delay Between Sequential Pulse Pumped Table-top Transient Collisional Excitation X-ray Laser*, **44th Annual Meeting of the International Symposium on Optical Science, Engineering and Instrumentation**, Denver, CO (1999).

Nilsen, J., Y. Li, J. Dunn, T.W. Barbee, Jr., A.L. Osterheld, *Modeling and Demonstration of a Saturated Ni-like Mo X-ray Laser*, **Proceedings of 7th International Conference on X-ray Lasers,** St. Malo, France (2000).

Nilsen, J., Y. Li, J. Dunn, and A.L. Osterheld, *Modeling Short-pulse-driven Collisional X-ray Lasers and Other New Schemes*, in proceedings of **Soft X-ray Lasers and Applications III**, J.J. Rocca and L.B. Da Silva, eds., **SPIE proc. 3776**, 14 (1999).

Nilsen, J., Y. Li, J. Dunn, A.L. Osterheld, A. Ryabtsev, and S. Churilov, *Measuring the Wavelengths of the Ni-like 4d 1So - 4p 1P1 X-ray Laser Line*, in proceedings of **6th International Conference on X-ray Lasers**, Kyoto, Japan, **Institute of Physics Conference Series 159**, 135 (1998).

Nilsen, J., Y. Li, J. Dunn, and A.L. Osterheld, *Progress in Understanding the Short-pulse-driven Collisional X-ray Lasers*, in proceedings of **6th International Conference on X-ray Lasers**, Kyoto, Japan, **Institute of Physics Conference Series 159**, 123 (1998).

Ng., J.S.T., P. Chen, W. Craddock, F.J. Decker, R.C. Field, M. Hogan, R. Iverson, F. King, R. Kirby, T. Kotseroglou, P. Raimondi, D. Waltz, H.A. Baldis, P. Bolton, D. Cline, Y. Fukui, V. Kumar, C. Crawford, R. Noble, K. Nakajima, A. Ogata, and A.W. Weidemann, *Results on Plasma Focusing of High Energy Density Electron and Positron Beams*, **International LINAC Conference,** Monterey, CA (2000).

Ng, J.S.T. H.A. Baldis, P. Bolton, P. Chen, D. Cline, W. Craddock, C. Crawford, F.J. Decker, R.C. Field, Y. Fukui, V. Kumar, R. Iverson, F. King, R. Kirby, T. Kotseroglou, K. Nakajima, R. Noble, A. Ogata, P. Raimondi, D. Waltz, and A.W. Weidemann, *Plasma Focusing of High Energy Density Electron and Positron Beams*, **Proceedings of the Advanced Accelerators Concepts 2000,** Santa Fe, NM (2000).

Osterheld, A.L. J. Dunn, S.J. Moon, K.B. Fournier, J. Nilsen, A.Y. Faenov, T.A. Pikuz, I.Y. Skobelev, A.I. Magunov, and V.N. Shlyaptsev, *Spectral and Imaging Characterization of Tabletop X-ray Lasers*, **Proceedings of 7th International Conference on X-ray Lasers,** Saint Malo, France (2000).

Osterheld, A.L., J. Dunn, and V.N. Shlyaptsev, *Characterization of Transient Gain X-ray Lasers*, in proceedings of **6th**

# CONFERENCE PROCEEDINGS

**International Conference on X-ray Lasers**, Kyoto, Japan, **Institute of Physics Conference Series 159**, 131 (1998).

Osterheld, A.L., J. Dunn, V.N. Shlyaptsev, Y. Li, J. Nilsen, and R. Shepherd, *Demonstration of Short Pulse Laser Pumped X-ray Lasers*, **5th Zababakhin Scientific Talks ZST 98 International Conference**, Snezhinsky, Chelyabinsk Region, Russia (1998).

Osterheld, A.L., V.N. Shlyaptsev, J. Dunn, J.J. Rocca, M.C. Marconi, C.H. Moreno, J.J. Gonzales, M. Frati, P.V. Nickles, M.P. Kalashnikov, and W. Sandner, *Modeling of Laser-produced Plasma and Z-pinch X-ray Lasers*, in proceedings of **6th International Conference on X-ray Lasers**, Kyoto, Japan, **Institute of Physics Conference Series 159**, 353 (1998).

Patel, R.R., H.E. Garrett, M.A. Emanuel, M.C. Larson, M.D. Pocha, D.M. Krol, R.J. Deri, and M.E. Lowry, *Compact, Low-Crosstalk, WDM Filter Elements for Multimode Ribbon Fiber Data Links*, **Proceedings of the 49th Electronic Components and Technology Conference,** 1261, San Diego, CA (1999).

Patel, F.D., E.C. Honea, D. Krol, S.A. Payne, J.S. Hayden, *A Diode-pumped Channel Waveguide Laser Fabricated in Nd:phosphate glass*, **OSA TOPS, 26,** Advanced Solid State Lasers, Martin M. Fejer, Hagop Injeyan and Ursula Keller eds., 172 (1999).

Remington, B.A., D. Arnett, R.P. Drake, and H. Takabe, *Using Intense Lasers in the Laboratory to Model Astrophysical Phenomena*, **ICF Quarterly** (1999).

Remington, B.A., S.G. Glendinning, K. Estabrook, R.J. Wallace, R. London, R.A. Managan, A. Rubenchik, D. Ryutov, K.S. Budil, J. Kane, D. Arnett, R.P. Drake, R. McCray, and E. Liang, *Supernova hydrodynamics experiments on Nova*, **Proceedings of the First International Conference on Superstrong Fields in Plasmas, AIP Conference Proceedings 426,** 551 (AIP, Woodbury, NY) (1998).

Rocca, J.J., M. Seminario, H.L. Mancini, J. Filevich, K. Kanizay, M.C. Marconi, M. Frati, B. Benware, A. Ozolos, J.L.A. Chilla, A. Vinogradov, I. Artioukov, V. Kondratenko, Y.A. Unspenskii, R. Depine, F.G. Tomasel, V.N. Shlyaptsev, *Applications of High Repetition Rate Tabletop Soft X-ray Lasers Become a Reality in Several Fields*, **Proceedings of 7th International Conference on X-ray Lasers,** Saint Malo, France (2000).

Rocca, J.J., B.R. Benware, C.D. Macchietto, and V.N. Shlyaptsev, *Generation of a High Average Power and Millijoule-level Pulses with a Tabletop Soft X-ray Laser*, **Proceedings of the SPIE - The International Society for Optical Engineering, 3776**, 152, **Soft X-Ray Lasers and Applications III**, Denver, CO (1999).

Rocca, J.J., B.R. Benware, C.D. Macchietto, and V.N. Shlyaptsev, *Generation of Millijoule-level Soft X-ray Laser Pulses at 4 Hz Repetition Rate in a Highly Saturated Tabletop Capillary Discharge Amplifier*, **1999 IEEE LEOS Annual Meeting Conference Proceedings**, LEOS'99. 12th Annual Meeting, **IEEE, 49** (1999).

Rocca, J.J., C.H. Moreno, M.C. Marconi, K. Kanizay, V.N. Shlyaptsev, C.D. Macchietto, and B. Benware, *Plasma Probing with a Table-top Soft X-ray Laser*, **Technical Digest. Summaries of papers presented at the Quantum Electronics and Laser Science Conference.** Opt. Soc. America, **156** (1999).

Rocca, J.J., M.C. Marconi, J. Filevich, K. Kanizay, C.H. Moreno, J.L.A. Chilla, R.J. Berglund, V.N. Shlyaptsev, Y.A. Unspenskii, A.V. Vinogradov, and Y.P. Pershin, *Plasma Diagnostics with a Tabletop Soft X-ray Laser*, **Proceedings of the SPIE - The International Society for Optical Engineering, 3886**, 266 (High-Power Lasers in Energy Engineering, Osaka, Japan) (1999).

Rocca, J.J., C.H. Moreno, B.R. Benware, M.C. Marconi, V.N. Shlyaptsev, C. Maccheitto, F.G. Tomasel, J.J. Gonzalez, M. Frati, and J.L.A. Chilla, *Tabletop Soft X-ray Lasers by Fast Discharge Excitation*, **Proceedings of the SPIE The International Society for Optical Engineering, 3343**, 138 (Santa Fe, NM) (1998).

Rocca, J.J.; C.H. Moreno, M.C. Marconi, V.N. Shlyaptsev, and C.D. Macchietto, *High Resolution Imaging of a Dense Plasma with a Table-top Soft X-ray Laser*, **Conference Proceedings. LEOS'98. 11th Annual Meeting. IEEE Lasers and Electro-Optics Society** 1998. (Orlando, FL). **IEEE, 44,1** (1998).

Schamiloglu, E., S.R.J. Brueck, F. Hegeler, F.V. Hartemann, et al., *A Smith-Purcell Free Electron Laser Based on an X-band Photoinjector*, IEEE Conference Record - Abstracts. **1999 IEEE International Conference on Plasma Science**. 26th IEEE International Conference, (Piscataway, NJ), **IEEE, 225** (1999).

Shlyaptsev, V., J. Dunn, A.L. Osterheld, Y. Li, and J. Nilsen, *Table-top Transient Collisional X-ray Lasers*, **29th Annual Anomalous Absorption Conference**, (Pacific Grove, CA) (1999).

Shlyaptsev, V.N., A.L. Osterheld, J. Dunn, J.J. Rocca, J.J. Gonzales, M. Moreno, M.C. Marconi, P.V. Nickles, M.P. Kalashnikov, K. Janulewicz, and W. Sandner, *Progress in Modeling of Table-top X-ray Lasers*, **44th Annual Meeting of the International Symposium on Optical Science, Engineering and Instrumentation**, (Denver, CO) (1999).

Shlyaptsev, V.N., J. Dunn, A.L. Osterheld, J. Nilsen, Y. Li, K.B. Fournier, J.J. Rocca, and P.V. Nickles, *Modeling of Transient X-ray Lasers: Comparison with Experiments*, 1999 IEEE LEOS Annual Meeting Conference Proceedings. **LEOS'99. 12th Annual Meeting. IEEE Lasers and Electro-Optics Society** (San Francisco, CA) IEEE, **113** (1999).

Tikhonchuk, V.T., J. Fuchs, C. Labaune, S. Depierreux, H.A. Baldis, S. Huller, J. Myatt, and D. Pesme, *Advanced Model for SBS of a Randomized Laser Beam and Application to Polarization Smoothing Experiments with Preformed Underdense Plasmas*, **ECLIM Proceedings,** (Prague, Czech Republic) (2000).

Zhang, G., S.G. Demos, and R.R. Alfano, *Far-red and NIR Emission from Tissues Under Photo-excitation*, in **Optical Biopsy: Advances in Laser and Light Spectroscopy to Diagnose Cancer and Other Diseases**, R.R. Alfano, ed., **SPIE, 3250**, 72 (1998).

# CONFERENCE PRESENTATIONS

Baldis, H.A., C. Labaune, J. Fuchs, and S. Depierreux, *Implications of Plasma Induced Smoothing to the Interpretation of Parametric Instabilities* (Invited), **Frontier-Science Research Conferences:P Science and Technology of Laser-Matter Interaction,** La Jolla, CA, July 2000.

Baldis, H.A., J. Dunn, M. Foord, and C. Andersen, *X-ray Thomson Scattering as a Diagnostic of Dense Hot Plasmas,* **7th International Conference on X-ray Lasers,** Saint Malo, France, June 2000.

Baldis, H.A., C. Labaune, J. Fuchs, S. Depierreux, A.V. Maximov, W. Rozmus, and D. Pesme, *Effect of Plasma-Induced Smoothing on Energy Transfer Between Crossing Beams,* **26th European Conference on Laser Interaction with Matter,** Prague, Czech Republic, June 2000.

Baldis, H.A. *Thomson Scattering of High Density Plasmas Using X-rays,* **20th ICFA Beam Dynamics Workshop,** Arcidosso, Italy, September 2000.

Baldis, H.A., C. Labaune, W. Rozmus, and A. Maximov, *Forward Scattering as a Potential Self-Smoothing Phenomena,* **3rd International Workshop on Laser Plasma Interaction Physics**, Banff, Alberta, February 1999.

Baldis, H.A., *Laser-Based Science Through the Institutes at LLNL*, **2nd International Workshop on Laboratory Astrophysics with Intense Lasers**, Tucson, AZ, 1998.

Baldis, H.A., *Parametric Instabilities and Thomson Scattering: A Perfect Marriage*, (Invited) **28th Annual Anomalous Absorption Conference**, Bar Harbor, ME, 1998.

Budil, K.S., M.J. Edwards, B. Lasinski, B.A. Remington, L. Suter, A.S. Wan, and P.E. Stry. *Ablation Front Rayleigh-Taylor Experiments at Nova*, **41st Annual Meeting of the American Physical Society Division of Plasma Physics**, Seattle, WA, November 1999.

Budil, K.S., M.J. Edwards, B.A. Lasinski, L. Suter, A.S. Wan, P.E. Stry, and B.A. Remington, *Hydrodynamic Eexperiments on the Nova Laser,* **41st Annual Meeting of the American Physical Society Division of Plasma Physics**, Seattle, WA, November 1999.

Calistru, D.M., S.G. Demos, V. Petricevic, A.B. Bykov, and R.R. Alfano, *Role of Intra-, Inter-molecular and Resonance Decay Pathways in Nonradiative Processes Taking Place in Impurity-doped Laser Crystals,* **CLEO-QELS,** QThM6, 250, Baltimore, MD, May 1999.

Calistru, D.M., S.G. Demos, and R.R. Alfano, *Role of Intra-, Inter-molecular and Resonance Decay Pathways in Nonradiative Processes Taking Place in Impurity-doped Laser Crystals,* **Optical Society of America 1998 Annual Meeting**, WDD15, Baltimore, MD, October 1998.

Chan, J.W., F.D. Patel, E.C. Honea, D.M. Krol, S.H. Risbud, *Photosensitivity of Rare Earth Doped Phosphate Glasses for Bragg Grating Formation,***102nd Annual Meeting of the American Ceramic Society,** St. Louis, MO, April 2000.

Chan, J.W., D.M. Krol, J.S. Hayden, S.H. Risbud, *Femtosecond Pulse Interactions with Phosphate Glasses for Waveguide Fabrication,* **Fall 2000 Meeting of the Glass and Optical Material Division of AcerS,** Corning, NY, October 2000.

Chan, J.W., D.M. Krol, S.H. Risbud, *Preparation and Characterization of Glasses from Fiber Bragg Gratings,* **101st Annual Meeting of the American Ceramic Society,** Indianapolis, IN, April 1999.

Chen, P., W. Craddock, F. Deker, R. Ivenson, F. King, R. Kirby, T. Kotseroglou, J.S.T. Ng, D. Walz, D. Cline, Y. Fukui, V. Kumar, P. Colestock, C. Crawford, R. Noble, T. Katsouleas, D.D. Meyerhofer, S. Masuda, A. Ogata, S. Chattopadhyay, A. Sessler, A.W. Weidemann, H.A. Baldis, P. Bolton, F. Esparza, and J. Foy, *Use of Localized Self-Induced Plasmas to Focus High Energy Electron Beams,* **International Conference on Plasma Science (ICOPS 2000),** New Orleans, LA, June 2000.

Cohen, B.I., H.A. Baldis, D.L. Berger, K.G. Estabrook, E.A. Williams, and C. Labaune, *Modeling of the Competition of Stimulated Raman and Brillouin Scatter in LULI Multiple Beam Experiments,* **30th Annual Anomalous Absorption Conference,** Ocean City, MD, June 2000.

Cohen, B.I., H.A. Baldis, R.L. Berger, C. Labaune, K.G. Estabrook, C.H. Still, and E.A. Williams, *The Competition of Stimulated Raman and Brillouin Backscatter in LULI Multiple Laser Beam Experiments,* **29th Annual Anomalous Absorption Conference**, Monterey, CA, June 1999.

# CONFERENCE PRESENTATIONS

Cohen, B.I., H.A. Baldis, R.L. Berger, E.A. Williams, and C. Labaune, *Modeling of the Competition of Stimulated Raman and Brillouin Scattering in LULI Multiple Beam Experiments*, **41st Annual Meeting of the American Physical Society Division of Plasma Physics**, Seattle, WA, November 1999.

De Yoreo, J.J., M. Yan, M. Runkel, M. Staggs, L. Liou, Demos, S.G., and L. Carman, *Characterization of Optical Performance and Defect Structures in Nonlinear Crystals for Large Aperture Lasers*, **CLEO-QELS**, 247, Baltimore, MD, May 1999.

Demos, S.G., *Defect Reactions in Optical Materials Using High Power Lasers*, **1999 Physics by the Bay**, IBM Almaden Research Center, CA, September 1999.

Demos, S.G., H.B. Radousky, and R.R. Alfano, *Subsurface Spectral Polarization Imaging Using NIR Laser Illumination*, **Optical Society of America,** 1998 Annual Meeting, Baltimore, MD, October 1998.

Demos, S.G., H.B. Radousky, M. Staggs, M. Yan, and J.J. De Yoreo, *Investigation of High-power Laser Conditioning of Defect Clusters in $KH_2PO_4$ Using Microscopic Fluorescence Imaging Defects: Doping and Microstructure*, **APS 1999 Centennial Meeting**, Atlanta, GA, March 1999.

Demos, S.G., H.B. Radousky, and R.R. Alfano, *Subsurface Imaging Using the Spectral Polarization Difference Technique and NIR Illumination*, 3597, **Optical Tomography and Spectroscopy of Tissue III, BIOS '99**, San Jose, CA, January 1999.

Demos, S.G., L.M. Sheehan, and M.R. Kozlowski, *Spectroscopic Investigation of Surface Defect Formations in $SiO_2$*, TuXX11, **Optical Society of America 1999 Annual Meeting**, Santa Clara, CA, September 1999.

Demos, S.G., M. Balooch, G.W. Marshall, and S.J. Marshall, *Spectroscopic Imaging and Characterization of Healthy and Transparent Root Dentin*, **Optical Society of America 1999 Annual Meeting**, Santa Clara, CA, September 1999.

Demos, S.G., M. Staggs, and H.B. Radousky, *Damage Induced Material Modification in the Bulk KDP Crystals*, **XXX Annual Symposium on Optical Materials for High Power Lasers**, Boulder, CO, October 1999.

Demos, S.G., M. Staggs, M. Yan, H.B. Radousky, and J.J. De Yoreo, *Observation of Photoexcited Emission Clusters in the Bulk of KDP and Laser Conditioning Under 355 nm Irradiation*, **XXX Annual Symposium on Optical Materials for High Power Lasers**, Boulder, CO, September 1998.

Demos, S.G., M. Staggs, M. Yan, H.B. Radousky, and J.J. De Yoreo, *Investigation of Steady-state and Transient Defect Populations in $KH_2PO_4$ Subsequent to High Fluence Laser Irradiation*, **Laser Material Crystal Growth and Nonlinear Materials and Devices**, 3610 LASE '99 San Jose, CA, January 1999.

Demos, S.G., M. Yan, M. Staggs, H.,B. Radousky and J. J. De Yoreo, *Microscopic Spectral Imaging of Defect Centers in KDP*, **Nonlinear Optics '98, Materials, Fundamentals and Applications**, Princeville, Kauai, HI, August 1998.

Demos, S.G., *New Approaches for Optical Sub-surface Imaging*, AWC1, **Advances in Optical Imaging & Photon Migration**, OSA Orlando Topical Meetings, Orlando, FL, March 1998.

Demos, S.G., M. Yan, M. Staggs, H.B. Radousky, and J.J. De Yoreo, *Investigation of Photoexcited Defect Clusters in KDP Using Microscopic Fluorescence Imaging*, **Optical Society of America, 1998 Annual Meeting**, Baltimore, MD, October 1998.

Depierreux, S., C. Labaune, H.A. Baldis, and J. Fuchs, *Experimental Observation of the Langmuir Decay Associated with Stimulated Raman Scattering*, **26th European Conference on Laser Interaction with Matter,** Prague, Czech Republic, June 2000.

Depierreux, S. C. Labaune, H.A. Baldis, J. Fuchs, D. Pesme, V. Tikhonchuk, S. Huller, and G. Laval, *Experimental Observation of Secondary Waves Produced in the Non-Linear Evolution of Stimulated Raman Scattering*, **30th Annual Anomalous Absorption Conference,** Ocean City, MD, June 2000.

Depierreux, S., C. Labaune, H.A. Baldis, J. Fuchs, and A. Michard, *Observation of Secondary Plasma Waves in Laser-plasma Interaction Experiments*, **International Fusion Science and Applications (IFSA)**, Bordeaux, France, September 1999.

# CONFERENCE PRESENTATIONS

Ditmire, T., K. Estabrook, K. Keilty*, B. Remington, A. Rubenchik, D. Ryutov, K. Shigemori, and V. Yanovsky, *Measurements of Radiative Blast Waves in Gases*, **AIRAPT-17 Meeting**, Honolulu, HI, July 1999.

Drake, R.P., J.J. Carroll III, T. Smith, H.A. Reisig, S.G. Glendinning, K. Estabrook, O. Hurricance, B.A. Remington, R. Wallace, E. Michael, and R. McCray, *Supernova Remnant Simulation Experiments Using the Nova Laser*, abstract submitted to the **First International Conference on Inertial Fusion Sciences and Applications: IFSA '99**, Bordeaux, France, September 1999.

Drake, R.P., S.G. Glendinning, K. Estabrook, J.J. Carroll, B.A. Remington, R. Wallace, E. Michael, O. Hurricane, and R. McCray, *Laser Experiments to Simulate Supernova*, **41st Annual Meeting of the American Physical Society Division of Plasma Physics**, Seattle, WA, November 1999.

Drake, R.P., T. Smith, H.N. Reisig, S.G. Glendinning, K. Estabrook, O. Hurricane, B.A. Remington, R. Wallace, J.J. Carroll III, E. Michael, and R. McCray, *Hydrodynamic Instabilities in Supernova Remnant Simulation Experiments*, **29th Annual Anomalous Absorption Conference**, Monterey, CA, June 1999.

Dunn, J., A.L. Osterheld, J. Nilsen, J.R. Hunter, Y.Li, A.Y. Faenov, T.A. Pikuz, and V.N. Shlyaptsev, *Saturated Output Tabletop X-ray Lasers* (Invited), **7th International Conference on X-ray Lasers,** St. Malo, France, June 2000.

Dunn, J., A.L. Osterheld, Y. Li, J. Nilsen, and V.N. Shlyaptsev, *Table-top Transient Collisional Excitation X-ray Lasers*, **IEEE International Conference on Plasma Science**, Monterey, CA, June 1999.

Dunn, J., A.L. Osterheld, Y. Li, J. Nilsen, and V.N. Shlyaptsev, *Transient Inversion Collisional X-ray Lasers*, **Optical Society of America Annual Meeting**, Santa Clara, CA, September 1999.

Dunn, J., Y. Li, A.L. Osterheld, J. Nilsen, S.J. Moon, B. Sellick, J.R. Hunter, and V.N. Shlyaptsev, *Table-top Transient Collisional Excitation X-ray Lasers*, **Soft X-ray Lasers and Applications III, 1999 International Symposium on Optical Science, Engineering and Instrumentation**, Denver, CO, July 1999.

Edwards, J., B. Lasinski, K.S. Budil, A.S. Wan, B.A. Remington, L. Suter, and P.E. Stry, *Ablative Rayleigh-Taylor Instability in Indirectly Driven Thin Aluminum Foils*, **29th Annual Anomalous Absorption Conference**, Monterey, CA, June 1999.

Edwards, J., S.G. Glendinning, L.J. Suter, T.D. Shepard, R.E. Turner, K.S. Budil, B. Lasinski, A.S. Wan, B.A. Remington, P. Graham, A.M. Dunne, and B.R. Thomas, *A Plasma Piston for Radiation Hydrodynamics Experiments*, **29th Annual Anomalous Absorption Conference**, Monterey, CA., June 1999.

Edwards, M.J., S.G. Glendinning, L.J. Suter, O. Landen, B.A. Remington, R.E. Turner, T.J. Shepard, P. Graham, A.M. Dunne, and B.R. Thomas, *Turbulent Hydrodynamic Experiments Using a New Plasma Piston*, **41st Annual Meeting of the American Physical Society Division of Plasma Physics**, Seattle, WA, November 1999.

Estabrook, K., B. Remington, D. Farley, G. Glendinning, S. Glenzer, C.A. Back, J.H. Harte, G.B. Zimimerman, R.J. Wallace, R. Turner, L.J. Suter, J.M. Stone, N. Turner, W.M. Wood-Vasey, and K. Shigemori, *Nova Laser Experiments of Radiative Astrophysical Jets*, **AAS January Meeting**, Austin, TX, January 1999.

Estabrook, K., B.A. Remington, K. Shigemori, D. Farley, S. Glenzer, R.E. Turner, S.G. Glendinning, G. Zimmerman, J.H. Harte, D.S. Bailey, R.J. Wallace, R.W. Lee, K. Fournier, R. Kodama, R. Koase, Y. Ochi, H. Azechi, J. Stone, and N. Turner, *LLNL Nova and Gekko Laser Experiments or Radiative Astrophysical Jets*, **29th Annual Anomalous Absorption Conference**, Monterey, CA., June 1999.

Estabrook, K., B.A. Remington, N. Turner, J. Stone, K. Shigemori, R. Kodama, T. Koase, Y. Ochi, H. Azechi, H. Takabe, D. Farley, P. Rambo, E. Alley, J. Hamster, G. Zimmerman, and J. Harte, *Astrophysical Jets Via Laser Plasma Interaction*, **41st Annual Meeting of the American Physical Society Division of Plasma Physics**, Seattle, WA, November 1999.

Fuchs, J. C. Labaune, S. Depierreux, and H.A. Baldis, *Self-Induced Plasma Smoothing of an Intense Laser Beam Propagating in Underdense Plasmas*, **30th Annual Anomalous Absorption Conference**, Ocean City, MD, June 2000.

Fuchs, J., C. Labaune, S. Depierreux, H.A. Baldis, V. Tikhonchuk, S. Huller, J. Myatt, and D. Pesme, *Polarization-Smoothing in Laser-Plasma Interactions,* **30th Annual Anomalous Absorption Conference,** Ocean City, MD, June 2000.

Fuchs, J., C. Labaune, S. Depierreux, H.A. Baldis, and A. Michard, *Polarization Smoothing in Laser-plasma Experiments,* **International Fusion Science and Applications (IFSA),** Bordeaux, France, September 1999.

Galmiche, D., C. Cherfils, P.A. Holstein, A. Richard, S.G. Glendinning, and B.A. Remington, *Ablative Rayleigh-Taylor Instability in Convergent Geometry,* abstract submitted to the **First International Conference on Inertial Fusion Sciences and Applications: IFSA '99,** Bordeaux, France, September 1999.

Gibson, D.J., F.D. Hartemann, E.C. Landahl, L. Song, A.L. Troha, J.R. Van Meter, H.A. Baldis, N.C. Luhmann, Jr., R.R. Freeman, D.U.L. Yu, and A. Kerman, *Design of a High Gradient Vacuum Laser Accelerator,* **41st Annual Meeting of the American Physical Society Division of Plasma Physics,** Seattle, WA, November 1999.

Glendinning, S.G., C. Cherfils, D. Galmiche, B. Remington, A. Richard, S. Haan, R. Wallace, L. Divol, N. Dague, D. Kalantar, O. Landen, W. Hsing, and B. Hammel, *Ablation Front Rayleigh-Taylor Growth Experiments in Spherically Convergent Geometry,* **41st Annual Meeting of the American Physical Society Division of Plasma Physics,** Seattle, WA, November 1999.

Glendinning, S.G., O.L. Landen, B.A. Remington, R.J. Wallace, D. Galmiche, C. Cherfils, P.A. Holstein, and A. Richard, *Ablative Rayleigh-Taylor Instability in Spherically Convergent Geometry,* **29th Annual Anomalous Absorption Conference,** Monterey, CA, June 1999.

Hartemann, F.V., H.A. Baldis, D.J. Gibson, J.P. Heritage, E.C. Landahl, A.L. Troha, and N.C. Luhmann, Jr., *Development of Tabletop Compton X-ray Sources for Advanced Biomedical Applications,* **7th International Conference on X-ray Lasers,** Saint Malo, France, June 2000.

Hartemann, F.V., A. LeFoll, A.K. Kerman, B. Rupp, D.J. Gibson, E.C. Landahl, A.L. Troha, N.C. Luhmann, Jr., and H.A. Baldis, *Three-Dimensional Theory of Emittance in Compton Scattering,* **Advance Accelerator Concepts 2000,** Santa Fe, NM, June 2000.

Hartemann, F., E. Lahdahl, A.L. Troha, J.R. Van Meter, H.A. Baldis, N.C. Luhmann Jr., D. Yu, J. Rosenzweig, and C. Pellegrini, *Development of a Laser Based Compton X-ray Source,* **40th Annual Meeting of the American Physical Society Division of Plasma Physics,** New Orleans, November 1998.

Hartemann, F., E. Landahl, L. Song, N.C. Luhmann, Jr., and H.A. Baldis, *Chirped Pulse Inverse Free-electron Laser: A High Gradient Vacuum Accelerator,* **40th Annual Meeting of the American Physical Society Division of Plasma Physics,** New Orleans, LA, November 1998.

Hartemann, F.V., E.C. Landahl, L. Song, A.L. Troha, J.R. Van Meter, D.J. Gibson, H.A. Baldis, and N.C. Luhmann Jr., *The Chirped-Pulse Inverse Free-Electron Laser,* **41st Annual Meeting of the American Physical Society Division of Plasma Physics,** Seattle, WA, November 1999.

Hartemann, F.V., H.A. Baldis, E.C. Landahl, N.C. Luhmann, Jr., T. Tajima, A.L.Troha, J.R. Van Meter, and A.K. Kerman, *Nonlinear Vacuum Electron-photon Interactions at Relativistic Intensities,* **JIFT Proceedings: Workshop on High Field Science,** Livermore, CA, November 1998.

Hurricane, O.A., B. Remington, R.P. Drake, H. Robey, J. Kane, and R. Teyssier, *CALE Simulation of the Spherically Divergent NLUF_2 Experiment,* **41st Annual Meeting of the American Physical Society Division of Plasma Physics,** Seattle, WA, November 1999.

Jiang, H., H.W.K. Tom, M. Yan, H.B. Radousky, J.J. DeYoreo, and S.G. Demos, *Time-resolved Studies of Laser Damage Processes in KDP Crystals,* **XXX Annual Symposium on Optical Materials for High Power Lasers,** Boulder, CO, October 1999.

Kalantar, D.H., B.A. Remington, J.D. Colvin, D.M. Gold, A. Loveridge, J.S. Wark, M. Meyers, and A. Hauer, *Shock Compressed Solids on the Nova Laser,* **29th Annual Anomalous Absorption Conference,** Monterey, CA, June 1999.

Kalantar, D.H., B.A. Remington, J.D. Colvin, D.M. Gold, K.O. Mikaelian, S.V. Weber, L.G. Wiley, A.M. Allen, A. Loveridge, J.S. Wark, M. Meyers, A. Hauer, and D. Paisley, *Laser Driven Shock Compressed Solid State RT and Diffraction Experiments,* **JOWOG37,** August 1999.

# CONFERENCE PRESENTATIONS

Kalantar, D.H., B.A. Remington, J.D. Colvin, K.O. Mikaelian, S.V. Weber, and L.G. Wiley, *Shock Compressed Solids on the Nova Laser,* submitted to the **11th Topical Conference on Shock Compression of Condensed Matter**, Snowbird, UT, June 1999.

Kalantar, D.H., J.D. Colvin, D.M. Gold, K.O. Mikaelian, B.A. Remington, S.V. Weber, L.G. Wiley, A.M. Allen, A. Loveridge, J.S. Wark, T.R. Boehly, A.A. Hauer, D. Paisley, and M.A. Meyers, *High Pressure Solid-state Experiments on Intense Lasers*, **NEDPC XII**, Los Alamos, NM, October 1999.

Kalanter, D.H., J.D. Colvin, D.M. Gold, K.O. Mikaelian, B.A. Remington, S.V. Weber, L.G. Wiley, A.M. Allen, A. Loveridge, J.S. Wark, T.R. Boehly, A.A. Hauer, D. Paisley, and M.A. Meyers, *Solid-state Experiments at High Pressure and Strain Rates*, **41st Annual Meeting of the American Physical Society Division of Plasma Physics**, Seattle, WA, November 1999.

Kane, J., D.D. Ryutov, B.A. Remington, *Hydrodynamic Instabilities in the Eagle Nebula,* **3rd International Workshop on Laboratory Astrophysics with Intense Lasers,** Rice University, Houston, TX, March 2000.

Kane, J., H.F. Robey, K.S. Budil, B.A. Remington, *Modeling of Multiple Layer and Divergent Geometry Laser Astrophysics Experiments,* **3rd International Workshop on Laboratory Astrophysics with Intense Lasers,** Rice University, Houston, TX, March, 2000.

Kane, J., B.A. Remington, D.D. Ryutov, D. Farnsworth, M. Pound, J. Stone, *Hydrodynamics of the Eagle Nebula,* **42nd Annual Meeting of the APS Division of Plasma Physics combined with the 10th International Congress on Plasma Physics,** Quebec City, Canada, October 2000.

Kane, J., K.S. Budil, and B.A. Remington, *Modeling of a Divergent-geometry Richtmyer-Meshkov Experiment on the Nova Laser,* **41st Annual Meeting of the American Physical Society Division of Plasma Physics**, Seattle, WA, November 1999.

Kodama, R., T. Koase, Y. Ochi, H. Nishimura, H. Azechi, H. Takabe, K. Shigemori, D.R. Farley, B.A. Remington, and K.G. Estabrook, *Experiments on a Radiative Collapse in Laser Produced Plasmas Relevant to Astrophysical Jet Formation*, **29th Annual Anomalous Absorption Conference**, Monterey, CA, June 1999.

Kozlowski, M.R., S.G. Demos, C.L. Battersby, *Spectroscopic Investigation of $SiO_2$ Surfaces Damaged by 351-nm Laser Illumination*, **XXX Annual Symposium on Optical Materials for High Power Lasers**, Boulder, CO, October 1999.

Labaune, C., H.A. Baldis, B.S. Bauer, E. Schifano, and A. Michard, *Effect of Crossed Beams Irradiation on Stimulated Brillouin and Raman Scattering,* (Invited), **25th European Conference on Laser Interaction with Matter**, Fiornio, Italy, May 1998.

Labaune, C., J. Fuchs, S. Depierreux, A. Michard, H.A. Baldis, B. Cohen, P.E. Young, and S. Glenzer, *Laser-Plasma Interaction Physics at LULI,* **International Fusion Science and Applications (IFSA)**, Bordeaux, France, September 1999.

Landahl, E., K. Li, R. Alvis, J.P. Heritage, F. Harteman, H.A. Baldis, N.C. Luhmann, Jr., E. Unreberg, D. Yu, J. Rosenzweig, and C. Pellegrini, *Optimization of a GHz UV Laser System for a High Gradient X-band PWT,* **40th Annual Meeting of the American Physical Society Division of Plasma Physics**, New Orleans, LA, November 1998.

Landahl, E.C., F.V. Hartemann, A.L. Troha, J.R. Van Meter, D.J. Gibson, J.P. Heritage, H.A. Baldis, N.C. Luhmann Jr., C.H. Ho, T.T. Yang, M.J. Horny, J.Y. Hwang, W.K. Lau, and M.S. Yeh, *RF Characterization of a Tunable, High-Gradient, X-Band Photoinjector,* **41st Annual Meeting of the American Physical Society Division of Plasma Physics**, Seattle, WA, November 1999.

Lee, R.W., R.C. Cauble, O.L. Landen, H.A. Baldis, J.S. Wark, A. Ng, S.J. Rose, C. Lewis, D. Riley, J-C. Gauthier, P. Audebert, *Science at the LCL: Plasma-based Studies,* **20th ICFA Beam Dynamics Workshop,** Arcidosso, Italy, September 2000.

Li, Y., J. Dunn, J. Nilsen, A.L. Osterheld, L.B. Da Silva, and V.N. Shlyaptsev, *Two-dimensional Near-field Images of the Table-top 18.9 nm Nickel-like Molybdenum Soft X-ray Laser Pumped by 1 ps Laser Pulses,* **Soft X-ray Lasers and Applications III, 1999 International Symposium on Optical Science, Engineering and Instrumentation**, Denver, CO, July 1999.

Maximov, A., W. Rozmus, D. Pesme, V. Tikhonchuk, C.E. Capjack, H.A. Baldis, and C. Labaune, *Nonlinear propagation of randomized laser beam: plasma-induced smoothing and scattering instabilities,* (Invited), **Frontier-Science Research Conferences: Science and Technology of Laser-Matter Interaction,** La Jolla, CA, July 2000.

Maximov, A., I. Ordev, D. Pesme, W. Rozmus, C.E. Capjack, and H.A. Baldis, *Field Distribution and Hot Spot Statistics in Plasmas Irradiated by Crossed RPP Beams*, **41st Annual Meeting of the American Physical Society Division of Plasma Physics**, Seattle, WA, November 1999.

Maximov, A., I. Ordev, W. Rozmus, D. Pesme, H.A. Baldis, C. Labaune, and C.E. Capjack, *Interaction of Two Crossed RPP Laser Beams with a Plasma*, **29th Annual Anomalous Absorption Conference**, Monterey, CA, June 1999.

Moon, S.J., J. Dunn, A.L. Osterheld, V.N. Shlyaptsev, Y. Li, and J. Nilsen, *Time Delay Between Sequential Pulse Pumped Table-top Transient Collisional Excitation X-ray Lasers*, **Soft X-ray Lasers and Applications III, 1999 International Symposium on Optical Science, Engineering and Instrumentation**, Denver, CO, July 1999.

Nilsen, J., Y. Li, J. Dunn, T.W. Barbee, Jr., and A.L. Osterheld, *Modeling and Demonstration of a Saturated Ni-like Mo X-ray Laser*, **7th International Conference on X-ray Lasers,** St. Malo, France, June 2000.

Nilsen, J., Y. Li, J. Dunn, and A.L. Osterheld, *Modeling Short-pulse-driven Collisional X-ray Lasers and Other New Schemes*, **Soft X-ray Lasers and Applications III, 1999 International Symposium on Optical Science, Engineering and Instrumentation**, Denver, CO, July 1999.

Ng, J.S.T., P. Chen, W. Craddock, F.J. Decker, R.C. Field, M. Hogan, R. Iverson, F. King, R. Kirby, T. Kotseroglou, P. Raimondi, D. Waltz, H.A. Baldis, P. Bolton, D. Cline, Y. Fukui, V. Kumar, C. Crawford, R. Noble, K. Nakajima, A. Ogata, and A.W. Weidemann, *Results on Plasma Focusing of High Energy Density Electron and Positron Beams*, **International LINAC Conference,** Monterey, CA, 2000.

Ng, J.S.T., H.A. Baldis, P. Bolton, P. Chen, D. Cline, W. Craddock, C. Crawford, F.J. Decker, R.C. Field, Y. Fukui, V. Kumar, R. Iverson, F. King, R. Kirby, T. Kotseroglou, K. Nakajima, R. Noble, A. Ogata, P. Raimondi, D. Waltz, and A.W. Weidemann, *Plasma Focusing of High Energy Density Electron and Positron Beams*, **Advance Accelerator Concepts 2000,** Santa Fe, NM, June 2000.

Patel, P.K. *High Energy Density Plasma Generation With the Ultra-intense JanUSP Laser*, **3rd International Conference on Laboratory Astrophysics with Intense Lasers,** Rice University, TX, March 2000.

Patel, R.R., H.E. Garrett, M.A. Emanuel, M.C. Larson, M.D. Pocha, D.M. Krol, R.J. Deri, and M.E. Lowry, *Compact, Low-Crosstalk, WDM Filter Elements for Multimode Ribbon Fiber Data Links*, **49th Electronic Components and Technology Conference,** San Diego, CA, June 1999.

Patel, F.D., E.C. Honea, D. Krol, S.A. Payne, J.S. Hayden, *A Diode-pumped Channel Waveguide Laser Fabricated in Nd:phosphate Glass*, **1999 OSA Topical Meeting on Advanced Solid-State Lasers,** Boston, MS, February 1999.

Radousky, H.B., S.G. Demos, M. Staggs, and J.J. De Yoreo, *Defect Cluster Dynamics in $KH_2PO_4$*, **WLL19, Optical Society of America 1999 Annual Meeting**, Santa Clara, CA, September 1999.

Radousky, H.B., S.G. Demos, M. Staggs, M. Yan, and J.J. De Yoreo, *Defect Clusters and Transient Defect Populations in $KH_2PO_4$, Defects: Doping and Microstructure*, JC30-5 **APS 1999 Centennial Meeting**, Atlanta, GA, March 1999.

Remington, B.A., *A Review of Astrophysics Experiments on Intense Lasers*, (Invited), **41st Annual Meeting of the American Physical Society Division of Plasma Physics**, Seattle, WA, November 1999.

Remington, B.A., D.H. Kalantar, S.V. Weber, J. Colvin, K. Mikaelian, and L. Wiley, *Solid-state Hydrodynamics Experiments on Laser Facilities*, **JOWOG37**, August 1999.

Remington, B.A., *Laboratory Astrophysics with High-power Lasers*, (Invited), Opening address at the **New Frontiers in Laboratory Astroplasma Physics Workshop**, Royal Astronomical Society, London, October 1999.

Remington, B.A., *Laboratory Studies of Supernovae and Astrophysical Jets with Intense Lasers*, abstract submitted to the **Asian Science Seminar**, Osaka University, Japan, February 1999.

Remington, B.A., *Laboratory Studies of Supernovae and Astrophysical Jets with Intense Lasers*, (Invited), **AIRAPT-17 Meeting**, Honolulu, HI, July 1999.

Remington, B.A., *Laser Experiments for Hydrodynamics and Astrophysics*, (Invited), **Centennial APS Meeting**, Atlanta, GA, March 1999.

# CONFERENCE PRESENTATIONS

Remington, B.A., Laser *Experiments for Hydrodynamics in a Variety of Settings*, **7th International Workshop on the Physics of Compressible Turbulent Mixing**, St. Petersburg, Russia, July 1999.

Robey, H., G. Burke, J. Edwards, G. Glendinning, J. Greenough, W. Hsing, D. Klem, P. Miller, B. Remington, P. Stry, and S. Weber, *Hydrodynamic Scaling Issues*, **NEDPC_XII**, Los Alamos, NM, October 1999.

Robey, H.F., B.A. Remington, J. Kane, O. Hurricane, R.P. Drake, D. Chin, R. Teyssier, J. Knauer, D. Bradley, and T. Boehly, *Recent Results from Astrophysically Relevant Hydrodynamic Experiments on the Omega Laser*, **41st Annual Meeting of the American Physical Society Division of Plasma Physics**, Seattle, WA, November 1999.

Rozmus, W.V. Bychenkov, A.V. Brantov, S. Glenzer, K. Estabrook, and H.A. Baldis, *Return Current Instability and its Effect on the Thomson Scattering Spectra in Laser Produced Plasmas*, **30th Annual Anomalous Absorption Conference,** Ocean City, MD, June 2000.

Rozmus, W., S. Glenzer, K. Eastabrook, H.A. Baldis, B. MacGowan, and P.E. Young, *Theoretical Analysis of Thomson Scattering from Laser Produced Plasmas*, **28th Annual Anomalous Absorption Conference**, Bar Harbor, ME, June 1998.

Rozmus, W., S. Glenzer, K. Estabrook, H.A. Baldis, J.S. DeGroot, B. MacGowan, and P.E. Young, *Calculations of Thermal Transport and Enhanced Ion-acoustic Fluctuations from Thomson Scattering Measurements in High-Z Laser Produced Plasma*, **40th Annual Meeting of the American Physical Society Division of Plasma Physics**, New Orleans, LA, November 1998.

Rozmus, W., V. Bychenkov, S. Glenzer, K. Estabrook, H.A. Baldis, and P.E. Young, *Modeling of Thomson Scattering Spectra from Laser Produced Plasmas*, **3rd International Workshop on Laser Plasma Interaction Physics**, Banff, Alberta, Canada, February 1999.

Rozmus, W., V. Bychenkov, S. Glenzer, K. Estabrook, H.A. Baldis, and P.E. Young, *Theory of Thomson Scattering Spectra from Laser Produced Plasmas*, **29th Annual Anomalous Absorption Conference,** Monterey, CA, June 1999.

Rozmus, W., V. Bychenkov, S. Glenzer, K. Estabrook, H.A. Baldis, and P.E. Young, *Theory of Thomson Scattering Spectra from Laser Produced Plasmas*, **International Fusion Science and Applications (IFSA)**, Bordeaux, France, September 1999.

Rubenchik, A.*, K. Budil, C. Brown, G. Glendinning, D. Gold, K. Estabrook, A. Komashko*, D. Pennnington, M. Perry, and B. Remington, *On Modeling of High Speed Meteorite Impact with Ultra-short Pulse Lasers*, **AIRAPT-17 Meeting**, Honolulu, HI, July 1999.

Ryutov, D., G. Glendinning, B. Remington, K. Shigemori, and T. Ditmire, *Simple Theory of a Blast Wave for Gases with Adiabatic Index Close to One*, **41st Annual Meeting of the American Physical Society Division of Plasma Physics**, Seattle, WA, November 1999.

Shigemori, K., D.R. Farley, B.A. Remington, K.G. Estabrook, R. Kodama, T. Koase, Y. Ochi, and H. Azechi, *Radiatively Cooled Jet Experiments Using High Intensity Lasers*, **41st Annual Meeting of the American Physical Society Division of Plasma Physics**, Seattle, WA, November 1999.

Shigemori, K., T. Ditmire, B.A. Remington, K.G. Estabrook, D.R. Farley, D.D. Ryutov, A.M. Rubenchik, R. Kodama, T. Koase, Y. Ochi, and H. Azechi, *Radiative Hydrodynamics Experiments for Astrophysics*, **29th Annual Anomalous Absorption Conference**, Monterey, CA., June 1999.

Shlyaptsev, V.N., A.L. Osterheld, J. Dunn, J.J. Rocca, J.J. Gonzales, C.H. Moreno, M.C. Marconi, P.V. Nickles, M.P. Kalashnikov, K.A. Janulewicz, and W. Sandner, *Progress in Modeling of Table-top X-ray Lasers*, **Soft X-ray Lasers and Applications III, 1999 International Symposium on Optical Science, Engineering and Instrumentation.** Denver, CO, July, 1999.

Shlyaptsev, V.N. & A.L. Osterheld, J. Dunn, Y. Li, and J. Nilsen, *Table Top Transient Collisional X-ray Lasers*, **29th Annual Anomalous Absorption Conference**, Pacific Grove, CA, June 1999.

Thamboon, P. D.M. Krol, *Thermal Poling Studies of Lanthanum Phosphate Glasses*, **Fall 2000 Meeting of the Glass and Optical Material Division of AcerS,** Corning, NY, October 2000.

Tikhonchuk, V.T., J. Fuchs, C. Labaune, S. Depierreux, S. Huller, J. Myatt, D. Pesme, and H.A. Baldis, *Advanced Model for SBS of a Randomized Laser Beam and Application to Polarization Smoothing Experiments with Preformed Underdense Plasmas*, **26th European Conference on Laser Interaction with Matter,** Prague, Czech Republic, June 2000.

Troha, A.L., E.C. Landahl, J.R. Van Meter, R.M. Alvis, N.C. Luhmann Jr., A.K. Kerman, F.V. Hartemann, R.R. Freeman, and H.A. Baldis, *Vacuum Electron Acceleration in a Coherent Dipole Field*, **41st Annual Meeting of the American Physical Society Division of Plasma Physics**, Seattle, WA, November 1999.

Turner, N., K. Estabrook, J. Stone, B. Remington, *Protostellar Jets: Laser Experiments and Astrophysical Simulations*, **41st Annual Meeting of the American Physical Society Division of Plasma Physics**, Seattle, WA, November 1999.

Wang, W.B., S.G. Demos, J. Ali, G. Zhang, and R.R. Alfano, *Enhancement of Visibility of Fluorescent Objects Hidden in Animal Tissues Using Spectral Absorption Difference Imaging*, BMB5, **Biomedical Optical Spectroscopy and Diagnostics, OSA Orlando Topical Meetings**, Orlando, FL, March 1998.

Weber, S.V., D.H. Kalantar, J.D. Colvin, D.M. Gold, K.O. Mikaelian, B.A. Remington, L.G. Wiley, A. Loveridge, J.S. Wark, M.A. Meyers, and A.A. Hauer, *Nova Experiments on Rayleigh-Taylor Instabilities in Solids*, **41st Annual Meeting of the American Physical Society Division of Plasma Physics**, Seattle, WA, November 1999.

Weber, S.V., D.H. Kalantar, J.D. Colvin, D.M. Gold, K.O. Mikaelian, B.A. Remington, and L.G. Wiley, *Nova Experiments Examining Rayleigh-Taylor Instability in Materials with Strength*, submitted to the **7th International Workshop on the Physics of Compressible Turbulent Mixing**, St. Petersburg, Russia, July 1999.

Wharton, K.B., J. Zweiback, G. Hays, D. Kalantar, B. Remington, T. Ditmire, and R.A. Smith, *Laser-driven Hard X-ray Source for Time-resolved Diffraction Experiments*, **41st Annual Meeting of the American Physical Society Division of Plasma Physics**, Seattle, WA, November 1999.

Yan, M., J.J. De Yoreo, B. Woods, M. Staggs, S.G. Demos, R. Torres, I.D. Hutcheon, and N.P. Zaisteva, *Impurity Segregation and its Affects on the Nonlinear Properties of* $KH_2PO_4$, **Solid State Lasers for Application to Inertial Confinement Fusion**, Monterey, CA, June 1998.

Yoreo, J.J., M. Yan, M.J. Runkel, B.W. Woods, R.W. Ryon, L. Carman, N.P. Zaitseva, Z.U. Rek, L.W. Liou, and S.G. Demos, *Characterization of Optical Performance and Defect Structure on Rapidly-grown Crystals of KDP and DKDP*, **Sixteenth Conference on Crystal Growth and Epitaxy**, Fallen Leaf Lake, CA, June 1998.

Young, P.E., H.A. Baldis, C.T. Hansen, J. Fuchs, S. Depierreux, and C. Labaune, *Characterization of SBS Growth in High Z Plasmas*, **40th Annual Meeting of the American Physical Society Division of Plasma Physics**, New Orleans, LA, November 1998.

# BOOKS AND BOOK CHAPTERS

## Books

**High-Field Science**, T. Tajima, K. Mima, and H.A. Baldis, Editors (Plenum, 2000).

## Book Chapters

*Nonlinear Vacuum Electron-Photon Interactions at Relativistic Intensities,* F.V. Hartemann, H.A. Baldis, E.C. Landahl, N.C. Luhmann, Jr., T. Tajima, A.L. Troha, and J.R. Van Meter, **High-Field Science,** edited by T. Tajima, K. Mima, and H.A. Baldis, (Plenum, New York, 2000).

*Coherence in Microwave and Laser Fields,* F.V. Hartemann, N.C. Luhmann, Jr., G.P. Le Sage, and H.A. Baldis, **Encyclopedia of Electrical and Electronics Engineering,** (Wiley & Sons, 1998).

*The Science and Technology of Silica Lightguides for Telecommunications,* C.R. Kurkjian and D.M. Krol, **Structure and Imperfections in Amorphous and Crystalline Silica**, (R.A. B. DeVine, J.P. Duraud, and E. Dooryhee, Eds.), (John Wiley & Sons Ltd., 2000).

# CONFERENCES WORKSHOPS

# CONFERENCES/WORKSHOPS

## 1998

September 30, 1998
***Mercury Laser Workshop***
Wente Conference Center, Livermore, CA

November 23-24, 1998
***Joint International Fusion Theory Workshop On High Field Science '98***
(United States and Japan)
Lawrence Livermore National Laboratory

## 1999

February 17-20, 1999
***3rd International Workshop On Laser Plasma Interaction Physics***
Banff Centre, Alberta, Canada

June 13-18, 1999
***29th Annual Anomalous Absorption Conference***
Asilomar Conference Center, Pacific Grove, CA

November 17, 2000
***Workshop on LLNL-ILSA's Compton X-ray Source for Protein Crystallography***
Wente Conference Center, Livermore, CA

# PARTICIPANTS

# PARTICIPANTS

ILSA Contact Information